TRACKER EFFECTOR-SPECIFIC AND MOTOR PLANNING SIGNALS IN HUMAN FRONTAL AND PARIETAL CORTICES: RELEVANCE FOR GOAL-DIRECTED ACTION AND NEURAL PROSTHETICS

Thesis by

Hilary Katherine Glidden

In Partial Fulfillment of the Requirements

for the Degree of

Doctor of Philosophy

California Institute of Technology

Pasadena, California

2009

(Defended July 3, 2008)

ACKNOWLEDGEMENTS

Starting a PhD is a bit like being dropped into the middle of the ocean in a dinghy. At first, you start paddling furiously in one direction, feeling sure of reaching your as-yet unknown destination as well as the path to get there. But, over the course of the next few years, your destination and the journey you take are strongly influenced by a variety of good breezes, currents, and co-paddlers. Below, I highlight people who influenced my thesis research work, but there are many other colleagues, friends, and family who supported me both scientifically as well as personally. Therefore, I dedicate this thesis to all of the good influences prior to and during my time here at the California Institute of Technology (Caltech).

I came to Caltech with the express interest of working for Dr. Richard Andersen. When I arrived, I was warmly welcomed into the fold of the Andersen Lab. Richard wisely steered me towards the Caltech Neural Prosthetic project and paired me with a postdoc in his lab, Daniel Rizzuto. Together, Dan and I spent many hours piloting human functional MRI (fMRI) experiments and learning the ropes of fMRI analysis, charting new territory in a lab with a primary interest in monkey electrophysiology. I am thankful that the past and present members of the Andersen Lab always encouraged me and took an interest in my work even though I was exploring the neuroscience of a different species (humans) with different techniques (mainly fMRI). The Andersen Lab staff have been very friendly and helpful for the past five years, so special thanks to Tessa Yao, Viktor Shcherbatyuk, and Kelsie Pejsa.

Shortly after I joined the lab, the Andersen Lab began to develop a program in monkey fMRI. Soon, I was no longer the only person in an electrophysiology lab using fMRI, or the only person running experiments with human subjects. Many thanks to my fellow Andersen Lab residents and fMRI scientists in the basement of Broad, including Igor Kagan, Axel Lindner, Daniele Procissi, and Asha Iyer, with whom I really enjoyed our scientific, collegial, and personal interactions.

A big thank you to my committee members for their advice and support during my PhD candidacy: Richard Andersen, Joel Burdick, Igor Fineman, Shinsuke Shimojo, and Yu-Chong Tai. This talented interdisciplinary committee kindly offered their basic science, clinical, and engineering perspectives on my research, and helped shape the direction of my thesis work as well as the formulation of this thesis.

The work presented in this thesis was completed in support of the Caltech Neural Prosthetic (CNP) Project. During my time at Caltech, the CNP Project has built on the Andersen Lab's strengths in monkey electrophysiology and brain-machine interfaces to further the transition to implantable human neural prosthetic devices. I eagerly anticipate the first human implants of the CNP as this device holds the potential to greatly improve the quality of life of people with severe paralysis. I would like to thank all the past and current contributors to the CNP Project, including our engineering and clinical partners.

Thanks also to the members and staff of the Caltech Brain Imaging Center, helmed by Dr. Scott Fraser. Steve Flaherty and Michael Tyszka taught me the mechanics of fMRI

acquisition, while Steve also provided assistance in many pilot studies. Mary Martin also did a wonderful job keeping the administrative side of things running smoothly.

The fMRI study of spinal-cord-injured patients in Part II of this thesis was made possible through collaboration with Dr. Steven Cramer, neurologist and professor at the University of California, Irvine (UCI). When I approached Dr. Cramer to initiate collaboration, he was very enthusiastic about working with the Andersen Lab and allowed us to piggyback on an ongoing study of his. I really enjoyed working with Dr. Cramer and his colleagues and staff at UCI, so many thanks to him and to Nuray Yozbatiran, Vu Lee, and Maggie Liu.

While they did not contribute directly to the work presented in this thesis, I would also like to thank the other people who played a role in my scientific experience at Caltech. Prior to joining Caltech as a graduate student, I completed a Summer Undergraduate Research Fellowship in Professor Christof Koch's lab, a positive experience that influenced my application to the Computation & Neural Systems Option at Caltech. Thanks to the CNS Class of 2003, including Ming Gu, Will Ford, Anusha Narayan, Matthew Nelson, Dirk Neumann, Jason Rolfe, Lavanya Reddy, Ueli Rutishauser and Casimir Wierzynski. Together we weathered the first year of classes and the qualifying exam. Thanks also to Professor Jerry Pine and his former graduate student, Daniel Wagenaar, with whom I completed a stimulating neuroengineering research rotation before officially joining the Andersen Lab. Early on, I also worked with Dan Rizzuto, Adam Mamelak, and the Epilepsy & Brain Mapping Unit at Huntington Memorial Hospital (HMH) to record intracranial electroencephalograms from patients undergoing surgery for intractable epilepsy. Dioni Rovello-Freking helped navigate the human subjects research approval at HMH. I also had very positive experiences with the Department of Radiology staff, with whom I piloted functional MRI at HMH. These partnerships with HMH clinicians and staff will facilitate the human implants of the CNP device in the future.

Thank you again to my advisor, Richard Andersen, for taking me on when I was an earnest first-year graduate student with an ambitious interest in brain-machine interfaces. Richard nurtured my interest in basic science and gave me the opportunity to also grow my interest in translational science. I would like to thank the Computation & Neural Systems Option, which flourished under the leadership of Christof Koch and Pietro Persona during my time at Caltech. Lastly, a special thanks to the campus-wide staff of Caltech. Here at Caltech, I encountered nothing but the most friendly and helpful people who made my experience with the administrative aspects of research and being a graduate student so easy and pleasant.

Be they breezes, currents, or co-paddlers, I am lucky to have had a multitude of beneficent influences at Caltech; influences that kept me on course and aided me in "reaching for" (part literally…) and achieving my PhD research goals of the last five years.

ABSTRACT

Delayed response tasks and functional magnetic resonance imaging were employed to map the neural architecture underlying goal-directed action planning in the human brain, examine interactions between motor planning and effector-specification (arm vs. eye), and explore other related processes and variables. Studies in healthy human subjects revealed a frontoparietal network of brain areas selectively involved in motor planning compared to control processes. Nodes within this network were characterized based on their functional properties, including effector-specificity. In frontal cortex, the dorsal premotor and supplementary motor areas preferentially encoded motor plans for arm reaches compared to saccadic eye movements, while the inferior frontal eye field was identified based on its selective involvement in eye movements. In parietal cortex, a similar dissociation of arm- and eye-specific brain areas was observed in the superior lobule. A medial branch of the intraparietal sulcus preferentially encoded eye movements, in contrast to more anterior medial, and posterior medial, portions of the intraparietal sulcus that preferentially encoded arm movements. Additionally, motor planning areas were engaged during voluntary shifts of spatial attention and during working memory for visual cues when these cues were relevant for upcoming movements. Many of these brain areas also encoded the type of arm movement (reach vs. point), arm posture, and limb contralaterality, a property that co-varied with increasing ties to motor execution. Also, a comparison of real vs. imagined arm movements revealed that the imagined arm could be used as a proxy for the real arm to drive activity in motor planning areas. Another study completed in healthy control and spinal cord-injured subjects demonstrated the preservation of a relatively normal pattern of brain activity after the brain is functionally disconnected from the limbs. The degree of preservation of

healthy/normal BOLD activity levels, particularly in the medial parietal cortex, strongly correlated with clinical and behavioral variables and could predict functional motor improvements in spinal cord-injured subjects six months later. These studies contribute to our understanding of the representation of goal-directed action planning in the human brain, elucidate human-monkey interspecies functional homologies, and have implications for the design and implantation of cortical neural prosthetic devices.

TABLE OF CONTENTS

List of Figures

List of Figures cont'd

List of Figures cont'd

List of Tables

NOMENCLATURE AND ABBREVIATIONS

ACC – Anterior cingulate cortex

AK - Attempted right knee movement

ASIA - American Spinal Injury Association

BOLD Signal – Blood oxygenation level dependent signal

CMA - Cingulate motor area

CNP - Caltech Neural Prosthetic

DC - Direct statistical comparison

dlPFC – Dorsolateral prefrontal cortex

ERA – Event-related average (see Part I: Methods)

FDR - False discovery rate (Genovese et al. 2002)

FEF – Frontal eye field

fMRI – Functional magnetic resonance imaging

GLM - General linear model (Friston et al. 1995)

HC - Healthy control (normal)

HRF - Hemodynamic response function

I or Imag. - Imagined

IL - Imagined right leg movement

IPL – Inferior parietal lobule

IPS – Intraparietal sulcus

IR - Imagined arm reaching

LIP – Lateral intraparietal area

M1 – Primary motor cortex

N - Null or NoGo: no movement condition

PC = Principal component

PM – Premotor

PPC – Posterior parietal cortex

PrCS - Precentral sulcus

PRR – Parietal reach region

NOMENCLATURE AND ABBREVIATIONS CONT'D

R - Real arm reaching, though "R" is sometimes used to indicate "Right"

RC - Relative Contribution

RFX - Random-effects analysis

ROI - Region of interest

S - Saccadic eye movement

S1 – Primary somatosensory cortex

SCI - Spinal cord-injured

SFS - Superior frontal sulcus

SMA – Supplementary motor area

SPL – Superior parietal lobule

Directional abbreviations:

a or ant – Anterior

d – Dorsal

i or inf - Inferior

l or lat - Lateral

m or med – Medial

mid – Middle

p or pos – Posterior

v – Ventral

R – Right, when separated from and modifying a noun,

else "R" is likely to be short for "Reach" or "Reaching"

L – Left

B - Bilateral

PREFACE

Good intentions are, at least, the seed of good actions

- Sir William Temple statesman and essayist

A thought which does not result in an action is nothing much,
and an action which does not proceed from a thought is nothing at all
- Georges Bernanos, author

I have always thought the actions of men the best interpreters of their thoughts

- John Locke, philosopher

The ancestor of every action is a thought
- Ralph Waldo Emerson, essayist, poet and philosopher

It was one of those parties where you cough twice before you speak, and then decide not to say it after all.

- P.G. Wodehouse, author and humorist

We are not passive observers of life, but actor-agents. As such, we make many plans in life; some are as long-term and ambitious as a five- or ten-year career plan, or as mundane as planning what to do next weekend. However, we also routinely make less ambitious, more immediate action plans: reaching out to grab a cup of coffee or to shake someone's hand, or glancing up to read the time off a clock or to meet someone's eye. This latter type of action plan may sometimes escape our conscious consideration but is of high ecological importance...Why? For example:

When meeting another person in the U.S., it is customary to shake hands. If another person reaches out their right hand, it is ecologically important to first recognize the gesture and any other contextual cues and then specify and narrow down a repertoire of potential behavioral responses. If this person is a friend, a typical response is an approach, reaching out one's own hand to engage in a handshake. If foe, the response domain may be less constrained, and the behavioral repertoire larger. For instance, one might either choose to ignore the hand offered (avoidance) or to swat the foe's hand away (an approach with a different intent). Whether friend or foe, the social gesture is first processed in the brain as visual input, and action execution is then predicated upon the transformation of the visual input into an appropriate motor output. Prior knowledge influences the recognition of the gesture and the specification of the response space, as well as the selection of an appropriate or optimal intent and corresponding response.

These cognitive "thoughts," or "intentions," that precede action are action plans. Hence, these action plans get pride-of-place in this thesis. Also highlighted are both the behavioral and clinical significance of the fact that the *brain encodes what you plan to do before you do it*. These intentional neural signals are encoded in a network of action-planning regions in the human brain and could be applied in the control of a neural prosthetic device.

To understand the planning of the actions mentioned above, a gross oversimplification of one possible trajectory of the handshake situation is:

Input: *Right hand offered*

Black box (aka "Brain"):

Perception/Recognition: *"Someone" is initiating a handshake*

Include prior knowledge: *Is this "someone" Friend or Foe? Friend*

Action selection: *Given the fact that "someone" is a friend, what is the appropriate response? Extend own right hand to shake hands*

Output: *Extend own right hand and shake hands*

It is tempting to classify this handshake as a simple stimulus-response mapping; however, a variety of contextual cues could influence the selection, preparation, and execution of a behavioral response (e.g., "intent" to shake or swat, approach or avoidance, right arm or left arm, hand shaping, grip force, current arm position, location of the other person's hand/spatial goal of movement, and timing of movement). A closer look at the "simple" handshake, like many other everyday movements, reveals it to be contextually rich and behaviorally flexible, such that it no longer belongs in the domain of reflexive stimulus-response mapping, but in the domain of goal-directed actions that are under voluntary, cognitive control.

To enable the experimental investigation of goal-directed actions, the behavioral context was pared down to embody only three relevant task instructions: where to move (the spatial goal of the movement), how to move (the mechanism of movement), and when to move (only move upon the presentation of a "go" stimulus). In the experiments described in Parts I and II of this thesis, the goal of an action and the mechanism of action are specified by external visual cues. The "goal" of the action is the spatial location of a visually-presented target. The mechanism of action is the means by which the agent acts or exerts an influence on the environment. Two mechanisms of action explored in depth in this thesis include arm movement (arm reaching or hand/finger pointing, real or imagined), and saccadic eye movement.

SPECIFIC AIMS

Part I of this thesis anatomically and functionally maps the neural architecture underlying the planning of goal-directed actions, and describes the interactions between motor planning and effector-specification in the human brain (Chapters 1 & 2). Chapter 3 explores other processes relevant for goal-directed action, including working memory and spatial attention and the representation of relevant visual cues. It also explores other variables related to goal-directed arm movements: the type of arm movement, brain lateralization for the arm employed, and arm posture. Lastly, Chapter 4 presents a novel functional magnetic resonance imaging (fMRI) data analysis technique and provides example applications. The results of the studies described in Part I have implications for our understanding of action planning in the human brain, as well as the interspecies functional homology of frontomotor and parietal cortices in monkeys and humans.

Part II of this thesis explores the clinical applications of the findings of Part I because, to quote the polymath Goethe, “Knowing is not enough; we must apply!” Therefore, Part II describes additional experiments demonstrating that imagined movements can be used as a proxy for real movements, discusses an fMRI study of brain plasticity that explores how the brain represents goal-directed actions following disconnection from the end effectors, and elucidates how the body of findings from Parts I & II will influence the design, implantation, and implementation of cortical neural prosthetic devices.

GENERAL INTRODUCTION

Goal-directed behavior

In the preface, I mentioned a few examples of goal-directed behavior. The "goal" of a behavior can be defined on several levels. A motivational outcome "goal" of the handshake could be to impress a new contact or to maintain a friendship, getting to the heart of the "why" of the movement intention. In contrast, a more immediate "goal" of the handshake, applicable across multiple action-motivational outcomes, could be to successfully navigate my right hand to meet with the other person's hand, and appropriately shape my grip so that our hands fit together and we can initiate the handshake. This latter definition of the goal of the handshake speaks more to the "what" of the movement intention, and can be decomposed into both a spatial/translational element (where to go), and a manipulative element (what to do when I get there.)

In this thesis, I mainly describe the translational components of simple actions, with the goal to acquire, rather than to manipulate, a spatial target. I concentrate on this decomposition of action, since it can be generalized across many different kinds of movements, including both arm reaching and saccadic eye movements. I also concentrate on elucidating the cognitive processes preceding, and brain areas engaged in, these spatial goal-directed movements.

The basic framework for the study of this kind of goal-directed action is to specify both the spatial goal of the action (the target location to be acquired), and the effector used to acquire the target. I commonly qualify the "effector" employed in a movement, defined in physiological terms as the "organ that carries out a response to a nerve impulse" (www.dictionary.com). In Part I, I extensively study how the brain represents two effectors and their related movements: the arm and the eye effectors, and pointing/reaching or saccadic eye movements, respectively.

Motor planning

This thesis treats the "what" content of movement intentions. Critical to the specification of a movement intention and subsequent action execution is the process of motor planning. A movement can only be planned and prepared in advance if both the spatial goal target ("where") and the effector ("how") are known. Once both target and effector are known, the full metrics of the movement are available and the brain network appropriate for the selected type of action can engage and specify a motor plan or intention.

For movements to visual targets/goals, sensory input informs action. Thus, the first step is to process sensory stimuli and extract spatial and contextual cues. Next, this sensory input needs to be linked with the action output, a step commonly known as sensorimotor transformation. Lastly, a resultant movement plan needs to be translated into descending corticospinal output in order to execute the movement.

In order for a brain area to participate in the formation of a motor plan, it should represent the effector to be employed in the upcoming movement, that is, be **effector-specific**. **Effector-specificity** is defined as significantly higher relative brain activity for one effector type (e.g., arm) compared to another (e.g., eye).

Cortical representations of effector in the human and monkey

The concept of effector-specificity is well studied in primary motor and somatosensory cortices. In 1890, Beevor & Horsley published a study of electrical stimulation of monkey motor cortex, revealing a map of the body on the cortical surface (Beevor & Horsley, 1890).

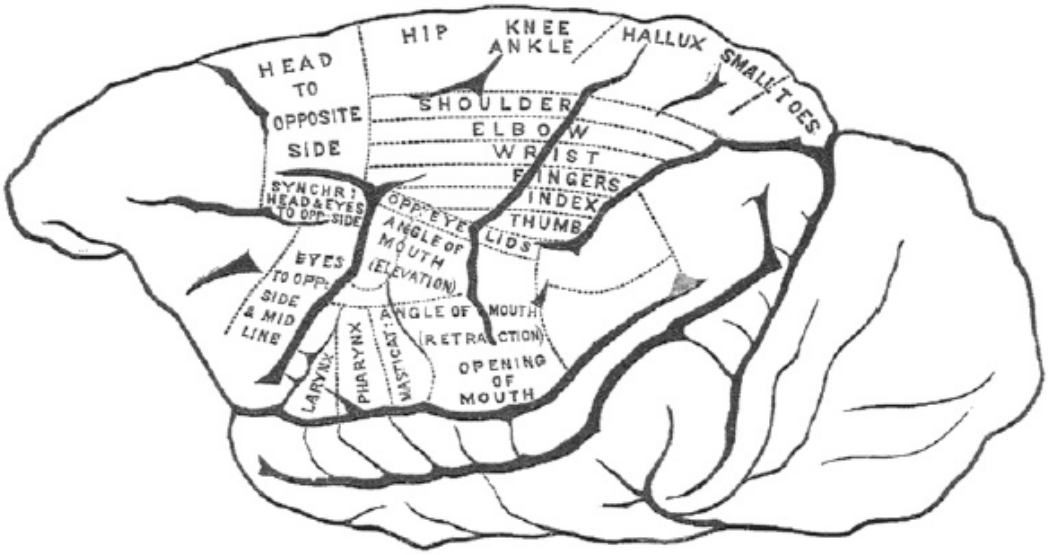

Figure G.1 – Topographic maps of the body in monkey cortex. From Graziano & Aflalo, 2007.

In the 20th century, neurosurgeon Dr. Wilder Penfield mapped these cortices in humans through electrical stimulation in his awake, epileptic patients, and identified topographic maps of the body, after stimulation evoked different movements or somatosensory experiences. This led to the concept of a body "homunculus," or "little man," within the brain. Instead of being a 1:1 mapping of body space onto the cortical surface, different parts of the body are overrepresented compared to their actual relative size, including the hands and the mouth/lips in motor cortex, and the hand, index finger, and lips in somatosensory cortex.

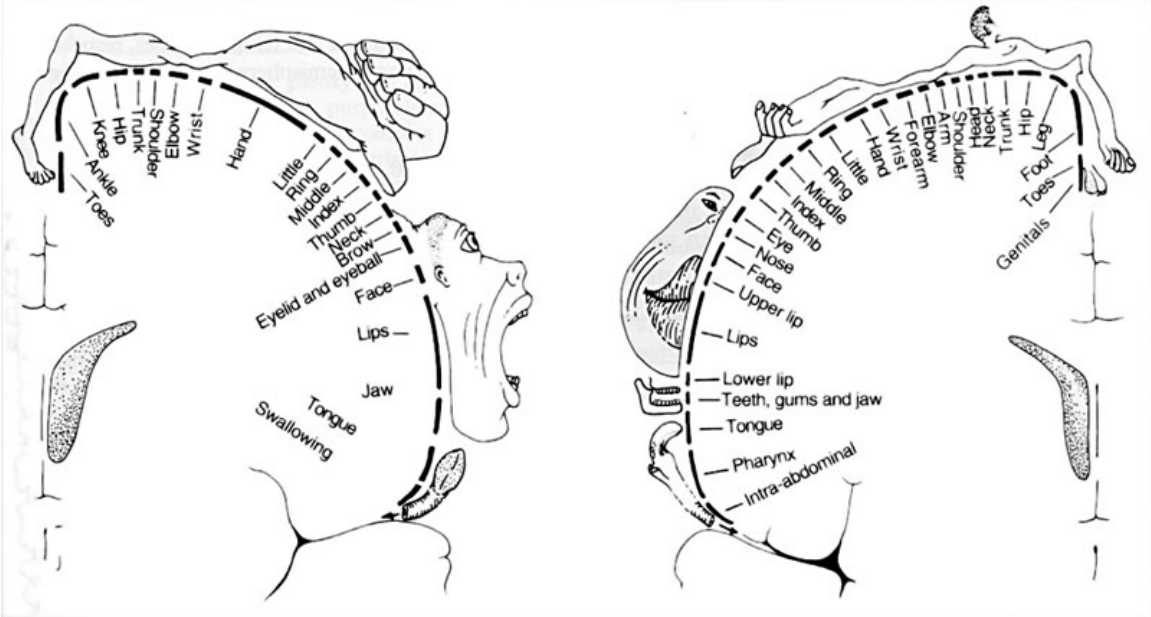

Figure G.2 – Human motor (left) and somatosensory (right) "homunculi." Based on the work by Dr. Penfield; image downloaded from:
http://www.ling.upenn.edu/courses/Fall_1997/ling001/neurology.html

However, the concept of the motor homunculus is a gross oversimplification. Localized lesions of primary motor cortex do not always elicit deficits in movements with single body parts, but rather lead to deficits in groups of synergistic muscles (Wikipedia entry for: cortical homunculus). Therefore, instead of discrete "body-space," the motor cortex may instead topographically represent overlapping maps of body parts/muscle groupings relevant for the control of coordinated movements of neighboring body-parts or functionally-linked actions (Nudo et al. 1996, Graziano & Aflalo 2007).

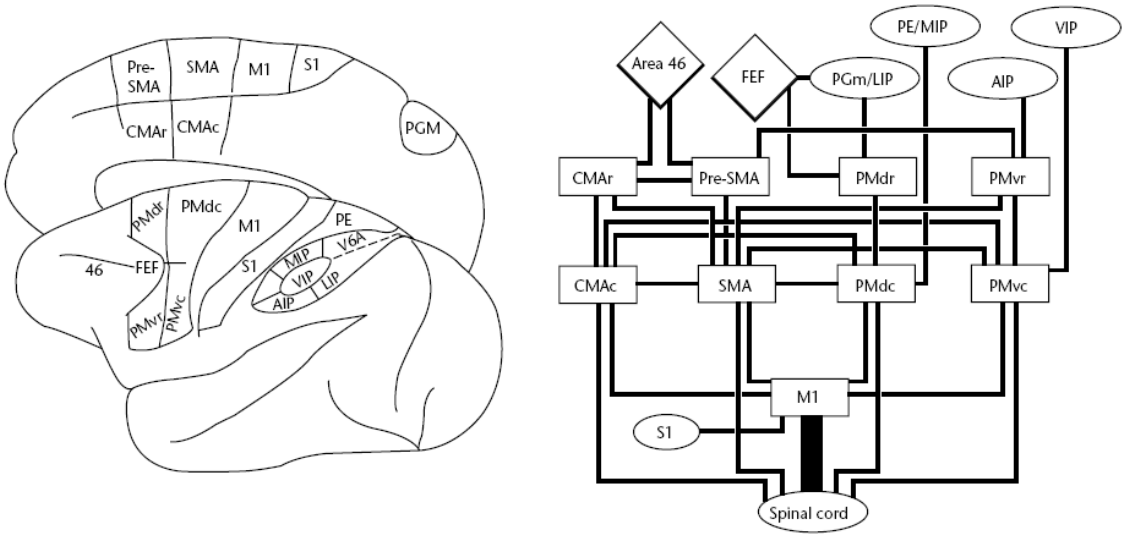

Figure G.3 – Left: Locations of monkey primary somatomotor (M1, S1) and motor association areas (premotor, supplementary motor, and posterior parietal cortices). Right: Anatomical interconnectivity of primary and association motor areas (Schieber & Fuglevand 2003).

There is also evidence of effector-specificity, or functional topography for effector, in premotor, supplementary motor, and parietal cortices, which are thought to play a role in motor planning and sensorimotor transformation critical to goal-directed actions (Hoshi & Tanji 2000, Hoshi & Tanji 2006, Beurze et al. 2007, Goodale & Milner 1992, Buneo & Andersen 2008). In the monkey brain, premotor areas PMd (dorsal premotor) and PMv (ventral premotor) strongly represent arm reaching and grasp/object manipulation, respectively. Eye movements can be evoked by stimulation of the frontal eye fields (FEF, Bruce et al. 1985), which are located lateral to the PMd representation of arm movements. However, parts of the rostral PMd are also relevant for eye movements (Boussaoud 1995, Fujii et al. 2000), and could perhaps play a role in the coordination of arm and eye movements. The most robust specificity for arm movements (compared to eye movements) is found in the caudal PMd. On the medial wall, the SMA is also involved in arm movements, while the more anterior SEF is generally classified as an oculomotor area. However, it is important to stress that the degree of arm- vs. eye-specificity in these brain areas is generally relative; PMd, PMv, and SMA have an oculomotor representation in addition to their involvment in arm movements, and reversely, SEF also plays a role in arm movements (Shadmehr & Wise, 2005).

In the posterior parietal cortex (PPC) of monkeys, the medial wall areas 7m and 5c/PEc encode current hand position, reaches, saccades, and visual inputs. In the intraparietal sulcus, the medial intraparietal area (MIP) and part of adjacent area V6A form the parietal reach region (PRR), a brain area that is effector-specific for arm reaching compared to saccade eye movements (Snyder et al. 1997, Snyder et al. 1998, Quian-Quiroga et al. 2006). This area receives sensory visual and proprioceptive inputs, and neurons respond to both visual inputs and arm posture (Johnson et al. 1996, Torres et al. 2006). It also contains both limb-dependent (contralateral arm preferred) and limb-independent neurons that encode upcoming arm movements (Chang et al. 2008). Neurons in MIP/PRR are directionally-tuned to different parts of visual space, and activity integrated across neurons in MIP/PRR to form a population vector encodes the direction of an upcoming arm movement. In contrast, the lateral intraparietal area (LIP) shows a preference for involvement in eye movements compared to arm movements, specifically planning saccades (Snyder et al. 1997, Snyder et al. 1998, Quian-Quiroga et al. 2006,) but also contains neurons that are visually-responsive, reflect the locus of spatial attention, and discharge during a saccadic eye movement (Bracewell et al. 1996, Gottlieb et al. 1998, Bisley & Goldberg, 2003, Colby et al. 1996).

Human lesion studies support a role for the medial PPC in goal-directed arm movements (Bálint 1909, Sirigu et al. 1999, Karnath & Perenin 2005). Transcranial magnetic stimulation over human medial PPC-induced endpoint variability during a memory-guided reaching task (Vesia et al. 2006), as well as several human neuroimaging studies, have reported a role in preparing arm movements (Astafiev et al. 2003, Connolly et al. 2000, Connolly et al. 2003), with a more lateral representation as the locus for eye movement planning and execution (Sereno et al. 2001, Medendorp et al. 2003, Medendorp et al. 2005). However, there is still debate in the human literature as to the degree of specificity for arm vs. eye effectors.

Part I: Chapter 1 of this thesis investigates effector-specific signals in human frontomotor cortex and PPC and the interaction between effector-specificity and motor planning, while the *Discussion* section of Part I expounds and attempts to resolve this debate within the human literature and discusses correspondence with findings in the rhesus macaque monkey.

Delayed response tasks

Delayed response tasks (DR tasks) are frequently employed by neurophysiologists to study the specification, preparation, and execution of movements. DR tasks impose a delay to separate a visual cue/instruction stimulus from a "go" stimulus that triggers a contingent motor response (Fig. G.4). A typical DR task instructs both where (target or spatial goal) and how (effector) to move prior to the delay. After initial cue and context processing, delay-period brain activity is thought to represent motor planning and other processes engaged prior to movement initiation. Importantly, a prerequisite for motor planning is that subjects can only plan a movement when it is fully-specified, that is, when they know the metrics of the movement, including both where to move and how to move.

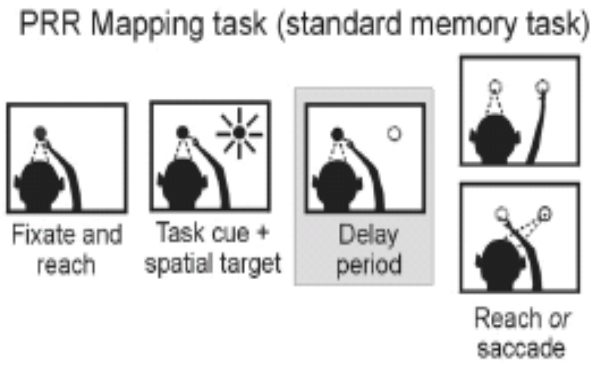

Figure G.4 – Typical delayed response task used in a monkey electrophysiological experiment. From Calton et al. 2002.

Introduction to fMRI and the BOLD signal

Functional magnetic resonance imaging (fMRI) measures the blood-oxygen-level dependent (BOLD) signal. Local increases in neural activity lead to greater oxygen consumption, triggering blood flow to the area (with a lag of 1-5 seconds) and changing the local ratio of deoxyhemoglobin/oxyhemoglobin. Ogawa (1990a and b) and Kwong (1992) discovered a linear relationship between this ratio and a magnetic susceptibility. This magnetic susceptibility is detected in fMRI, and an increase in local metabolism correlates positively with an increase in the amplitude of the BOLD signal.

One caveat is that the BOLD signal is an indirect measure of neural activity. The precise relationship between increased metabolism and oxygen consumption and single neuron activity is not completely understood and is still under active investigation. However, a recent study in awake, behaving macaque monkeys used single-unit and multi-unit neuronal activity and local field potentials (LFPs) from electrophysiological recordings to predict the BOLD response. The authors found that the LFP was a more reliable predictor of the BOLD response than multi-unit activity (Goense & Logothetis 2008), and that the gamma range band of the LFP (20-60Hz) explained the most variance. The LFP integrates information from large numbers of neurons, and reflects both inputs to a brain volume and local processing, since it is related to dendritic synaptic activity. In contrast, single-unit and multi-unit activity usually reflect action potentials in large pyramidal neurons (which are easier to record using implanted electrodes), the output/projection neurons of a brain volume.

The impulse hemodynamic response function (HRF) has a lag of 1-4s, then takes 4-5s to reach its peak. This impulse HRF is convolved with box-car predictors spanning periods of visual stimulation (the cue), or other task epochs (the delay and response periods) to develop a profile of the predicted BOLD response to a certain task or trial. Individual predictor HRFs are assumed to add linearly. A statistical regression, the general linear model (GLM) (Friston et al. 1995), then scales these task-epoch predictors to best fit the observed BOLD response signal.

The GLM is set up as follows:

$$\mathbf{Y = XB + U}$$

Y is the measurement observed (the BOLD signal, amplitude x time), X is the design matrix (the separate predictor HRFs), and U is the noise/error term. Solving for B finds the beta weights (beta values) for the different predictors that generate the best overall fit of the model design matrix to the observed data. Secondary statistical contrasts between different beta values can then be calculated, for instance to determine whether the Cue-related HRF or the Delay-related HRF contributes more to the BOLD signal observed in a particular brain area.

A)

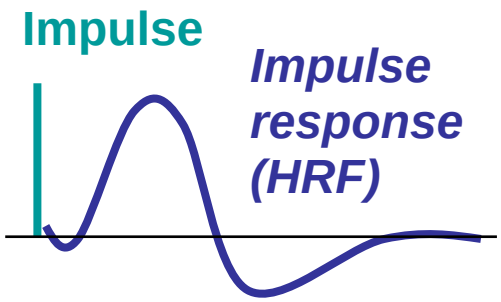

B)

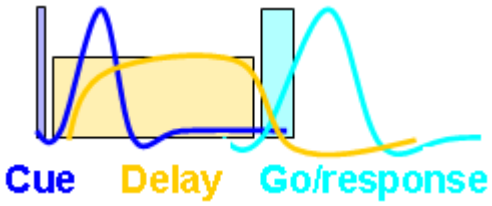

Figure G.5 – A) BOLD impulse response function: The HRF lags an impulse by 1-5s, then takes 4-5s to peak. An undershoot sometimes follows the main modulation. The whole temporal profile of the impulse HRF lasts ~20s. B) Predicting the BOLD response to a delayed response task: Task epochs (Cue, Delay, Go) are convolved with the expected impulse HRF (A), to generate an expected Task-epoch BOLD response predictor. These predictors are assumed to add linearly, and are scaled to fit the data in a general linear model.

It can be difficult to directly translate delayed response task paradigms used in monkey electrophysiology to be appropriate for fMRI investigations because of the sluggish nature of the BOLD impulse response function and the limited temporal resolution of the fMRI acquisition (sample or repetition rate, the TR, is usually 1-3s instead of in the 10^2-10^3 Hz range). These considerations are discussed in greater detail in the *Methods* section for Part I: Chapters 1 and 2.

PART I: BASIC SCIENCE OF GOAL-DIRECTED ACTION

CHAPTER 1 – The best of intentions

ABSTRACT

Two event-related fMRI experiments were used to investigate effector-specificity during motor planning. Effector-specificity was defined as a significant preference for one effector over another (e.g., arm > eye). The main experiment characterized effector-specificity in frontal and parietal cortices, with a special focus on brain areas involved preferentially in planning real and imagined reaches. A second experiment employed a modified delayed response task to investigate the interaction between effector-specificity and processes related to motor planning, including non-spatial effector preparation and default motor planning. This study provides converging evidence for the human functional homologues of the monkey dorsal premotor cortex (PMd) and parietal reach region (PRR), and demonstrates a double dissociation between arm-specific and eye-specific brain areas.

INTRODUCTION

The current study was designed to characterize human supplementary motor, premotor, and posterior parietal cortices in terms of their preference for planning goal-directed movements made with one motor effector vs. another (e.g., arm vs. eye).

Mapping of effector-specific brain areas in the human cortex is important for two reasons. The first motivation is to determine the degree of inter-species correspondence between human and monkey functional brain areas in frontal and parietal cortex. Relative effector-specificity (arm vs. eye) is well characterized in the monkey during the memory period of delayed response tasks, when neural activity reflects variables regarding upcoming goal-

directed reaches and/or saccades (Snyder et al. 1997, Snyder et al. 1998, Musallam et al. 2004, Scherberger et al. 2005, Scherberger et al. 2007, Quian Quiroga et al. 2006, Cisek & Kalaska 2002, Mazzoni et al. 1996, Bruce & Goldberg 1985, Mushiake et al. 1996, Lawrence et al. 2005). Two monkey brain areas with greater neural activity prior to reaches than prior to saccades include dorsal premotor cortex (PMd) and parietal reach region (PRR), while two saccade-specific brain areas include the frontal eye fields (FEF) and lateral intraparietal area (LIP). Effector-specific intentional signals are not as well characterized in the human brain, and previous human fMRI studies have reported strongly overlapping brain networks for goal-directed arm and eye movements (Connolly et al. 2000, Simon et al. 2002, Astafiev et al. 2003, Medendorp et al. 2003, Medendorp et al. 2005, Connolly et al. 2007, Levy et al. 2007). The current study provides evidence for the human functional homologues of monkey PMd and PRR, and demonstrates a double dissociation between arm-specific and eye-specific brain areas.

The second motivation for mapping effector-specificity in the human brain is to restore communicative and motor function to severely paralyzed patients. Intentional signals for reaches recorded from monkey PMd and PRR have been used to directly control the movement of an external effector (Musallam et al. 2004, Mulliken et al. 2004). A neural prosthetic device implanted into a functionally homologous areas of the human brain could allow patients to interface with and control an external effector such as a computer, a prosthetic arm, or even their own limb just by thinking about reaching, greatly improving quality of life and independence. This clinical application will be discussed in greater detail in Part II of this thesis.

RESULTS

Effector-specificity during the delay period in Experiment 1

The main experiment (Experiment 1) investigated relative effector-specificity (i.e., arm vs. eye) in a delayed response task. Because the main analysis epoch was the Delay period, comparisons between effectors are not confounded by differences in visual stimulation, motor output, or sensory feedback related to the movement. Both the results of the statistical models and raw BOLD activity confirm the observed patterns of significant effector-

specificity. Abbreviations are used in the GLM contrasts detailed below, with R=reach, I=imagined reach, S=saccade, and N=nogo. Motor planning should occur during the delay period, while motor execution processes are engaged during the go/response period. The inclusion of a variable delay interposed between the cue instruction period and go/response period ensured that subjects began to plan the upcoming movement at the start of the delay. Further details about the experiment are available in the *Methods* section at the end of Part I, and a diagram of the task is available in the *Figures* section.

Areas were defined as reach or arm-specific if they survived the GLM contrast [R_{Delay} > S_{Delay}] AND [R_{Delay} > N_{Delay}]. Specificity for imagined arm movements relative to saccades was tested separately with the contrast [I_{Delay} > S_{Delay}] AND [I_{Delay} > N_{Delay}]. Importantly, imposing the constraint that real- or imagined reach delay activity be greater than NoGo delay activity ensures that the brain areas identified in the contrast are significantly active above baseline (NoGo) levels. Similarly, brain areas were defined as eye-specific if they survived the GLM contrast [S_{Delay} > R_{Delay}] AND [S_{Delay} > N_{Delay}].

The main arm-specific regions of interest (ROIs) were located mainly in frontal and parietal cortices, contralateral to the arm used, including the dorsal premotor cortex (PMd: ROIs PMd and PMd/SMA), supplementary motor cortex (SMA: ROIs PMd/SMA and SMA/Cing.), anterior superior parietal lobule (aSPL: ROI aIPS/PoCS), and medial superior parietal lobule (mSPL: ROI medPPC/pIPS) (Fig. E1.1B, Table E1.1). Significant specificity for arm movements compared to eye movements is visible in the across-subjects, random-effects statistical parametric map (Fig. E1.1B).

In contrast, eye-specific activations were located in a distinct, bilateral frontoparietal network including the inferior frontal eye field (infFEF), middle SPL (midIPS), and the right supplementary eye field (SEF).

In general, the effector-specificity observed during the Delay period was maintained throughout the Go period (Table E1.1, Fig. E1.2), though the degree of effector-specificity changed. One major exception is the right SEF, which showed specificity for saccades during

the Delay period but was not significantly specific for saccades during the Go period. Several brain areas increased their effector-specificity during the Go period, including infFEF, midIPS, parts of PMd, and aIPS/PoCS; while in the SMA/Cing. and medPPC/pIPS, effector-specificity was maintained but not potentiated. Looking at the raw BOLD ERAs in SMA/Cing. and medPPC/pIPS (Fig. E1.3), it appears that, relative to BOLD activity at the end of the Delay period, the Go period BOLD signal increases roughly equally on reach and saccade trials; hence, the effector-differences observed throughout the response period in these ROIs could either be carried over from the Delay period into the Go period, or could be in part due to smear of the Delay period HRF into the beginning of the Go period HRF.

Because the GLM contrasts for effector-specificity are biased against areas showing relatively equal activity on reach and saccade trials, a Relative Contribution (RC) analysis was performed (see *Methods*). Using this analysis, the changing profile of effector-preference can be visualized on the cortical surface, during the Delay (Fig. E1.1A) and Go (Fig. E1.2) periods. While confirming the significant effector-specificity revealed by the GLM, the RC analysis also shows that there are parts of the PMd, SMA, and SPL which are roughly equally active during both arm and eye movement planning (light blue and light yellow in Fig. E1.1A). Activity in these brain areas may reflect non-specific aspects of motor planning, a possibility discussed later in the text. Several additional arm-preferring ROIs not visible in the random-effects (RFX) map (Fig. E1.1B) still demonstrate significant arm-specificity in the GLM, including the dlPFC, preSMA/Cing., putamen, and SMG/IPL, and posterior ascending cingulate sulcus (pCing) (see Table E1.1). Two additional areas with reach-preference in the RC map include the inferior frontal gyrus extending into ventral premotor cortex (IFG/PMv), and bilateral anterior insula (antInsula); however, these areas were difficult to define on a single-subject basis as described below and are not considered “main” ROIs.

Effector-specificity in frontal and parietal cortex was further analyzed on a subject-by-subject basis. Even in Talairach space, there is substantial inter-subject anatomical variability in brain shape and sulcal patterns. Despite these variations, single-subject RC maps reveal consistent relative locations of infFEF and PMd moving from lateral to medial PrCS, and of

midIPS and medPPC/pIPS moving medially from the middle IPS into the mSPL (Fig. E1.9). The greatest RC value for eye vs. arm in parietal cortex is located in a large medial branch of the IPS, about halfway between the anterior end of the IPS and where the IPS approaches the parietal occipital sulcus (ROI: midIPS). The greatest RC values for arm vs. eye are located in the medial SPL extending onto the medial surface of the PPC (medPPC). Compared to eye-preference, reach-related preference emerges in the next medial branch of the IPS, posterior to the branch containing midIPS, and extends into the transverse parietal sulcus (TPS) and onto the medial wall of parietal cortex in the ascending branch of the superior parietal sulcus (SPS). In several subjects, this medial branch of the IPS intersects with the TPS; this intersection or spanning reach-preferring region of the mSPL was termed pIPS. The medial wall reach-preferring region was termed medPPC. MedPPC was often contiguous with and indistinguishable from the pIPS activation, especially when viewed in the 3D brain instead of on the inflated cortical surface. The functional activation profiles were also indistinguishable from each other; hence, these areas were considered one region of interest: medPPC/pIPS.

Single subject-based regions of interest (ssROIs) were defined based on peak reach- or saccade-delay activity relative to the baseline condition (i.e., [R_{Delay} > N_{Delay}] or [S_{Delay} > N_{Delay}] in the single-subject GLM). These ssROIs were then analyzed across subjects (Table E1.1). Timecourses of BOLD activity were extracted from these areas in each subject. Delay period-aligned, trial-averaged event-related BOLD timecourses (ERAs) were calculated for each ssROI and then averaged across subjects. These ERAs confirm the significant effector-specificity previously revealed by the whole-brain across-subjects GLM (pictured in Fig. E1.1). Calculation of ERAs, which are based on the raw BOLD activity and not on a model of the expected HRF, also allows for visualization of the evolution of effector-specificity during the course of the delay period. Fig. E1.3 shows ERAs for the main arm- and eye-specific ROIs and for two control regions, M1 and V1. Fig. E1.3A shows the ERAs for trials with the longest delay length, 8s. The effective delay period in these 8s delay trials is from 2-10s relative to actual delay onset, since there is a lag in the onset of the impulse HRF (~2s). This latency is clear in M1 (Fig. E1.3A), as BOLD activity does start rising above the zero baseline until >2s after Go period onset. Left hemisphere SMA/Cing., PMd/SMA, PMd (not shown, very similar to PMd/SMA), aIPS/PoCS, and medPPC/pIPS exhibit reach-specificity,

and bilateral infFEF and midIPS/LIP exhibit eye-specificity. M1 and V1 do not significantly distinguish between effectors during the Delay period, but clearly show significant specificity during the Go period, as expected, when motor output and sensory feedback drive activity in these areas. The ERA curves also reveal that infFEF and midIPS have larger initial transient responses than the arm-specific ROIs, best observed in NoGo trials (yellow curves, Fig. E1.3A). In arm-specific ROIs, these transient visual- or context-processing responses quickly decay back to baseline during the delay period.

Experiment 1 utilized variable delay lengths of 2, 4, 6 and 8s, to ensure that subjects began planning the cued movement immediately after the cue instruction and could not predict when the instructed movement would be made. Fig. E1.3B better resolves the evolution of effector-specificity during the Delay period by isolating Delay period activity and averaging across trials with different delay lengths and then subtracting out NoGo delay activity from reach, imagined reach, and saccade trials. The NoGo condition served as a control for the effects of visual stimulation during the Cue period and any initial visual cue/context-processing that occurs during the Delay period. Thus, by subtracting out NoGo activity, the true profile of evolving effector-specificity can be observed (Fig. E1.3B).

Significant real/imagined arm-specificity starts to evolve about 4s after delay onset, peaks around 8s after delay onset, and is maintained throughout the rest of the delay. While both real- and imagined-arm movement planning activates arm-specific regions to a greater extent that saccade planning, there are some slight differences between real- and imagined-arm trials. The least subtle modulation appears in the left aIPS/PoCS, where real-arm planning is significantly greater than imagined-arm planning, though both are significantly greater than saccade. This ROI also showed the highest ratio of Delay/Cue GLM beta values (R_{Delay}/Cue = 36.9%), reflecting a smaller Cue predictor contribution to the GLM than in other ROIs (~1/3 the size of the Cue predictor contribution in midIPS and medPPC/pIPS).

Interestingly, saccade vs. reach specificity evolves later in infFEF and midIPS. Eye-specificity is strongest at 8-10s after delay onset, but still appears before any effector differences are observable in V1 (Fig. E1.3B). The profile of delay activity after subtracting

out the NoGo curve is lower than for arm-specific areas, reflecting the strong visual cue/context processing response in these brain areas (see NoGo curves in Fig. E1.3A) relative to motor planning activity. Strong visual cue responses could also explain why saccade-specificity evolves later in the delay period. Modulations of BOLD activity by the preferred effector tend to be fairly small in size relative to the amplitude of modulation by the cue in these ROIs, with a lower ratio of Delay/Cue predictor beta values in these ROIs compared to in reach-specific ROIs. This ratio is about half as big in saccade-specific ROIs as it is in reach-specific ROIs for the dominant effector (midIPS S_{Delay}/Cue = 4.3% vs. medPPC/pIPS: R_{Delay}/Cue = 10.4%; infFEF S_{Delay}/Cue = 11.1% vs. PMd R_{Delay}/Cue = 20%).

While curves for reach/imagined reach/saccade trials diverge from the NoGo condition at 2-4s in all effector-specific ROIs, relative effector-specificity for arm vs. eye evolves with different temporal profiles in reach-specific ROIs (~4s relative to delay onset) compared to in eye-specific ROIs (from +8s relative to delay onset) (see Fig. E1.5C). This later evolution of saccade-specificity could explain why the strength and significance of relative effector-specificity assessed based on GLM results is lower in eye-specific ROIs (where eye is greater than arm) than in arm-specific ROIs (where arm is much greater than eye). Delay periods of 2-8s were employed in Experiment 1, with equal probability. If significant saccade-specificity tends to evolve at +8s relative to delay onset in eye-specific ROIs, BOLD activity would only diverge for saccade vs. reach in comparisons of trials of the longest delay lengths (6s and 8s delay lengths). However, in reach-specific ROIs, reach vs. saccade effector-specificity should be evident across all employed delay lengths. Hence, a GLM contrast between saccade and reach predictors, when predictors are defined to span the entire delay period, will be less significant in eye-specific compared to arm-specific ROIs. These differences in the temporal evolution of dissociable arm vs. eye specificity might warrant further investigation, as a greater proportion of delay activity in eye-specific ROIs infFEF and midIPS might reflect non-specific/effector-independent processes such as spatial attention or working memory. This possibility is discussed later in the context of Experiment 2.

To further quantify the degree of effector-specificity in these ROIs, single-subject GLM beta weights for the reach and saccade delay predictors were used to calculate a paired relative effector-specificity index (RES). RES is defined as:

$$(R_{Delay} - S_{Delay}) / (| R_{Delay} | + | S_{Delay} |)$$

The RES ranges from +1 ("absolute" reach-specificity) to -1 ("absolute" saccade-specificity). A value of 0 indicates no specificity for one effector over another, while a value of +/- 0.33 indicates that one effect has a beta value that is 2x the beta value for the other effector. In theory, the "chance" level RES value should be zero. For each ROI, an actual "chance" level RES value was calculated by taking the actual beta values for the two predictors for all subjects, randomly permuting the assignment across effectors/subjects 1000 times; then, for each assignment permutation, the RES was recalculated, to derive a mean "chance" RES. For all of the ROIs, the actual "chance" level RES value was less than 0.005.

Mean RES value for arm-specific ROIs (SMA, PMd, aIPS/PoCS, and medPPC/pIPS) was 0.6, reflecting a four times greater GLM contribution of the R_{Delay} predictor compared to the S_{Delay} predictor. This value was -0.13 in eye-specific ROIs (bilateral infFEF and midIPS), reflecting a 1.3 times greater contribution of the S_{Delay} compared to the R_{Delay} predictor. However, in all of these ROIs, at least one subject showed absolute reach- or saccade-specificity in their RES value. RES values are plotted in Fig. E1.4. Similar RES values were calculated using the raw BOLD data by extracting the mean percent BOLD signal change on reach vs. saccade trials over the epoch 6-10s relative to delay onset (Fig. E1.5), confirming the results obtained using the GLM-derived beta values.

Despite the presence of significant differential relative effector-specificity signals in frontal and parietal cortices, much of the brain network engaged during motor planning is still recruited by all three motor effectors (R, I, S), and by other task-related processes (see previous two *Results* sections). A GLM contrast of [R>N] AND [I>N] AND [S>N] for either delay- or go-period predictors was used to identify brain areas that are significantly active for all three motor effectors compared to the NoGo condition in Experiment 1 (Fig. E1.6B).

Because of their engagement when any motor effector is cued, some of the BOLD activity in these brain areas could be considered "non-specific," and may reflect processes like cue/context processing, spatial attention and working memory, general action readiness, or the prediction of upcoming sensory or motor events. However, the results of Experiment 2 (described below) confirm that these non-specific processes alone do not fully explain BOLD activity in these brain areas, and at least a portion of brain activity is attributable to the process of motor planning.

Effector-specificity, and interactions with motor planning and other processes in Experiment 2

Experiment 2 characterized the cognitive basis of the BOLD signal observed during the delay period of traditional DR tasks by separately manipulating the presentation of target and effector information prior to the delay period. While Experiment 2 was primarily designed to look at the processes driving delay period activity rather than at effector-specificity (see next Chapter), the interaction between effector and the motor preparation condition (PIS_E) relative to the motor planning condition (PIS_{ET}) is of interest, since it is conceivable that the effector-specific modulations observed in Experiment 1 could be attributable to non-spatially specific, but effector-specific, motor preparation. Point, Imagined Point, and Saccade effectors were collapsed into a "motor" effector group (PIS, designating an average-across-predictors for different motor effectors), for comparison with a "non-motor" effector (NoGo trials, N). GLM predictors are named based on the effector instructed on the trial in either the first or the second cue period; thus, the name designates the movement type made during the Go period rather than explicit knowledge of the effector during the Delay period. Subject "knowledge" is captured in predictor name subnotation, and denotes the information presented on that type of trial *prior* to the delay period (ET=effector+target, E=effector only, T=target only, 0=no cues, see *Methods* section). Any task instructions that were not presented in the first cue period, prior to the delay, were instructed in a second cue period that directly preceded the go/response period. Further details of Experiment 2 are available in the *Methods* section at the end of Part I, and the task is diagrammed in the *Figures* section.

Shorter delay periods were employed in Experiment 2 given the larger number of conditions (n=16) and the need for statistical power for inter-condition comparisons. Due to the sluggish nature of the HRF, the tail of delay-related BOLD activity probably continues into the early Go period. This additional delay-related activity is of interest but cannot be disambiguated from response-related activity when looking at the BOLD timecourse from the early Go period. It is important to mention that this contamination effect does not work in reverse: there is no confound of response-related activity affecting ERAs extracted during the Delay period. Hence, in order to best resolve all delay-related BOLD activity and any modulations by effector in Experiment 2, the HRF related to Delay period activity was isolated from the HRF related to Go period activity using a deconvolution analysis, implemented in BrainVoyager QX.

Brain areas selectively activated during motor planning compared to control processes (see next Chapter) were selected for the deconvolution analysis. The intersection between effector-specificity and processes engaged during the delay period was investigated across different cueing paradigms to reveal how effector-specific signals manifest in brain areas involved in motor planning, as well as any interactions between effector-specificity and processes related to motor planning such as non-spatial effector preparation and default motor planning.

The results of the deconvolution analysis confirm the previously demonstrated pattern of effector-specificity in the main motor planning-related ROIs (Fig. E2.2) and no specificity during the delay period in M1 (control). Additional insight into the nature of the delay activity for the non-preferred effector can be gleaned from the deconvolved responses.

In the frontal cortex in SMA/Cing. (medial wall), PMd/SMA (surface dorsal premotor cortex, in the PrCS medial to the PrCS/SFS junction, not shown in Fig. E2.2 but appears in Fig. E2.1), and PMd (located in the PrCS), the predominant result revealed by the deconvolution analysis is an effector modulation where there are clear differences between hand and eye planning (P_{ET}>S_{ET}, Fig. E2.2). However, there is still a strong effect for S_{ET} compared to other conditions, so these brain areas probably play a role in planning both hand and eye

movements, as well as encode a motor readiness or preparatory set, with the strongest effect for hand movements but also an effect for eye movements (P_E and S_E>0 cond., also see Fig. E2.1 where $PIS_E>N_E$).

In the parietal cortex, a role for the aIPS/PoCS in planning and specifying upcoming hand/arm movements is confirmed since activity for P_{ET} is maintained throughout the delay period and is greater than activity in all other conditions, though S_{ET} also demonstrates some maintained activity above the rest of the conditions (Fig. E2.2). There is also a mild effect of effector preparation (P_E, S_E) in the late delay period compared to the T condition, which could encode non-specific motor preparedness.

The medPPC/pIPS is specific for hand movement planning activity (P_{ET}>all), and also maintains activity in the motor preparation condition, but does not differentiate between arm and eye preparation (no differences between P_E and S_E) (Fig. E2.2). Another effect of interest is that S_{ET} activity is not greater than either T or S_E activity, suggesting that the recruitment of medPPC/pIPS in trials where a saccade is fully specified prior to the delay may reflect the non-effector-specific components of the task, such as spatial attention/working memory, mnemonic encoding of the cue context, and general action readiness, and that this area is only engaged in motor planning for hand/arm movements and not for saccade eye movements.

In infFEF and midIPS, the only condition that differentiates at the beginning of the delay is S_{ET}, while S_E starts to diverge from T later (at 4s+); hence, the modulation by the saccade effector may be twofold: these areas may subserve saccade planning when the metrics of the saccade are known, and could underlie non-spatially specific saccade preparation prior to the second cue, instructing the target and fully specifying an imminent saccade movement (Fig. E2.2). Another interesting effect is the maintained non-zero activity and positive slope of the 0 (baseline) condition curve, similar to in Fig. E2.1, and the fact that $P_E>P_{ET}$ and $T>P_{ET}$ in the late delay period, effects that, when combined, suggest the possibility that these brain areas might anticipate upcoming visual cue presentation relevant for behavior, rather than encode a form of non-specific general arousal, motor preparation, or readiness. Similar to the

medPPC/pIPS, delay activity in these two ROIs for the "planning condition" with the non-preferred effector (P_{ET} trials) does not differ from activity on T-type trials, suggesting that despite the recruitment of infFEF and midIPS during P_{ET} trials, these areas do not "plan" hand movements. Instead, in addition to planning saccade eye movements, they may play a role in non-specific spatial attention or working memory processes that could subserve hand/arm movement planning in other brain areas.

Effector-neutral (non-specific) delay activity in Experiment 1

The RC analysis in Experiment 1 revealed that there are some parts of PMd, SMA, and the SPL with very weak effector-preferences (Fig. E1.1A), even though the nearby centers of these areas still show significant motor planning activity in Experiment 2 compared to control conditions (Fig. E1.1C). Thus, is it possible that the BOLD signal in these parts of PMd, SMA, and the SPL might reflect a more prominent role in other task-related processes (such as spatial attention and working memory), or these areas could subserve default planning of coordinated arm/eye movements. However, the current study always dissociated arm- and eye-movements, which explains why the effector-neutral parts of PMd, SMA, and SPL were less task-related (contribute less to the GLM) than other effector-specific regions in frontal and parietal cortices. A future study could investigate the possible role of these effector-neutral brain areas in the coordination of arm and eye movements.

Target contralaterality

In Experiment 1, contralateral target selectivity was assessed in all reach- and saccade-specific ROIs, and in control ROIs, by binning trials by visual hemisphere of target presentation.

ERAs from the arm- and eye-specific brain areas are plotted in Fig. E1.7 with separate curves for targets in the left visual field (LVF) and in the right visual field (RVF), revealing some contralaterality. Cue-responsive V1 is strongly contralateral during the cue period, while bilateral eye-specific areas infFEF and midIPS are significantly contralateral for visual field during the Cue period and show a degree of contralaterality during the delay period (Fig. E1.7B, Table E1.1). In arm-specific brain areas, while there is some contralaterality for

visual field (except in aIPS/PoCS), the strongest modulation of BOLD activity during the delay period is the modulation by effector (Fig. E1.7A), with significant arm-specificity (compared to saccades) for targets presented in either visual field.

Effector-specificity during long delays

Because saccade-specificity seems to evolve later than reach-specificity, perhaps due to swamping of the BOLD signal in saccade-related areas by visual cue responses, one repeat subject (S6) was scanned in the Experimental 1 paradigm with even longer delays (up to 18s in length). Raw BOLD timecourse ERAs for the main ROIs are plotted for trials of delay length 14s (Fig. E1.8). The plot demonstrates that reach-specificity is maintained in reach-specific areas throughout even 14s delays, and very strong saccade-specificity is evident in infFEF and midIPS 10-16s after delay onset, when there is a second peak of delay activity on saccade trials. Thus, even at very long delays, effector-specificity is maintained in the main motor planning ROIs, but does not emerge in control ROIs M1 or V1 until the response period.

Rostrocaudal division of premotor and supplementary motor cortices: Distinction between relative vs. absolute effector-specificity

While rostral portions of the PMd and SMA exhibit relative effector-specificity (Figs. E1.1 and E1.3, Figs. E2.2 and E1.6B), the caudal-most portions show evidence of absolute effector-specificity. The caudal-most portions of these frontal ROIs were identified in Experiment 2 with the conjunctive GLM contrast [P_{ET} > S_{ET}] AND [P_{ET} > N_{ET}], demonstrating *absolute* arm-specificity during motor planning for both real and imagined pointing movements, and strong specificity for real pointing compared to other effectors during the response period (Fig. E2.3A, Table E2.1). Absolute effector-specificity is defined here as a significant above-baseline BOLD response to one type of motor effector cue and not to another: in this case, the presence of significant point but not saccade activity during the delay period. ROI-based GLM results from Experiment 2 confirmed that the saccade delay predictor did not significantly contribute to the GLM in these caudal ROIs, in contrast to the same predictor's positive contribution in more rostral portions of these ROIs. The same is true of caudal PMd and SMA/Cing. identified in Experiment 1 by directly contrasting real

and imagined reach planning activity. Experiment 1 ERA curves confirmed absolute effector-specificity for arm vs. eye movement planning, as well as an increasing difference between real and imagined reach planning with longer delays (not shown).

Experiment 2 ERAs from caudal PMd, PMd/SMA, and SMA/Cing. also confirm a functional distinction between these caudal ROIs (Fig. E2.3A) and more rostral portions of the same ROIs (Fig. E2.1). In sum, the functional properties that differentiate them from the more rostral portions include 1) little to no visual cue-related response, 2) no ramping baseline activity, 3) little to no target cue/spatial attention/working memory activity, 4) some preference for real/imagined hand preparation, 5) strong preference for real and imagined hand planning, and 6) a shift to a much larger recruitment of these caudal areas during real hand movement execution compared to motor planning. Importantly, these properties were not observed in M1 (which did not differentiate between effectors or cueing paradigms during the delay period); hence, they are unlikely to be due to either confounding motor output or somatosensory or proprioceptive feedback related to anticipatory movements.

The relative positions of frontal ROIs demonstrating absolute (caudal, orange) and relative (rostral, pink) arm-specificity are shown in Fig. E2.3B. This pattern of relative arm-specificity in rostral portions of the ROIs and absolute arm-specificity in more caudal portions of these regions may correspond with the distinctions between monkey pre-SMA/SMA and monkey PMdr/PMdc (see Fujii et al. 2000, Boussaoud 2001, Fujii et al. 2002, Simon et al. 2002).

Metastudy analysis

To compare results of the current study with other studies in the literature, a meta-analysis of ROI locations was performed. First, the centers of several meta-ROIs were calculated across studies, by averaging reported Talairach and MNI coordinates (see *Methods*). Then, these meta-ROI locations were compared with the locations of ROIs from the current study (Fig. E1.10, also see Fig. E1.1). Linear Talairach distances between the meta-ROIs and ROIs from Experiment 1 were also computed (Table E1.2). The locations of the proposed human functional homologues of monkey LIP and PRR (midIPS and medPPC/pIPS) reported in the

current study correspond with meta-ROIs involved in some aspect of saccades or hand/arm movements, respectively (meta-ROIs: “LIP” and “PRR,” see Table E1.2 and *Methods: Meta-analysis*). In comparison with reported visual/directional topographic maps in the posterior parietal cortex (PPC), midIPS is located near IPS2 and IPS3 (though it may be closest to IPS3), and medPPC/pIPS is located medial to the reported center of IPS2 (Fig. E1.10, Table E1.2). Findings from the current study suggest that the center of IPS2, just lateral to medPPC/IPS in the SPL, may be equally activated by reach- and saccade-planning (Fig. E1.1A, also see Fig. E1.6B). Thus, topographic map IPS2 in human PPC may be recruited by both eye- and arm-movement planning.

Parietal ROI locations in the context of structural maps of the human PPC

Several recent investigations of the structural maps of the human PPC are also of interest in the interpretation of possible functional and anatomical homologies between human and monkey parietal brain areas (Scherperjans et al. 2008a and b). The location of the medPPC/pIPS (hPRR) ROI in the current study seems to span structural areas 7M and 7P on the medial wall, and extends into medial 7A, while aIPS/PoCS corresponds with area 7PC as defined by Scherperjans and colleagues. In contrast, midIPS (hLIP) seems to be located in area 7A and may extend into hIP3 (Scherperjans et al. 2008a and b).

CONCLUSIONS

The current study separately tracks effector-specificity for arm and eye movements during motor planning and movement execution. Advantages over prior studies of effector-specificity include 1) a focus on the delay period as the main analysis epoch, which is not confounded by differences in sensory input or motor output between effectors, 2) investigation effector-specificity during motor planning, when the full metrics of the upcoming movement are known, compared to roles in other processes engaged when the movement is partially-instructed or a cue instructs the subject to withhold a movement, 3) the use of arm reaching instead of the smaller finger/hand pointing employed in most previous studies, and 4) dual confirmation of effector-specificity from both model-based and model-independent analyses (GLM results and timecourse ERAs). It is also the first study to demonstrate a double-dissociation of reach- and saccade-specific brain areas during motor

planning, an important prediction from the monkey electrophysiological literature. Findings from this study also suggest a motor-related rather than a simple attentional or working memory role for both frontal areas in PMd and the SMA, and parietal areas in the SPL.

Experiment 1

The first experiment characterized relative arm vs. eye effector-specificity during goal-directed motor planning for real and imagined reaches and saccades. Despite strong overlap of delay-period activity for different effectors (Fig. E1.6B), both direct GLM contrast comparisons and plots of trial-averaged BOLD activity reveal dissociable arm vs. eye effector-specificity in frontal and parietal cortices. Arm-specificity was observed in the SMA/Cing., PMd/SMA, PMd, aIPS, and medPPC/pIPS, while eye-specificity was observed in the bilateral infFEF and midIPS. Effector-specificity evolves during the course of the delay period (Figs. E1.1 and E1.3, Figs. E1.7 and E1.8), though it may take on different temporal profiles in arm- and eye-specific brain areas. Pre-movement effector-specificity established during the delay period was usually maintained during the response period (Fig. E1.3A, Fig. E1.2).

Experiment 2

Effector-specificity observed during the traditional delayed response task, when both target and effector are instructed prior to the delay period, probably reflects a modulation of the BOLD signal related to motor planning. An investigation of the interaction between effector-specificity and processes related to motor planning revealed that, in the majority of effector-specific brain areas, the instruction of effector only modulates the BOLD response if the target of the movement is also known, i.e., when the movement can be planned. Effector preparation in the absence of spatial target information did not differentiate BOLD activity based on effector, except in the SMA/Cing. and towards the tail end of the delay in infFEF and midIPS. And rather than encoding motor plans for both preferred and non-preferred effectors, BOLD activity during the delay of “motor planning” trials with the non-preferred effector could be explained as domain-general activity related to the allocation of spatial attention or working memory. These findings support the notion that the “relative” effector specificity observed in Experiment 1 may actually be an “absolute” effector-specific

modulation riding on top of the BOLD signal related to other task-related processes, but not directly related to motor planning. These findings also support the idea that while frontal and parietal cortices do engage in domain-specific processes, they are also engaged in domain-general processes. The global encoding of spatial information may be relevant not just for the successful execution of the next probable action, but could be used to update motor plans in a dynamic environment, or to predict sensory and spatial relationships relevant for planning and executing the next subsequent action. Differential but parallel engagement of two related brain networks, one for arm movements and one for eye movements, may facilitate flexible behavior in a dynamic environment, the specification of sequences of movements, or the coordination of actions involving multiple effectors.

CHAPTER 2 – The best laid plans

ABSTRACT

An fMRI experiment employing a modified delayed response task was used to investigate the cognitive processes engaged during the delay period of traditional delayed response tasks. This experiment confirms that the regions of interest described in the previous chapter exhibit delay-period activity attributable to motor planning processes. The experiment included built-in controls for transient encoding of visual stimuli, cue context processing, spatial working memory, spatial attention, effector preparation in the absence of a motor goal, and default motor planning as sole drivers of BOLD activity. This study provides further evidence of a motor role for frontal and parietal cortices in involvement vision-for-action, not just vision-for-attention or the perception of space.

INTRODUCTION

A complex network of brain activity in human frontal and parietal cortices underlies goal-directed action planning. Within this network, supplementary motor, premotor, and posterior parietal cortices are often reported as active during the memory period of delayed response tasks, which temporally separate an instructional visual cue from a motor response via the introduction of an intervening memory delay period. Several prior studies in humans and monkeys interpreted these delay activations as evidence of involvement in motor planning, target and effector integration, and response preparation (Sweeney et al. 1996, Deiber et al. 1996, Hoshi & Tanji 2002, Hoshi & Tanji 2004, Hoshi & Tanji 2006, Cunnington et al. 2006, Schluppeck et al. 2006, Beurze et al. 2007). Other studies have suggested that activity in these brain areas can also be driven by voluntary shifts of spatial attention, spatial working memory, effector preparation in the absence of spatial information, and stimulus-response mapping, and may not necessarily reflect movement plans or intentions (Rowe et al. 2000, Simon et al. 2002, Kincade et al. 2005, Silver et al. 2005, Wilson et al. 2005, Curtis 2006, Curtis & D'Esposito 2006, Hahn et al. 2006, Beurze et al. 2007, Connolly et al. 2007).

The current study was designed to investigate the cognitive nature of the BOLD signal observed in human supplementary motor, premotor, and posterior parietal cortices during the memory period of the delayed response task, and to assess whether it reflects motor planning, or other related processes.

RESULTS

Motor planning and other processes in Experiment 2

Experiment 2 characterized the cognitive basis of the BOLD signal observed during the delay period of traditional DR tasks, by separately manipulating the presentation of target and effector information prior to the delay period.

Due to the large number of trial types (n=16), to maximize statistical power in the investigation of motor planning activity using GLM contrasts, the effectors Point, Imagined Point, and Saccade were collapsed into a "motor" effector group (PIS, designating an average-across-predictors for different motor effectors), for comparison with a "non-motor" effector (NoGo trials, N). Subnotation denotes the information presented on that type of trial *prior* to the delay period (ET=effector+target, E=effector only, T=target only, 0=no cues, see *Methods* section).

In this second experiment, balanced GLM contrasts between cueing conditions (see Fig. 1 and *Methods*) were used to isolate brain areas with significant activity in the motor planning condition (PIS_{ET}) compared to conditions that control for alternative possible explanations of delay activity, including: non-spatial motor preparation/readiness or planning a movement to a default/preferred target location [PIS_{ET}>PIS_{E}], spatial attention/working memory or planning a movement with a default/preferred effector [PIS_{ET}>T], and visual stimulation/bottom-up attentional capture/non-motor mnemonic cue/context activity and movement inhibition [PIS_{ET} > N_{ET}]. The conjunctive AND of these three contrasts controls for the possibility that any of the processes recruited by the control conditions are sole drivers of the delay activity observed in the PIS_{ET} condition, such that brain areas surviving the conjunction most likely participate in the formation of a motor plan or intention. The

statistical parametric map generated by the conjunction of these three contrasts is shown in Fig. E1.1C.

There is a remarkable degree of overlap between the activation map of motor planning areas from Experiment 2 (Fig. E1.1C) and the map of effector-specificity from Experiment 1 (Fig. E1.1B), suggesting that the effector-differences observed in Experiment 1 are most likely related to differential motor planning activity (also see Fig. E2.2).

ROIs significantly involved in motor planning are listed in Table E2.1, and included bilateral antInsula, IFG/PMv, infFEF, SMA/Cing., PMd/SMA, IPL, several ROIs in anterior IPS and SPL, midIPS, SPL, and left-hemisphere medPPC/pIPS. Because Experiment 2 only employed movements of the right and not the left hand, collapsing across arm and eye effectors in the analysis could have introduced a bias towards better resolving motor planning activity in the contralateral left hemisphere. In spite of this potential contralateral bias, for the most part motor planning ROIs were bilateral, though the extent of activation tended to be larger in the left hemisphere. MedPPC/pIPS and some anterior PPC ROIs were fully left-lateralized, possibly reflecting their strong involvement in arm- compared to eye-movement planning (Fig. E1.1, Fig. E1.3).

Delay activity in Experiment 2 across different conditions is better resolved in Fig. E2.1, which displays the ERAs calculated from the raw BOLD timecourses (epoch-based averaging from -4 to 0s relative to delay onset, across-subjects: n=6). The effective delay period in this task is from 2-6s relative to actual delay onset, since there is a lag in the onset of the impulse HRF (~2s). This latency was clear in M1 (not shown), which is not visually-responsive, as BOLD activity does not start to rise above the zero baseline until >2s after the Go period onset. Hence, activity in the ERAs up to 6s after delay onset can be considered to reflect activity during the Delay epoch of the task.

In spite of the relatively short (4s) delay period (compared to the temporal profile of the hemodynamic response function, HRF), activity in the motor planning condition (PIS_{ET}) diverges from activity related to other processes/conditions as early as 2-4s after delay onset

in most ROIs. However, this divergence appears slightly later in midIPS and infFEF, because of the strong relative effect of the N_{ET} condition, which probably reflects retrospective visual processing of the cue, non-spatial contextual mnemonic processes, the inhibition of a saccade to the previously flashed target, or the prospective inhibition of movement upon future presentation of the "Go" stimulus. In all ROIs except infFEF, N_{ET} activity quickly decays back to a zero baseline percent BOLD signal change (by 6s), and even in infFEF, N_{ET} activity begins to decay from 4s relative to delay onset. These properties indicate that retrospective visual cue/context processing or the inhibition of a response to a previously cued spatial target are the most viable explanations of N_{ET} activity in these brain areas, rather than forward context/rule memory or the preparation to inhibit a motor response upon presentation of a "Go" signal.

ERA plots in Fig. E2.1 confirm the significant involvement of these ROIs in motor planning compared to related processes. DlPFC, reported as arm-specific in Experiment 1 (not visible in Fig. E1.1B, but see Table E1.1 and Fig. E1.1A), did not survive the GLM conjunction contrast at q(FDR)<0.05, though the trend towards significant involvement in motor planning towards the end of the delay period is evident in the ERA plot (Fig. E2.1).

Despite their demonstrated involvement in motor planning, many frontoparietal ROIs still exhibited significant activity during other processes related to the task. SMA/Cing., PMd/SMA, PMd, and medPPC/pIPS also encode a spatial target that is relevant for future action ($T>0$ and $T>N_{ET}$) even when the action type is not yet known, suggesting a possible role in spatial attention or working memory (Fig. E2.1). These areas also show sustained activity when a motor effector is specified in the absence of spatial target information, suggesting a possible role in the maintenance of effector information relevant for future action, effector preparation, or default planning to a preferred spatial location. In infFEF and midIPS, while activity on T-type trials was significantly above baseline, it did not diverge substantially from activity on N_{ET}- or N_E-type trials except towards the end of the delay period; thus, the encoding of target or effector information in these two ROIs may be less related to future motor output than in the other nodes in the frontoparietal network, or these ROIs may be more swamped by activity related to visual cue or context-processing in the

early delay period (other effects in these two ROIs will be described later). The functional characteristics of aIPS/PoCS distinguish it from most other nodes in the frontoparietal motor planning network, since it exhibits only a mild effect of motor preparation (activity during PIS_E trials) and there is little evidence that it encodes a spatial target relevant for future action (T is only slightly greater than 0, also see Fig. E2.2, and there is no difference between T and N_{ET}).

Additionally, in SMA/Cing. and PMd (but not PMd/SMA) there is strong "ramping" activity during the delay period of baseline (0) trials even though the upcoming movement was completely unspecified during the delay (Fig. E2.1). This ramping baseline activity is not an artifact of the ERA calculation: in these ROIs, the 0 condition has a significant and positive GLM beta value. In baseline (0-type) trials, no visual cues preceded the Delay period, and both target and effector information were instructed instead during the 2nd Cue period. Thus, subjects could always expect two relevant visual cues after the Delay period (with 100% probability). Also, in the majority of baseline trials (75%), an immediate real or imagined motor response was required after the 2nd cue period, while in the remaining 25% of trials the 2nd cue subsequently instructed NoGo. In order to successfully complete a trial, subjects had to minimize reaction time, which could have contributed to an increase in arousal or the need for encoding of elapsed time and stimulus or behavioral expectation during baseline-type trials. However, in NoGo "planning" (N_{ET}) trials, the NoGo effector was instructed in the 1st Cue period, so subjects knew they would not have to make a movement during the response period and should also not expect additional cues during the 2nd Cue period. The fact that N_{ET} trial activity dipped below baseline trial activity at the end of the delay period in SMA/Cingulate and PMd supports a probable, but not a dominant, role for these two ROIs in processes relevant for immediate behavior such as general arousal or non-specific preparation, response/task timing, or behavioral cue anticipation (see Deecke & Kornhuber 1978, Macar et al. 2002, Cunnington et al. 2003, Coull et al. 2004, Hinton et al. 2004, Macar et al. 2004, Hoshi, Sawamura & Tanji 2005, Hoshi & Tanji 2006, Macar, Coull & Vidal 2006). Activity could also reflect the need to ***withhold*** an eye movement to an imminent, flashed visual target (to appear during the 2nd Cue period); but then N_{ET} should be greater than N_E activity at the beginning of the delay period, which is not the case. Instead, $N_E > N_{ET}$

at the end of the delay (Fig. E2.1), again suggesting that these two areas may also play a role in the anticipation of salient visual stimulus (such as a visually-flashed target, even if no behavior is required, e.g., in the NoGo condition).

Rostrocaudal division of premotor and supplementary motor cortices: Domain-specific (motor planning) vs. domain-general (motor planning and associated processes) distinction

A large swath of frontal activity along the PrCS extending onto the medial frontal wall and related to motor planning was divided into three separate ROIs based on peaks in GLM-map activity in Experiment 2. These three ROIs were previously identified as arm-specific in the previous chapter, with a significant relative specificity for planning arm vs. eye movements (Figs. E1.1 and E1.3, Table E1.1). The ROI labeled PMd, located in premotor cortex along the PrCS, probably corresponds with monkey PMd (Fujii et al. 2000, Hoshi & Tanji 2000, Pesaran et al. 2006). Like monkey PMd, this ROI is involved in motor planning but also showed strong activity during effector preparation in the absence of a spatial goal, as well as a response to behaviorally-relevant visual cues (Fig. E2.1). Another premotor ROI (PMd/SMA) localized to the most medial aspect of the PrCS and was sometimes medial to the junction with the superior frontal sulcus (SFS). This ROI was functionally very similar to PMd. A third frontal ROI, termed SMA/Cing., localized to the frontomedial wall, above and including the cingulate sulcus mainly posterior to the anterior commissure. It probably corresponds with monkey areas pre-SMA, the rostral portion of the SMA, and CMAr (Hoshi & Tanji 2004; Hoshi, Sawamura & Tanji 2005).

CONCLUSIONS

Experiment 2

The second experiment investigated the cognitive nature of the BOLD signal during the delay period in traditional memory-delayed response tasks (DR tasks) by employing a modified version of the DR task. Motor planning, compared to control conditions, most strongly activated supplementary and premotor cortex, and superior posterior parietal cortex (PPC) along the IPS. Most ROIs that exhibited motor-planning activity were also active during the maintenance of a spatial target in the absence of effector information, or during

the maintenance of a motor effector instruction in the absence of information about the target (Fig. E2.1, T-type and E-type trials, respectively). However, effector-only and target-only BOLD activity was significantly smaller in amplitude than activity for the motor planning condition that cued both pieces of information prior to the delay period, indicating that delay activity in these ROIs cannot solely be explained by maintenance of target or effector information alone, or by related attentional, non-specific preparatory, or default-planning processes.

In addition, the fact that many ROIs in premotor and parietal cortex survive the contrast $PIS_{ET} > N_{ET}$ is evidence that these regions do not just reflect retrospective sensory information or encode a memory of the effector cue, since even in N_{ET} trials subjects need to remember to withhold movement during the "Go" period. Instead, BOLD activity reflects the motor demands of the trial, and these ROIs remain active only if the effector cue instructs an upcoming real or imagined movement. Because of its unique design and built-in controls, this experiment could confidently attribute a significant proportion of delay activity in these ROIs to the formation of a motor plan, ruling out alternate explanations such as transient visual sensory encoding or context-processing, spatial working memory or voluntary attentional shift, effector preparation, and default or implicit motor planning. These findings support a role for frontal and parietal cortices in the formation of a motor plan and, combined with the evidence of effector-specificity from Experiments 1 and 2, further support the proposition that these brain areas subserve motor-related processes, not just attention- or memory-related processes (see *Introduction*).

DISCUSSION OF CHAPTERS 1 & 2

Arm-specificity, and hSMA, hPMd, and hPRR

Several reach-specific ROIs were characterized in frontal cortex, including SMA/Cing., PMd/SMA, and PMd. These brain areas were reach-specific during both motor planning and motor execution. Left SMA/Cing. was arm-specific during motor planning, like monkey SMA/pre-SMA (Fujii et al. 2002). PMd likely corresponds with monkey PMdc (Fujii et al. 2000), while PMd/SMA may include PMdc extending into PMdr (Hoshi & Tanji 2000, Pesaran et al. 2006). In addition to their role in preferentially planning arm vs. eye movements, SMA/Cing., PMd/SMA, and PMd also encode both target and effector information in isolation, but only when they are relevant for a future action (Fig. E2.1, Fig. E2.2).

In the posterior parietal cortex, two ROIs exhibited significant specificity for reach- compared to saccade-planning (medPPC/pIPS and aIPS/PoCS). AIPS/PoCS was located in the anterior SPL. A functional correspondence with Area 5 is supported both by the region exhibiting weak responses to visual cues, greater activity during motor execution than during motor planning, and greater recruitment by real than by imagined reaching (Fig. E1.3). As summarized by Pellijeff and colleagues (2006), monkey areas 5 and 7b "have few visual inputs, are strongly interconnected with somatosensory and motor cortices, [and] are dominated by somatic and motor responses." Also, aIPS/PoCS does not strongly encode either target or effector information in isolation, and the most robust modulation of delay BOLD activity is due to arm/hand movement planning (Fig. E2.1, Fig. E2.2).

This study also offers converging functional and anatomical evidence that medPPC/pIPS is the likely human functional homologue of monkey PRR. Like monkey PRR, it is located in the SPL medial to the posterior segment of the IPS and extending onto the medial parietal wall. This ROI also responded transiently to behaviorally-relevant visual cues, as does monkey PRR (Snyder et al. 1997, Gail 2006). However, if no future motor output was specified (e.g., in NoGo trials, Fig. E2.1), this visual response quickly decayed back to zero.

MedPPC/pIPS was significantly more active during the planning of an upcoming movement when both target and effector were specified, but was still active if either only the target or effector was known. These same properties have been reported for neurons in monkey PRR (Calton et al. 2002). Experiment 2 showed that the motor preparatory activity observed in medPPC/pIPS appears to be effector-neutral, not differentiating between arm and eye, while motor planning delay activity demonstrated significant (but not absolute) specificity for reaching (and other hand movements) compared to saccades, a property characteristic of the neuronal population in monkey PRR (Figs. E1.3 and E1.4, see Snyder et al. 1997, Snyder et al. 2000). Additionally, saccade planning activity is not significantly different from target-related or motor preparatory activity (Fig. E2.2). Hence, recruitment of this ROI during the delay period on trials when the metrics of a saccade are known may reflect a role in effector-neutral processes or task components such as spatial attention, working memory, or general action readiness. This area only engages in motor planning for arm/hand movements, and not for saccade eye movements.

Several recent human studies additionally support the proposed designation of medPPC/pIPS as functionally homologous to monkey PRR. Prior fMRI studies of hand/finger pointing compared to saccades suggested that there is an area in the medial PPC that preferentially encodes arm vs. eye movements (Astafiev et al. 2003, Connolly et al. 2003), though there is still some debate as to the degree of effector-specificity (e.g., Simon et al. 2002, Levy et al. 2007), and this debate will be discussed later. In other related studies, Fernandez-Ruiz and colleagues (2007) found that medial PPC represents the direction of reaches in retinotopic rather than motor coordinates, just like monkey PRR (Batista et al. 1999). Postural information about the upper limbs may also be present in human medial PPC (Pellijeff et al. 2006, and unpublished results), and some neurons in monkey PRR encode in limb posture as a gain modulation of spatially-tuned spiking activity (Torres & Andersen 2006). This postural information may be useful for sensorimotor transformations and the formation of a motor plan. There is also good correspondence between medPPC/pIPS and the locus of lesions causing deficits in visually-guided reaching in humans (Karnath & Perenin, 2005), but not saccades (Trillenberg et al. 2007).

Compared to recently identified spatial topographic maps in the PPC, medPPC/pIPS localizes medially to the center of one map termed IPS2 (Fig. E1.10, see Table E1.2 for references). The area medial to IPS2 has also been found to respond to tactile stimulation of the fingers (Swisher at al 2007). Levy and colleagues (2007) report a small bias for reaching in IPS2, but the relatively small preference for reaching may reflect confounds in their experimental design and analysis methods, including the fact that they did not independently assess and compare maps of visual topography and effector-specificity.

Saccade-specificity, and hFEF and hLIP

The area of human frontal cortex usually termed "FEF" in the fMRI literature is located at the junction of the PrCS and SFS. This area contains a topographic map of visual space, and is active during memory-delay and visually-guided saccade tasks (Hagler et al. 2007, Koyama et al. 2004, Kastner et al. 2007). However, there is some debate regarding effector-specificity in this region in the human brain, which will be further discussed later. Importantly, results of the current study confirm that the PrCS/SFS junction ("FEF") is not selective for saccades compared to reaching, as might be expected if it were the human functional homologue of monkey FEF. Instead, it is recruited by multiple effectors but is significantly specific for reaches compared to saccades during both motor planning and execution, with the caudal-most portions of "FEF" even showing evidence of absolute hand- vs. eye-specificity.

In contrast, an ROI located more laterally in the PrCS, designated infFEF in the current study, had strong visual cue responses, contralateral target selectivity, specificity for saccade execution, and significant specificity for saccade planning at the end of the delay period (Figs. E1.1 and E1.3, Figs. E1.7 and E1.8). These findings are in keeping with the results of Amiez and colleagues (2006), who report saccade-related activity in the ventral PrCS, and colocalization of hand- and saccade-related activity at the junction of the SFS and PrCS.

Human fMRI studies have also reported topographic maps of visual space, as well as saccade-related activity, in more lateral PrCS extending into the junction with the inferior frontal sulcus (IFS), near infFEF (Luna et al. 1998, Berman et al. 1999, Brown et al. 2006,

Hagler & Sereno 2006, Connolly et al. 2007, Kastner et al. 2007, Levy et al. 2007). The human functional homologue of monkey FEF may thus include two oculomotor subregions, one near the junction of the fundus of superior PrCS and the SFS ("deep" FEF), and one in lateral PrCS extending onto the precentral gyrus ("lateral" or "inferior" FEF) (for examples, see Grosbas et al. 2001, Lobel et al. 2001, Lachaux et al. 2006).

The ROI termed midIPS in the current study is proposed to functionally correspond with monkey LIP. Recent probabilistic tractography work demonstrated that human medial IPS has the strongest probability of connection with the superior colliculus, and that the projection pattern strongly resembles that of LIP to the superior colliculus in monkeys (Rushworth et al. 2006). This may explain why "LIP," as localized by tasks involving saccades, is reported to be medial to the IPS in humans whereas LIP is on the lateral bank of the IPS in monkeys. The current study provides convergent evidence of inter-species functional homology, including strong visual cue responses, and specificity for saccade planning and execution (Figs. E1.1 and E1.3). Additionally, contralateral cue selectivity was observed for all visual targets, independent of effector, suggesting visual-like properties of this ROI. Neurons in monkey LIP have access to information about the whole visual field and may play a role in spatial updating (Heiser & Colby 2006), a finding that is supported by human fMRI studies demonstrating contralateral field selectivity, topographic mapping of visual space, saccade-related activity, and spatial updating across saccades in the vicinity of midIPS (see Fig. E1.10 and Table E1.2 for references).

An event-related fMRI study of antisaccades (Medendorp et al. 2005b) showed that BOLD activity in a parietal region termed retIPS (located near midIPS) did not reflect the retrospective visual cue, but instead the actual (anti-cued) saccade target location. However, the delay-period activity observed by Medendorp and colleagues (2005b) could be interpreted as either a voluntary attentional shift, the maintenance of target information (Medendorp et al. 2006), or as a prediction of the sensory consequences of the upcoming saccade, since it would lead to foveation of the visual field containing the anti-cue location.

Because of the strong modulation by visual input during the cue period and saccade execution, the argument could be made that this area may be less related to the motor aspects and metrics of saccade planning and execution and more to the representation of visual space relevant for multiple forms of action. Indeed, the execution-epoch difference between saccades and small hand movements (e.g., the index finger moving a trackball) essentially disappears if the targets reappear upon presentation of the "Go" stimulus such that both saccades and trackball movements are "visually-guided" instead of "memory-guided" and the subject is provided visual feedback of the movement of the trackball in the form of a cursor moving on the screen (unpublished results). However, in the current study, midIPS was significantly more engaged when the subject was planning a saccade during the delay period compared to an arm/hand movement or NoGo delay activity (Fig. E1.1, E1.3, E2.1, Fig. E2.2), and this modulation of delay activity cannot be explained by differences in visual input, but could perhaps still be explained by an internal model of the predicted sensory consequences of an upcoming, planned gaze shift. Still, the presence of delay-period activity in midIPS modulated by effector type suggests a probable motor, and not just sensory/attentional, role for this ROI.

The current study confirms several findings from these previous studies of proposed human "LIP" and further extends them by demonstrating significant saccade planning specificity, an effect that cannot be explained by differences in visual stimulation or gaze updating and an important prediction from the monkey electrophysiological literature. Moreover, the manipulation of information available to the subject prior to the delay period in Experiment 2 allowed for further investigation of functional properties of saccade-specific infFEF and midIPS. Findings from Experiment 2 suggest that these brain areas may encode a spatial target regardless of its direct relevance for future action, and also encode a non-spatial saccadic preparatory set at the end of the delay period (Fig. E2.1 and Fig. E2.2). Similar to the results observed in medPPC/pIPS, delay activity in these two ROIs for the "motor planning condition" with the non-preferred effector (arm) does not differ from activity on T-type trials, suggesting that despite their recruitment during arm movement "planning" trials, these areas do not actually "plan" hand movements. Instead, infFEF and midIPS may contribute to effector-neutral spatial attention or working memory processes that could

subserve hand/arm movement planning in other brain areas, in addition to their demonstrated role in planning saccadic eye movements.

The debate on effector-specificity in frontal and parietal cortices

There is some debate in the literature regarding the degree of effector-specificity in human frontal and parietal cortices. Previous human fMRI studies have reported specificity for arm-movements in PMd or putative human PRR (Astafiev et al. 2003, Connolly et al. 2003, Medendorp et al. 2005, Connolly et al. 2007), while other studies have reported strong overlap of arm- and eye-related activity (Medendorp et al. 2003, Simon et al. 2002) and limited effector-specificity in posterior parietal cortex (Levy et al. 2007, Hagler et al. 2007). There are several reasons why the current study was able to resolve dissociable reach- and saccade-specificity where previous studies reported limited effector-specificity, including: 1) a focus on the delay period as the main analysis epoch, which is not confounded by differences in sensory input or motor output between effectors, and the use of longer delays; 2) investigation of the role of the frontal and parietal cortices in motor planning when the full metrics of the upcoming movement are known, compared to roles in other processes engaged when the movement is partially-instructed or a cue instructs withholding a movement; 3) the use of arm reaching instead of finger/hand pointing employed in most previous studies; and 4) confirmation of effector-specificity from both model-based and model-independent analyses (GLM results and timecourse ERAs).

Amongst previous studies of effector-specificity, those reporting the most limited effector-specificity in parietal cortex did not resolve different task epochs (Medendorp et al. 2005, Simon et al. 2002, Levy et al. 2007); hence, their experimental designs were confounded by differences in visual stimulation, motor output, and sensory feedback between effectors. Also, a whole-trial assessment of effector-specificity does not address the issue of effector-specific signals during pre-movement motor planning, an important prediction from previous monkey electrophysiology studies (Snyder et al. 1997, Snyder et al. 2002, Lawrence & Snyder 2006). The current study was able to successfully resolve cognitive differences between arm and eye effectors because it concentrated on effector comparisons during the

delay period, when there were no differences between sensory input/feedback and motor output between effectors.

As an investigation of effector-specificity, the study by Levy and colleagues was further confounded by the fact that visual stimulation was different on saccade and reach trials. Another confound of the study is that they defined their ROIs based on visual topographic map borders, and activity during a block-design saccade experiment, and then assessed arm- vs. eye- effector-specificity within these maps, instead of independently assessing and comparing maps of visual topography and effector-specificity (Levy et al. 2007). Levy and colleagues admit that "the maps we obtained in this way were thus a conservative estimate of the extent of these topographically mapped areas." This could explain the small bias for reaching compared to saccades. Also, while Levy and colleagues did place some emphasis on the pre-movement period, they only cued which effector to use (arm or eye) and not the target of the movement. Hence, subjects were not able to construct a motor plan during the pre-movement effector-cue task epoch. The presence of both target and effector information may be a requirement for resolving effector differences in some brain areas (Connolly et al. 2003, Fig. E2.2).

The results of the current study suggest that human PRR (medPPC/pIPS) is actually located medial to topographic map IPS2 identified by Levy and colleagues and others (see metastudy analysis in *Supplementary Materials*), and that the center of IPS2 may instead be activated fairly equally by reach-, imagined reach-, and saccade-planning (see Fig. E1.1A and Fig. E1.6B). Thus, the relatively small preference for reaching observed by Levy and colleagues in IPS2 located in the medial PPC may reflect confounds in their experimental design and analysis methods (Levy et al. 2007).

Two previous studies compared smaller hand/finger pointing with saccades during a pre-movement delay and found some evidence of arm-specific brain areas in frontal and parietal cortices. However, real or imagined hand/finger movements activate the fronto-parietal network to a smaller degree than real or imagined reaching (unpublished results), meaning that these prior studies might not reveal the true extent of effector-specificity for arm vs. eye

movements. Astafiev and colleagues employed a delayed response task, but the metrics of the movement were not fully specified during the delay. Instead, the effector was cued prior to the delay, as was some spatially-relevant information (but not the actual target location). They reported one ROI with specificity for pointing vs. saccades in medial PPC as well as peak point-preparatory activity near the center of pIPS defined in the current study, and a point-specific ROI near the junction of the PrCS and SFS, close to the ROI we designate as PMd (Astafiev et al. 2003). However, because the metrics of the movement were not fully specified during the delay period, and arm- and eye-movement trials were not interleaved, the results of the study probably do not reflect the true extent of effector-specificity in human cortex and these experimental design issues may explain why they did not report any saccade-specific ROIs.

The second study by Connolly and colleagues again employed a delayed response task, this time with a long delay (9s), and looked only at effector-specificity in the medial PPC. They found significant point vs. saccade specificity assessed by a post-hoc direct comparison of peak delay-period activity in medial PPC only if both the target and effector were presented prior to the delay (motor planning), in contrast with trials where only the effector was cued (effector preparation) (Connolly et al. 2003). However, a fixed hand posture (hand/index finger pointed at the central fixation spot) was maintained throughout both hand and eye trials, and hand posture seems to be strongly encoded in both monkey and human PRR (Torres et al. 2006, and unpublished results), which parietal ROI instead of resolving effector-specificity in the whole brain.

Interestingly, none of the previous studies of effector-specificity reported significant saccade-specificity during a pre-movement period, or compelling evidence of functional correspondents of monkey LIP and FEF. Medendorp et al. 2005 did report contralateral visual-field preference and saccade-specificity in retIPS, located near midIPS, in a comparison of pointing and saccade activity in a block-design task. However, differences between saccade and point could be adequately explained by differences in visual stimulation/gaze updating during the response period of the task. While looking directly at delay-period activity, other event-related studies of this ROI by the same research group did

not directly test for arm vs. eye specificity (Medendorp et al. 2005b, Medendorp et al. 2006, Beurze et al. 2007).

The current study replicates the result of contralateral visual field preference and saccade-specificity during the response period in midIPS (located near retIPS as identified by Medendorp and colleagues), but also resolves the evolution of saccade-specificity during the late delay period, and demonstrates that activity in midIPS cannot be explained solely by the maintenance of target information or by voluntary attentional shift. Given its demonstrated preferential role in saccade planning compared to arm-movement planning, and the summation of other functional properties of the ROI, the current study strongly intimates functional correspondence between midIPS and monkey LIP.

In frontal cortex, Medendorp et al. 2005 and Levy et al. 2007 report that the area commonly termed "FEF" in the human fMRI literature, while exhibiting contralateral visual preference, "showed little or no effector selectivity." Connolly et al. 2007 claim that for a memory delay task with short delay periods (<4s), pre-movement activity is higher for pointing than for saccades in "FEF" with this pattern extending into PMd, though this same pattern was observed in M1 and hand movements were not recorded in the scanner; thus, one possible interpretation for this higher arm vs. eye activity is that subjects were tensing or moving their hands prior to the cued response period. However, results from the current study confirm that this area near the PrCS/SFS junction, while it may exhibit contralateral target topography, is not selective for saccades compared to reaching. Instead, it exhibits the reverse preference of significant reach-specificity during both motor planning and motor execution. An ROI located more laterally in the PrCS, designated infFEF in the current paper, is strongly modulated by visual cues and shows specificity for saccade planning and execution. Levy and colleagues (2007) also reported saccade activations near infFEF, and their findings probably reflect the strong saccade-execution related activity in this ROI. Due to its functional properties, saccade-related infFEF may better correspond with monkey FEF than the human frontal brain area located near the PrCS/SFS junction that is typically termed "FEF" in the literature.

SUMMARY

This study extends prior fMRI studies of effector-specificity by focusing on a pre-movement delay period not confounded by differences in sensory input or motor output between effectors, demonstrating dissociable arm- vs. eye- specificity, characterizing the evolution of these effector-specific signals over the course of the pre-movement delay and response periods, and employing real and imagined arm reaching instead of smaller hand/finger movements. It also attempts to expound and resolve the debate regarding effector-specificity in human cortex and reconcile previous conflicting studies in the literature.

The findings of the current study provide compelling evidence of dissociable significant relative arm and eye effector-specificity throughout the brain network engaged in the planning of goal-directed action, manifested as a modulation of the BOLD signal by different effectors. This effect emerges during a delay period when the subject is planning a movement, prior to movement initiation. The cognitive difference between reach and saccade during the delay period cannot be explained by sensory stimulation, motor output, or the monitoring of an ongoing movement and its sensory and motor consequences. Attentional, memory, and default-planning processes were also ruled out as drivers of this effector modulation (see next Chapter). Instead, these cognitive differences reflect differential engagement of nodes in the network in arm or eye movement planning, supporting a role for these brain areas in motor-related and not just attentional or working memory-related processes. The detailed investigation of the functional properties of these effector-specific brain areas allowed for the proposition of likely human functional homologues of monkey PMd, FEF, PRR, and LIP, with important implications for neural prosthetics, which will be discussed in Part II of this thesis.

METHODS FOR CHAPTERS 1 & 2

Subjects

Seven subjects (6 right-handed, 1 left-handed, 3 males, 4 females, aged 23-33, mean 30 years) participated in the main task in Experiment 1. An additional four subjects participated in a modified version of the main task, excluding the imagined arm condition (4 right-handed, 4 males, aged 19-47, mean 31 years). Two subjects (DR, HG) in Experiment 1 are authors on this paper. Six different subjects (all right-handed, 4 males, 2 females, aged 25-39, mean 31 years) participated in Experiment 2. Handedness was assessed via the Oldfield Handedness Inventory (Oldfield 1971). All subjects in both experiments gave informed consent in accordance with the Caltech Institutional Review Board guidelines.

Functional and Anatomical Imaging

Functional magnetic resonance imaging (fMRI) was performed in the Siemens 3-Tesla TRIO scanner at Caltech's Brain Imaging Center. The blood-oxygen-level-dependent (BOLD) signal was measured using T2*-weighted echo-planar images (TR=2000ms, TE=30ms, flip angle=90°) acquired with an 8-channel phased-array head coil. The scan volume covered parietal and premotor cortices, and most of prefrontal and occipital cortices, in 30 axial slices (slice thickness=3mm, gap=0mm, in-plane voxel size=3x3mm, FOV=192x192, resolution=64x64). Since the scan volume did not provide full coverage of subcortical areas and the cerebellum in all subjects, the Results and Discussion sections will focus on cortex. In Experiment 1, subjects completed 12-16 runs, each 346s in duration with 16 trials per run, in two or three separate scan sessions. In Experiment 2, subjects completed 20 runs, each 196s in duration with 8 trials per run, in two separate scan sessions.

Anatomical images were acquired using a T1-weighted MP-RAGE sequence with the same head coil used for functional image collection. The whole brain volume was scanned in 176 slices (slice thickness=1mm, gap=0mm, in-plane voxel size=1x1mm, TR=1500ms, TE=3.05ms, FOV=256x256, resolution = 256x256).

Experimental Setup and Behavior

Subjects lay supine on the scanner bed and viewed the task backprojected onto a screen viewed through a mirror attached to the headcoil, subtending 21.6° visual angle. Stimuli appeared frontoparallel to the subject, in the natural plane of motion, and subjects made arm or eye movements towards the virtual target location. No mirror transformation of the target was required. For Experiment 1, when real or imagined (internal simulation) arm movements were instructed, right armed reaching was employed. Reaching movements involved extension of the right arm from the elbow combined with right hand pointing towards the remembered visual target location. Because of the constraints of the scanner bore, resting arm posture, and the nature of reaching movements in the ipsi- vs. contra-arm field, leftwards reaching movements involved mainly elbow extension and hand pointing with little to no elbow/forearm rotation, while rightwards reaching movements additionally involved elbow/forearm rotation to approach the target, though the path traversed by the endpoint of the arm (the hand) was similar for both movements. This outward movement was followed by a return to resting arm posture, with the right arm lying parallel to the right side of the body and the elbow bent such that the right hand rested comfortably on the subject's chest. Subjects were instructed to keep their right upper arm and shoulder fixed during reaching, to minimize head movement and any effects of mass displacement on BOLD activity observed during these movements. Experiment 2 utilized pointing instead of reaching. Real and imagined right handed pointing movements involved extending and rotating the wrist from its resting position on the chest combined with extension of the right index finger to point at a remembered target location, followed by a return to resting position.

Eye movements (ASL infrared eyetracker, Bedford, MA) and arm/hand movements (Measurand ShapeTape, Fredericton, NB) were monitored inside the scanner during at least one scan session for each subject in Experiment 1. Central visual fixation was required at all times unless a subject was making a cued eye movement, while resting arm posture was required at all times unless a subject was making a cued real arm movement. Eye data from four subjects were discarded because the infrared eye signal in these subjects was too noisy for stable recording of eye position. In the remaining two subjects, eye behavior was analyzed offline in Matlab. In the experimental task, subjects were required to dissociate arm

and eye movements, making arm movements with the eyes fixed, or eye movements with the arm fixed. One subject made a single coordinated reach-saccade on the first trial of the first scan run (a reach-type trial), but later behavior was accurate, with all subject making accurate instructed saccades during the response period and making no saccades during other trial epochs or trial types.

In experimental sessions during which arm/hand position was recorded, ShapeTape was fixed to allow for natural reaching movements. The flexible tape ran longitudinally along the left side of the subject, wrapped around under the neck, and attached to the right upper arm using Velcro, while the end of the tape was attached to a golf glove worn on the right hand. Offline, ShapeTape recordings of arm position were exported from the accompanying recording/playback program, ShapeWare II, as Cartesian coordinates. Then, the 3D Cartesian end point of the ShapeTape was plotted over time in Matlab, for each scan run, indexed by behavioral markers. All six subjects exhibited accurate arm behavior, making reaching movements towards the correct target during the response period of every reach trial, and making no arm movements during other trial epochs or other trial types (e.g., imagined reach).

Experimental Tasks

Prerequisites for planning and executing a motor response include knowing both where to move (the target, or goal) and how to get there (the type of movement, or effector). Traditional effectors include the eyes and the arm (i.e., saccade and point/reach), but in this study, the operational definition of effector also includes imagined arm movement and the NoGo condition, in which subjects were instructed to withhold movement to a cued target location.

In a typical delayed response (DR) task, both target and effector are cued prior to the delay period on a given trial. Because the response is fully-instructed, subjects are asked to plan the upcoming movement during the delay period. The main experiment in this study investigated effector-specific signals (i.e., arm vs. eye) during motor planning by utilizing a typical DR task and modulating effector type.

To further characterize the cognitive basis of the BOLD signal observed during the memory period of the typical DR task, a second control experiment independently cued target and effector information such that the motor response was either partially- or fully-instructed prior to the delay period on a given trial.

In both experiments, eye fixation and resting arm posture were required at all times unless a subject was making an instructed real eye or arm movement during the response period; hence, there were no confounds of motor activity during the delay period. Visual stimulation was identical across all trials during the delay period (only the central fixation spot was "on"), and the inclusion of NoGo trials controlled for the effects of residual transient visual activity from the preceding cue period. By eliminating these potential confounds, brain activity observed during the delay epoch represented cognitive processes related to task demands, including those involved in motor planning.

Experiment 1

The main experiment was designed to investigate effector-specificity during motor planning. Effector-specificity was defined as a relative preference for one effector over another (e.g., arm>eye) during the pre-movement delay period.

Four types of effectors (Real Reach, Imagined Reach, Saccade, or NoGo) and four delay lengths (2, 4, 6, or 8s) yielded 16 total trial types which were pseudo-randomized and balanced for trial order in an event-related design. Each trial began with an initial fixation period (3.5s), followed by a visual cue that flashed for 500ms at a horizontal eccentricity randomized between 6.2° and 7.3° (mean 6.75°) to the left or right of the fixation point (Fig. 1A). This visual cue indicated the target location, while its color further instructed which effector was to be used to acquire the target. Thus, target and effector information was presented simultaneously at the same peripheral spatial location. A red cue indicated an upcoming real right arm reach to the remembered target location, a purple cue indicated an upcoming imagined right arm reach, a blue cue indicated an upcoming saccadic eye movement, and a yellow cue indicated no upcoming movement (NoGo). Following a

memory delay of 2, 4, 6, or 8s, variable and unpredictable to ensure that subjects planned the cued motor response as soon as the delay period began, the white central fixation circle became a hollow white circle, which indicated the "Go" signal. The response period lasted 2s, and subjects were required to perform the cued motor response to the remembered visual target location and to return to resting eye or arm position upon extinction of the "Go" stimulus. A fixation cross indicated the end of the response period and remained on during the intertrial interval (12s). Onsets of the initial fixation, memory delay, and response periods were synchronized with the TR (TR=2s) of the functional data acquisition.

Experiment 2

The second experiment in this study separately manipulated the presentation of target and effector information prior to the delay period in order to isolate brain activity attributable to movement planning, controlling for other associated processes. Trials were pseudo-randomized and balanced for trial order in an event-related design. In contrast to the reaching movements employed in Experiment 1, Experiment 2 utilized real and imagined pointing movements (see *Methods: Experimental Setup and Behavior*). Differences between Experiments 1 and 2 are further discussed in the *Methods*.

Each trial consisted of an Initial Fixation period (1.5s), a 1st Cue period (500ms), a Delay period (4s), a 2nd Cue period (500ms), and a Go (response) period (1.5s). Trials were separated by a fixed intertrial interval of 10s (Fig. 1B). Initial Fixation, Delay and Go epochs were synchronized with the TR (TR=2s) of fMRI data acquisition.

The design included four cueing paradigms (four rows of Fig. 1B), in which the information instructed during the 1st Cue period was varied (effector+target, effector only, target only, no cues), thus engaging different cognitive processes during the Delay period. Any information not presented during the 1st Cue period was always instructed in the 2nd Cue period, so that on each trial the response was fully-instructed prior to the Go epoch.

Spatial targets were presented either to the left or to the right of the central fixation spot at 8° horizontal eccentricity, and were always green. The only stimulus on the screen during the

Delay period was the white central fixation spot, and a change in this central fixation spot from solid to hollow indicated the “Go” signal.

In addition to the inclusion of four different cueing paradigms, described below, Experiment 1 also modulated effector type, with four different effector cues (right hand point, P; imagined right hand point, I; saccade, S; NoGo, N). Effector information was conveyed centrally at the fixation spot as a change in color of the fixation stimulus in either the 1st or the 2nd cue period, depending on the cueing paradigm. A red cue indicated a right hand point, a purple cue indicated an imagined right hand point, a blue cue indicated a saccade, and a yellow cue indicated a NoGo trial. On NoGo trials, a NoGo effector cue was presented in either the 1st or 2nd cue period, and subjects were instructed to rest quietly and neither plan nor execute a movement.

In the main cueing paradigm, both target and effector were instructed in the 1st Cue period, and no additional cues were presented in the 2nd Cue period. This cueing paradigm was called ET, since both effector (E: P, I, S, or N) and target (T) were specified in the 1st Cue period, prior to the Delay period. Subjects could begin planning the upcoming movement during the Delay period, since it was fully-specified. Thus, delay-period activity in these ET-trials was thought to represent motor planning.

A second cueing paradigm instructed only effector information (E-type trials, effector only: P, I, S, or N) prior to the Delay period, to engage processes related to context processing, motor effector preparation, and response readiness in the absence of a movement goal. In the 2nd Cue period, the target was instructed so that the movement was fully-specified prior to the response period. Delay-period activity in trials of this type was thought to represent non-spatial effector preparation. Alternatively, it is possible that during the Delay period of trials of this type, subjects began preparing a movement to a preferred or predicted target location, or planned both leftward and rightward movements of the instructed effector. Thus, comparing ET-type trials vs. E-type trials at the analysis stage would control not only for non-spatial effector preparation as the main driver of delay-period activity, but also for the formation of an implicit/default motor plan as described above.

The third cueing paradigm instructed only the spatial target (T-type trials, target only) prior to the Delay period. In 75% of trials of this type, the 2nd Cue period subsequently instructed an immediate movement (real or imagined point or saccade) to the previously cued target location, while the remaining 25% of trials instructed the subject to withhold a response. Subjects needed to encode and remember the target location during the Delay period, for integration with upcoming effector information in the 2nd Cue period. Maintaining the location of the target across the memory delay period for an upcoming, as yet unspecified movement should engage processes related to memory encoding, maintenance and retrieval, working memory, and voluntary spatial attention. The inclusion of T-type trials, contrasted against trials where the movement is fully-specified prior to the delay period (ET-type), controls for these processes as a sole explanation of observed delay activity.

A brain area may also encode a "default" covert or implicit motor plan to a flashed visual target, which may reflect the underlying effector-preference of that brain area. For example, in the monkey PRR, some neurons are nearly as active in a memory saccade DR task as they are in a memory reach DR task. However, rather than reflecting a saccade plan during the saccade task, a further dissociation task revealed that these neurons were representing potential reach plans (Snyder et al. 1997). Thus, a reach-specific brain area might encode a potential reach plan to any visual target, regardless of effector instruction, while a saccade-specific brain area might encode a potential saccade plan. If present, these types of implicit, "default" motor plans would become active during the Delay period of T-type trials. The inclusion of this cueing paradigm in Experiment 2, and directly contrasting ET-type trials vs. T-type trials at the analysis stage, controlled for default motor planning as a complete explanation of observed delay activity.

A final cueing paradigm, where neither goal nor effector information were presented prior to the Delay period (baseline, 0-type trials, no cues), controlled for behavioral arousal related to task timing and anticipation of behaviorally-relevant stimuli or upcoming motor action, since subjects knew that the missing information (both target and effector) would always be instructed in the 2nd Cue period. In 75% of these trials, the 2nd Cue period instructed an

immediate real or imagined motor response to the flashed target, while in the remaining 25% of trials, a NoGo cue instructed no movement.

With four cueing paradigms (ET, E, T, 0) and four possible effectors (P, I, S, N), the entire experiment consisted of a total of 16 trial types: "Motor planning" trials - P_{ET}, I_{ET}, S_{ET}, and N_{ET}; "effector preparation" trials - P_E, I_E, S_E, and N_E; "spatial attention" trials - P_T, I_T, S_T, and N_T; and "Baseline" trials - P_0, I_0, S_0, and N_0. The flexible design of Experiment 2 allowed for the isolation of brain areas exhibiting delay-period BOLD activity that could not be explained solely by effector preparation, spatial working memory or attention, default or implicit motor planning, or behavioral arousal/anticipation. During experimental analyses, these controls were implemented by isolating brain areas exhibiting delay-activity that was significantly higher for ET trials than for all other trial types (E, T, 0). These brain areas are likely to play a role in motor planning.

In addition, the inclusion of NoGo trials in the experimental design and analysis served as a built-in control for residual cue-period visual activity, bottom-up capture of spatial attention by a flashed target, and initial cognitive cue processing, since within each cueing paradigm there were no differences between visual stimulation on P, I, S, and N trials other than the color of the cue that instructed the effector context. Another requirement for brain areas defined as playing a role in motor planning was higher delay-period BOLD activity on P_{ET}, I_{ET}, and S_{ET} than on N_{ET} trials (also see *Methods: Data Preprocessing and Analysis* and *Results*).

Data Preprocessing

Anatomical images were reconstructed into a 3D brain with voxel resolution of 1x1x1mm and transformed first to AC-PC and then to Talairach space via an 8-parameter affine transformation in BrainVoyager QX (Brain Innovation B.V., Maastricht, The Netherlands). Functional images were imported into BrainVoyager QX as DICOM images. The first functional run of each scan session was carefully coregistered to the anatomical scan using BrainVoyager QX's initial alignment and manual final alignment. Functional data preprocessing included slice scan time correction, trilinear 3D motion correction (in addition

to the scanner's on-the-fly correction), spatial smoothing (8mm or 4mm Gaussian kernel for Experiments 1 and 2, respectively), linear trend removal, and temporal high pass filtering (0.005Hz). Functional data were also converted to Talairach space, to facilitate analyses across subjects.

Analysis of Experiment 1

Experiment 1 was first analyzed using both whole-brain across-subjects fixed-effects and random-effects (RFX) general linear models (GLM, Friston et al. 1995) with 9 total predictors of interest per subject: the cue period (Cue), delay period separated by effector (R_{Delay}, I_{Delay}, S_{Delay}, N_{Delay}), and go period separated by effector (R_{Go}, I_{Go}, S_{Go}, N_{Go}). A "+" after a predictor indicates that a predictor has a significant positive beta value (positively contributes to the GLM). An "AND" indicates a conjunction of two or more GLM contrasts. All reported statistics are corrected for False Discovery Rate (Genovese et al. 2002) at q(FDR)<0.05 unless stated otherwise. Seven subjects were included in the fixed-effects analysis. The main experimental contrast to test for significant arm-specificity during motor planning was the conjunction contrast: [$R_{Delay} > S_{Delay}$] AND [$R_{Delay} > N_{Delay}$]. Similarly, to test for significant imag. arm-specificity, the following contrast was employed: [$I_{Delay} > S_{Delay}$] AND [$I_{Delay} > N_{Delay}$]. Regions of interest (ROIs) were only classified as arm-specific if they were significant in this conjunctive contrast comparison at q(FDR)<0.05. The M1 hand knob was localized with the contrast [$R_{Go} > S_{Go}$] AND [$R_{Go} > N_{Go}$] AND [R_{Go}+], making no assumptions about imagined reach activity. The contrast [$S_{Delay} > R_{Delay}$] AND [$S_{Delay} > N_{Delay}$] was used to localize potential human functional homologues of monkey FEF and LIP, which are more active prior to and during saccades than reaches. Further analyses of Experiment 1 included ROI-based analyses. The ROIs identified by the main contrasts in the fixed-effect analysis in seven subjects were further subjected to a random-effects analysis, which included the original seven subjects and an additional four subjects. These additional four subjects completed trials in all of the experimental conditions except for imagined arm movement. The RFX GLM included 7 total predictors of interest per subject (as in the fixed-effects analysis, but now excluding predictors for imagined movement since the 4 additional subjects did not complete imagined movement trials). The random-effects analysis was used to confirm arm or eye effector-specificity in the across-subjects ROIs using the contrast

[R_{Delay} > S_{Delay}]. Whole brain RFX analysis was also performed to confirm the generalization of the results from the fixed-effect analysis.

Single subject-based ROI analyses were also performed. For each of the seven subjects in the main experiment, a single-subject GLM with 18 predictors (two predictors each for Cue, R_{Delay}, I_{Delay}, S_{Delay}, N_{Delay}, R_{Go}, I_{Go}, S_{Go}, N_{Go}, separated by target direction: Right/Left) was used to identify subject-based ROIs. Subject-based ROIs were defined by the following contrasts: 1) the conjunction of [R_{Go} Right/Left > S_{Go} Right/Left] AND [R_{Go} Right/Left+] to identify M1 and related arm motor-execution areas; 2) the conjunction of [S_{Go} Right/Left > N_{Go} Right/Left] AND [S_{Go} Right/Left+] to identify V1 and saccade-related areas; 3) [R_{Delay} Right/Left > N_{Delay} Right/Left] OR [R_{Delay} Right/Left+] to identify reach planning-related brain areas; and 4) [Cue Right/Left+] to identify peak cue-related activations. For each subject, these contrasts were used to define the following ROIs: left primary motor cortex (M1), left peak post-central somatosensory cortical activation (Somat), left cingulate motor area (CMA), left primary visual cortex (V1), **left VP**, right and left inferior frontal eye fields (infFEF), right and left middle intraparietal sulcus (midIPS), left dorsal premotor cortex (PMd), left PMd/supplemental motor area (SMA), left SMA/cingulate, left dorsolateral prefrontal cortex (dlPFC), left putamen, left anterior intraparietal sulcus (aIPS), left posterior intraparietal sulcus (pIPS), and left medial posterior parietal cortex (medPPC). For each of these ROIs, an ROI-based GLM across subjects was used to assess effector-specificity.

To further quantify the degree of effector-specificity in these ROIs, single-subject GLM beta weights for the reach and saccade delay predictors were used to calculate a paired relative effector-specificity index (RES). RES is defined as:

$$(R_{Delay} - S_{Delay}) / (| R_{Delay} | + | S_{Delay} |).$$

The RES ranges from +1 (“absolute” reach-specificity) to -1 (“absolute” saccade-specificity). A value of 0 indicates no specificity for one effector over another, while a value of +/- 0.33 indicates that one effect has a beta value that is 2x the beta value for the other effector. In theory, the “chance” level RES value should be zero. For each ROI, an actual “chance” level

RES value was calculated by taking the actual beta values for the two predictors for all subjects, randomly permuting the assignment across effectors/subjects 1000 times; then, for each assignment permutation, the RES was recalculated to derive a mean "chance" RES. For all of the ROIs, the actual "chance" level RES value was less than 0.005.

Event-related averaged (ERA) BOLD timecourses were calculated for across single-subject defined ROIs. Trial-averaged ERAs were aligned to the onset of the delay period, and the baseline used for calculating percent BOLD signal change was the epoch including the 2 TRs prior to the onset of the delay period. In addition to calculating ERAs separately for different delay lengths, ERA plots were also generated by extracting delay-period activity and averaging across different delay lengths. These mean delay-period activity ERAs were calculated to better resolve the evolution of effector-specificity in frontal and parietal brain areas, and better observe the transition from initial transient visual cue response/context processing to sustained motor-planning activity in these ROIs. Timecourses of delay activity averaged across trials of different delay lengths were calculated by extracting only delay-period activity for each trial and sorting trials by effector type, then plotting time relative to actual delay onset vs. mean % BOLD signal change after subtracting out the NoGo curve (to control for visual stimulation and initial cue/context processing) (Fig. E1.7B).

Relative Contribution (RC) analyses were calculated in BrainVoyager QX, according to methods described previously (in Munk et al. 2002, Cohen Kadosh et al. 2005). The advantage of RC analyses is that, while the maps do not directly test for significant statistical differences between predictors, even task-related voxels with similar contributions of both predictors are visible. This allows for the visualization of a "latency" map, which shows how the differential relative contributions of two experimental predictors change across the cortical surface.

The color of a voxel in the RC maps depicts the relative weighting of two predictors (P1 and P2) in terms of their contribution to explaining the variance in a given voxel (e.g., Reach Delay predictor vs. Saccade Delay predictor). The minimum multiple correlation coefficient

of voxels shown in the maps is listed in the RC figure legends (as the R-value), and the color code for each RC map is also described. The RC value for each voxel is calculated as:

$$\text{RC value} = (Pb1 - Pb2)/(Pb1 + Pb2).$$

where Pbi is calculated as an incremental multiple correlation coefficient according to the extra sum of squares principle (see Cohen Kadosh et al. 2005 and Draper & Smith 1998). The RC value can range between +1 (only predictor P1 contributes to the model) and -1 (only predictor P2 contributes to the model), and an RC value of 0 indicates that both predictors P1 and P2 contribute equally to the model. Statistical differences between predictors P1 and P2 can be confirmed by performing a t-test of the beta-weights for P1 and P2, such as was done in the subject-group GLM and RFX comparisons described above.

Analysis of Experiment 2

Experiment 2 was analyzed by running two whole-brain, across-subjects GLMs, which modeled three task epochs: 1) combined Initial Fixation/1st Cue, 2) Delay, and 3) combined 2nd Cue/Go. One predictor was included for the Initial fixation/1st Cue, which would capture activity common to the beginning of all trials and the non-specific visual response related to cue presentation. In the first GLM, an additional 32 predictors modeled the Delay and Go periods separately for each of 16 trial types (a Delay and Go predictor each for P_{ET}, I_{ET}, S_{ET}, N_{ET}, P_E, I_E, S_E, N_E, P_T, I_T, S_T, N_T, P_0, I_0, S_0, N_0 trials) to resolve modulations by instruction and effector. Predictor main notation (P, I, S, N) indicates the effector used during the response period, regardless of whether the effector was instructed in the 1st or 2nd Cue period. Subnotation denotes the information presented during the 1st Cue period, prior to the delay epoch (ET=effector+target, E=effector only, T=target only, 0=no cues). In the second GLM, the Delay period was modeled using only 6 separate predictors. Four predictors modeled motor planning and effector preparation contexts separated by whether the effector instructed a subsequent motor response ("motor": P_{ET}, I_{ET}, S_{ET} were combined into a single predictor PIS_{ET}; P_E, I_E, S_E were combined into PIS_E) or whether the effector cue instructed withholding a motor response ("nonmotor": N_{ET} and N_E). Two more Delay predictors were collapsed across all effector types, since the effector was not instructed prior to the delay period on

these trials (target trials: P_T, I_T, S_T, N_T were combined into T; baseline trials, P_0, I_0, S_0, N_0 were combined into 0) (also see *Methods: Experimental Tasks*). The Go period was modeled with 4 predictors, one for each different effector/movement type, irrespective of cueing paradigm (P_{Go}, I_{Go}, S_{Go}, N_{Go}). These boxcar predictors were convolved with the standard 2-gamma BOLD hemodynamic response function in BrainVoyager QX. A "+" after a predictor indicates that a predictor has a significant positive beta value (positively contributes to the GLM). An "AND" indicates a conjunction of two or more GLM contrasts. All reported statistics are corrected for False Discovery Rate at $q(FDR)<0.05$ unless stated otherwise.

ROIs were defined based on statistical contrasts at the threshold specified. Event-related average timecourses were generated by averaging raw delay period-aligned data across trials, and across voxels in the ROI. The 2 TRs prior to the delay were used to baseline each trial (epoch-based averaging). Error bars were calculated either across trials or across subjects, as specified.

Because of the large number of experimental conditions in Experiment 2, a fixed, 4s delay period was employed. To better resolve delay-related activity and effector-specificity, a deconvolution analysis was implemented in BrainVoyager QX. For every delay- and go-period predictor, 10 consecutive impulse functions (each 1 TR long) were convolved with the standard HRF. The beta values (weights) for each impulse for each predictor were extracted from the GLM, and the amplitude of the beta values were plotted as a function of impulse number/time for each predictor to reveal the effective shape of the separate deconvolved delay and go HRFs for each predictor.

Viewing of statistical parametric maps

Statistical parametric maps were either projected onto segmented 3D brain surfaces of a representative single subject (neurological image convention: left hemisphere on the left, right hemisphere on the right), or onto 2D un-segmented brain slices (radiological image convention: left hemisphere on the right, right hemisphere on the left) for viewing.

Translation of electrophysiological experiments into fMRI experiments

Direct translation of monkey electrophysiological experiments for fMRI is complicated both by spatial and temporal resolution limits of fMRI and by the hemodynamics of the BOLD response. fMRI measurements are made for individual "voxels," and a voxel of size 3x3x3mm will sum the activity across hundreds of thousands of neurons, so only neuronal properties which survive on a population level will be resolvable using fMRI. As an example, the property of spatial tuning in individual neurons will be impossible to detect unless there is a topographic distribution of these neurons within a brain area. The lower bound of 1-2s repetition time typically employed in functional imaging also limits the temporal resolution of experimental tasks. Finally, for any impulse input, the BOLD hemodynamic response function (HRF) acts as a low-pass filter, with both an initial lag of 1-2s and a slow rise to peak (~6s). Convolving any two closely spaced events with the HRF illustrates the potential for temporal "smear" and overlap of BOLD responses. Thus, in order to fully separate BOLD responses to visual input and motor execution, and to increase the chance of resolving intervening processes, the delay between cue instruction and response in a delayed response task must be long enough to allow transient BOLD activity related to visual stimulation to decay back to baseline before the start of the response period. Practically, this means that experimental designs with short delay periods risk temporal "smear," confounding additive effects of the BOLD response over different trial epochs, and also hinge upon the assumption that these BOLD responses add linearly and do not saturate. However, there is a fine balance between improving the resolution of different trial epochs within an fMRI task by lengthening delays and losing control over the cognitive processes employed by subjects if the delays become too long.

Differences between Experiments 1 and 2

Some important differences between Experiments 1 and 2 must be noted. Experiment 1 utilized right arm reaching movements involving hand and lower arm extension from the elbow, while Experiment 2 utilized right hand/wrist pointing movements and no movement of the elbow or lower arm. Previous controls (unpublished data) testing pointing vs. reaching movements suggested strong overlap of the brain areas involved in point and reach planning, a finding that was again confirmed by comparing results from Experiments 1 and 2. The

main contrast for "motor planning" in Experiment 2 ($PIS_{ET} > N_{ET}$ AND $PIS_{ET} > PIS_{T}$ AND $PIS_{ET} > PIS_{E}$, see main text *Methods* and *Results*) is rather conservative and assumes no saturation of BOLD responses to target and effector information in brain regions involved in motor planning. It is possible that this conservative contrast excluded some brain areas which could also play a role in motor planning, such as dorsolateral prefrontal cortex.

Another difference between Experiments 1 and 2 is that in Experiment 1, since both target and effector were always cued simultaneously, both were instructed at the same peripheral location, whereas in Experiment 2, effector and target information were independently manipulated and thus presented at different locations (target peripherally, effector centrally). The cognitive dimensions of cueing, spatial cue for target and color cue for effector, were preserved across both experiments, and a central fixation stimulus was always on in both experiments; thus, we feel it appropriate to compare results from Experiments 1 and 2.

Meta-analysis

In order to compare the current study of effector-specificity with other studies in the literature that have topographically mapped visual/directional space in frontal and parietal cortices, or have reported BOLD activity related to eye- or arm-movements, we performed a meta-analysis. The average Talairach location of various meta-ROIs determined across studies were calculated based on reported Talairach and MNI coordinates.

Reported Talairach or MNI coordinates from a frontal or parietal ROI were extracted for each study, and MNI coordinates were converted to Talairach coordinates with mni2tal.m. If a study reported multiple coordinates for one ROI, these multiple coordinates were averaged to determine a single mean ROI location for each included study. Coordinates were also averaged across brain hemispheres. For each meta-ROI, these study-based ROI locations were then averaged across studies to determine mean Talairach X, Y, and Z-coordinates, as well as standard deviation along each axis across studies. Meta-ROI coordinates are reported in Table E1.2.

Meta-ROIs selected for comparison with ROIs from Experiment 1 of the current study included the topographic parietal maps IPS1, IPS2, IPS3, and IPS4, saccade-related areas FEF, infFEF, retIPS, and "LIP," and arm-related areas SMA, PMd, aIPS, and "PRR." Meta-ROIs "LIP" and "PRR" and other eye- and arm-related areas were not necessarily reported to be eye- or arm-specific, respectively; rather, they were calculated from single-study ROIs shown to be active during some component of an eye- or arm-movement related task.

Arm-specific ROIs from Experiment 1 compared to meta-ROIs included SMA/Cing., PMd/SMA, PMd, aIPS/PoCS complex, medPPC/pIPS and, separately, medPPC and pIPS (see Table E1.1). Eye-selective ROIs from Experiment 1 included in the comparison were FEF (active during the cue or saccade-delay periods), infFEF (saccade-specific during the response period and tail end of the delay period), and LIP (also referred to as midIPS/LIP; saccade-specific during the response period and tail end of the delay period). Experiment 1 ROI coordinates were collapsed across hemispheres and task-epochs where appropriate to determine a single average ROI location for comparison with the meta-ROIs. The locations of the parietal meta-ROIs and ROIs from the current study are shown in Fig. E1.10.

We also calculated the linear Talairach distance between the meta-ROIs and ROIs from Experiment 1, reported in Table E1.2. Studies included in the meta-analysis are listed in Table E1.2.

TABLES AND FIGURES FOR CHAPTERS 1 & 2

Figure 1 – Design of Experiments 1 and 2

A) Design of Experiment 1. See *Methods* for a description of the task. The color of the visual target instructed which effector to use on a given trial, and was always presented prior to the delay period. Red = Real Reaching. Purple = Imagined Reaching. Blue = Saccade. Yellow = NoGo. The main analysis epoch, the delay period, is indicated by the gray box.

B) Design of Experiment 2. See *Methods* for a description of the task. Each row represents a different cueing paradigm, named based on information provided to the subject in the 1st Cue period, *prior* to the delay period. Effector + Target (ET) reflects motor planning. Effector only (E) reflects effector preparation. Target only (T) reflects spatial working memory and attention. No cue (0) reflects baseline activity during the delay period. The color of the central fixation cue during the 1st or 2nd Cue period instructed which effector to use on a given trial. Red = Real Pointing (P). Purple = Imagined Pointing (I). Blue = Saccade (S). Yellow = NoGo (N). The target was always green. The main analysis epoch, the delay period, is indicated by the gray box.

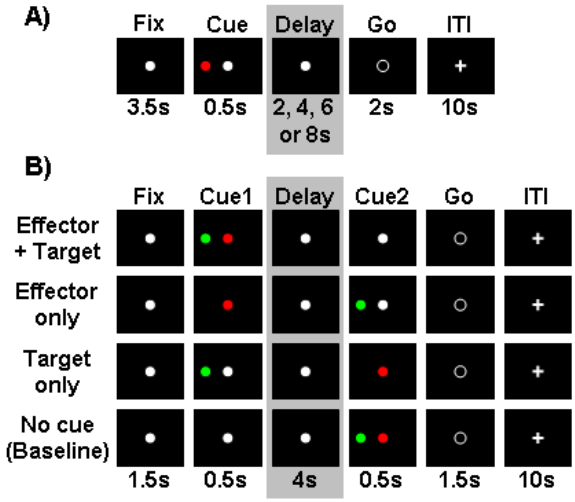

EXPERIMENT 1: TABLES AND FIGURES

TABLE E1.1 – Effector-specific and control ROIs from Experiment 1. ROI locations and summary of functional properties.

									Relative Effector-Specificity (RES)				
ROI Name	**BA**	**Tal X**	**Tal Y**	**Tal Z**	**std X**	**std Y**	**std Z**	**Contra-laterality**	**Delay RES**	**RES in both vis. fields?**	**Go RES**	**RES (RDvs.SD) in RFX? (n=11)**	**Real vs. Imag. Diff.?**
Motor planning ROIs: Reach, Imag. Reach or Saccade Delay predictors > NoGo Delay predictor													
L. dlPFC	9	-29	34	36	3.7	5.1	5.5	RD	**R, I**	yes	I	yes	ID, IG
L. preSMA/ Cing. (n=6)	24,32	-5	4	44	3.9	8	4.8	RD	**R, I**	yes	none, trend I>S>R	yes	RD, IG
L. Putamen	na	-23	0	14	2.4	6	3.3	RD	**R, I**	yes	R>S>I	yes	RD, RG
L. SMA/Cing.	6	-5	-7	52	2.3	7.6	4.1	RD	**R, I**	yes	R	yes	RD, RG
L. infFEF	*4,6*	*-40*	*-10*	*47*	*6.6*	*4.7*	*5.8*	*Cue, RD*	*S*	*LVF, trend RVF*	*S*	*trend LVF (p<0.13), no SG>RG or contra cue*	*ID, IG*
R. infFEF	*4,6*	*43*	*-13*	*52*	*2.3*	*3.3*	*3.2*	*Cue, SD*	*S*	*LVF*	*S*	*yes: BVF, contra cue*	*IG*
L. PMd/SMA	6	-13	-17	63	2.6	7.2	4.5	RD	**R, I**	yes	R	yes	RD, RG
L. PMd	6	-23	-17	56	2.4	4.8	3	RD	**R, I**	yes	R, I	yes	RD, RG
L. pCing	7	-11	-43	46	4.3	4.2	5.7	RD	**R, I**	yes	R>S>I	yes	RD, RG
L. SMG/IPL (n=6)	40	-52	-45	32	5.7	5.4	6	no	**R, I**	yes	I, S	yes	RD, IG
L. aIPS/PoCS	5,7	-38	-48	55	7.2	4.6	3.7	no	**R, I**	yes	R, I	yes	RD, RG
L. medPPC	7	-12	-59	54	2.1	5.2	3.4	RD	**R, I**	yes	R	yes	RG
L. midIPS	*7*	*-24*	*-61*	*48*	*2.5*	*7.1*	*3.4*	*Cue*	*S*	*LVF*	*S*	*trend LVF (p<0.09), contra cue*	*IG*
R. midIPS	*7*	*25*	*-62*	*48*	*2.1*	*5.6*	*5.3*	*Cue, SD*	*S*	*LVF*	*S*	*trend LVF (p<0.06), contra cue*	*no*
L. medPPC/ pIPS	7	-15	-65	49	2.2	3.8	4	RD	**R, I**	yes	R	yes	RD, RG
L. pIPS	7	-12	-66	40	4.7	6.8	7.6	RD	**R, I**	yes	R	yes	RG
Visual ROIs (cue or response, no delay activity)													
L. v1cuelat	*19*	*-25*	*-67*	*-5*	*5*	*2.1*	*7.5*	*Cue*			*S*		*no*
R. v1cuelat	*19*	*24*	*-67*	*-7*	*3.2*	*3.1*	*5.2*	*Cue*			*S*		*no*
L. v1cuemed	*18*	*-10*	*-78*	*-5*	*3.5*	*8.1*	*5.9*	*Cue*			*S*		*no*
R. v1cuemed	*18*	*9*	*-79*	*-5*	*1.8*	*6.1*	*5.4*	*Cue*			*S*		*no*
L. VisPar	*18*	*-17*	*-85*	*20*	*3.1*	*3.9*	*4.5*	*Cue*			*S*		*no*
Motor execution ROIs (response only, no delay activity)													
L. CMA	6,31	-2	-17	47	1.7	2.4	2.7	no			R>S>I		RG
L. M1	4	-28	-25	65	2.9	3	2.2	no			R>S>I		RG
L. M1/S1 (n=5)	3,4	-32	-31	53	5.2	3.8	4.1	no			R		RG
L. S1/PoCG	5,2	-32	-42	62	2.5	2.7	3.3	no			R, I		RG

Region of interest (ROI) abbreviations: dlPFC=dorsolateral prefrontal cortex, Cing.=cingulate, CMA=cingulate motor area, FEF=frontal eye fields, IPL=inferior parietal lobule, IPS=intraparietal sulcus, M1=hand/arm area of primary motor cortex, PM=premotor cortex, PoCS=postcentral sulcus, PPC= posterior parietal cortex, PrCS=precentral sulcus, PRR=parietal reach region, S1=primary somatosensory cortex, SEF=supplementary eye fields, SMA=supplementary motor area, SMG=supramarginal gyrus, SPL=superior parietal lobule.

Figure E1.1 – Arm- and eye-specificity in frontal and parietal cortices: Effector-specific regions of interest and motor planning areas. A) A visualization of transitions in effector preference across the cortical surface based on a relative contribution (RC) analysis of Reach Delay and Saccade Delay predictors (see *Methods*). Positive RC values (yellow to red) indicate that the Reach Delay predictor contributes more to the GLM than the Saccade Delay predictor. Negative RC values (cyan to blue) indicate that the Saccade Delay predictor contributes more than the Reach Delay predictor. N. subjects = 11, based on Experiment 1. B) Random-effects contrasts for effector-specificity: In red: [R_{Delay} > S_{Delay}] AND [R_{Delay} > N_{Delay}]. In blue: [S_{Delay} > R_{Delay}] AND [S_{Delay} > N_{Delay}]. N. subjects = 11, based on Experiment 1. C) Motor planning activity compared to control conditions, based on Experiment 2. Brain areas involved in motor planning were identified by the conjunction contrast PIS_{ET} > N_{ET} (Motor planning condition > NoGo "planning" condition) AND PIS_{ET} > PIS_{T} (Motor planning condition > Spatial attention/working memory condition) AND PIS_{ET} > PIS_{E} (Motor planning condition > Motor preparation condition). q(FDR)<0.05, number of subjects = 6. The precentral sulcus is outlined in blue, the central sulcus in purple, the postcentral sulcus in light purple, the main intraparietal sulcus in light green, and the posterior-most segment of the intraparietal sulcus in dark green.

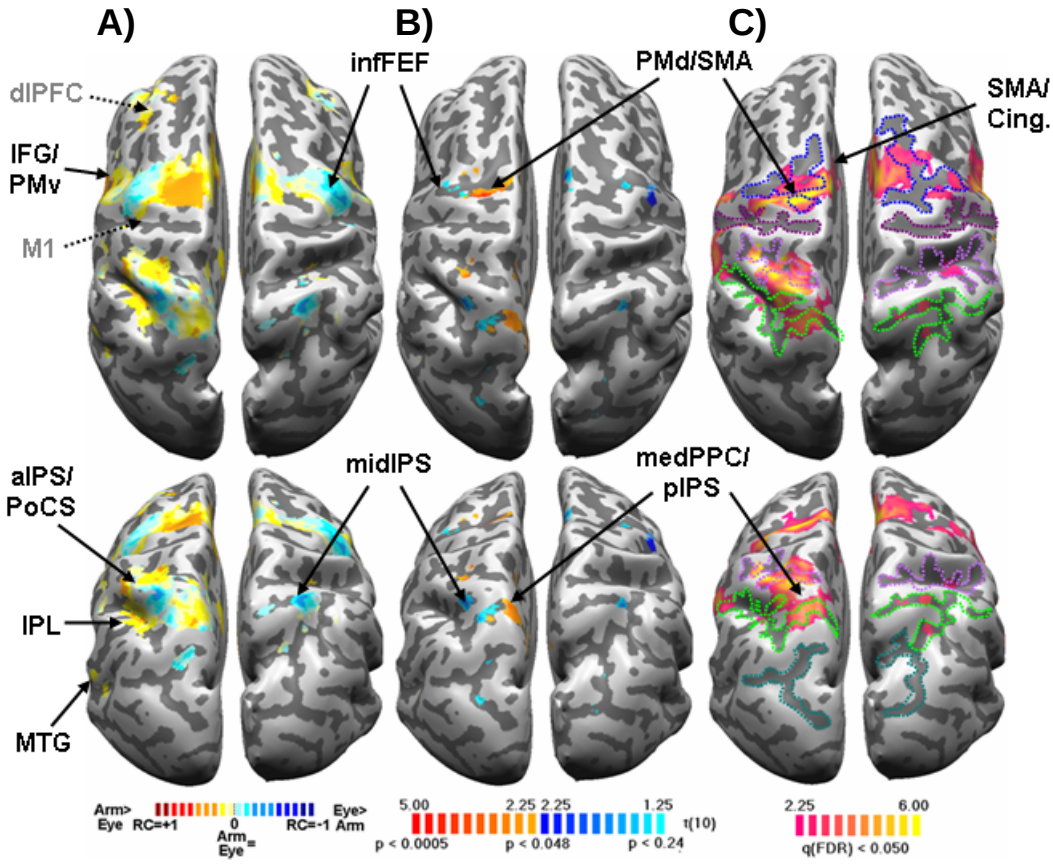

Fig. E1.2 – Effector-specificity during the Go period, across-subjects. Effector-preference during the Go period visualized as a RC map (A), and a direct random-effects test for effector-specificity (B). Across-subjects, n=11. Based on Experiment 1. Compare with the delay-period RC and RFX maps in Figs. E1.1A, E1.1B. The precentral sulcus is outlined in blue, the central sulcus in purple, the postcentral sulcus in light purple, the main intraparietal sulcus in light green, and the posterior-most segment of the intraparietal sulcus in dark green.

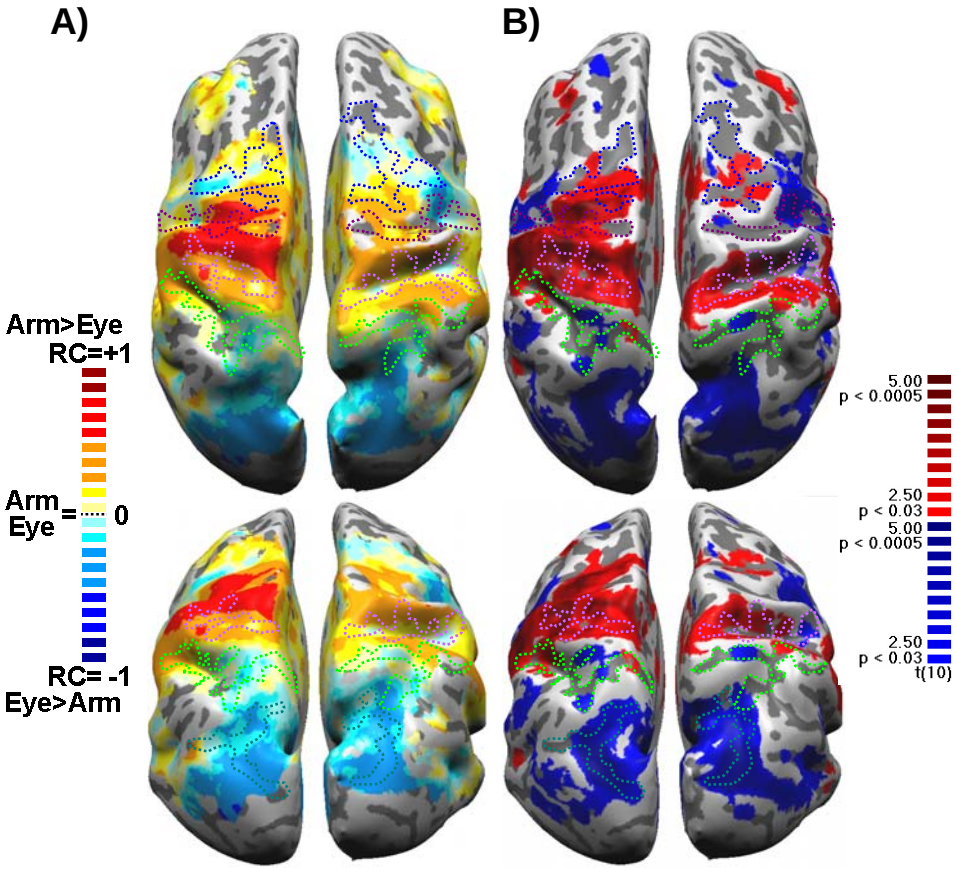

Figure E1.3 – Timecourses of BOLD activity in arm- and eye-specific ROIs reveal the evolution of effector-specificity during the trial. Event-related average (ERA) timecourses from the main ROIs exhibiting significant effector-specificity for arm or eye effectors during motor planning, and two non-specific control ROIs (M1, V1).

A) Event-related BOLD timecourses for 8s delay trials only. Averaged across individual, subject-based ROIs (N. subjects=7). Left – Reach-specific ROIs show stronger BOLD activity in reach trials than in saccade trials, and recruitment in imagined reach trials. Middle – Saccade-specific ROIs show strong visual cue/context responses (not effector-specific, see high activity in NoGo trials when there are no requirements for motor planning), and an increasing separation between saccade and reach trials towards the end of the delay period that is maintained throughout the execution period. Right – Control ROIs M1 and V1 show strong effector-specificity during movement execution for reaches and saccades, respectively, but not during the delay period. Curves are aligned to actual delay onset, with the preceding initial fixation period as baseline. Gray shading indicates the effective delay period (not used in the ERA calculation, for viewing only), shifted by the expected hemodynamic response onset latency (2s). Notice that neither M1 activity on reach trials nor V1 activity on saccade trials begin to increase above baseline until ~2s after the actual onset of the response period (actual onset at 8s), confirming the expected 2s hemodynamic response onset latency. Red = Real reach. Purple = Imag. Reach. Blue = Saccade. Yellow = NoGo. Timecourses are based on Experiment 1.

B) BOLD activity during the delay period only. ERA curves are raw BOLD signal timecourses averaged across single-subject ROIs (N. subjects=7), and calculated across all delay lengths and with visual/context cue activity subtracted out (i.e., the NoGo curve was subtracted from the three remaining curves). Effector-specificity evolves earlier for arm than for eye movements, and is maintained throughout the rest of the delay period. Left – In reach-specific ROIs, reach-specificity evolves at 4+ seconds after delay onset and is maintained throughout the duration of the delay period. Middle – In saccade-specific ROIs, saccade-specificity evolves towards the end of the delay period (~8s), and is maintained during the execution period (not shown, see Fig. E1.3A). Right - Control ROIs M1 and V1 do not show effector-specificity during the delay period, nor do they show significantly delay activity above the baseline (NoGo) condition, but are strongly reach- (M1) and saccade (V1)-specific during the execution period (not shown, see Fig. E1.3A).

(figure on next page)

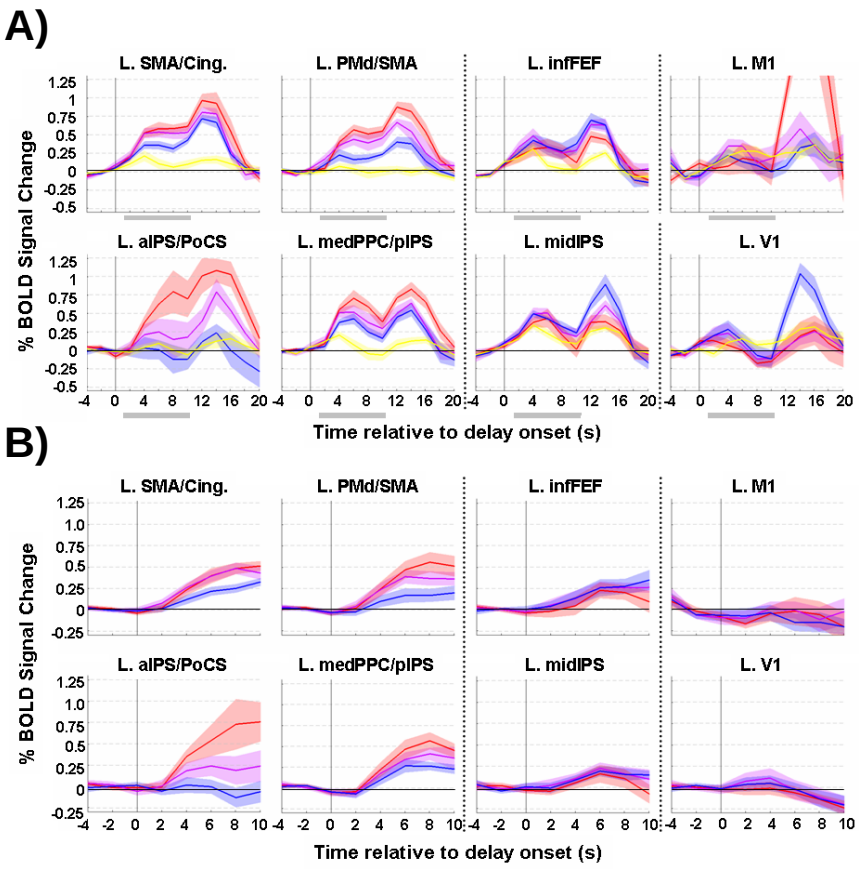
A)
L. SMA/Cing.
L. PMd/SMA
L. infFEF
L. M1
L. aIPS/PoCS
L. medPPC/pIPS
L. midIPS
L. V1
% BOLD Signal Change
Time relative to delay onset (s)
B)
L. SMA/Cing.
L. PMd/SMA
L. infFEF
L. M1
L. aIPS/PoCS
L. medPPC/pIPS
L. midIPS
L. V1
% BOLD Signal Change
Time relative to delay onset (s)

Figure E1.4 – Relative effector-specificity indices for the main ROIs. Relative effector-specificity (RES) is calculated on a per-subject basis using GLM predictor beta values: $(R_{Delay} - S_{Delay})/(|R_{Delay}| + |S_{Delay}|)$. RES ranges from +1 (very reach-specific) to -1 (very saccade-specific). A value of |0.33| means that one predictor's beta value is twice the other predictor's beta value. Chance level was calculated by randomly permuting the predictor beta values across subjects and effector predictors in a given ROI 1000x, and then re-calculating the RES index. Mean chance level RES was <0.005. Shown: mean RES with SE bars, and max value across subjects (n=7), based on Experiment 1. A) SMA, PMd, aIPS/PoCS, and medPPC/pIPS are strongly reach-specific. Across subjects, bilateral infFEF and midIPS were specific for saccades, but the mean RES values tended to be lower than for reach-specific ROIs. B) RES calculated separately for targets in the right visual field (RVF) and left visual field (LVF).

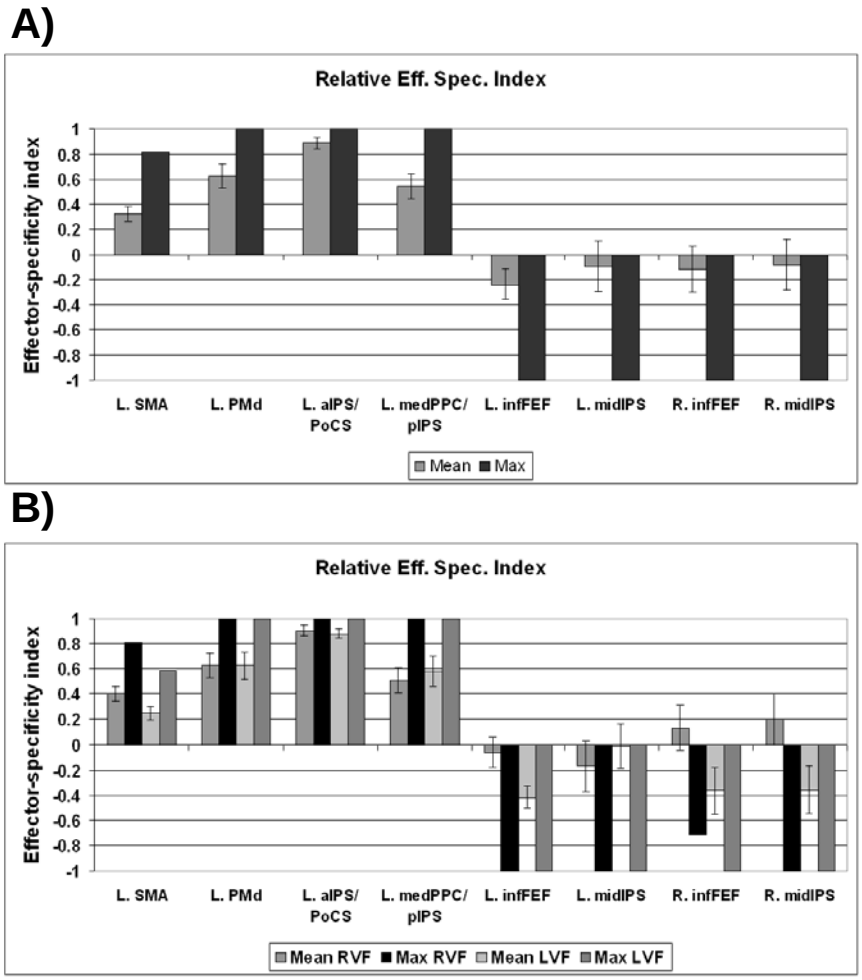

E1.5 – Relative effector-specificity (RES) indices for the main ROIs, where RES was calculated based on raw delay BOLD activity. Relative effector-specificity (RES) was calculated on a per-subject basis using raw BOLD activity from the delay period. This delay activity was averaged across 6-10s relative to delay onset, and then was averaged across subjects. The formula used is: (Reach – Saccade)/(|Reach| + |Saccade|). RES ranges from +1 (very reach-specific) to -1 (very saccade-specific). A value of |0.33| means that one effector's mean delay activity (over the period 6-10s relative to delay onset) is 2x the other effector's mean delay activity. Shown: mean RES with SE bars, and max value across subjects (n=7), based on Experiment 1. RES values calculated based on raw delay-period BOLD activity strongly mirror those calculated based on GLM predictor beta values; compare with Figure E1.4. A) SMA, PMd, aIPS/PoCS, and medPPC/pIPS are strongly reach-specific. Across subjects, bilateral infFEF and midIPS were specific for saccades, but the mean RES values tended to be lower than for reach-specific ROIs. B) RES calculated separately for targets in the right visual field (RVF) and left visual field (LVF). C) Paired (within-subject) t-tests compared Reach and Saccade delay activity in the main ROIs. Arm-specific ROIs demonstrate significant effector-specificity within- and across-subjects earlier (2-4s) than eye-specific ROIs (8s).

(figure on next page)

A)

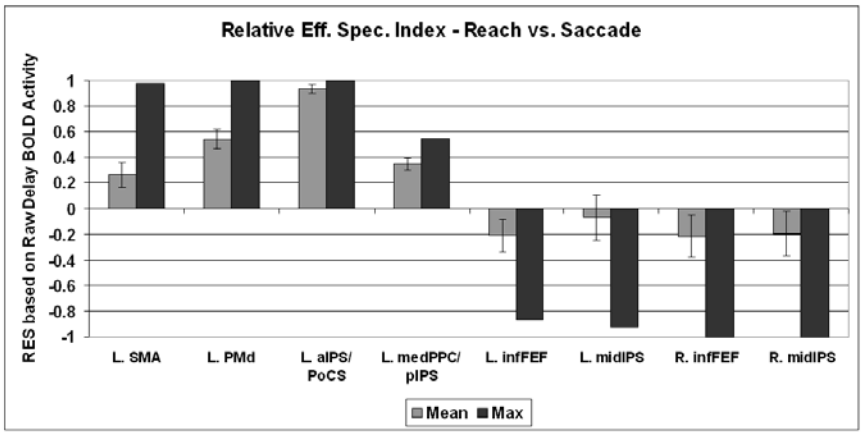

B)

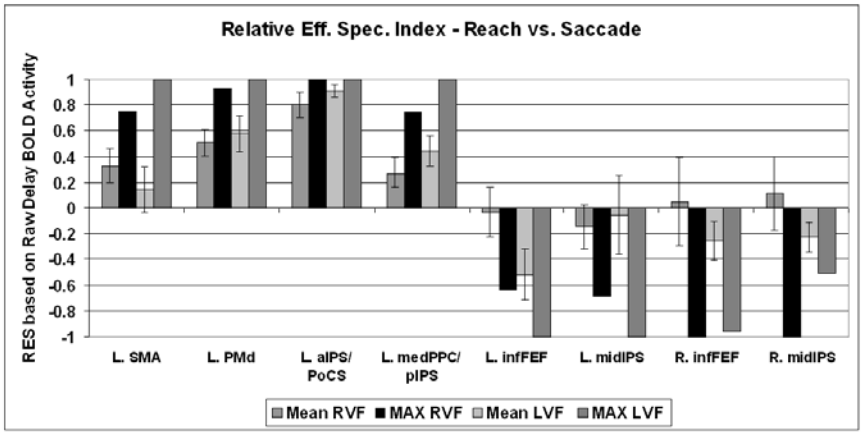

C)

ROI	L. SMA	L. PMd	L. aIPS/ PoCS	L. medPPC/ pIPS	L. infFEF	L. midIPS	R. infFEF	R. midIPS
Eff.-spec.	Arm	Arm	Arm	Arm	Eye	Eye	Eye	Eye
Time?	4s	2-4s	4s	2-4s	8s	8s	8s	8s
Paired t-test for 6-10s:	p<0.083	p<0.0048	p<0.0115	p<0.0042	p<0.004	p<0.015	p<0.0008	p<0.028

Fig. E1.6 – Comparison of real- and imagined reach-specificity, and non-specific task-related activations. A) Comparison of real- and imagined reach-specificity during the delay (top) and go (bottom) periods. Across-subjects (n=7), maps are at q(FDR)<0.005. During motor planning, both real and imagined reach-specificity maps (relative to saccade) strongly overlap, but specificity-for these two effectors segregates during motor execution. Based on Experiment 1. B) Overlap of motor planning (pink) and motor execution (salmon) for the three motor effectors: Real Reach, Imag. Reach, and Saccade. Across-subjects (n=7), maps are at q(FDR)<0.001. Based on Experiment 1.

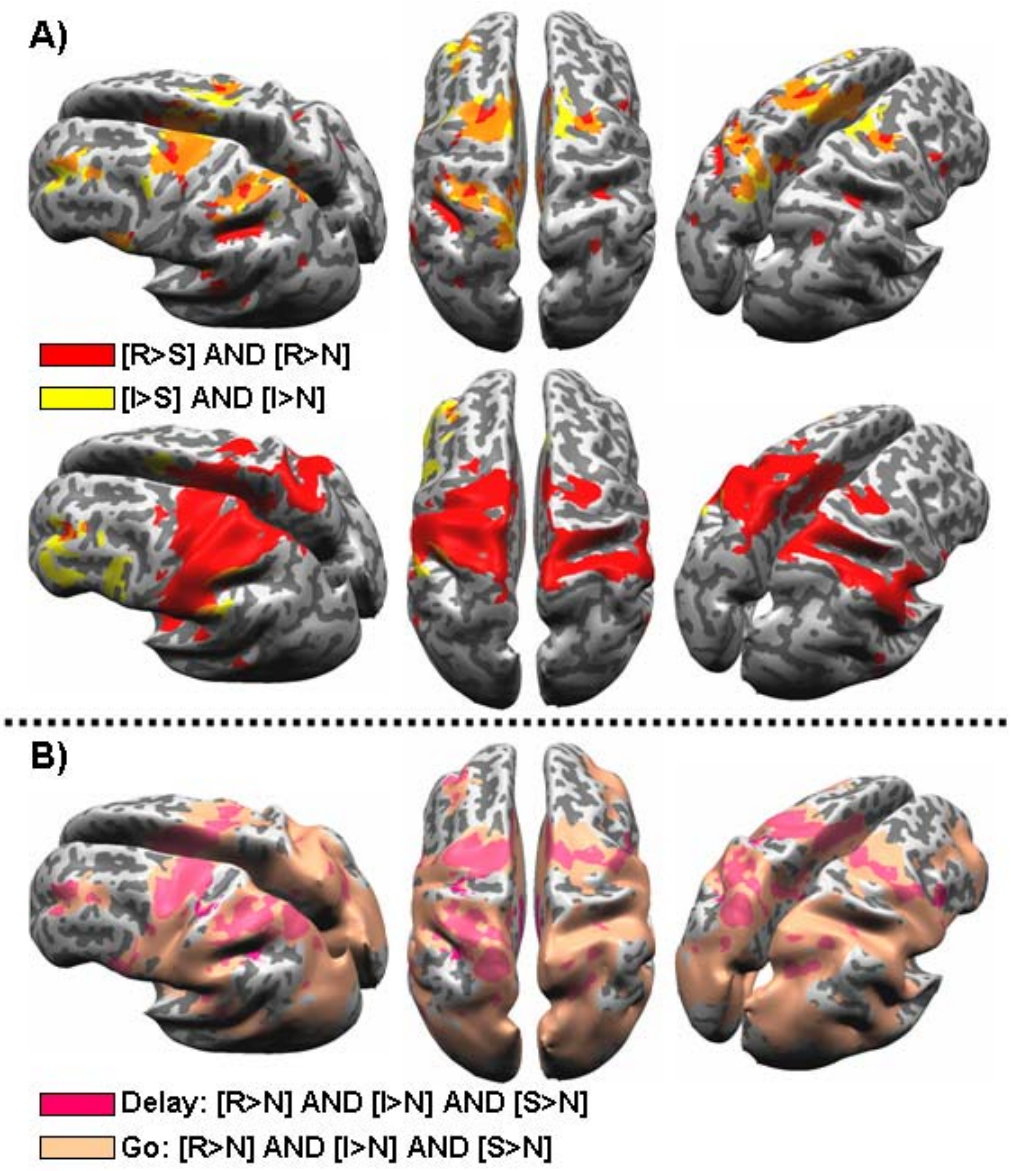

Fig. E1.7 – ERAs for reach- and arm-specific ROIs and controls, separated by target visual field. ERAs for 8s delay trials, separated by target visual field. Most effector-specific ROIs demonstrate some degree of cue/delay contralaterality. The main effect in reach-specific ROIs is the reach-specific modulation rather than the contralateral effect. In contrast, there is a stronger contralateral effect in saccade-specific ROIs, though saccade vs. reach specificity is also evident. A) Reach-specific motor planning ROIs (and control M1). B) Saccade-specific motor planning ROIs and controls (L/R. V1). Lighter curves: right visual field (RVF); darker curves: left visual field (LVF). Based on Experiment 1.

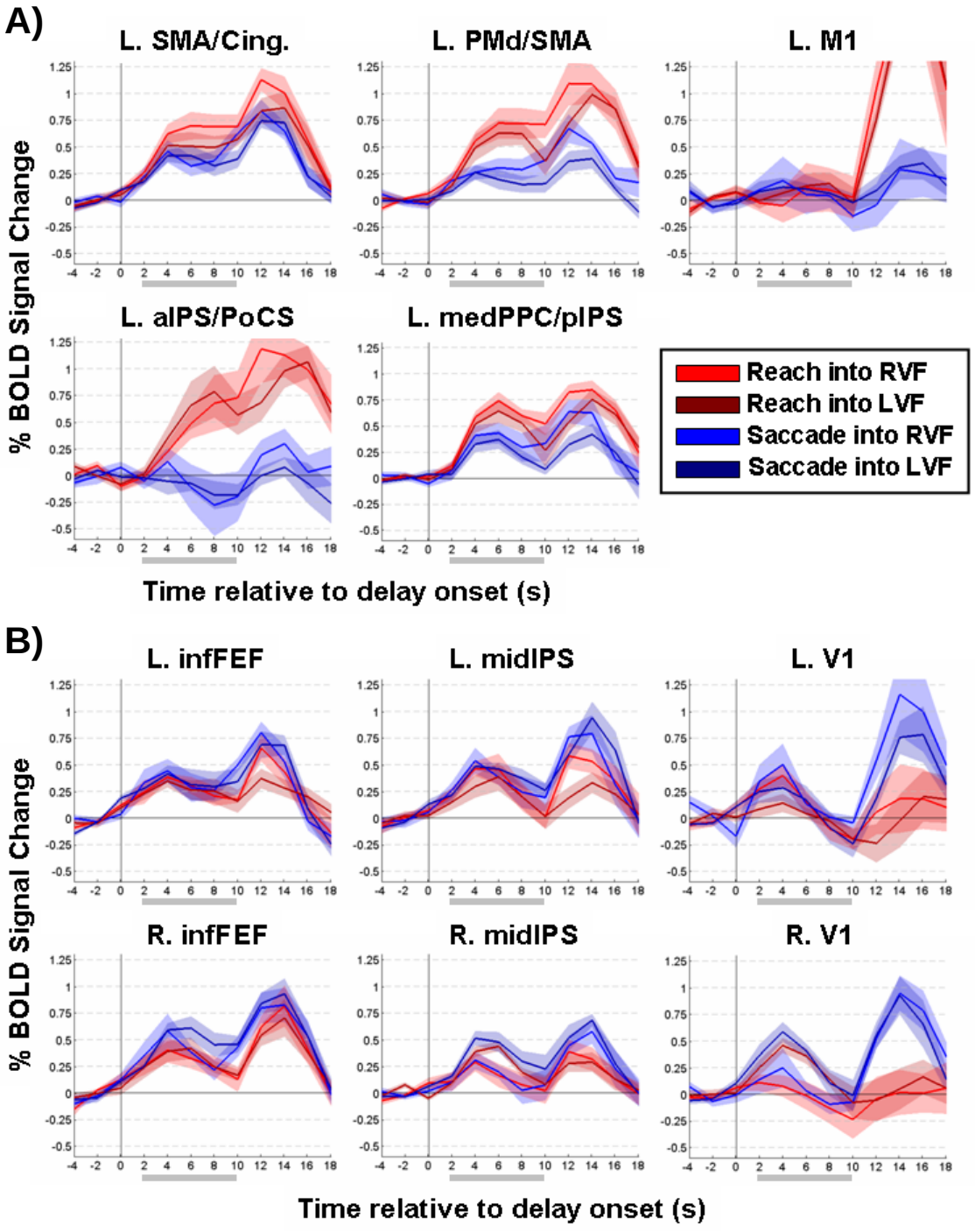

Fig. E1.8 – ERAs from a single subject demonstrate that effector-specificity is maintained throughout even very long delay periods. ERAs from main ROIs in a single subject scanned in the same task with longer delays (6-18s). ERAs shown are for 14s-delay trials only. Saccade-specific BOLD activity evolves during the late delay period, after the BOLD response to the initial visual cue decays to baseline. Reach-specific BOLD activity is maintained throughout the whole delay period. M1 and V1 are not effector-specific during the delay period, but are strongly arm- and eye-specific (respectively) during the execution period. V1 activity during the execution period on reach-trials is probably due to visual feedback of the hand moving (as the hand approaches the target).

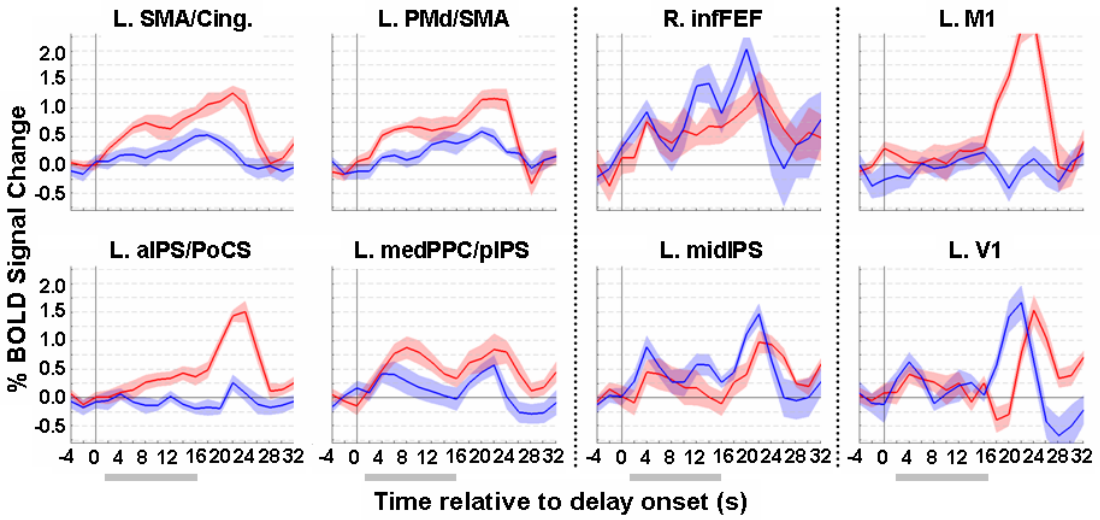

E1.9 – Effector-preferences during the Delay period visualized as RC maps in single subjects. RC maps visualize transitions in effector-preferences on the cortical surface in single subjects. RC maps are for task-related voxels only, thresholded at R>0.04, and q(FDR)<0.05 (see *Methods*). In the medial PrCS, and medial to that, effector-preference tends to be Arm>Eye. In the lateral part of the PrCS (and ventro-caudal to it), effector-preference tends to be Eye>Arm. In superior parietal cortex, Arm>Eye activity lies in the SPL and PreCun. This arm-preference starts in a branch of the IPS and extends into the transverse parietal sulcus (TPS), and again onto the medial wall to include the ascending portion of the superior parietal sulcus (SPS). In contrast, Eye>Arm activity lies in a medial branch of the IPS (anterior and lateral to the branch with arm-preference), about halfway between the anterior end of the IPS and a line drawn to the POS. Top: A transverse view of the left hemisphere of the brain. Bottom: A back view of the left hemisphere of the brain. The IPS/TPS are outlined in solid black; the SPS is outlined in dotted black. Single subject hemispheres are aligned in Talairach space. Based on Experiment 1.

(figure on next page)

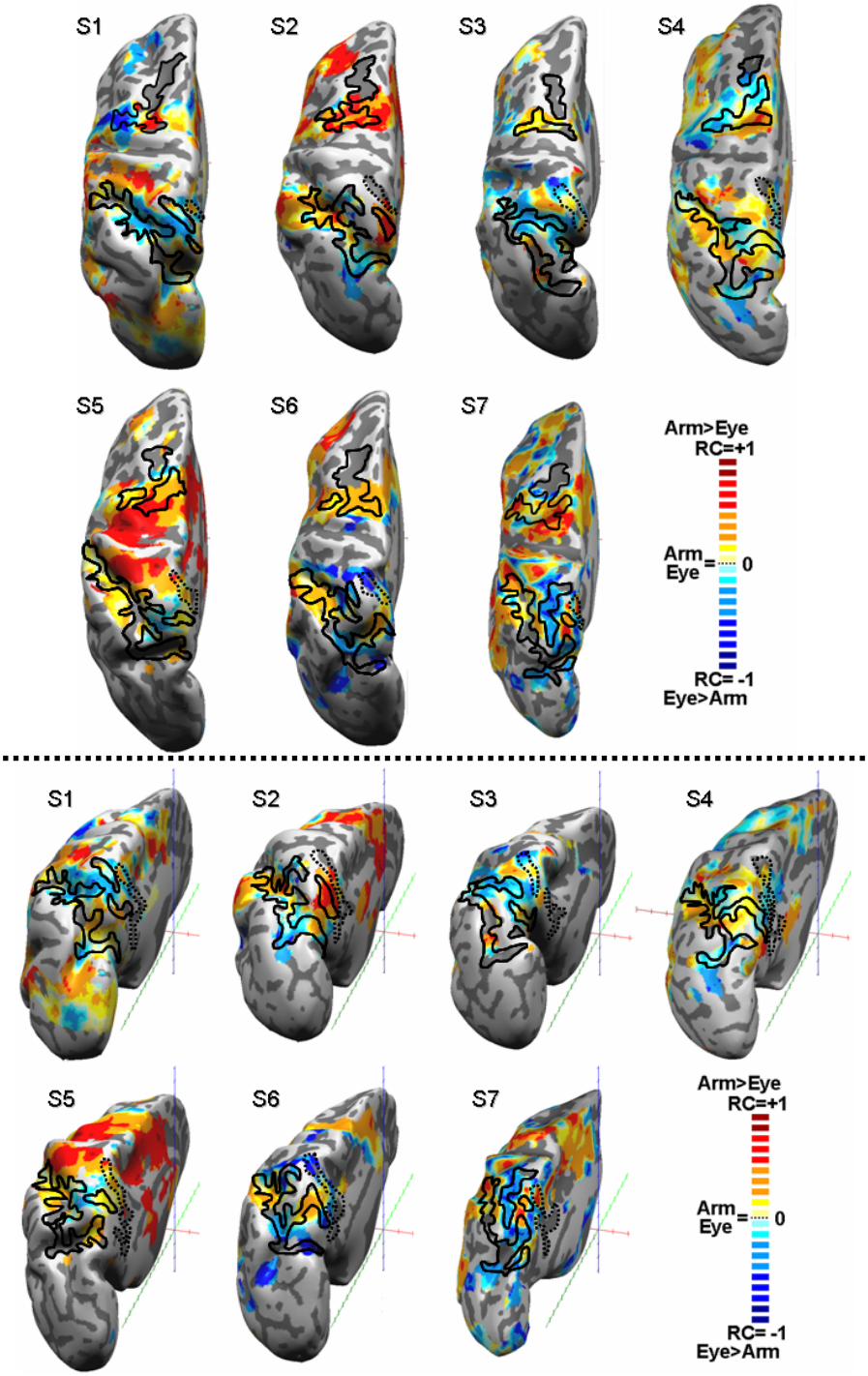
S1
S2
S3
S4
S5
S6
S7
Arm>Eye
RC=+1
Arm
Eye
=
0
RC= -1
Eye>Arm
S1
S2
S3
S4
S5
S6
S7
Arm>Eye
RC=+1
Arm
Eye
=
0
RC= -1
Eye>Arm

TABLE E1.2 – Average Talairach coordinates of meta-ROIs calculated across studies, and linear distances to ROIs from Experiment 1. Talairach X-coordinates have been collapsed across left and right hemispheres. See *Methods: Meta-analysis* for further details.

Meta ROI	TalX	TalY	TalZ	StdX	StdY	StdZ	# Studies	Studies
B. IPS1	22	-73	38	2.4	3.9	4.8	6	8,9,12,16,18,19
B. IPS2	21	-67	49	3.7	6.5	2.9	6	8,9,12,16,18,19
B. IPS3	24	-53	51	2	6.5	2.5	3	8,9,19
B. IPS4	26	-53	52	0.2	0	0	1	19
B. retIPS	22	-61	44	2.5	1.9	2.2	3	13,14,15
B. "LIP"	26	-59	47	5.1	5.9	5.3	5	1,2,5,6,17
B. "PRR"	11	-68	47	1.9	6.4	6.3	5	2,4,6,8,9
L. aIPS	37	-50	46	5.3	15.3	5.3	3	1,2,6
B. FEF	32	-10	51	4.4	3.2	2.8	10	1,2,3,5,7,8,10,11,12,14
B. infFEF	42	-3	37	5.5	4.6	8.3	6	5,7,8,10,11,12
B. PMd	26	-13	57	3.1	2.5	3.9	4	1,2,5,14
L. SMA	4	-2	48	1.1	2	2.8	3	1,2

Our ROI	TalX	TalY	TalZ
LIP	24	-58	49
medPPC/pIPS	11	-63	50
medPPC	10	-56	55
pIPS	12	-67	48
aIPS Complex	35	-48	53
FEF	30.5	-11	52
infFEF	43.5	-10	52
PMd	25	-18	55
SMA/Cing.	7	1	46

TAL DISTANCES		
Meta ROI	**Our ROI**	**Tal. Dist.**
IPS3	LIP	5.4
retIPS	LIP	6.2
"LIP"	LIP	3
IPS2	medPPC/pIPS	10.8
"PRR"	medPPC/pIPS	5.8
"PRR"	pIPS	1.7
aIPS	aIPS complex	7.6
PMd	PMd	5.5
SMA	SMA/Cing.	4.7
FEF	FEF	2.1
infFEF	infFEF	16.6

Included studies:	
1	Amiez et al. 2006
2	Astafiev et al. 2003
3	Brown et al. 2007

4	Connolly et al. 2003
5	Connolly et al. 2007
6	Fernandez-Ruiz et al. 2007
7	Grosbas et al. 2001
8	Hagler et al. 2006
9	Hagler et al. 2007
10	Kastner et al. 2007
11	Lachaux et al. 2006
12	Levy et al. 2007
13	Medendorp et al. 2003
14	Medendorp et al. 2005a
15	Medendorp et al. 2005b
16	Schluppeck et al. 2005
17	Sereno 2001
18	Silver et al. 2005
19	Swisher et al. 2007

Fig. E1.10 – Comparison of parietal ROIs (identified in Experiment 1) with a meta-analysis. Comparison of across-subjects ROIs identified in Experiment 1 (pIPS, medPPC/pIPS complex, medPPC, midIPS/LIP) with parietal meta-ROIs (IPS1, IPS2, IPS3, retIPS, "LIP," and "PRR"). The meta-ROIs were calculated over several studies (see Table E1.2 and *Methods: Meta-analysis*). A) Left to right: transverse/axial view, coronal view, sagittal view. The blue ellipses indicate the standard deviation in each plane around the center of the ROI. The centers of ROIs from Experiment 1 of the current study are indicated by red dots. B) The centers of meta-ROIs (italic labels and dotted lines) and ROIs from Experiment 1 (bold labels and solid lines) visualized on a representative left-hemisphere surface.

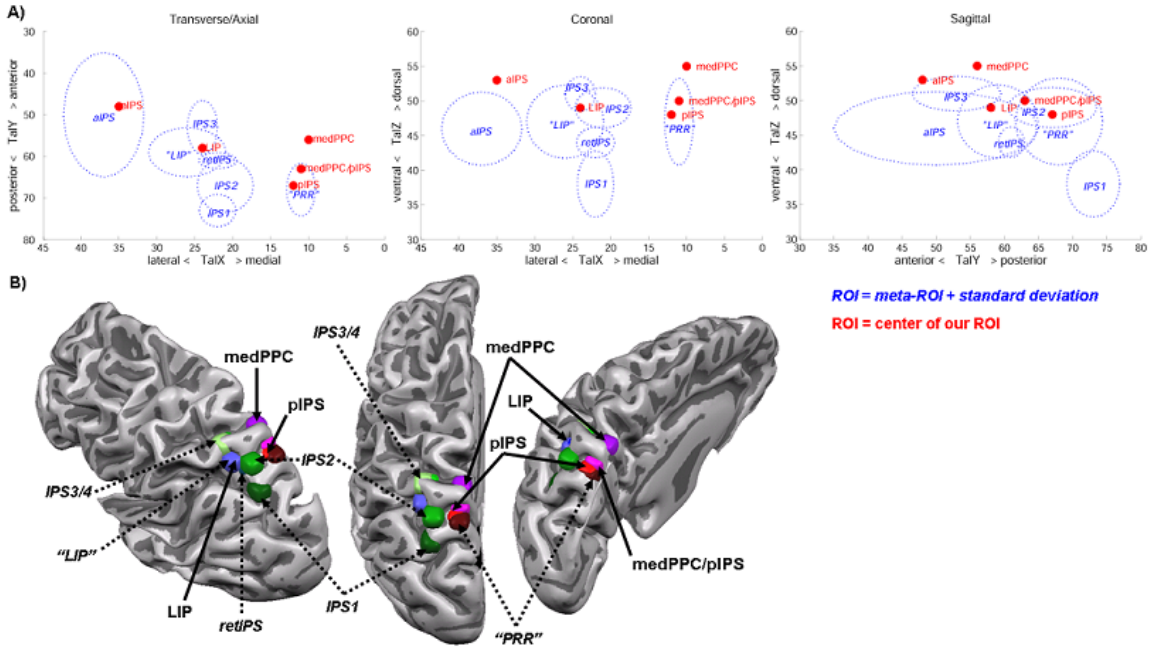

EXPERIMENT 2: TABLES AND FIGURES

TABLE E2.1 – Talairach coordinates of ROIs from Experiment 2

ROI NAME	TAL X	TAL Y	TAL Z
Motor Planning > All Controls			
R. antInsula	32	23	11
L. antInsula	-31	16	12
R. IFG/PMv	50	7	29
R. PMv/BA44	44	6	9
L. PMv/BA44	-50	6	6
L. IFG/PMv	-53	2	32
B. SMA/Cing.	0	-6	53
L. infFEF	-45	-10	52
R. infFEF	42	-5	50
L. PMd/SMA	-22	-16	60
R. PMd/SMA	16	-8	60
L. IPL/BA40	-52	-28	29
R. IPL/BA40	57	-30	24
L. aIPS/PoCS	-36	-37	44
L. aIPS fundus	-39	-40	49
L. aIPS fundus	-28	-45	35
R. aIPS fundus	34	-43	41
L. aSPL	-24	-53	61
L. aSPL/aIPS	-30	-53	50
L. midIPS/LIP	-24	-60	49
R. midIPS/LIP	28	-52	49
R. midIPS/LIP	23	-63	45
L. medPPC	-12	-64	55
R. SPL	15	-67	46
L. SPL	-16	-68	49
L. pIPS	-18	-71	46
Point/Imag. Point Planning > Saccade Planning AND NoGo "Planning"			
L. cSMA/Cingulate	-5	-12	47
L. cPMd/SMA	-19	-19	56
L. cPMd	-29	-17	59
Saccade Planning/Execution > Point AND NoGo Planning/Execution			
L. infFEF	-43	-10	47
R. infFEF	47	-11	49
L. midIPS/LIP	-21	-58	40
R. midIPS/LIP	25	-65	44

Directional abbreviations: d=dorsal, v=ventral, r=rostral, c=caudal, L=left hemisphere, R=right hemisphere, a/ant=anterior, p/pos=posterior, mid=middle, med=medial, inf=inferior. ***Region of interest (ROI) abbreviations:*** dlPFC=dorsolateral prefrontal cortex, CMA=cingulate motor area, FEF=frontal eye fields, IFG=inferior frontal gyrus, IPL=inferior parietal lobule, IPS=intraparietal sulcus, LIP=lateral intraparietal area, M1=hand/arm area of primary motor cortex, PM=premotor cortex, PoCS=postcentral sulcus, PPC= posterior parietal cortex. PrCS=precentral sulcus, PRR=parietal reach region, S1=primary somatosensory cortex, SEF=supplementary eye fields, SMA=supplementary motor area, SPL=superior parietal lobule.

Figure E2.1 – Timecourse plots from main ROIs confirm a role in motor planning compared to control processes. Event-related average timecourses from the left-hemisphere ROIs in Figure 2C. Curves are aligned to actual delay onset, with the preceding initial fixation period as baseline. The gray bar indicates the effective delay period shifted by the expected hemodynamic response onset latency (2s). ERAs are based on Experiment 2.

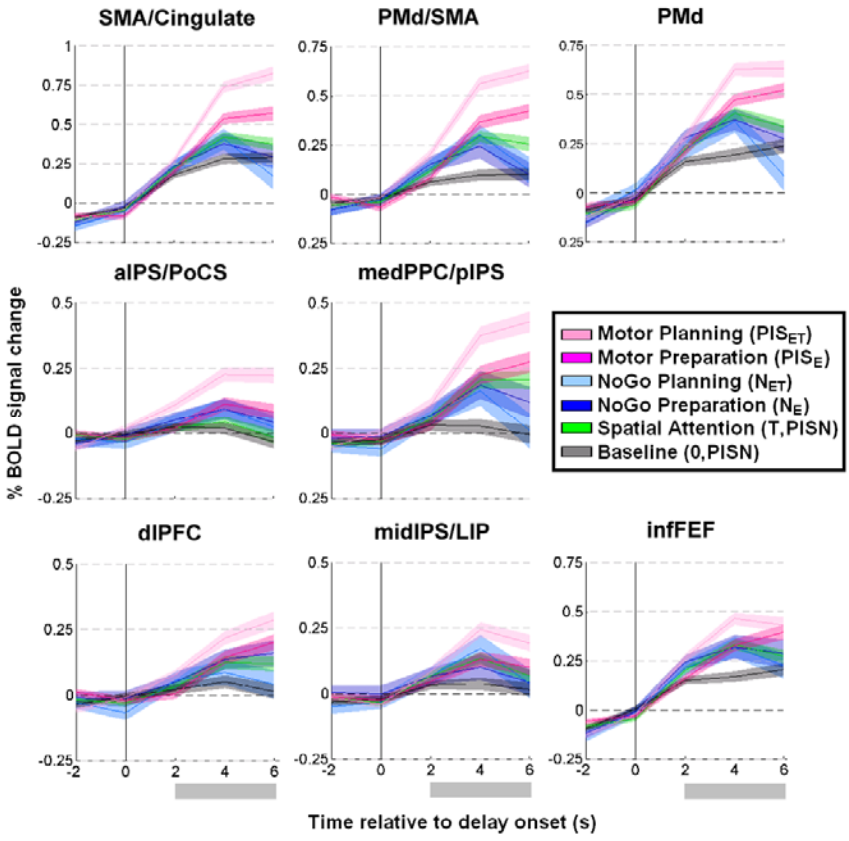

Fig. E2.2 – Deconvolved delay-period BOLD responses from motor planning ROIs shown in Fig. E1.1C demonstrate effector-specificity. The main ROIs identified as effector-specific in Experiment 1, and as playing a role in motor planning in experiment 2 (see Fig. E1.1), are also effector-specific in Experiment 2. Deconvolved delay-period BOLD activity is plotted relative to delay onset. The 1st Cue period (see Fig. 1B) starts 500ms before the beginning of the delay period, and explains the rapid rise in early BOLD activity in these ROIs.

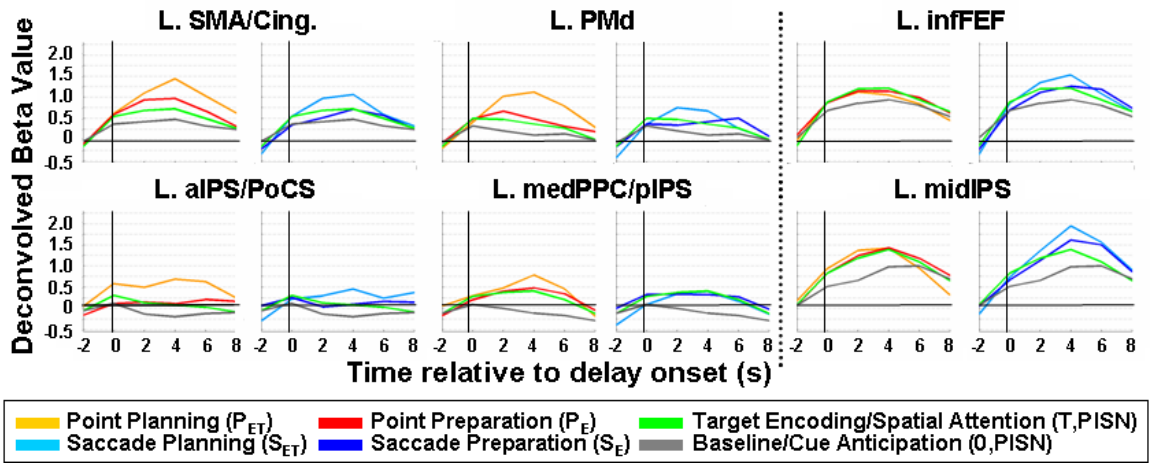

Fig. E2.3 – Rostrocaudal functional gradient in PMd and SMA
The caudal-most portions of left frontal ROIs with activity attributable to motor planning (Fig. E1.1C and Fig. E2.1) demonstrate absolute specificity for real and imaging point planning and real point execution. A) ERAs of caudal SMA/Cing., PMd/SMA, and PMd. B) The anatomical relationship between the main frontal ROIs identified in Figure E1.1C (pink), and the caudal-most, point-specific portions of these ROIs (orange) is shown. Talairach x, y, z coordinates for cSMA/Cing. (-5,-12,47); cPMd/SMA (-19,-19,56); and cPMd (-29,-17,59).

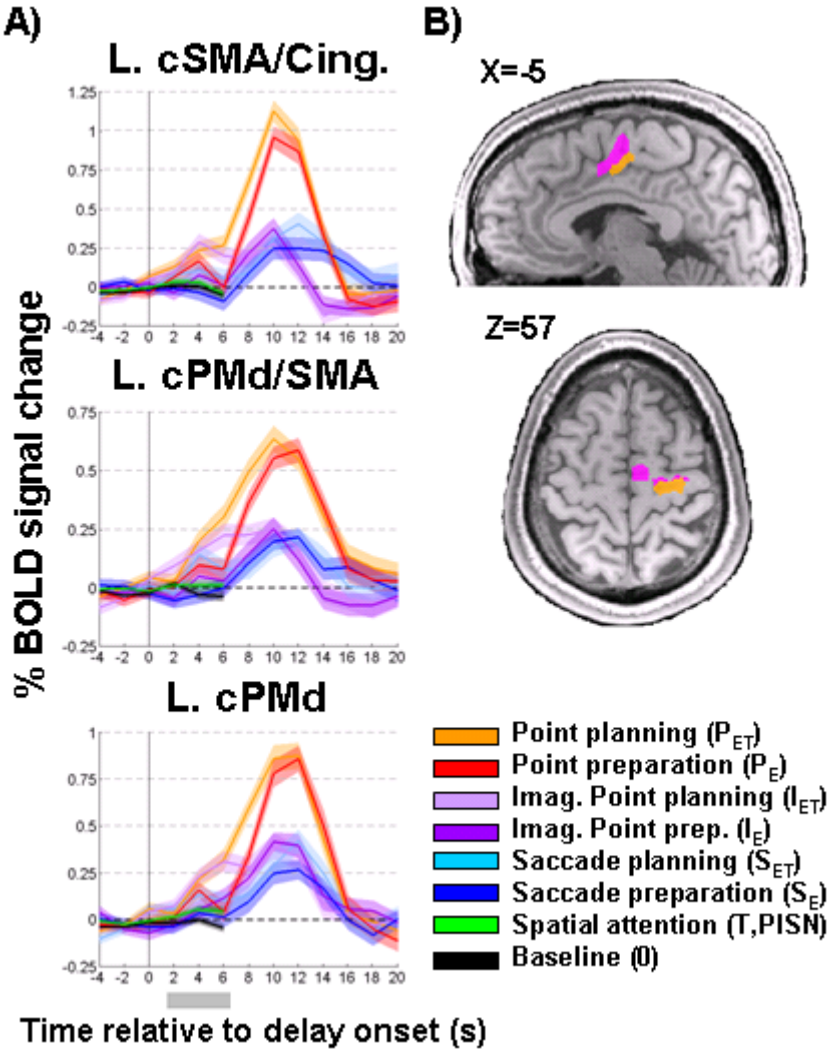

CHAPTER 3 - Other signals relevant for goal-directed action

3.1 While I've got your attention…

Experiment 2 described in the last two chapters revealed that the brain network involved in motor planning is also significantly active when either only the effector or the target are instructed.

The design of Experiment 2 allowed for the disambiguation of exogenous, retrospective spatial attention/working memory related to a flashed visual target, or endogenous forward attention/working memory independent of an upcoming movement, from endogenous spatial attention/working memory related to a prospective movement, via the contrast [$T>N_{ET}$] AND [T+]. Exogenous, "bottom-up" attention is usually stimulus-driven and reflexive, while endogenous, "top-down" attention is usually volitional. This same contrast also controls for visual stimulation, since the same visual target is flashed in both T and N_{ET} conditions. It simultaneously controls for initial perceptual cue and cognitive color-effector rule processing, since in N_{ET} trials the NoGo effector is instructed in the first cue period and the subject needs to recognize both that no future motor output is required and that the previously flashed visual target is irrelevant for action. The main distinction is that in N_{ET} trials, the effector cue instructs the subject that no future movement will be required. Activity in the frontoparietal network is highest when a movement is fully specified compared to when only the spatial goal of the movement is specified, and lowest when the pre-delay cues instruct the subject to withhold a movement ($M_{ET}> T > N_{ET}$). A prediction of BOLD activity based on retrospective visual cue/context processing and retrospective attention would be $M_{ET}=N_{ET}>T$, which is not the ordering observed in this brain network (Fig. I.3.1.i).

An additional control, a block-design fMRI delayed response experiment, was run in five subjects, who either had to prepare and execute a saccade, right hand point, or voluntary shift

of spatial attention to the remembered target location. Unlike the previous experiment, in this experiment the endogenous attention shift was unrelated to a prospective movement, and the experimental design did not resolve different task epochs. While a highly overlapping pattern of brain activity was observed for the saccade, point, and attention conditions, the saccade and point networks segregate as would be expected from Experiment 1 (Part I – Chapter 1). Additionally, there is an interesting effect of voluntary spatial attention. When no physical movement is specified, preparing and executing an endogenous shift of spatial attention to a particular location more strongly recruits the bilateral IPL, preSMA, IFG, and dlPFC than preparing and executing a saccade or pointing movement to the same location (Fig. I.3.1.ii, left, yellow map). Unlike a saccade, an endogenous shift of spatial attention does not generate sensory consequences. This distinction may be reflected in BOLD activity in the brain network most active during saccade execution, since this network is recruited to a greater extent during the saccade task than during the attention task (Fig. I.3.1.ii, left, blue). These patterns of activity were confirmed in the ERAs, though only the statistical parametric maps are pictured in Fig. I.3.1.ii.

There is greater overlap between the saccade and attention tasks than between the point and attention tasks, reflecting a tight coupling between attention and eye movements (see overlap of Attention+ and Saccade+ in Fig. I.3.1.ii., right).

Greater recruitment of the bilateral IPL, IFG, preSMA, and dlPFC during the endogenous attention task compared with the real movement tasks cannot be explained by differences in attentional or working memory load, since memory load (1 spatial target) was controlled across tasks. However, this phenomenon could be explained by the need to decouple the eye and attention, or because a voluntary shift of spatial attention involves an internal simulation similar to the imagined movement tasks explored in Part II of this thesis, perhaps approximating an imagined eye movement or gaze shift. This hypothesis is supported by the result from Experiment 1 (described in Part I: Chapter 1) that a direct comparison of imagined reach planning and execution compared conjunctively to real reach, saccade or nogo planning, and execution selectively engages the left IPL, IFG, preSMA, and dlPFC (Fig. I.3.1.ii B). The difference in laterality between the maps related to covert shift of spatial

attention and imagined reaching could be explained by the fact that only the right arm was used in Experiment 1 (contralateral to the dominant hemisphere). The saccadic eye movement network is fairly symmetrical across brain hemispheres. Therefore, if the attentional task approximates an imagined saccade movement, it follows that the imagined eye movement network, and hence activity during the attention task, would be similarly symmetrical.

Conclusions

Shifting spatial attention in the absence of overt movement engages much of the task-related brain network, though to a lesser degree than motor planning. Sustained delay activity is related not to a retrospective encoding of visual or context information or attention, but to a prospective encoding of spatial attention or working memory necessary for an upcoming movement (Fig. I.3.1.i) or an internal cognitive “shift” of attention that might approximate an imagined eye movement (Fig. I.3.1.ii). Findings from the built-in controls in Experiment 2 and a separate attentional control experiment suggest that, while this frontoparietal network may play a role in generalized spatial attention and the representation of space, it is also crucially linked to prospective action planning.

3.1 FIGURES

Figure I.3.1.i – Left: Spatial attention/working memory related to an upcoming movement, when the movement type is still unspecified ([T>N_{ET}] AND [T+]). PMv, infFEF, PMd, SMA, midIPS, and medPPC/pIPS are engaged in this prospective, effector-neutral process. Middle: Relative contribution comparison of M_{ET} vs. T, with M_{ET} > T in orange tones; T > M_{ET} in green tones; M_{ET} = T in white. Only part of the bilateral IFG/PMv is more engaged when only the spatial goal is known compared to when the full metrics of the movement are known. Right: If the movement is fully specified prior to the delay, and the subject can plan the upcoming movement, much of this same network becomes even more engaged ([M_{ET}>T] AND [M_{ET}+]).

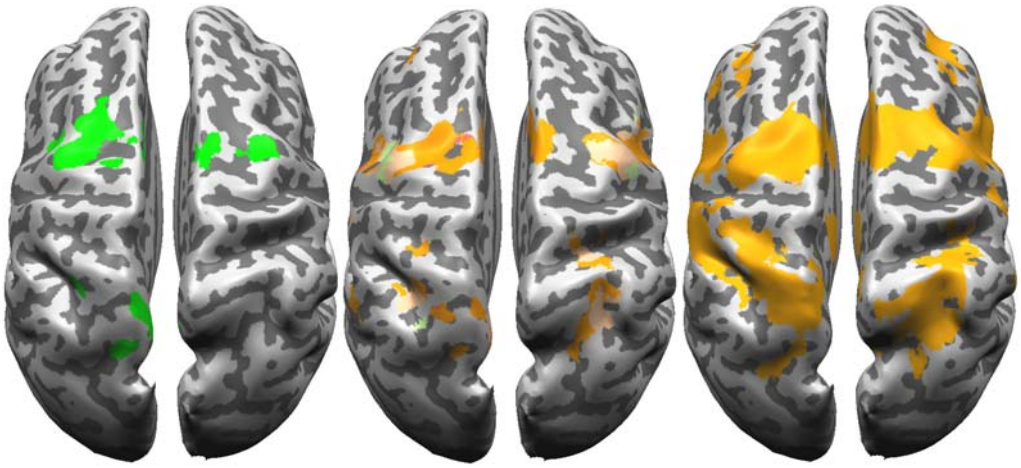

Figure I.3.1.ii – A) Left: Brain networks recruited more strongly by Saccade than Attention task (blue) or more strongly by Attention than by the Saccade or Point tasks (yellow). Middle: RC analysis of Saccade vs. Attention tasks. Most of the task-related network is equally recruited by the Saccade and Attention tasks (yellow), except for primary visual and infFEF areas (Saccade>Attention, blue), as well as IPL, pre-SMA, IFG, dlPFC, and left M1 (Attention>Saccade, but in M1 Point>>Attention, green). Right: Conjunction contrast of [Attention+] in every subject (green) and [Saccade+] in every subject (blue) shows strong overlap of activations for the two tasks. B) Previous experiment (Experiment 1 in Part I: Chapter 1) - Imagined reach planning and execution > AND (Real reach, Saccade, Null planning and execution)

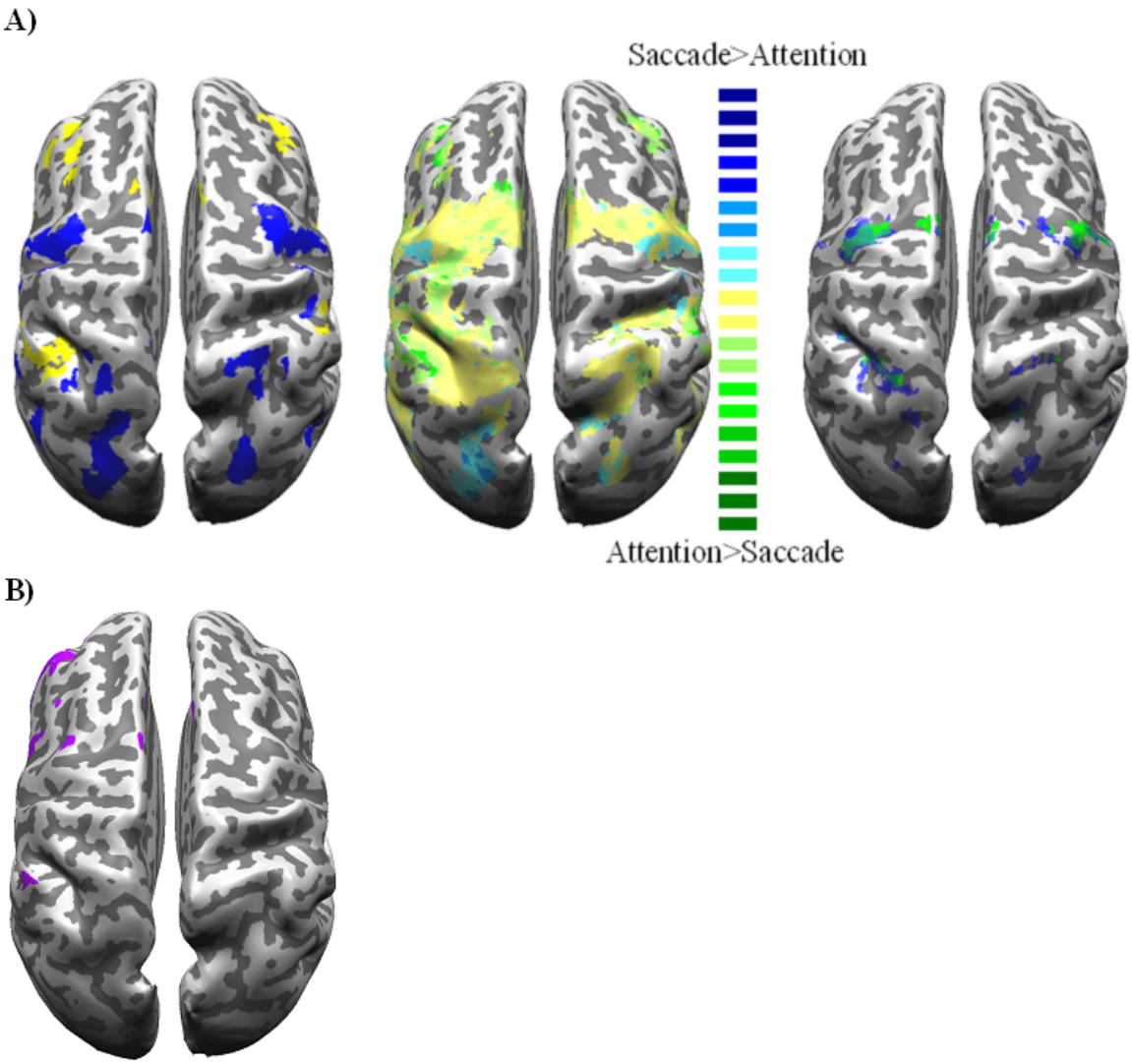

3.2 Where I see what I see - Sensory and bottom-up attentional effects of central vs. peripheral visual cueing

In the traditional delayed response task, a visual cue is used to instruct an upcoming movement. This cue period is usually just prior to a memory delay period. Because the PPC receives such strong sensory visual input, it is possible that a large cue response could preclude the observation of modulations of delay BOLD activity due to the effector used, the processes engaged during the delay period, or other variations in task parameters and demands. Also, much of the frontoparietal cortex plays a role in spatial attention. Therefore, the spatial location of task-relevant stimuli could affect both bottom-up (exogenous) and top-down (endogenous) allocation of attention.

A single subject was scanned in two similar delayed response tasks in order to investigate any effects of central (foveal) vs. peripheral visual cueing in the frontoparietal brain network. In one task variant, the effector cue was presented centrally as a change in the color of the fixation spot, while in the other task variant the effector cue was presented peripherally, as a change in the color of the target cue (Figure I.3.2.i). In both tasks, the effectors instructed were included a right hand point (red cue), a saccade (blue cue), or nogo (yellow cue). The central cueing paradigm was the same paradigm employed in the effector-specificity experiment in Chapter 1, while the peripheral cueing paradigm was employed in the motor planning experiment in Chapter 2.

One possible confound of the current experiment as a basic investigation of central vs. peripheral visual instruction is that the target/goal was always instructed in peripheral vision, and that there are two relevant cue locations/stimulus changes in the central cueing paradigm, and only one in the peripheral cueing paradigm. The goal of this experiment was not to elucidate the brain networks involved in central vs. peripheral vision, but instead to consider how to minimize the cue response in the frontoparietal network to better facilitate other experimental investigations of delay period activity in the network.

Cue-responsive brain areas, including many ROIs in the frontoparietal network, exhibit increased BOLD activity when the effector cue is presented centrally compared to when it is presented peripherally (Figure I.3.2.iiA and B). This effect is evident in both direct contrast and relative contribution comparisons of the central vs. peripheral cue predictors, across trials instructing all effectors. To better quantify the difference between cueing paradigms, a Relative Cue Selectivity (RCS) index was calculated (Figure I.3.2.iiC; similar to the RES index calculated in Chapter 1, see *Methods* for that chapter).

As expected, bilateral V1 that responds to foveal visual stimulation demonstrates absolute selectivity for central vs. peripheral cueing. In the rest of the cue-responsive brain network, central effector cueing engages these areas to a greater degree than peripheral effector cueing, but the effects are relative and not as dramatic as in V1. Neural processing in the entire cue-responsive brain network is also likely to be modulated by bottom-up attentional orienting and top-down spatial attention; thus, these cue period differences probably reflect both differential visual stimulation and attention.

These findings highlight the importance of using peripheral visual cues where possible in any detailed fMRI investigations of delay period activity in order to minimize the visual cue/attentional response that could otherwise confound delay period BOLD activity.

3.2 FIGURES

Figure I.3.2.i – Central (CC) vs. peripheral cueing (PC) paradigms. Left: Task schematic. In both task, a color rule instructs the effector to be used on a given trial. Right: In the PC task, both target and effector were cued at the same peripheral location, while in the CC task, the target was cued peripherally and the effector was cued centrally.

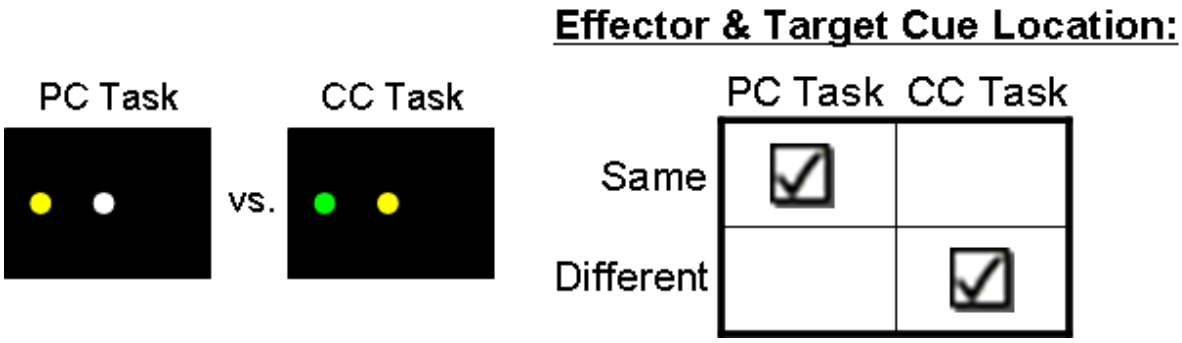

Figure I.3.2.ii – Central vs. peripheral visual cueing. The majority of the cue-related network is more strongly engaged when the effector cue is presented centrally than when it is presented peripherally. The largest differences between central vs. peripheral cueing are in occipital cortex (V1l, VP); these effects are damped but still visible in frontoparietal brain areas. A) Relative contribution map for central vs. peripheral presentation of the effector cue. B) Direct GLM contrast map for central vs. peripheral cueing. C) The Relative Cue Selectivity (RCS) index was calculated similarly to RES, discussed in the *Methods* in Chapter I.1 of this thesis. A value of +1 indicates absolute selectivity for central vs. peripheral cues; a value of +0.33 indicates that the BOLD response to the central cue is twice the value of the response to the peripheral cue; negative RCS values would indicate selectivity for peripheral vs. central visual cues.

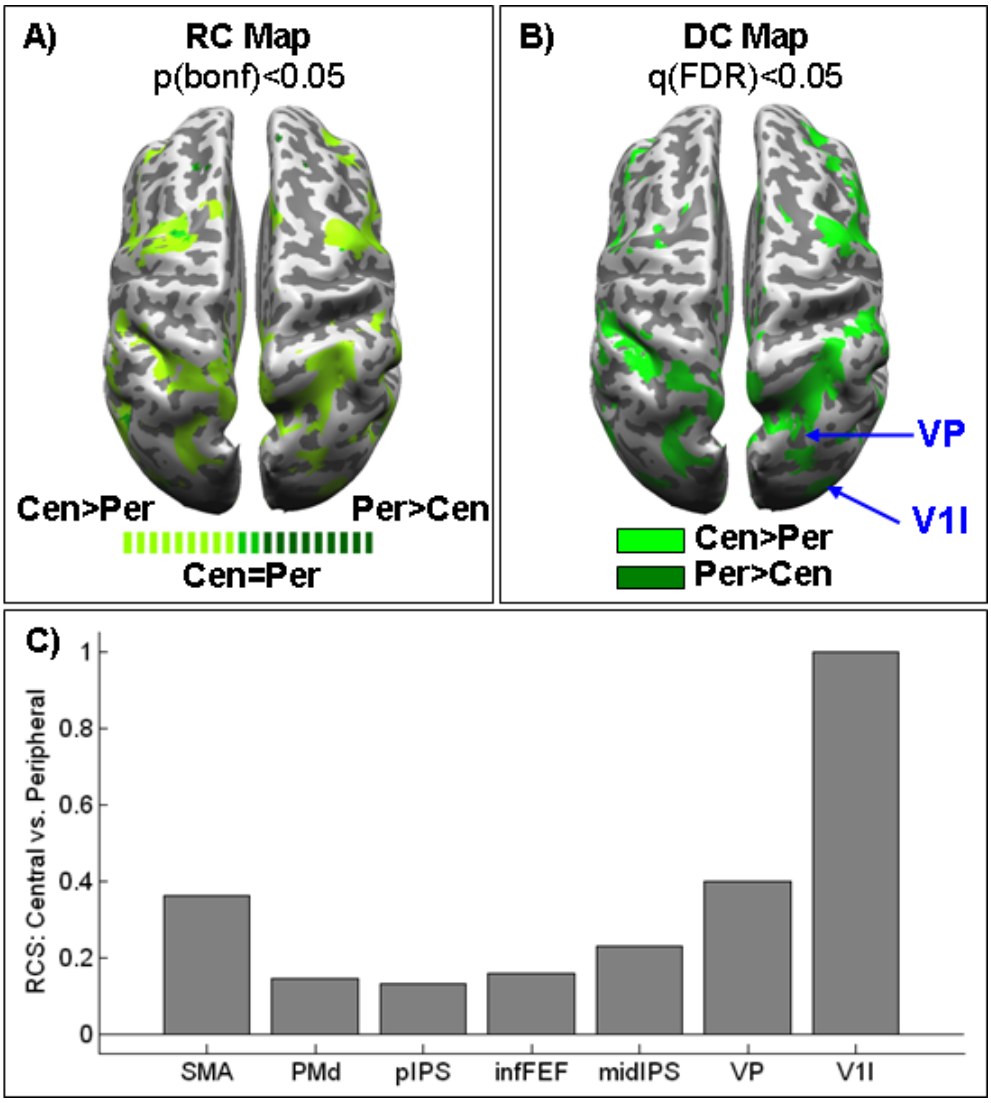

3.3 What's the point of reaching? Arm reaching activates the frontoparietal network more than hand/finger pointing

In Part I: Chapter 1, I provided evidence of effector-specific brain networks that are differentially engaged during the planning of goal-directed arm and eye movements. Effector-specificity is an additional argument for a motor-related, instead of a pure attentional/spatial, role of the PPC, SMA, and PMd. However, the kinds of computations and sensory expectations involved in planning and executing arm and eye movements might bias the relative engagement of these two circuits, including the need for additional coordinate transformations for arm movements and the fact that the arm activates a more lateralized brain network than saccadic eye movements (also see Chapter 3.4 and discussion of laterality related to the arm used).

The existence of modulations of the arm-specific motor planning network by the type of arm movement employed would provide additional evidence of an action-related role for nodes in the network, particularly since the same coordinate transformations would be necessary across movement types while the kinematics of the instructed movements vary. Here, I present evidence that the type of arm movement employed in a delayed response task modulates BOLD activity in the arm-specific motor planning network, with more kinematically complex movements (e.g., reaching) recruiting this network to a greater extent than simpler movements (e.g., pointing). This computational/kinematic complexity effect applies to both real and imagined arm movements.

A single subject was scanned in a block design fMRI experiment, using a traditional delayed response task with four effectors: Point (P), Imagined Point (IP), Imagined Reach (IR), or NoGo (N). A direct comparison of IR vs. IP revealed that imagined reaching more strongly recruits the left PPC (aIPS, pIPS, medPPC) and PMd than imagined pointing (Figure I.3.3.i.A) The effect was also evident in the timecourses from the SMA, but was not significant at q(FDR)<0.05 in the direct GLM contrast comparison. Because no real movement is made in either the IR or IP blocks, and visual stimulation was identical across

all block types, these signal amplitude differences cannot be explained by differential sensory input. Similarly, both IR and IP trials require the transformation of a visual target into a coordinate frame appropriate for arm movement. Therefore, increased activity on IR compared to IP trials probably reflect the more complicated kinematics of the imagined movement, including longer trajectory travel and the involvement of more joints during imagined reaching (elbow + wrist in IR trials vs. wrist only in IP trials). IR activated the pIPS and SMA more than real pointing, despite the generation of somatosensory consequences in real pointing trials (Figure I.3.3.ii.B). In medPPC and PMd, while IR > IP, P ~= IR, probably due in part to the somatosensory consequences of movement and efference copy.

Since arm reaching (at least the imagined variety) seems to activate the frontoparietal motor planning network more than hand/finger pointing, we decided to resolve this modulation in different task epochs. A new single subject was scanned in two event-related delayed response experiments, one employing real hand/finger pointing, and one employing real arm reaching.

Both relative contribution and direct contrast comparisons between real reach and real point trials (whole-trial, includes the delay and response but not cue periods) reveal that the frontoparietal motor planning network is more strongly recruited during reaching (Figure I.3.3.ii). Brain areas related to motor execution, including M1 arm, S1, putamen, posterior insula, thalamus, and cerebellum, are more active during real reach execution than during real point execution, reflecting the increased kinematic complexity of the movement, but amongst these ROIs only the putamen is also active during the delay period. In contrast, the M1 hand knob is recruited by both reach and point execution, as expected since both movements involve hand kinematics.

The statistical maps and ERA timecourses demonstrate that parts of the dlPFC and premotor cortex along the PrCS and medial wall, while arm-specific (compared to the eye), do not differentiate between real reaching and pointing during the delay period. Typically thought to play a role in motor planning, the fact that delay period BOLD activity in these areas does not reflect the additional movement complexity suggests either that these areas are

downstream of the brain areas computing the movement plan, or that this fMRI/task technique is not able to resolve the distinction. The latter possibility seems unlikely given the delay period activity profiles in arm-specific ROIs in the PPC (pIPS, aIPS) and the PMv, which are more strongly recruited during real reach planning than during real point planning. A direct contrast comparison between reach and point delay predictors and an exploratory investigation of ERA timecourses revealed no delay-period differences between reach and point in any part of primary or secondary somatosensory cortex. Hence, the higher profile of activity in pIPS, aIPS, and the PMv during reach planning is likely not explained by a difference in the somatosensory inputs to these areas between arm movement types. Instead, it is likely that these brain areas are involved in the computations related to the transformation of a visual target/goal into a movement plan, and that a computational, rather than a somatosensory, difference between reach and point trials explains the BOLD activity in these ROIs.

Conclusions

Reaching (both real and imagined), compared to pointing, is a more potent driver of BOLD activity in the cortical networks related to arm movement planning and execution. Reaching movements are more kinematically complex and traverse a longer trajectory path than pointing movements; hence, they are likely to require additional computations in both the delay/motor planning and go/motor execution phases of the task. Response period differences were observed in the entire network, including frontoparietal and motor execution-related areas, but only the pIPS, aIPS, and PMv distinguished between reaching and pointing during the delay period. Thus, we propose that these brain areas are critically linked to the planning of arm movements, and reflect the computational complexity associated with a movement. This finding provides additional evidence of a motor- rather than a simple attentional functional role of the PPC.

3.3 FIGURES

Figure I.3.3.i – A) Direct GLM comparison of Imagined Reaching vs. Imagined Pointing reveals stronger recruitment of the PPC (aIPS, pIPS, medPPC) and PMd during imagined reaching. B) ERA BOLD timecourses from frontoparietal ROIs, showing amplified activity during imagined reaching compared to imagined pointing blocks, and transition from recruitment during both real and imagined arm movement (left) to recruitment during mainly real arm movement (right). Control ROI M1 is only active during real point blocks.

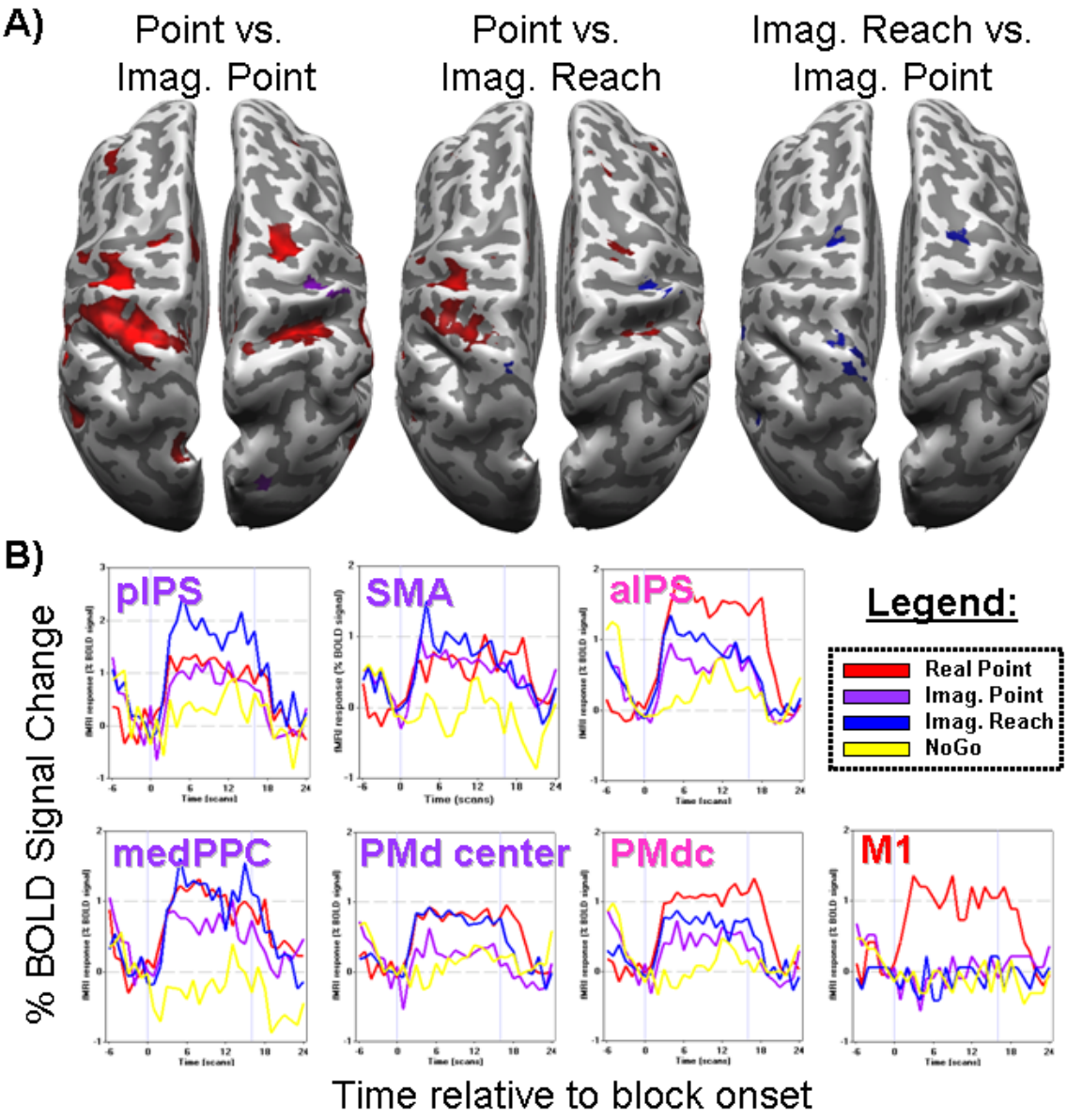

Figure I.3.3.ii – Event-related fMRI investigation of arm movement type and effects on motor planning and motor execution. Whole-trial (delay+response periods) RC and DC comparisons show that the motor planning network is more strongly recruited by real reaching than by real pointing. The M1 hand knob/S1 hand, however, is equally activated by both, as are parts of the PrCS. ERA BOLD timecourses from frontoparietal and motor execution control areas reveal that three ROIs (pIPS, aIPS and PMv) are more active during planning of reaches than points, while frontomotor dlPFC, SMA, and PMd do not differentiate between reach and point planning. All ROIs, except the M1 hand knob, are more active during reach execution than during point execution.

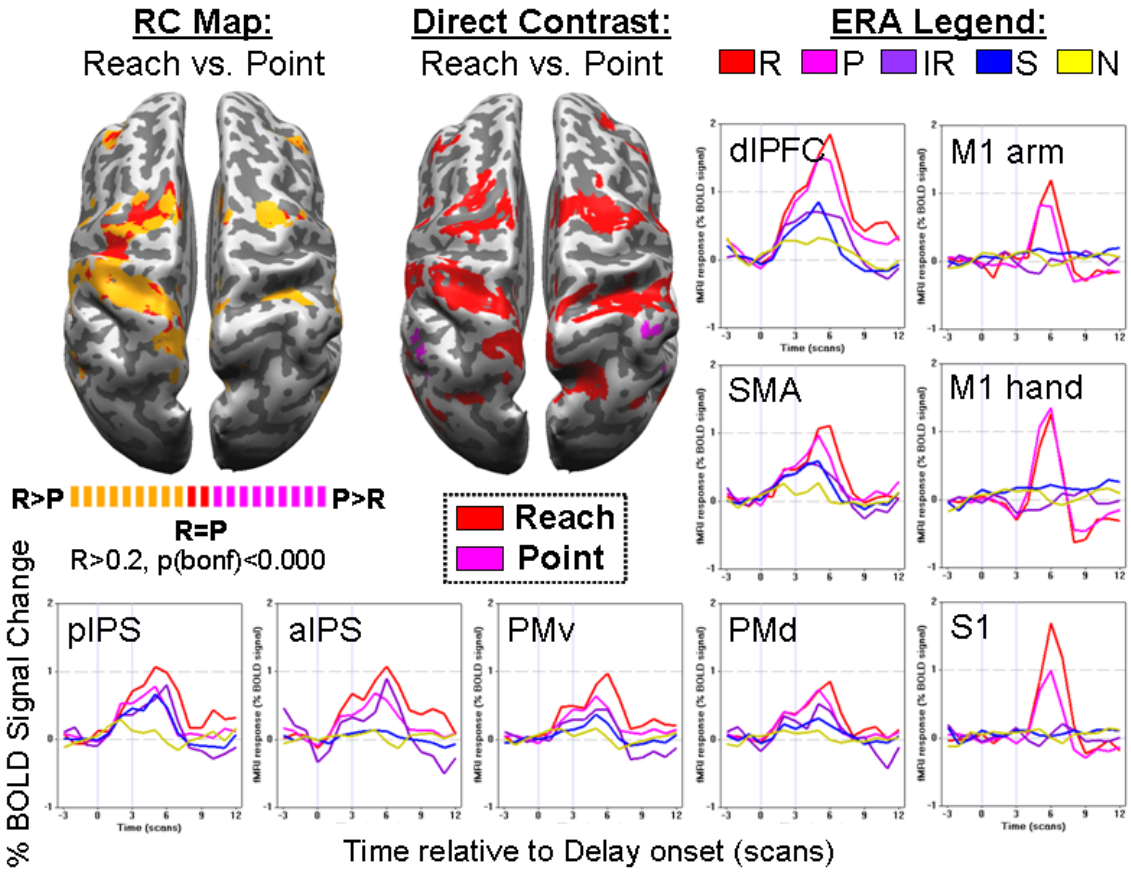

3.4 – On the one hand, on the other hand: Differential degree of contralaterality for the arm used in motor planning and motor execution areas

In order to assess the degree of contralaterality for the arm used in motor planning and motor execution areas of the brain, a single subject was scanned in a block design fMRI experiment. The task paradigm was a typical memory delayed response task, where the effector cued on a given block was either 1) reach with the right arm(R-RA), 2) reach with the left arm (R-LA), 3) imagined reach with the right arm (IR-RA, 4) imagined reach with the left arm (IR-LA), 5) saccade (S) or 6) nogo/fixation (N). The current experiment utilized a block design task; hence, it was not possible to separately consider arm laterality during the delay (motor planning) and go (motor execution) periods. Therefore, we note that it is possible that the arm is encoded differentially during these two trial epochs.

A GLM that modeled the different task block types (R-RA, R-LA, IR-RA, IR-LA, S, and N) was used to test for task-related brain areas and arm laterality. There is very strong overlap in brain activity during the use of the right and left arm in both real and imagined reaching blocks, when compared to nogo/fixation (a control for visual stimulation). This overlap is pictured in Figure I.3.4.i for the real reaching blocks only, as is a conjunction of the two contrasts [R-RA > N] AND [R-LA > N]. Both direct contrast comparisons and relative contribution (RC) maps for reaching with the right arm vs. left arm reveal strong contralaterality in primary somatomotor cortex (M1/S1), the medial wall cingulate motor area (CMA), putamen, thalamus (Thal), and posterior insula. These areas are most active during movement execution compared to movement planning (see Part I: Chapter 1); hence, contralateral arm selectivity is expected. In addition, the cerebellum (Cereb) strongly represented the ipsilateral arm, also as expected. The rest of the frontoparietal network was only very weakly contralateral for the arm used. However, the RC map in Figure I.3.4.i suggests that arm contralaterality may be stronger in the right hemisphere. It is possible that this effect that may be related to handedness. The experimental subject was left-handed; therefore, the left arm may be more robustly represented than the right arm in the brain.

Next, we looked at the timecourse of BOLD activity in our ROIs to better observe arm laterality effects. Consistent with the GLM results, brain areas that are active during both real and imagined arm movement planning (pIPS, medPPC, SMAr/center, PMdr/center) exhibit little to no contralaterality for the arm used (Figure I.3.4.ii), but demonstrate slightly stronger contralaterality in the right hemisphere. In contrast, areas that are involved preferentially in planning and executing real arm movements compared to imag. arm movements (aIPS, SMAc, PMdc) demonstrated stronger contralateral arm selectivity, while absolute contralateral arm selectivity was observed in motor execution areas M1, S1, and Thal, and absolute ipsilateral arm selectivity was observed in the cerebellum (Cereb).

Conclusions:

Motor execution-related areas including M1/S1, CMA, the putamen, thalamus, and posterior insula were all strongly contralateral for the arm used, as expected. Similarly, the cerebellum was strongly ipsilateral for the arm used to reach. The more interesting finding is weaker contralaterality in ROIs in the frontoparietal motor planning network, including parietal areas pIPS, medPPC, and aIPS and frontomotor areas SMA and PMd. The degree of contralaterality observed in these brain areas is consistent with their relative level of activity during arm movement planning vs. arm movement execution (see event-related timecourses in Part I: Chapter 1) and level of recruitment during imagined arm movements. Arm contralaterality increases with the ratio of relative BOLD signal amplitude observed during the go/delay periods of the task in Part I: Chapter 1, while decreasing with decreased involvement in imagined arm movements (Figure I.3.4.ii). This effect is particularly evident in the transition from SMAr→SMAc→CMA on the medial wall and PMdr→PMdc→M1 on the superior cortical surface. Therefore, it is possible that laterality for the arm used is differentially encoded during motor planning and motor execution. Planning a movement with either arm may activate the bilateral motor planning network, with a mild degree of contralaterality, while executing a movement may predominantly activate the contralateral cortical motor execution network.

Since motor planning areas pIPS, SMA, and PMd are arm effector-specific (compared to saccade, see Part I: Chapter 1) but exhibit weak contralaterality for the arm employed, it may be possible to decode movements of either arm by implanting a cortical neural prosthetic device into only one brain hemisphere.

3.4 FIGURES

Figure I.3.4.i – Laterality for the arm used during reaching. Brain areas with the strongest links to motor execution, including M1/S1, CMA, Thal, putamen, and posterior insula, exhibit absolute arm contralaterality. In contrast, frontoparietal motor planning areas exhibit weaker, relative arm contralaterality. RC = Relative Contribution analysis, see *Methods* in Part I: Chapter 1.

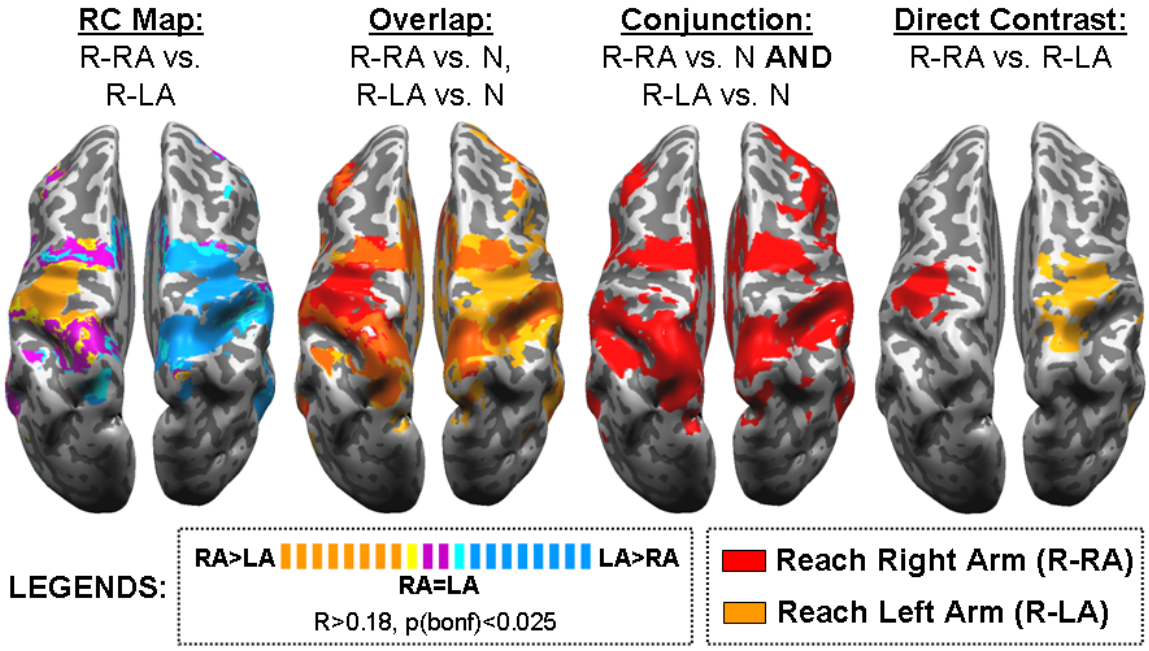

Figure I.3.4.ii – ERA BOLD timecourses (Time vs. % BOLD Signal Change) from left hemisphere, arm movement planning and execution ROIs. Only ROIs from the left hemisphere are displayed; however, the pattern of arm laterality completely reverses in the right hemisphere: the left hemisphere is dominant for the representation of movements of the right arm, while the right hemisphere is dominant for the representation of movements of the left arm.

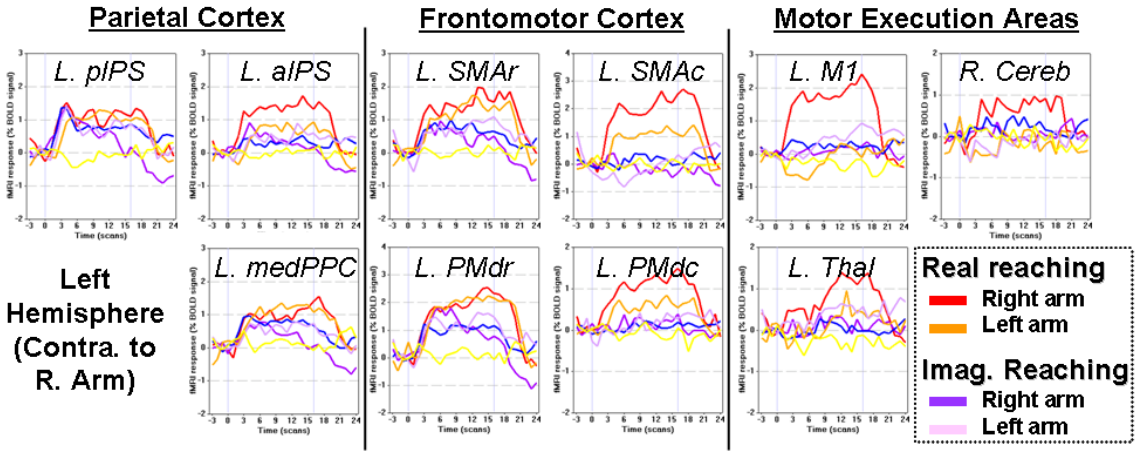

3.5 Pre-posture-rous – Limb posture affects delay period BOLD activity in frontal and parietal cortices

Introduction

Posterior parietal cortex receives not only strong visual sensory input, but also tactile somatosensory and proprioceptive inputs from the anterior parietal lobule. In order to plan an arm movement, information about the current state of the limb needs to be combined with information about the desired goal/target of the movement. This raises certain questions: How does hand posture affect activity in brain areas involved in effector-specific motor planning? Are any postural modulations due to enhanced somatosensory input to brain areas, or instead due to a direct influence of arm posture on the computational processes involved in motor planning? Does a change in hand posture differentially affect the arm- and eye-specific networks?

To answer these questions, a single subject was scanned in two traditional delayed response tasks. In both tasks, the subject had to plan and execute hand pointing or saccadic eye movements to the remembered location of a flashed visual target. However, between tasks the posture of the hand/arm was varied. In the first task, the subject maintained a static hand posture with the index finger pointing at the central fixation spot throughout the experimental run, unless making a cued hand movement. This fixational hand posture was maintained throughout arm movement, eye movement, and nogo trials. In this second task, resting hand/arm position (when the subject was not executing a cued arm movement) was a loose fist on the chest, with no fixational element. Therefore, the subject's general arm- or action-readiness may have been enhanced in the posture task compared to the second, no posture task. Only during the go period on trials when the subject was executing a cued arm movement did this arm posture change. Task schematics appear in Figure I.3.5.i.

Model-based and BOLD timecourse analyses (standard techniques, compare with I.4.1)

The effect of hand posture was studied separately for arm and eye movement planning and execution. The left side of Figure I.3.5.ii shows the GLM activation maps for the Saccade

Delay predictor with (light blue) and without (dark blue) a static hand posture relative to their respective NoGo control predictors; at right is the relative contribution map of the Saccade Delay (with hand posture) and Saccade Delay (without hand posture) predictors.

A limb posture that is task-engaged biases the differential activation of the arm- and eye-specific planning networks even when no limb movement is instructed on that trial. When there is a static fixational arm posture compared to when there is no posture of the arm, eye movement planning more strongly recruits the arm-specific network, and less strongly recruits the eye-specific network. This finding indicates an upregulation of the arm-specific network and a downregulation of the eye-specific network when there is a fixed, task-engaged hand posture. However, this trend is only evident in the saccade planning trials; postural modulations during point planning trials will be discussed below. This network shift based on hand posture may reflect the induction of default arm movement planning circuits that become active when the arm is in a posture that is "ready" for movement compared to when it is in a fully relaxed resting posture, or could reflect an increased difficulty in dissociating eye- and arm-movements on saccade trials (see movement vector overlap in Figure I.3.5.i).

An alternative explanation of this finding is related to coordinate reference frames. Monkey PRR and LIP represent movement targets in a retinotopic reference frame, while Area 5 and PMd have more complicated reference frames, with neurons that either separately code in retinotopic and arm-centered reference frames or encode the spatial relationship of the arm, eye, and target. Because both the eyes and the arm are "fixating" the central fixation spot in the hand posture task, the retinotopic movement vector is identical for both eye and arm movements (see Figure I.3.5.i). There is a very close association between starting arm- and eye-position and the arm- and eye-movement vectors in the posture task. Therefore, on saccade trials the in-plane movement vector could more easily activate the default arm movement planning network, or there may be a lower threshold for coordinated eye and arm movement because of the tighter coupling, thereby engaging the brain network involved in planning arm movements. However, we may then expect this movement vector-overlap

modulation to generalize to an upregulation of the eye movement network during arm movement trials, which is not the case.

To further investigate this postural shift, we looked at the effect of a static hand posture on delay activity during trials when an arm movement is instructed. Rather than appearing as an independent, postural modulation riding on top of an effector-specific modulation, static hand posture interacts differently with the existing signals in nodes of the motor planning network.

The overall pattern observed was that when there was no static hand posture during the experimental run, point planning more strongly recruited the arm-specific motor planning network (PMd, PPC), and point execution more strongly recruited the arm-execution network (M1, S1). Hence, a task-engaged hand posture linked to enhanced proprioception, somatosensation, or enhanced "action readiness" does not appear to be the dominant effect in the arm-specific brain network. However, merely instructing an upcoming hand movement may be sufficient to "ready" the arm for movement, thus masking any potentiation of "action readiness" due to the presence of a task-engaged arm posture. In saccade trials, a task-engaged hand posture could enhance arm-movement readiness in the way that a flashed visual target attracts bottom-up, reflexive attention and is likely to induce an eye movement.

Another explanation for the finding that point trials in the no posture task more strongly recruiting the arm planning/execution network than point trials in the posture task is that the movement vector for the no posture vs. the hand posture task was always longer (the hypotenuse of the triangle), and the no posture task not only required wrist rotation but also extension of the index finger. Thus, point planning and execution in the no posture task may be more computationally demanding than during the posture task, which may explain the effects observed in Figure I.3.5.iii.

The ERA timecourses in Figure I.3.5.iv reveal more detailed information regarding the effects of hand posture across the motor planning network. The SMA and PMd are strongly modulated by a static hand posture on both point and saccade trials at the beginning of the

delay period. At the end of the delay period, however, the main modulation of BOLD activity is due to the effector to be used (arm>eye). This pattern of activity would be consistent with a bottom-up default arm movement plan "activated" by a static hand posture on saccade trials, and then cognitively overridden such that these ROIs reflect the selected upcoming movement at the tail end of the delay period.

In the parietal cortex, aIPS shows a combinatorial modulation by hand posture (posture>no posture) and by effector (arm>eye), while pIPS is strongly modulated by hand posture and by effector in a more interactive way. If hand posture and effector were fairly independently encoded (as appears to be the case in aIPS), the top curve in arm-specific pIPS would be Point w/ posture, and the bottom curve with would be Saccade w/out posture. Since this is not the case, rather than an independent coding of posture and effector, it appears that pIPS encodes a signal related to a default arm movement plan that may be triggered by the ready hand posture. While the default plan in frontomotor cortex fades as the delay period progresses to reflect the selected action, the persistence of a default arm-movement plan in pIPS might be important for flexible, goal-directed behavior in a dynamic environment. The possibility that the persistence of a default movement plan in pIPS helps to facilitate rapid changes to existing action plans warrants further study.

M1 is more active during point execution in the no posture task than in the posture task, suggesting a greater movement complexity (computationally or kinematically) in the no posture task. If planning the arm movement vector in the no posture task was more computationally expensive than planning the arm movement vector in the posture task (as proposed earlier in this section), then in arm-specific motor planning ROIs we would expect the delay period activity rise above baseline to be higher (Point w/out posture curve would be above the Point w/ posture curve), which is not the case (except perhaps in PMd). However, since many of these same brain areas encode a hand posture, it is possible that separate modulations of the BOLD signal by hand posture (posture task>no posture task) and any modulation of BOLD signal by increasing movement complexity or distance to target (no posture task>posture task) are confounded in the ERA timecourses. A future experiment that both independently and combinatorially considers posture and movement

complexity/distance would be necessary to disambiguate the two signals during motor planning.

Conclusions:

Two delayed response tasks, one with a static, task-engaged arm posture and one with a resting arm posture were used to investigate the questions of whether posture affects brain activity in the motor planning network, whether postural effects are due to enhanced somatosensation or are more directly related to the computational requirements for motor planning, and lastly whether arm posture differentially modulates activity in arm-specific and eye-specific brain areas.

Hand posture does modulate activity in the motor planning network, but the presence of a static, task-engaged posture does not enhance delay period activity in either M1 or S1 (see Figs. I.3.5.iii and I.3.5.v). Hence, postural effects observed in frontal and parietal cortices are not likely to simply reflect differential sensory input. Instead, tactile and proprioceptive sensation probably interacts with the perception of body space and the computations necessary for motor planning, including default motor planning.

During saccade trials, the presence of a static arm posture enhances recruitment of the arm-specific planning network and dampens recruitment of the eye-specific planning network, relative to activity when there is a resting arm posture. Across the whole task-related brain network, a “ready” arm posture increases delay activity more in saccade trials than in point trials, which overall minimizes the differences between these two effectors. At the beginning of the delay period, frontal secondary motor areas SMA and PMd seem to reflect a default arm movement plan, which is then refined by the end of the delay period to reflect a selected arm- or eye-movement plan (with arm>eye). AIPS reflects both an arm movement plan and the position of the arm, while pIPS encodes both selected arm movement plans as well as a default plan arm plan on saccade trials when the subject maintains a task-engaged, “ready” hand posture. The enhanced activity in arm-specific planning areas on saccade trials of the posture task may be a signature of the tight coupling between starting eye and arm positions and movement vectors throughout the task, or could reflect greater posture-induced arm

motor readiness mediated by sensory input or motor attentional processes. In contrast, the eye-specific planning network (including infFEF, SEF, and midIPS) is most engaged during saccade planning in the no posture task.

Planning the arm movement vector may be more computationally intensive in the no posture task than in the posture task, supported by the fact that M1 and S1 are more strongly recruited during motor execution in the no posture task, which could be a hallmark of more complicated kinematics. Even though we were able to rule out a simple somatosensory explanation of postural effects, unfortunately we were not able to disambiguate spatial perception (including body-world relational space) from movement complexity, both of which are relevant for the successful preparation and execution of goal-directed actions.

3.5 FIGURES

Figure I.3.5.i – A) Differences between the posture and the no hand posture tasks. B) Schematic diagram of the posture and no posture tasks. The blue dotted line is the saccade movement vector, which is the same across both tasks. The bright red dotted line is the hand movement vector in the posture task. The dark red dotted line is the hand movement vector in the no posture task.

A) **<u>No posture (NP) vs. posture (P) task differences:</u>**

1) Same retinotopic target position

2) Different starting hand position
   - P task: 'movement ready'
   - NP task: 'resting' position

3) Movement vector and angle for eye and arm movements same in P task, different in NP task

4) The distance traveled by the index finger is greater in the NP than in the P task, as **$|c| > |a|$**, and in the NP task, subject needs to plan to both extend the finger and rotate the wrist, instead of a simple wrist rotation

B)

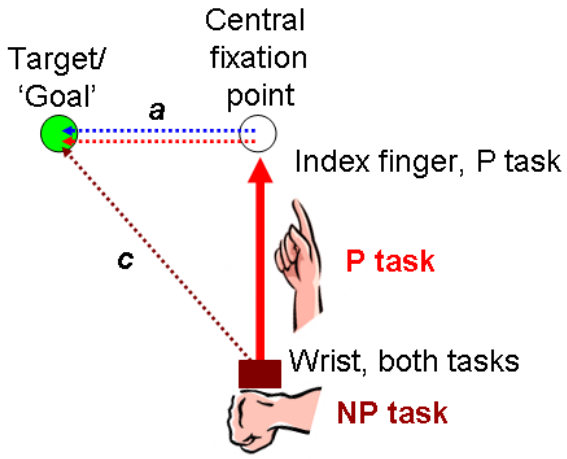

Figure I.3.5.ii – Left: Activation maps for Saccade Delay predictors compared to NoGo Delay predictors, with a static hand posture (light blue) and without a static hand posture (dark blue). Threshold is q(FDR)<0.05. Right: RC map for Saccade Delay predictors with static hand posture (light blue), and without static hand posture (dark blue). The medium blue color signifies that the two predictors contribute roughly equally to the GLM. Note that despite substantial overlap in the map (at left), the eye-specific network including bilateral infFEF, SEF, and LIP is more strongly recruited when there is no static hand posture, and the arm-specific network including the PMdc, aIPS, and medPPC/pIPS is more strongly recruited with there is a static hand posture (at right).

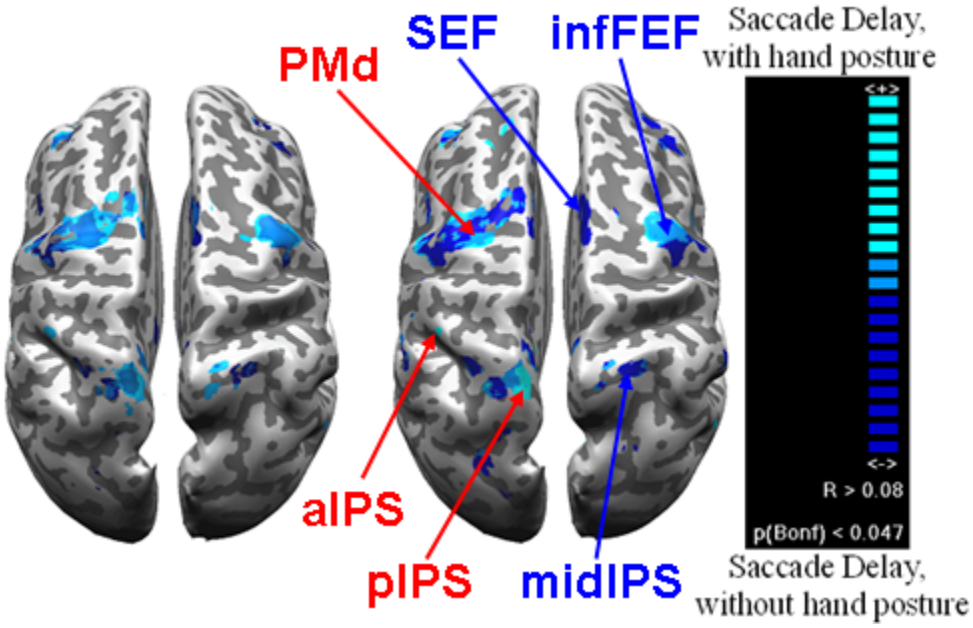

Figure I.3.5.iii – Direct GLM test for posture: Point no hand posture (dark red) vs. Point with hand posture (orange). Threshold at q(FDR)<0.05.

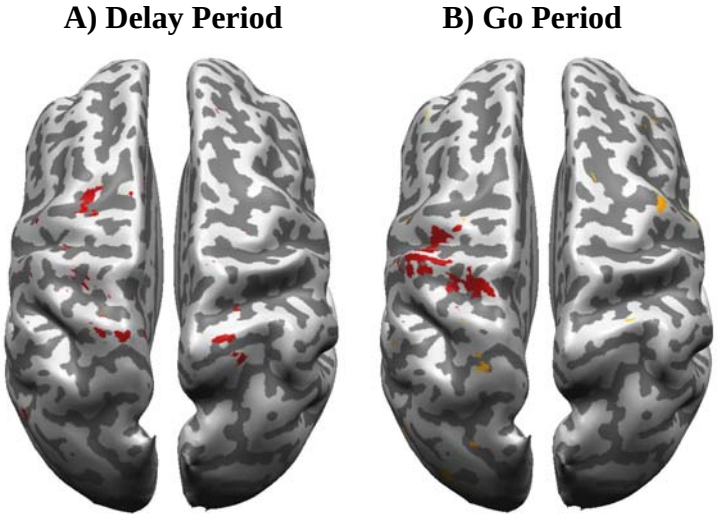

Figure I.3.5.iv – Effects of hand posture in arm-specific and eye-specific brain networks. Left: RC Map for Point Delay predictors without and with static hand posture. Right: RC Map for Saccade Delay predictors without and with static hand posture. Middle: ERA timecourses from select ROIs. SMA, PMd, aIPS, and pIPS are arm-specific; infFEF and midIPS are eye-specific. ERAs are calculated relative to the NoGo curve in each task, which subtracts out BOLD activity related to initial visual cue/context processing.

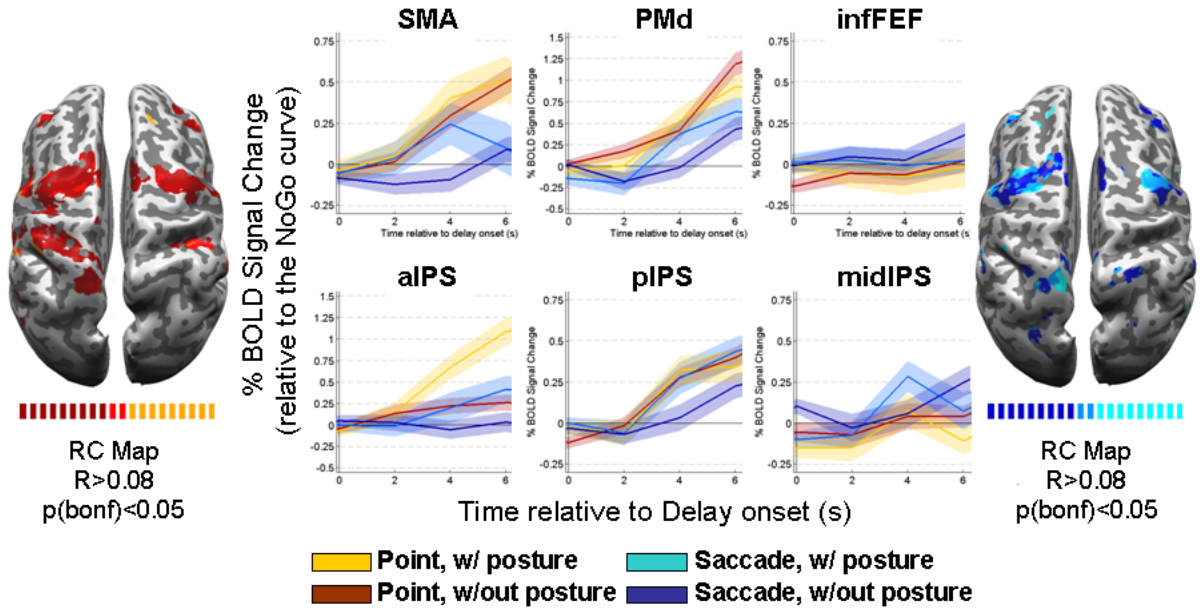

Figure I.3.5.v – ERA timecourse from left M1 hand knob, relative to delay onset. Point no posture=red. Point w/ posture=orange. Saccade no posture=blue. Saccade w/posture=sky blue. NoGo no posture=yellow. NoGo with posture=light yellow. The onset of the Go period occurs between scans 3-4 (6-8s relative to delay onset).

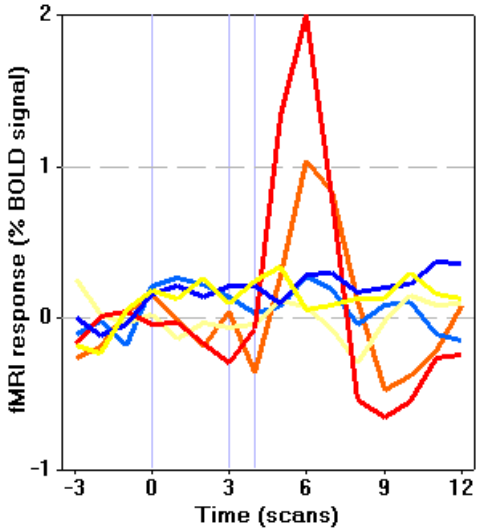

CHAPTER 4 - On principal (components): Novel fMRI analysis technique combining model- or hypothesis-based and data-driven (principal component analysis) approaches: Dimensionality reduction, framework identification, and predictive power

Novel data-driven analysis technique: Background and Description

The analysis of this fMRI experiment, as well as many others presented in this thesis, is complicated by the high-dimensionality of the dataset. Not only are there tens of thousands of voxels in the brain, with a particular 3D spatial configuration, but there are thousands of time samples, and many task conditions or trial epochs that could all be considered separately. Some recent methods papers have described pure data-driven approaches to fMRI analysis (e.g., independent components analysis, a.k.a. ICA, which when applied can preserve the spatial configuration of the voxels and reveal separable task-related brain networks), or combined data-driven (e.g., temporal ICA) and model-based (e.g., GLM) approaches (Hu et al. 2005). Unfortunately, most of these data-driven or combined methods are not routinely applied in fMRI analysis, and pure ICA can be very difficult to interpret since it can reveal tens of "independent networks" in any one simple task.

Here, we describe an alternative method, a pre-filtered data-driven analysis of fMRI data. The approach I've developed is less computationally expensive than other similar approaches, allows the researcher to focus the analysis on a variable number of user-defined ROIs (model- or hypothesis-filtered), and generates data that are easier to interpret.

Principal components analysis (a.k.a. PCA) is a method for data dimensionality reduction that projects data onto a new, orthogonal coordinate system. The coordinates are known as the principal components (PCs), and are ordered such that the first PC explains the greatest variance in the data, and so on. Invented in 1901 by Karl Pearson, PCA is employed as an exploratory data analysis tool, and is commonly used in pattern recognition, spectroscopy, and bioinformatics, but has only recently been applied to the analysis of MRI and fMRI images.

I propose a combined model/hypothesis-driven and PCA approach that can be implemented in several ways. After the researcher defines a variable number of brain ROIs based either on the results of simple GLM contrasts or initial hypotheses, the timecourse of BOLD activity is averaged across every voxel within each ROI (spatial averaging). This raw BOLD timecourse then can be fed directly into the PCA as BOLD signal amplitude across an element of time such as a single experimental run, can be appended across multiple experimental runs in the same subject or across subjects, or can be subjected to further temporal averaging. Because the BOLD signal measure is fairly noisy, it is important to average data either across subjects, across identical runs in the same subject, or across trial types/task conditions. For the PCA described in this section, the dataset was derived from a single subject who completed 18 fMRI experimental runs. Since the trial order was pseudo-randomized across the whole experiment, many different run types were employed, and it was not possible to average across runs. Therefore, I chose to average the BOLD time course across trials in each separate task condition. Each trial consisted of an initial fixation epoch (used as the baseline to calculate % BOLD signal change) and three epochs of interest: the cue, delay, and go/execution periods. Trial-averaged BOLD activity spanning the whole trial (initial fixation, cue, delay, and go periods) and aligned to the onset of the delay period (i.e., the same data typically plotted in ERAs) was calculated for each task condition. These trial averages were then concatenated across different task conditions (after data centering) to create a new “time/sample” axis (see next paragraph). The input to the PCA was a matrix: “Time/sample” x ROI. I will not go into further detail about the PCA here; I will just mention that it was implemented in Matlab R13 (version 7.1) using the standard script princomp.m.

Results

After a PCA with an input of BOLD activity from 9 ROIs (delay-active ROIs: SMA, PMd, infFEF, aIPS, midIPS and pIPS; control ROIs with strong go- and cue-period activity: M1, VP, V1l) concatenated in time/samples across 5 task conditions (Point no posture, Point with posture, Imagined point with posture, Saccade no posture, Saccade with posture), the first principal component (PC1) accounted for 66% of the variance, and the second principal component (PC2) accounted for an additional 17.5% of the variance, such that combined PCs 1 and 2 accounted for the majority of the variance (84.1%). The high proportion of variance explained by PCs 1 and 2 is indicative that the dimensionality reduction, from 9 ROIs to 2 PCs, was effective. Compared to standard plots of ERA curves (number of curves = 5 in this experiment), the effective dimensionality reduction, from 45 ROI-Curves to 2 PCs, was very effective; however, the PCA was probably aided by the fact that all of the inputs were task-related brain areas with fairly stereotyped trial behavior (i.e., most regions exhibit at least some cue-, some delay-, and some go-period activity above baseline on every trial).

I was then able to look at the PCA results in several different and uniquely informative ways: 1) stationary across time/task conditions (Figure I.4.1.i: ROI biplot output), 2) trajectories through trial-time (condensed into cue/early delay, late delay, and execution epochs but separated by task condition, Figure. I.4.1.i dotted line paths), 3) trajectories through posture changes (separated by trial epoch and effector, Figure I.4.1.ii), and 4) trajectories through effector-space (separated by trial epoch and posture, Figure I.4.1.iii).

Looking at the PC1-PC2 plot from 2) above, moving from the early delay (ED, 2-4s post delay onset) to the late delay (LD, 6-8s), the path trajectories decrease in PC2 while increasing in PC1 (Figure I.4.1.i, dotted line paths). The main effect when transitioning from the LD to the Go epochs is an increase in PC2. Combining these results with the locations of the ROIs in PC1-PC2 space (Figure I.4.1.i, biplot output), we can infer that PC2 is more strongly related to movement execution, followed by cue/visual stimulation, while PC1 is most strongly related to delay activity and arm movement execution.

Next, I considered the PC1-PC2 trajectories through posture changes, separated by epoch and effector (Figure I.4.1.ii). When moving from resting hand posture to a stationary task-engaged hand posture, the predominant effect across time and effector is an increase in PC1. Therefore, PC1 seems to be more strongly related to hand posture than PC2.

Finally, I investigated PC1-PC2 trajectories through effector, separated by epoch and posture (Figure I.4.1.iii). Moving from the eye (saccade) to an arm effector (point), the predominant effect is an increase in PC1 and little change in PC2; therefore, PC1 is likely to be more related to effector-specificity than PC2, with higher PC1 values corresponding with increasing arm- vs. eye-specificity.

Table I.4.1.i summarizes the results of the PC trajectories. The addition of a static task-engaged hand posture leads to increased recruitment of posterior parietal cortical areas that are involved in hand movement planning and that receive strong proprioceptive and tactile sensory inputs, even on saccadic eye movement trials.

Combining the above inferences about the functional interpretations of PCs 1 and 2 (that PC1 encodes both effector-specificity and hand posture while PC2 encodes trial epoch) with the ranked ROI contributions to these principal components informs us of the functional properties of these ROIs and their placement in a network architecture. Placement along PC1 does a good job of assigning ROIs to an arm- or eye-specific network and qualifying the degree to which arm posture affects delay-period, motor planning activity. Similarly, placement along the PC2 dimension does a good job of predicting the relative delay-to-go period signal amplitude. ROIs with the largest PC2 contribution value tend to have larger execution BOLD activity relative to delay activity (i.e., higher signal amplitude). The emergence of these effects is interesting and truly data-driven since we did not directly inform the principal components analysis about the task condition (effector/posture) or temporal structure of the task.

Conclusions:

The application of a novel combined hypothesis-guided and data-driven approach helped us further investigate the posture effects previously described in section I.3.5 of this thesis. The PCA correctly grouped the PMd, SMA, aIPS, and pIPS in the arm-specific planning network, and V1, VP, midIPS, and infFEF in the eye-specific planning/execution network. It also informed us that the arm-specific ROIs are more strongly modulated by an arm posture, even during saccade trials, than eye-specific ROIs. Placement along the second PC did a good job of predicting the relative level of engagement of a brain area during the cue and go periods in comparison with engagement during the delay period.

While many of these insights are replicated in the GLM- and ERA-based analyses, the PCA approach significantly reduced the amount of data we had to sift through and interpret. This approach is a powerful tool that can help us qualify functional similarity amongst ROIs even in very complicated tasks, and also help predict activation patterns/network placement in other tasks. For instance, a separate subject was run in a block design fMRI, delayed response experiment. Instead of just two postures, this experiment had nine different effector-posture combinations. Running a GLM contrast for each potentially interesting comparison would generate on the order of 50 contrast maps! And if the design had been event-related instead of blocked, separately considering the 3 main task epochs (Cue, Delay, Go) would bring the tally to around 150 different maps.

ERAs from task-related brain areas in this second experiment are pictured in Figure I.4.1.iv. Even though only a subset of the total number of data curves are shown, describing a pattern of modulation across the task-related brain network, or imposing a network architecture, becomes intractable. Without making any hypotheses about the characteristics of these modulations, PCA employed on the dataset effectively performed a rapid pattern recognition that grouped ROIs based on their functional similarities. Knowing that V1 is a visual area and M1 is related to arm movement execution, data in PC1-PC2 space were re-projected onto a line from V1 to M1, and the network architecture pictured in Figure I.4.1.v emerged.

This same network architecture applied to the organization of separate single-ROI PCA results from the same experiment in the same subject correctly predicts two functional properties of the ROIs: clustering of posture by effector employed (real arm, imagined arm, or saccade), as well as an increasing separation between the cluster groups of real- and imagined-arm postures moving left to right (Figure I.4.1.vi).

The original PCA-derived framework also has predictive power for the functional properties of ROIs in separate experimental tasks in different subjects, correctly organizing ROIs along the dimension of increasing arm contralaterality (Figure I.4.1.vii) and increasing specificity for real vs. imagined arm movements (Figure I.4.1.viii).

These are just a few of the many possible applications of this novel combined hypothesis-drive and PCA/data-driven approach, which successfully groups ROIs or task conditions based on their functional properties and similarity within a single task, and successfully organizes ROIs into a predictive framework that correlates well with functional neural properties observed in homologous ROIs is different tasks, and different subjects.

4.1 FIGURES

Figure I.4.1.i – PC1-PC2 trajectories through time/epoch, separated by task condition. When moving from the early delay (ED, 2-4s) to the late delay (LD, 6-8s), paths decrease in PC2 and increase in PC1. When moving from the LD to the Go epoch, the predominant effect is an increase in PC2. Given these properties, PC2 seems to be most strongly related to movement execution, followed by cue/visual stimulation, while PC1 is most strongly related to delay activity and arm movement execution.

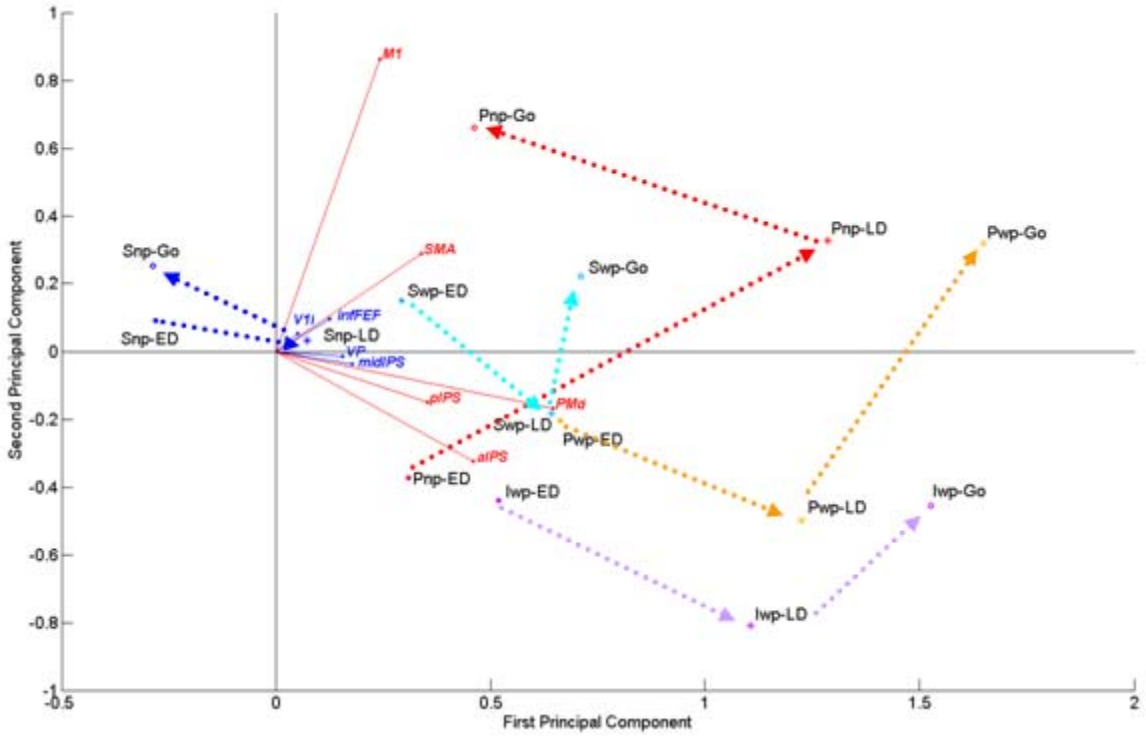

Figure I.4.1.ii - PC1-PC2 trajectories through posture, separated by epoch and effector. When moving from resting hand posture to a stationary task-engaged hand posture, the predominant effect across time and effector is an increase in PC1; therefore, PC1 seems to be more strongly related to hand posture than PC2.

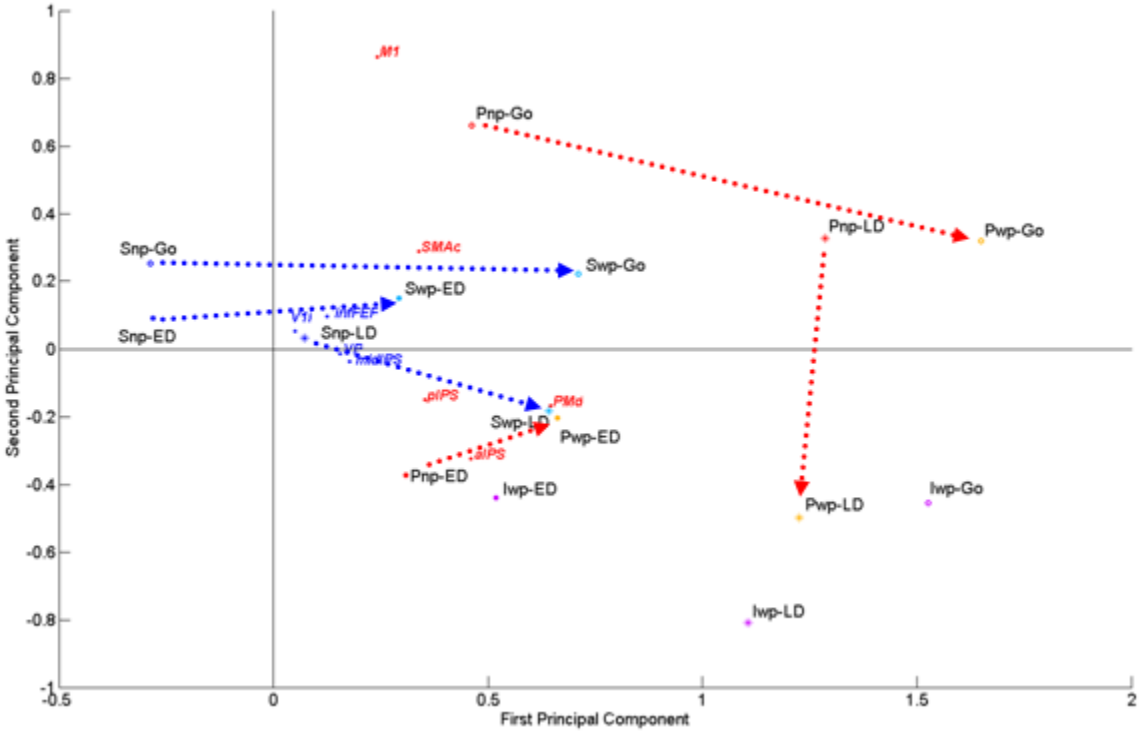

Figure I.4.1.iii - PC1-PC2 trajectories through effector, separated by epoch and posture. When moving from the eye (saccade) to an arm effector (point), the predominant effect is an increase in PC1; therefore, PC1 is likely to be more related to effector-specificity than PC2.

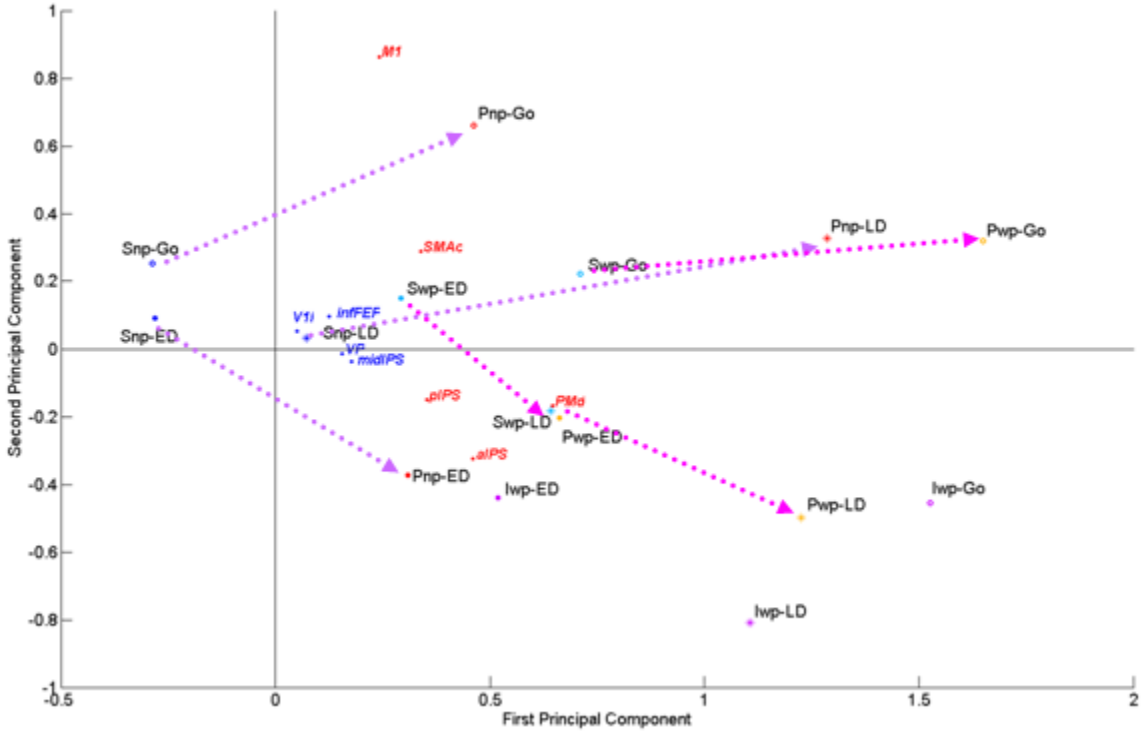

Table I.4.1.i – Summary of principal components trajectories separated by task epoch and condition. For every trial epoch/task condition pairing, the ROIs listed in the table are the ROIs that were close to the task condition in PC1-PC2 space (considering both angle and linear distance; see Figure I.4.1.i). The addition of a static task-engaged hand posture more strongly recruits posterior parietal cortical areas involved in hand movement planning and that receive strong proprioceptive and tactile sensory inputs. Starred ROIs were the closest to the task condition in PC1-PC2 space.

Trial epoch/ Task Condition	**Early Delay (ED)**	**Late Delay (LD)**	**Go Period (Go)**
Point no posture (Pnp)	aIPS*, pIPS, PMd	PMd, SMA	M1, SMA
Point with posture (Pwp)	aIPS, pIPS, PMd*	aIPS, pIPS, PMd	PMd, SMA*
Saccade with posture (Swp)	SMA, V1l, VP, infFEF*, midIPS	PMd*, aIPS, pIPS, midIPS	PMd, SMA*, V1l, VP, infFEF,* midIPS
Saccade no posture (Snp)	V1l*, VP, infFEF, midIPS	V1l, VP, infFEF*, midIPS	SMA, V1l*, VP, infFEF*, midIPS

Table I.4.1.ii – Ranked ROI contributions to principal components 1 and 2, and possible interpretations of PC1 and PC2 dimensions. PC1 seems to encode both effector-specificity and hand posture influences, while PC2 seems to encode BOLD activity across different task epochs. ROIs with the largest PC2 contribution value tend to have larger execution BOLD activity relative to delay activity (i.e., higher signal amplitude). The emergence of these effects is interesting and truly data-driven since we did not directly inform the principal components analysis about the task condition (effector/posture) or temporal structure of the task.

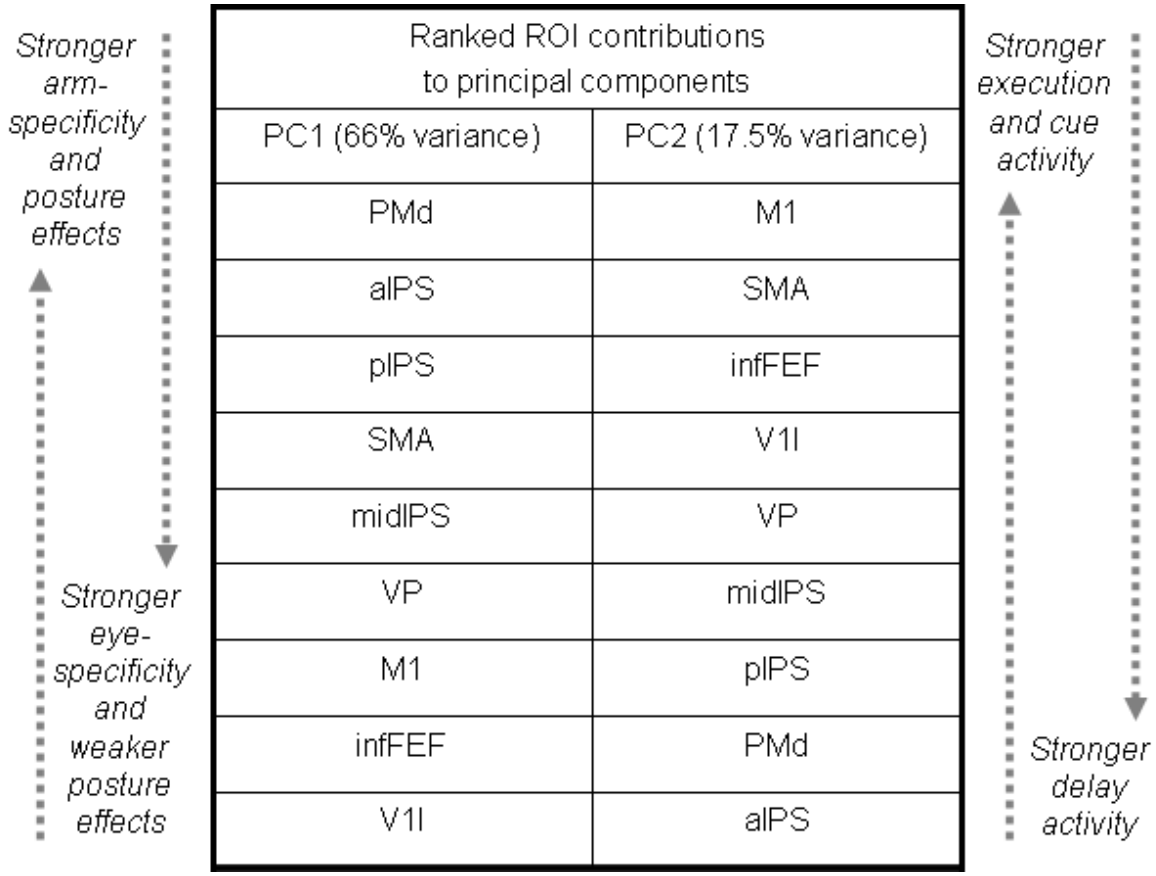

Ranked ROI contributions to principal components	
PC1 (66% variance)	PC2 (17.5% variance)
PMd	M1
aIPS	SMA
pIPS	infFEF
SMA	V1l
midIPS	VP
VP	midIPS
M1	pIPS
infFEF	PMd
V1l	aIPS

Figure I.4.1.iv – ERAs from a second experiment employing nine different effector-posture combinations (direct pointing, point to center then out to target, pointing with a posture that switches on/off at the end of every trial, pointing with a fixed posture, reaching, saccade with fixed hand posture, saccade with no hand posture, imagined point with fixed hand posture, imagined point with no fixed hand posture). Only four effector-posture curves are shown across the task-related brain network; however, the high-dimensionality of the data and complexity in data interpretation, which approaches intractable, is clear.

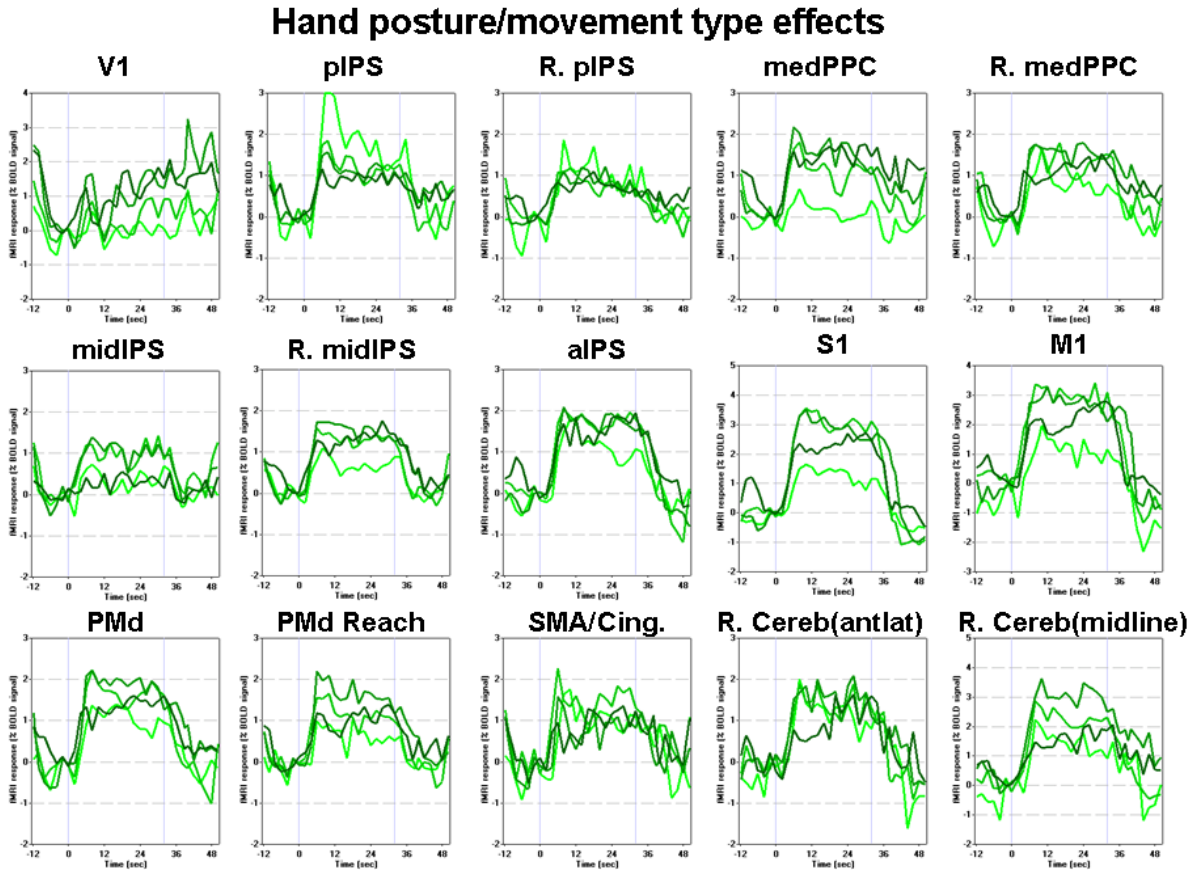

Figure I.4.1.v – PCA-remapped projection of task-related ROIs onto V1-M1 line.

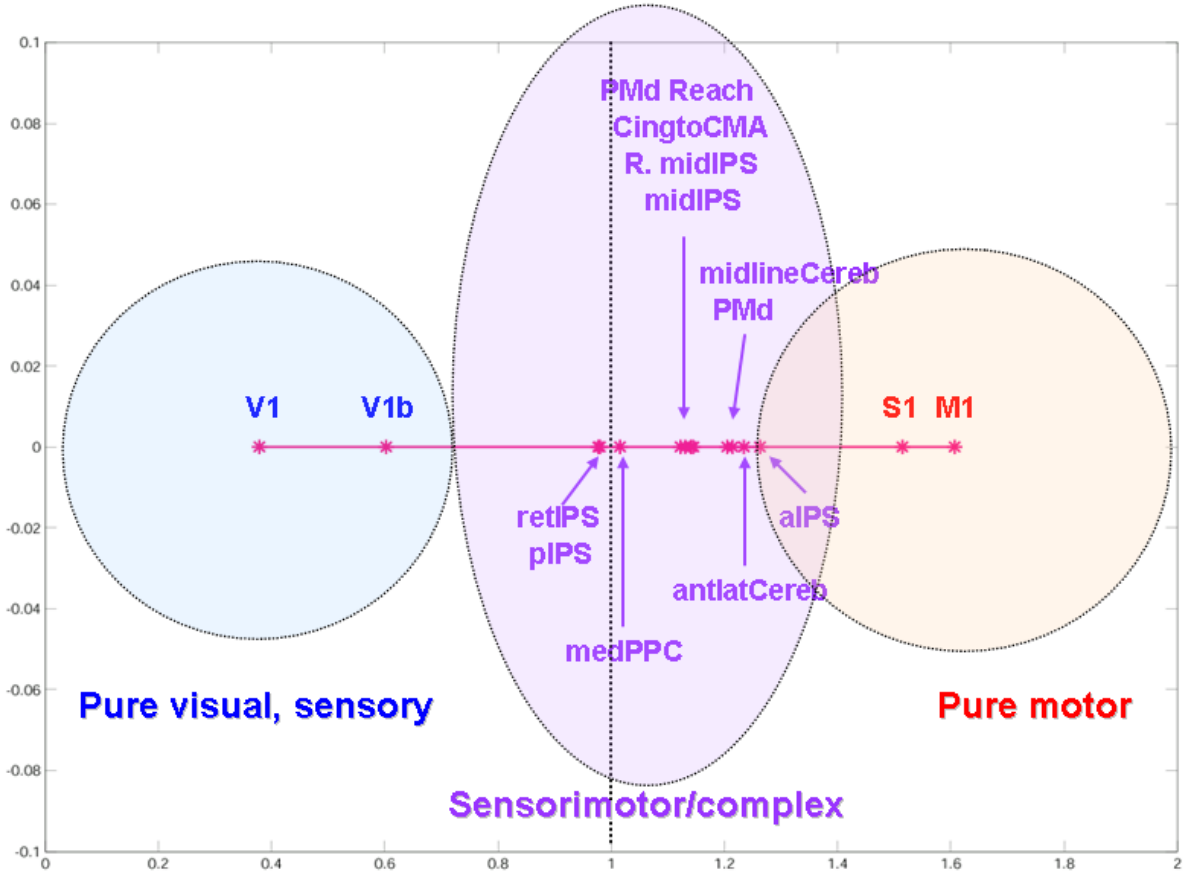

Figure I.4.1.vi – Effector-posture projections for different ROIs organized based on functional network architecture observed in Figure I.4.1.v. This PCA-derived network organization has predictive power for separate PCAs performed on single ROIs: the groupings of real arm-related postures (orange circles) and imagined arm-related postures (purple circles) demonstrate increasing PC1-PC2 space distance/separation for real vs. imagined arm movements moving from left to right.

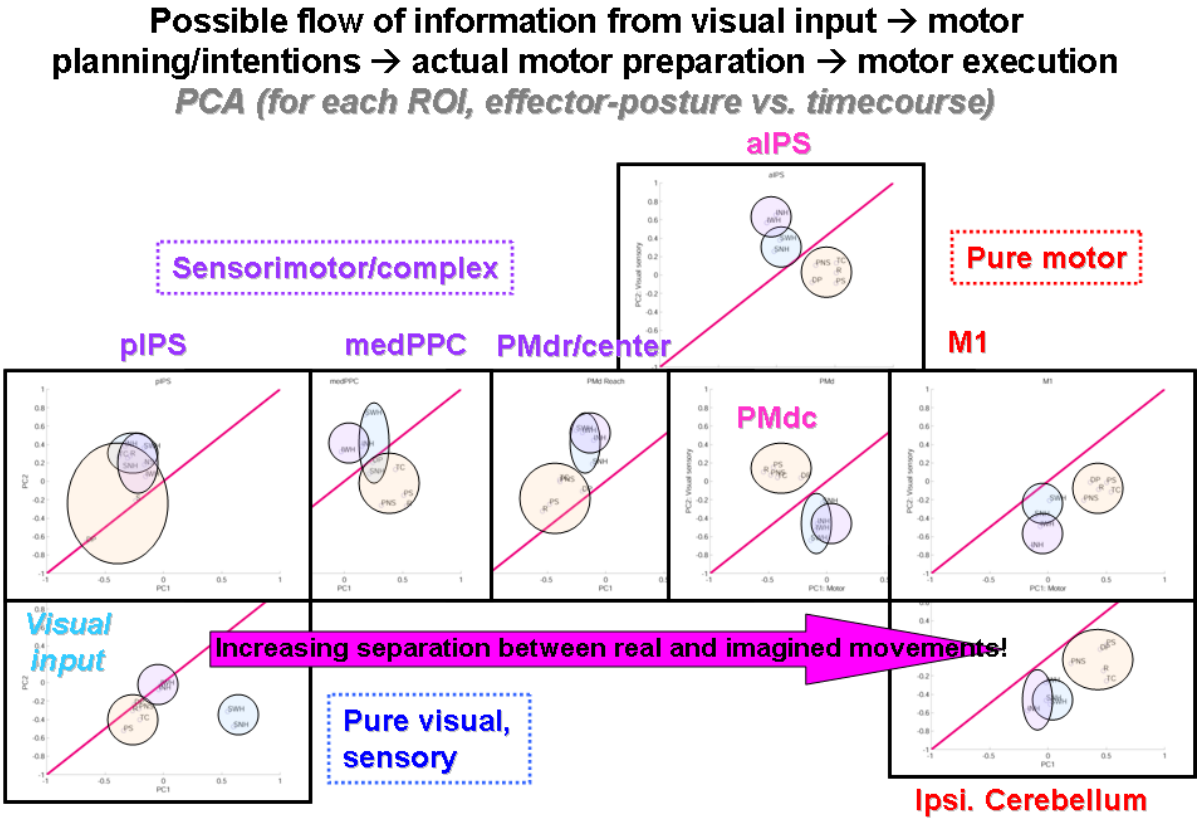

Figure I.4.1.vii – ROIs from the experiment presented in I.3.4, organized based on functional network architecture observed in Figure I.4.1.v. The PCA-derived network organization has predictive power for the functional properties observed in a different experiment in a different subject! Moving from left to right, ROI ERAs exhibit evidence of increasing arm contralaterality.

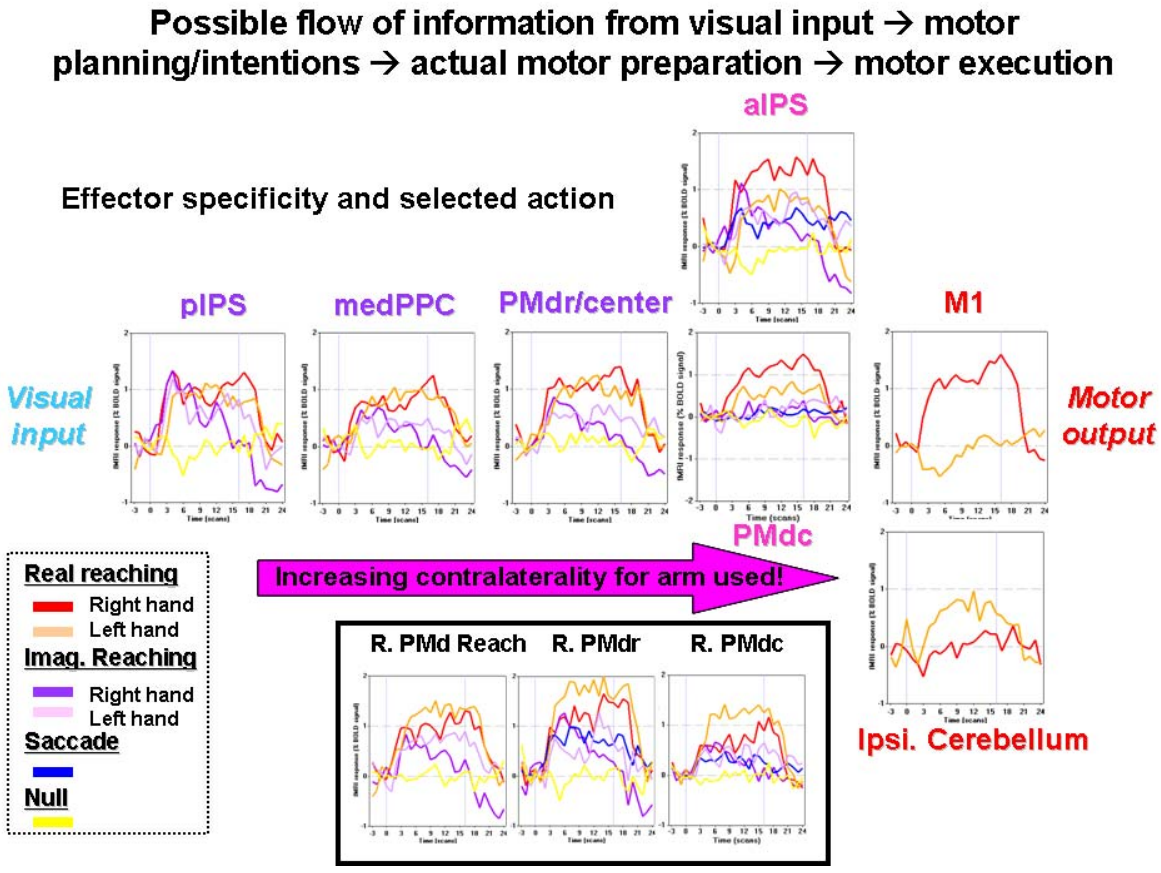

Figure I.4.1.viii – ROIs from one experiment presented in I.3.3, organized based on functional network architecture observed in Figure I.4.1.v. The PCA-derived network organization has predictive power for the functional properties observed in a different experiment in a different subject! Moving from left to right, ROI ERAs exhibit evidence of increasing specificity for real arm movements compared to imagined arm movements. The roughly linear decrease in the relative amplitude ratio of the Imag. Reach vs. Real Point curves moving from pIPS → medPPC → PMdr/center → PMdc → M1 is particularly striking.

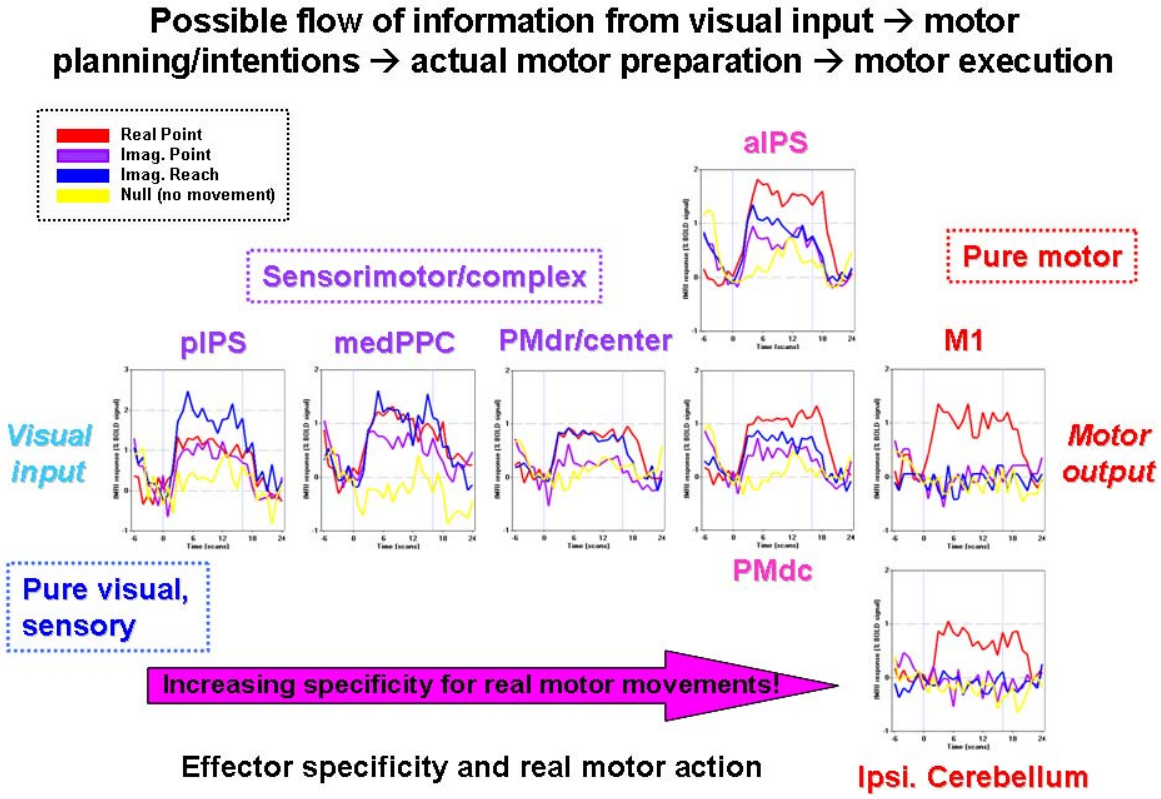

PART II: CLINICAL APPLICATIONS

CHAPTER 1 - Comparison of real and imagined reaching: Imagined arm movement can be used as a proxy for real arm movement in the identification of brain areas involved in motor planning

Implications for neural prosthetics, and motivation for exploring imagined movements

Part I of this thesis identified several arm- and eye-specific planning regions in frontal and posterior parietal cortices, including the likely human functional homologues of monkey PMd, FEF, PRR, and LIP. The task utilized in Experiment 1 (Part I: Chapter 1) reliably activated PMd and PRR, which were previously demonstrated to contain neural signals in monkeys appropriate for the control of an external device (Musallam et al. 2004, Mulliken et al. 2004, Mulliken et al. submitted). Implantation of human PMd or PRR with a cortical neural prosthetic should yield neural signals suitable for brain control of an external device that could restore communicative and motor function to severely paralyzed patients.

Monkey PRR and PMd are localized during neurophysiological recordings based on the functional neuronal properties of directional tuning and reach vs. eye specificity. In Part I of this thesis I presented evidence of similar, potentially functionally homologous human brain areas. Human PRR and PMd were identified based on the property of significant reach vs. saccade specificity during motor planning.

Unfortunately, for the purposes of neural prosthetics it will not be possible localize human PRR and PMd in severely paralyzed patients using a task involving real arm movement. Hence, it is important to determine whether human PMd and PRR are also active during imagined reach planning and execution. If so, it may be viable to utilize imagined arm

movements as a viable proxy for real arm movements to both localize and target PMd and PRR for the implantation of a neural prosthetic device, and to train and implement neural prosthetic decode algorithms.

A previous block design fMRI experiment in healthy control subjects suggested that goal-directed imagined point planning/execution activates the PMd and PPC to nearly the same extent as real point planning/execution (Rizzuto et al. 2004). However, the block design task did not separately resolve the delay (motor planning) and response (motor execution) task epochs. Here, we employed an event-related experimental design and imagined reaching instead of imagined pointing (see task description in Part I: Chapter 1) to compare real and imagined arm movements and assess the degree of imagined arm movement (vs. eye movement) specificity in the frontoparietal motor planning network and in particular, in putative neural prosthetic implant areas.

Comparison of Real vs. Imagined Movement Planning and Execution

Real reaching and imagined reaching activate strongly overlapping brain networks, particularly during motor planning (Figure II.1.i.B). Arm-specificity was tested separately for real and imagined reach-planning, revealing strong overlap of real and imagined reach-specific brain areas (top of Figure II.1.ii, also see Figure II.1.iii). During the delay period, a direct contrast comparison of real and imagined reach planning revealed some differences in the amplitude of BOLD activity within this task-related network (compare Figure II.1.i.A and top of Figure II.1.ii). Real reach planning activated parts of the PMv, SMG, middle temporal gyrus (MTG), IPL along the IPS, SPL/PoCS, posterior ascending cingulate sulcus (pCing) and caudal PMd and SMA/Cing more than imagined reach planning. Most of these areas (except for the IPL and MTG) were also specific for imagined reach planning compared to the saccade and NoGo conditions. In contrast, imagined reach planning activated part of the dlPFC, lateral segment of the PrCS, medial-most PMd at the cusp of the medial wall, and medial-most medPPC/pIPS more than real reach planning (Figure II.1.i.A). All of these areas (except for medPPC/pIPS) are specific for imagined reach planning but not for real reach planning compared to the saccade and NoGo conditions, while medPPC/pIPS is significantly effector-specific for both real and imagined reaching compared to saccade and NoGo (Figure

II.1.ii, top). The RC analysis comparing real and imagined reach conditions during the delay period provides evidence that most of the real vs. imagined effector biases within the task-related brain network are mild (Figure II.1.i.B, also see Figure II.1.iii)

During the go period, both motor output and sensory feedback are different between the real and imagined reaching conditions. These differences could explain the greater real vs. imagined reach segregation during the go period (Figure II.1.i.B, bottom; Figure II.1.i.A, bottom, Figure II.1.ii, bottom). As expected, real reach execution activates primary somatomotor cortex more than imagined reach execution (Figure II.1.i.A, bottom). It also engages PMd, PMv, SMA, MTG, and the SPL more than imagined reach execution. In contrast, imagined reach execution more strongly recruits parts of frontal cortex, including the bilateral dlPFC, IFG, SFG, preSMA, and the left SMG/IPL.

These findings are in accord with other published findings comparing real and imagined movements (Deiber et al. 1998, Johnson et al. 2002, Hanakawa et al. 2003, Nair et al. 2003, de Lange et al. 2006, Michelon et al. 2006, Szameitat et al. 2007, Filimon et al. 2007), though the current task differs from most published work due to the visuospatial, goal-directed aspect of the movement and the placement of emphasis on the pre-movement, motor planning epoch.

Conclusions:

Real and imagined reach planning and response execution co-activate large portions of cortex. Significant differences between real and imagined arm effectors are most evident during the response period, when real reaching activated primary motor and somatosensory cortex while imagined reaching recruited additional rostral premotor and supplementary motor cortex as well as more of dlPFC and IPL. These findings are in accord with other published findings comparing real and imagined movements (Filimon et al. 2007, de Lange et al. 2006, Hanakawa et al. 2003, Szameitat et al. 2007, Deiber et al. 1998, Michelon et al. 2006, Johnson et al. 2002, Nair et al. 2003), though the current study differs from most published work due to the visuospatial goal-directed aspect of the movement and the placement of emphasis on the pre-movement, motor planning period.

Imagined reach planning activates reach-specific brain areas to nearly the same degree as real reach planning, suggesting that imagined arm movement could viably replace real arm movement during a pre-surgical fMRI localizer of neural prosthetic implant targets and also during training and implementation of decode algorithms for the control of a brain-machine interface device. Findings from another recent experiment (discussed in the subsequent chapter) suggest that both PMd and medPPC/pIPS are still active during goal-directed imagined movements in subjects with spinal cord injury.

II.1 FIGURES

Figure II.1.i - Direct comparisons and relative contributions of real- and imagined reaching. A) Direct comparison of real vs. imagined reach activity in task-related brain areas during the delay period (top) and go period (bottom). Maps are at q(FDR)<0.05. Real reaching (R) > Imagined Reaching (I) in red, the reverse in yellow. Based on Experiment 1 described in Part I: Chapter 1. B) Relative contribution (RC) analysis (see *Methods*, Part I: Chapter 1) shows the relative contribution of the Reach and Imag. Reach predictors during the delay period (top, task-related at R>0.1), and go period (bottom, task-related at R>0.15).

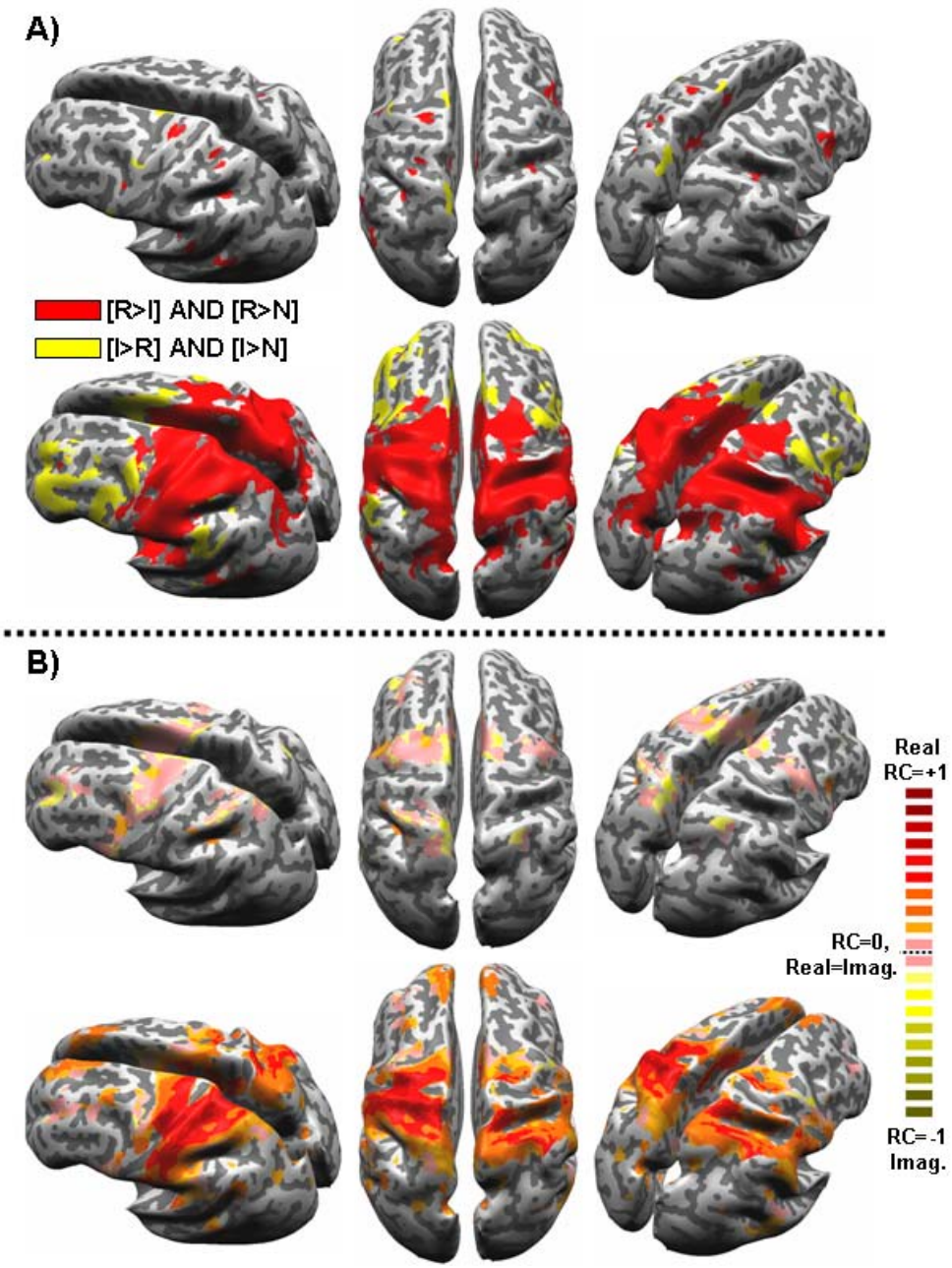

Figure II.1.ii - Comparison of real reach and imagined reach-specificity. Comparison of real- and imagined reach-specificity during the delay period (top) and go period (bottom), from Experiment 1 discussed in Part I: Chapter 1. Across-subjects (n=7), maps are at q(FDR)<0.005. During motor planning, both real- and imagined reach-specificity (relative to saccade) strongly overlap, but specificity-for these two effectors segregates during motor execution.

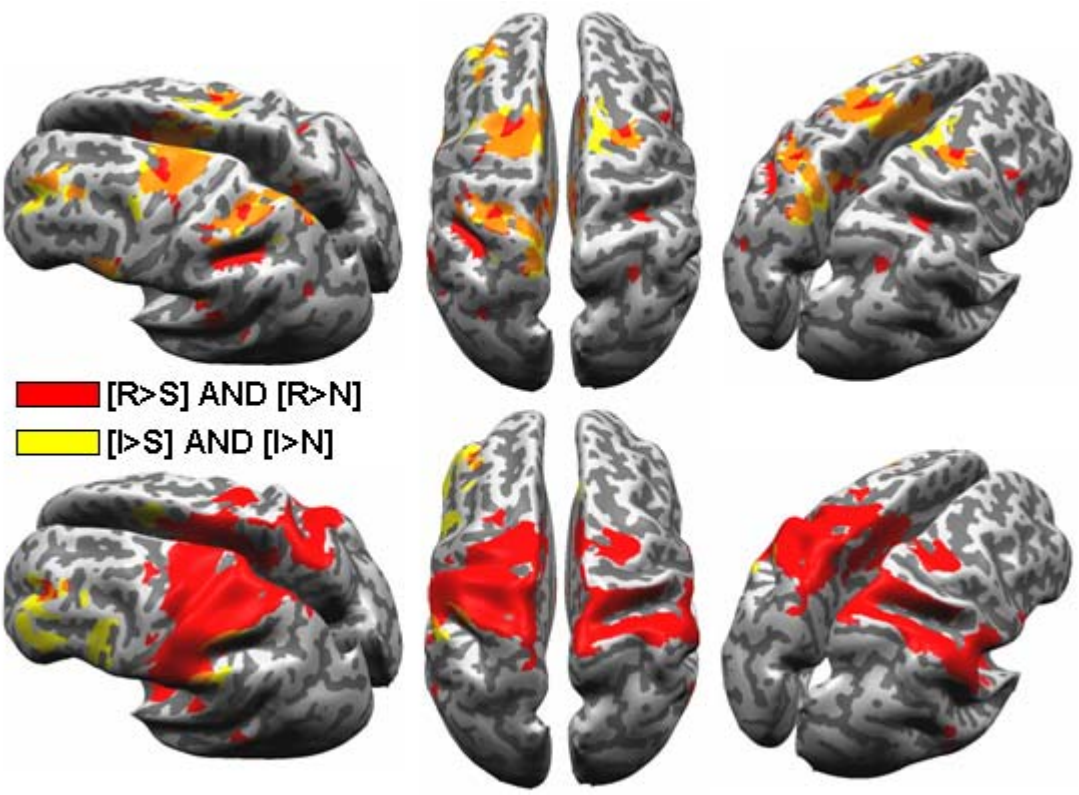

Figure II.1.iii – Timecourses of BOLD activity in arm- and eye-specific ROIs reveal the evolution of effector-specificity during the trial. Event-related average (ERA) timecourses from the main ROIs exhibiting significant effector-specificity for arm or eye effectors during motor planning, and two non-specific control ROIs (M1, V1), for 8s delay trials only. Averaged across individual, subject-based ROIs (N. subjects=7). Reach-specific ROIs (left) show stronger BOLD activity in reach trials than in saccade trials, and recruitment in imagined reach trials. Curves are aligned to actual delay onset, with the preceding initial fixation period as baseline. Gray shading indicates the effective delay period (not used in the ERA calculation, for viewing only) shifted by the expected hemodynamic response onset latency (2s), since neither M1 activity on reach trials nor V1 activity on saccade trials begin to increase above baseline until ~2s after the actual onset of the response period (actual onset at 8s), confirming the expected 2s hemodynamic response onset latency. Timecourses are based on Experiment 1 from Part I – Chapter 1.

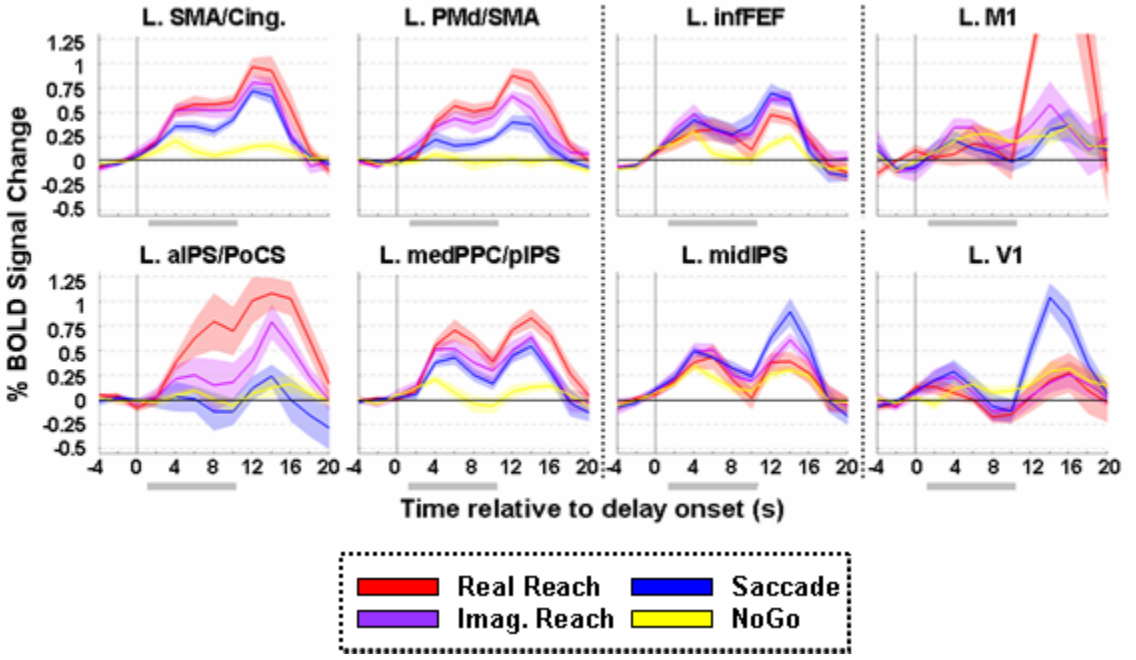

CHAPTER 2 – Goal-directed action following spinal cord injury: Brain plasticity and viability of recording from hPRR and PMd in paralyzed patient populations

ABSTRACT

Functional magnetic resonance imaging was used to investigate changes in the neural circuits underlying action planning and motor execution following traumatic injury to the spinal cord. Spinal cord injured (SCI) and healthy control subjects (HC) were scanned in two experimental tasks: one emphasizing motor imagery and action planning for spatial goal-directed leg movements (IL task) and another requiring visually-paced attempted knee extension (AK task). Despite the functional disconnection between the brain and the lower limbs and accompanying significant motor and sensory impairments in SCI subjects, a relatively normal pattern and amplitude of brain activity was observed across the distributed brain networks subserving motor planning and execution, including the supplementary motor area (SMA), dorsal premotor (PMd) cortex, and posterior parietal cortex (PPC), and primary somatomotor cortex (M1, S1, and the cingulate motor area). However, there was an expansion of the normal motor map for knee movement in SCI subjects, with activity spreading into neighboring somatomotor cortex as well as the ipsilateral, homologous cortex. Our findings suggest the presence of compensatory mechanisms during attempted motor execution, but a fairly normal cortical network for planning movements with the disconnected limb.

Brain activity correlated with several clinical and behavioral variables in the SCI subject group. Hours of exercise per week correlated with normalizing influences on brain activity in M1/S1/CMA and the medial PPC. Interestingly, brain activity in the medial PPC not only correlated with current preserved motor functionality, but also robustly predicted future functional motor gains. There were no significant correlations between continuous time-

since-injury and brain activity; however, comparisons between early-SCI and late-SCI subgroups are consistent with the hypothesis of early hyper-activity and late hypo-activity in somatomotor cortex following SCI. We discuss these and other findings in terms of implications for the understanding and treatment of spinal cord injury, as well as for the development and control of cortical neural prosthetics (next chapter, Part II: Discussion).

INTRODUCTION

Spinal cord injury (SCI) can severely disrupt both the normal outflow of information from the brain to the muscles of the limbs as well as inflow from sensory and proprioceptive sources. Without the confound of cortical injury, SCI proffers an opportunity to study changes in the cortical networks for limb movement after a limb is functionally disconnected from the brain. When a subject is paralyzed as a result of SCI, plasticity may occur in both primary somatomotor and motor association cortical areas involved in normal limb movement. Cortical changes could limit functional recovery as well as inhibit the efficacy of future treatments that directly target and repair the subcortical damage, since descending cortical signals to the spinal cord and limbs/muscles may be altered. The current study investigates these changes, and correlates them with clinical and behavioral measures.

Several previous studies investigated cortical plasticity and reorganization in SCI patients (Alkadhi et al. 2005, Cramer et al. 2005, Hotz-Boendermaker et al. 2008). These studies reported divergent results, which could potentially be explained as an effect of time-since-injury. In the current study, we correlate time-since-injury, as well as other clinical and behavioral variables, with activity in brain areas recruited during motor planning and execution.

These previous studies also employed experimental tasks that robustly recruit primary somatomotor cortex. However, most natural behaviors recruit a much wider network of brain activity including parts of the premotor (PM), supplementary motor (SMA), and posterior parietal cortices (PPC), and reorganization in these motor association areas may also occur as a consequence of SCI. Given the putative role of these regions in planning/preparing goal-directed actions (Glidden et al. submitted), alterations in the spatial extent of activity, level of

activity, or overall excitability in these brain areas could dramatically interfere with normal behavior. For this reason, it is also imperative to assess plasticity and reorganization in these motor association areas.

We hypothesized that primary somatomotor areas (e.g. M1, S1) would be more plastic than motor association areas (e.g. PM, SMA, PPC) in the wake of spinal cord injury. With direct descending corticospinal fibers and strong somatosensory and proprioceptive inputs, primary somatomotor cortex is both anatomically and functionally "close" to the site of injury. In contrast, motor association areas are more anatomically and functionally distant from the site of injury, retain several sensory inputs following SCI, and are recruited to some degree by a variety of cognitive and motor tasks. These characteristics could limit the degree of plasticity and reorganization in these areas following SCI; it is even possible that these areas might still compute the sensorimotor transformations necessary for goal-directed action and continue to pass high-level motor plans to M1.

This study also addresses whether brain areas involved in planning real and imagined goal-directed limb movements are still active during imagined movements of a functionally disconnected, paralyzed limb. A previous study in healthy control subjects identified several brain areas including dorsal premotor cortex (PMd) and parts of posterior parietal cortex (PPC) that are strongly activated during real and imagined arm-movement planning and execution; in fact, imagined arm movement planning and execution activated these areas to nearly the same degree as real arm movement planning and execution (Glidden et al. submitted, Glidden et al. 2005, Rizzuto et al. 2004). These motor planning areas show promise as targets of an implanted cortical neural prosthetic device for severely paralyzed subjects, which would allow them to directly communicate with an external effector, such as a computer or a robotic arm, via thought alone. Because severely paralyzed patients lack the ability to execute real movements, it may be necessary to use imagined or attempted movements to activate these potential neural prosthetic implant sites; both for pre-surgical identification/surgical targeting and for cortical control of the device after implantation. Thus, another aim of the current study was to assess whether these brain areas could still be recruited by imagined limb movement in/by SCI subjects.

To address these aims, we utilized functional magnetic resonance imaging (fMRI) to assess BOLD activity in both healthy control (HC) subjects and subjects with chronic cervical and high thoracic spinal cord injury (SCI) while they performed two tasks. The first task was a delayed-response task in which the response was an imagined right leg "reach" toward the remembered location of a flashed visual target. The response was directed towards a target in visual space (the "goal"); hence, it can be considered a visuospatial goal-directed movement. This kind of movement differs substantially from movements such as self-paced finger tapping or limb flexion/extension. Finger tapping and simple limb flexion/extension are commonly employed in studies of cortical plasticity and reorganization following brain injury; however, these movements are strongly driven by proprioception and have no visuospatial goal.

The imagined leg movement used in the first task also differs from the movement required in a second task. In the second task, subjects were asked to watch a video of a cartoon leg and to pace attempted right knee movement with the extension and flexion of the cartoon leg. This task, while visually-driven, does not involve visuospatial transformations for motor planning, just visually-guided pacing of the repeated movement.

We expected the paced knee extension task to recruit primary somatomotor areas including M1, S1, and the cingulate motor area (CMA). In contrast, with the further requirements of spatial motor planning and goal-directed imagined action, the imagined leg movement task should strongly recruit association areas but recruit primary somatomotor areas to a lesser degree than real or attempted leg movement.

In our analyses, SCI-induced plasticity in network nodes and reorganization across the networks for visually-paced and goal-directed action was assessed by comparing fMRI activations in healthy control and SCI subjects. We correlated fMRI activations in SCI subjects with clinical variables such as time-since-injury (TSI), American Spinal Injury Association (ASIA) impairment scale and motor scores, ASIA SCI level, amount of exercise, and investigated relationships between spinal cord cross-sectional area and task-related brain

activity. Interestingly, we were also able to predict future functional motor improvements based on brain activity. Functional motor improvements were assessed as changes in ASIA motor scores between the baseline/fMRI scan (T1) and second set of clinical measurements taken 6 months later (T2). We hypothesized that the maintenance of a relatively "healthy" brain organization would facilitate long-term functional recovery.

RESULTS

In order to investigate brain plasticity following complete functional disconnection from the effector limb, it made more sense to employ leg movements instead of arm movements in our experimental task, since most SCI patients retained some motor functionality of the upper limbs. Bilateral ASIA upper motor extremity scores ranged from 18-50 with mean 32.5, compared to bilateral ASIA lower motor extremity scores ranging from 0-25 with mean 1.75, or 0-6 with mean 0.7 on the right side only. The lower the ASIA motor score, the more limited the functionality of the limb-effector. Both behavioral control electromyogram (EMG) recordings from the lower leg muscles during attempted right knee extension and leg kicks, and during transcranial magnetic stimulation of the knee area of M1 (see *Methods*) revealed little evidence of retained motor functionality of the lower limbs in any of the SCI subjects included in this study, corresponding with the lower low ASIA motor scores for the lower limbs.

However, since we are interested in recording from human PRR and PMd in severely paralyzed patients, both brain areas that are arm- vs. eye-specific, we first needed to assess the degree of overlap of imagined arm- and imagined leg-movement planning and execution networks. To do this, we ran four healthy subjects in a control fMRI experiment, directly comparing goal-directed imagined arm and imagined leg movements.

Comparison of Imagined Arm and Imagined Leg "Reaching" Activity in Healthy Control Subjects

In order to facilitate the comparison between the current study and prior studies of goal-directed limb movements and motor planning, a control experiment was conducted in four

healthy control subjects directly comparing imagined movement planning and execution for right arm reaching and right leg "reaching." Motor planning and execution for both imagined arm and imagined leg movement activated a strongly overlapping frontoparietal network of brain activity including the dorsal and ventral premotor cortex (PMd, PMv), supplementary motor area (SMA), superior parietal lobule (SPL), and portions of the inferior parietal lobule (IPL) (Fig. 2).

A direct comparison between imagined arm reaching and imagined leg "reaching" revealed that movement of the imagined arm recruited the left M1 hand knob and IPL to a greater degree than movement of the imagined leg, while the reverse was true in the left premotor and M1 leg area, SMA, globus pallidus, and anterior commissure (see Table 2 and Figure 2). However, given the high degree of overlap between networks for imagined arm reaching and imagined leg reaching, and the fact that no BOLD amplitude statistical differences were observed in the SPL or PMd, we concluded that it was viable to use imagined leg movements as a proxy for imagined arm movements.

Comparison of Imagined Leg "Reaching" in Healthy Control and SCI Subject Groups

Random effects (RFX) analyses of healthy control (HC) and spinal cord injured (SCI) subject groups in the imagined leg movement task revealed strong overlap of activity in association areas bilaterally along the precentral sulcus (PrCS, including PMd) extending onto the medial wall (to include the SMA), and along the intraparietal sulcus (IPS, including both SPL and IPL). Figure 3 shows the activation maps for both HC and SCI groups, as well as the overlap (Fig. 3, middle). Task-related ROIs are listed in Table 3.

A direct contrast of activity between HC and SCI groups was computed, revealing several task-related brain areas that were more active during imagined leg movement planning and execution in HC subjects compared to SCI subjects. These brain areas included left premotor cortex at the junction of the PrCS and superior frontal sulcus (SFS), left M1/S1 hand area, and parts of the SPL along the postcentral sulcus (PoCS) and the IPS. There were no brain

areas that were more active in the SCI group than in the HC group (see Table 4 and Figure 4).

Event-related average BOLD timecourses from the most task-related ROIs and ROIs exhibiting significant inter-group amplitude differences are plotted in Figure 5. The most task-related ROIs are plotted on the left. There were no significant differences in brain activity between the healthy control and SCI subject groups in these ROIs. However, a trend towards reduced activation in the left PMd, SMA, and medPPC (human PRR) in SCI subjects was apparent. On the right of the figure are the timecourses from ROIs with significant differential HC vs. SCI activity.

The most important finding from these between-group comparisons was that most of the frontoparietal motor planning network (including PMd, SMA, and PRR) was still active in SCI subjects. In contrast, primary motor cortex and parts of the PoCS involved in somatosensation and proprioception were more active in healthy control subjects than in the SCI subjects, though these brain areas were in general less task-related (and probably more related to movement execution rather than movement planning) than the frontoparietal areas.

Comparison of Attempted Knee Movement in Healthy Control and SCI Subject Groups

Random effects analyses of healthy control (HC) and spinal cord injured (SCI) subject groups in the attempted knee extension task also revealed strong overlap of BOLD activity in the premotor, primary motor, and somatosensory cortex related to leg movement (SFG, M1, S1) and on the medial wall in the cingulate motor area (CMA). However, visual inspection of the activation maps (Fig. 6) demonstrated a shift in laterality from a biased left-lateralized to a bilateral or even slightly right-lateralized brain network from the HC to the SCI subject group. Task-related ROIs are listed in Table 3.

A direct RFX comparison of HC and SCI subject groups revealed several brain areas that were task-related and more active in the SCI subject group than in the HC subject group (see Table 4). Brain areas recruited more robustly in the SCI group compared to the HC group

included the left SFG, CMA, M1/S1 leg area, posterior corpus callosum (pCC), and part of the left SPL (medPPC), and in the right hemisphere, premotor and primary motor areas (M1/PrCG, M1/S1 leg, M1 hand), the pCC, medPPC, and the medial SPL (medSPL). These regions are listed in Table 4, while which also shows that in the centers of task-related brain regions recruited in the HC group, there were no significant differences between BOLD activity level and HC and SCI subjects. Again, the shift in laterality of the task-related brain network was evident in these direct comparisons, and for better visualization, a relative-contribution analysis was computed (see Fig. 9). Timecourses of BOLD activity from cortical task-related ROIs are plotted in Fig. 7.

Subcortically, bilateral cerebellum was significantly more active in the SCI group than in the HC group (Fig. 8). Timecourses of BOLD activity from subcortical AK task-related ROIs are plotted in Fig. 8. A ROI in the posterior corpus callosum (pCC) also exhibited increased BOLD activity in the SCI group. Statistical models incorporating head motion correction parameters and direct comparisons of head motion between HC and SCI revealed that the activity observed in the pCC cannot be attributed to head motion.

These patterns of activity in the brain network for attempted knee movement suggest the presence of compensatory activations. Compared to the imagined leg movement task, in which both health control and SCI subjects can successfully plan and simulate movements of the lower limb, attempted knee movement in these SCI subjects is extremely difficult, frustrating, and fruitless. The main cortical (M1, S1, CMA) and subcortical (ipsilateral cerebellum) brain areas engaged during knee movement in healthy controls were still active in SCI subjects. However, there was also a local “spreading” of activity in the M1/S1 and onto the medial wall in SCI subjects, such that parts of the somatomotor cortex responsible for movements of parts of or muscle groups in the leg, and even the adjacent arm representations, were additionally recruited. The right motor cortex, ipsilateral to the right knee effector, was also engaged in SCI subjects, again suggesting that SCI subjects compensate for the severely disrupted functional connectivity of the knee M1 to the spinal cord by attempting to recruit additional corticospinal fibers for neighboring body parts and muscle groups and for the analogous limb in the opposite hemisphere. SCI subjects had

increased activity in the posterior corpus callosum (pCC, Fig. 8) compared to healthy controls. The pCC, which mediates interhemispheric transfer of information, is not task-related in the HC group. This upregulation of pCC activity could reflect heightened communication between the contralateral and ipsilateral primary motor cortices, since it correlated with increased right hemisphere somatomotor activity.

Relative Contribution Analysis: HC Group vs. SCI Group

In the relative contribution (RC) analysis, the amplitudes of the task predictors for the HC and the SCI groups were computed across the cortical surface for the two tasks: Imagined Leg movement and Attempted Knee movement. The RC maps were masked by task-involvement in the healthy controls. The RC of the HC and SCI predictors are visualized in Fig. 9 for each of the two experimental tasks.

Within the task-related network in healthy controls in the imagined leg movement task, RC values indicated fairly equal contributions of the HC and SCI predictors in most task-related brain areas (orange/lime colors), with the primary exception in the medial SPL (orange to red colors), where the HC predictor contributed more than the SCI predictor. The RC value in the center of the human PRR exhibited fairly balanced contributions of the HC and SCI predictors (orange), while in the anterior edge of PRR extending towards the medPoCS, the balance of predictors shifted more towards HC. These findings offer confirmation of the overlap of the HC and SCI GLM activation maps, the locations of significant differences between groups in the GLM-RFX comparison, and the observed ERA BOLD timecourses discussed previously.

The more interesting finding was in the RC map for the attempted knee movement task. In the AK task, the contributions of HC and SCI in the M1/S1 leg area were balanced (orange/lime), but there was also enhanced recruitment of left SFG and the medial-most part of left M1/S1 as well as greater relative activity in the right primary somatomotor cortex in the SCI subject group compared to age-matched healthy control subjects (bright and darker green). Blue arrows graphically depict this shift, which reflects a spread in recruitment of

parts of the left somatomotor cortex and up-regulation of task-engagement in the right somatomotor cortex (Figure 9).

Relative Contribution Analysis: IL Task vs. AK Task

An additional RC analysis which separately compared active predictor contributions across the two tasks (IL, AK) was calculated for the different subject groups in each hemisphere (see Figs. 10 and 11). This analysis was a useful visualization of the relative recruitment of different brain areas in each of the two tasks and was used to detect any breakdown in the distinction between imagined and attempted movement networks in the SCI subject group.

In the SCI subject group, the activity balance between experimental tasks remained normal in bilateral frontomotor (PMd, SMA) and temporal areas (MTG). However, there was a shift in the M1 hand area such that it was recruited not only during the IL task but also during the AK task in these subjects.

In several SPL regions (recruited by HC subjects in the IL task: medPPC, retIPS, aIPS) there was a shift in the SCI subjects towards enhanced recruitment of these areas during the performance of the AK task. In HC subjects, the SPL regions were more active in the IL task than in the AK task. However, in the SCI group, these same areas were much more equally recruited during both tasks. These RC map changes correspond with the fact that in SCI subjects compared to healthy controls, these ROIs were more active above baseline in the AK task (GLM analyses), perhaps reflecting compensatory recruitment of the goal-directed action network during a simple attempted movement that would otherwise not engage this circuit.

In HC subjects, the M1 hand knob was typically recruited only in the IL task, while in SCI subjects it was additionally recruited in the AK task. In the centers of healthy control AK task ROIs, there were no differences between the HC and SCI subject groups either in level or BOLD activity (please see bottom of Table 4) or in the balance of activity between tasks. However, in SCI subjects compared to HC subjects, there was a shift in other knee-related

areas. In these bilateral task-related areas, identified in the SCI group using GLM contrasts (SFG, M1 leg area, CMA, pCC), not only was there a significantly higher level of activity in the SCI group (see Table 4 and Fig. 9) but there was also a shift between tasks in the SCI subject group such that these areas became more active in the AK task. This effect is particularly striking in the RC map of the right hemisphere (Fig. 11).

Linear Correlation Analyses

In addition to the standard GLM maps and group comparisons, we checked for linear correlations between clinical and behavioral variables and BOLD activity in the SCI subject group. One SCI subject was excluded from a subject of these analyses since the subject did not return for additional assessment of neurological and clinical variables six months after the baseline tests and fMRI data acquisition; hence, certain correlations were calculated for the 15 remaining SCI subjects. A subset of correlations in the IL task can be seen in Fig. 12, while the statistics for the correlations and any interactions are located in Table 5.

Hours per week of any exercise:

IL Task

Hours per week of any exercise correlated positively with activity in the inferior parietal cortex (IPL/MTG: $r=0.6$, $p<0.019$), medPPC/SPL, and aIPS. It also correlated positively with activity in frontomotor cortex bilaterally in the SMA, PMd, M1 hand area, and further extending along the bilateral CS into parts of premotor, primary motor, and somatosensory cortex associated with leg movement (see Fig. 12). Most of these influences were normalizing, except in the right ACC and SMA, where mean SCI group activity was slightly higher but not significantly different from mean HC group activity.

AK Task

In the AK task, this variable showed a trend positive correlation with activity in the left SFG/SMA, and a trend negative correlation with activity in the right SMA, which was a normalizing influence. Increasing hours per week of any form of exercise also decreased

activity in the right medial SPL (normalizing), and increased activity in the left ventral somatosensory cortex and anterior IPL (also normalizing).

Hours per week of IE program exercise:

Increasing hours per week spent in an intense-exercise program (Project Walk, Carlsbad, CA) helped to maintain a more normal pattern of brain activity in both IL and AK tasks (see Fig. 12).

IL Task

The strongest correlations in the IL task were observed in the parietal cortex. Hours per week of intense-exercise (at Project Walk, Carlsbad, CA) correlated positively with activity in the medPPC, left IPL/MTG, and bilateral M1/S1 hand area. There was also a strongly positive correlation with activity in the right ACC, right pCing, and right IPL, and a weaker correlation in the right latPrCS.

AK Task

In the AK task, significant negative correlations were observed in certain left knee related motor areas including S1 and M1/CMA, with a trend negative correlation in the M1 leg area. Negative correlations were also observed in the anterior and medial-most portions of the bilateral SFG/SMA, in the right PMv/IFG and SMA, and in parts of the left M1/S1 hand/arm areas and SMG/IPL (all normalizing influences).

Total hours of IE program exercise prior to fMRI:

IL Task

Total hours spent in the IE program prior to the fMRI experiments correlated positively with activity in bilateral parietal and frontomotor cortex. Significant and near significant correlations were observed in the left medPPC (LH – $r=0.66$, $p<0.007$), bilateral aIPS (LH – $r=0.62$, $p<0.014$; RH – $r=0.45$, $p<0.09$), left IPL/MTG ($r=0.54$, $p<0.038$), and in bilateral M1 hand area (LH – $r=0.66$, $p<0.007$; RH – $r=0.67$, $p<0.007$), ACC (LH – $r=0.55$, $p<0.034$; RH – $r=0.56$, $p<0.03$), left SMA (LH – $r=0.51$, $p<0.053$), right Cing. (RH – $r=0.56$, $p<0.03$), latPrCS (RH – $r=0.5$, $p<0.058$), and PMd (RH – $r=0.46$, $p<0.08$).

AK Task

There were no significant correlations in the AK task; however, trend negative correlations were observed in the left CMA, pCC, and right medPoCS.

Time-since-injury (days between SCI and fMRI):

IL Task

Time-since-injury correlated positively with activity in the left ACC, SMA, aIPS, and in the right IPL/MTG ($r=-0.43$, $p<0.11$). The center of the left IPL/MTG did not show this effect, but a positive correlation was observed nearby.

AK Task

In the AK task, there were no significant correlations between brain activity and time-since-injury in the main task-related ROIs. In the right latPoCS, there was a significant positive correlation with BOLD activity (denormalizing).

ASIA Impairment Scale (AIS A-C):

The ASIA Impairment Scale (AIS, i.e., A-E) also correlated with brain activity during the IL task, but not during the AK task.

IL Task

With less complete SCI, BOLD activity increased in the bilateral medPPC, left SPL and medPoCS, and the left SFG/SMA. In Figure 12, positive correlations can be observed in part of the right SFG/SMA and the right M1 leg area, all normalizing influences.

AK Task

There were no significant correlations between brain activity and AIS in this task.

SCI Level:

IL Task/*AK Task*

SCI level (i.e., C4-T8) did not correlate significantly with brain activity in either task. However, in the IL task, with lower-level injuries there were trend-positive correlations in the right PMv/IFG, right M1/S1 hand area, and the bilateral MTG. In addition to these main effects, there were interesting interactions effects, described below.

SCI Group (e.g., IE-SCI or C-SCI):

SCI subjects included in this study were either enrolled in an intense exercise program (IE-SCI) or participated in their own exercise regime (C-SCI). See the *Methods* for more on these groups and their distinctions.

IL Task

SCI Group correlated with activity in the left medPPC/SPL, right pCing and right ACC, with lower BOLD activity in the C-SCI group.

AK Task

Activity in the left CMA and S1 knee area increased in the C-SCI group. There were also correlations in the right hemisphere in the latCS ($r=0.52$, $p<0.048$), PMv/IFG and SPL, again with higher activity in the C-SCI group compared with the IE-SCI group.

Age:

IL Task

There was a trend negative correlation in the left medPoCS and medPPC, and a trend positive correlation in the right medPPC and MTG. Significant interactions were observed between age and other variables in many task-related brain areas, detailed in the description of interaction effects below.

AK Task

In the AK task, increased age positively correlated with BOLD activity in the medial-most portion of the PrCS, indicating a less healthy level of brain activity, but no significant correlations were observed in any of the main ROIs (see Table 5).

Change in Right ASIA LEMS:

IL Task

Change in Right ASIA LEMS strongly correlated with activity in the parietal cortex. In bilateral medPPC/SPL and medPoCS, r-values were in the 0.52-0.75 range, with the peak r-value of 0.88 observed in a portion of the medPPC (see Figure 13). Change in Right ASIA LEMS also correlated strongly with activity extending onto the medial wall of the left SPL ($r=0.68$, $p<0.006$). Additionally, the variable also correlated with activity in the bilateral pCing and SFG/SMA, a positive correlation was observed in the right MTG ($r=0.58$, $p<0.02$), and a positive trend correlation was observed in the bilateral SMA. Even though the bilateral M1/S1 leg areas were not main task-related ROIs in the IL task, these areas still showed significant positive correlations with change in Right ASIA LEMS, suggesting that even recruitment of primary somatomotor areas by imagined movement can predict functional recovery.

AK Task

The only significant correlation was in the right SMA, and was a negative correlation with BOLD activity ($r=-0.61$, $p<0.015$). There were also trend negative correlations in the right latPrCS, right M1 leg area, and the left CMA.

Right ASIA LEMS:

IL Task

Right ASIA LEMS correlated positively with activity in the bilateral medPPC and left SPL, right SFG/SMA ($r=0.61$, $p<0.02$), with a trend effect in the ROI left SFG/SMA, but the parts of left SFG/SMA clearly show a significant effect in Fig. 12, as does part of the left M1 leg area. There was also a correlation in the right hemisphere in the PMv/IFG, and near significant positive correlations in parts of bilateral MTG.

AK Task

This variable correlated positively with activity in the bilateral medPPC, and there was a trend correlation in the left IPL/MTG ($r=0.44$, $p<0.1$). There was also a positive correlation

with right M1/S1 hand area activity, and a similar trend in the right M1 extending into the SFG.

Change in Right ASIA UEMS:

IL Task

A positive change in Right ASIA UEMS strongly correlated with activity in the bilateral medPPC ($r=0.55$ to 0.71, $p<0.003$ to $p<0.03$), and also the right aIPS and left IPL/MTG, and bilateral MTG. Positive trend correlations were observed in the right ACC and right PMv/IFG.

AK Task

In the AK task, this variable again correlated positively with activity in the bilateral SPL, right pCC, and right M1/S1 leg area, but not with recruitment of the M1 hand area by either task. A trend negative correlation was observed in the left SFG/SMA ($r=-0.4$, $p<0.13$), while additional positive correlations were observed in the bilateral ACC, left Cing., and left medial-most PrCS. Interestingly, both the left Cing. and the left medial-most PrCS were recruited by healthy controls performing the IL task, not strongly task-related in HC subjects during the AK task.

Right ASIA UEMS:

IL Task

This variable correlated positively with activity in the MTG bilaterally. It also correlated negatively with activity in the left cSMA/CMA, which was not a main ROI.

AK Task

Baseline right ASIA UEMS correlated positively with activity in the right SPL. There was also a trend towards a negative correlation in two motor-related areas that were overactive in SCI subjects compared to healthy controls: the left SFG/SMA ($r=-0.29$, $p<0.3$) and the right SFG/M1 ($r=-0.43$, $p<0.11$).

Change in bilateral ASIA motor score:

IL Task

There were strong positive correlations between baseline brain activity assessed via fMRI and improvements in bilateral ASIA Motor Score 6 months later. The most significant correlations were in the bilateral medPPC extending onto the medial wall (to include the medPoCS and pCing), with r-values up to 0.81 ($p<0.00022$). Additional parietal correlations were observed in the bilateral SPL, aIPS, MTG, and left IPL/MTG. In frontomotor cortex, there were positive correlations in bilateral SFG/SMA, and right ACC, SMA, PMd (extending into PMdc), latPrCS, and PMv/IFG. A significant positive correlation was also observed in the bilateral medial CS extending onto the medial, part of primary somatomotor cortex associated with leg movement (a normalizing influence).

AK Task

There were no significant correlations between BOLD activity and change in bilateral ASIA motor score in the AK task.

Bilateral ASIA motor score:

IL Task

Baseline bilateral ASIA motor score correlated positively with activity in the bilateral MTG, bilateral SPL/medPPC extending onto the medial wall, and right aIPS and PMv/IFG.

AK Task:

There were no significant correlations in the AK task.

Interaction Effects:

We also looked for interaction effects between Change in Right ASIA LEMS (cMLEr) and other variables (via ANOVA). There were no interaction effects with SCI Group, but there were significant interaction effects between cMLEr and other variables, including baseline Right ASIA LEMS (MLEr), Change in Right ASIA UEMS (cMUEr), ASIA Impairment Scale (AIS), SCI Level, Time-Since-Injury (TSI), Age, Hours per week any exercise (HpW-Any), Hours per week of IE (HpW-IE), Days in the IE program prior to fMRI (Days-IE), and Total Hours in the IE program (TotHours-IE) (see Table 5).

In bilateral SFG/SMA (surface extending onto the medial wall in SMA proper), there were interaction effects between cMLEr and Age, cMLEr and AIS, and cMLEr and TSI. In the PMd, while there was no main effect of cMLEr, there were interaction effects bilaterally. In the left PMd, there were interactions between cMLEr and: Age, AIS, SCI Level, and cMUEr. In the right PMd, there were interactions between cMLEr and: Age and AIS. In the left M1/S1 hand area, there was no main effect of cMLEr, but there was a significant interaction effect with HpW-IE ($p<0.03$).

In the right latPrCS, there was an interaction between two variables with main effects: cMLEr and HpW-IE ($p<0.08$). In the right pCing, there were trend interactions between cMLEr and: AIS, SCI Level, and cMUEr.

In the left aIPS, there was no main effect of cMLEr, but significant interactions between cMLEr and: Age, AIS. Conversely, in the right aIPS there was an interaction with HpW-IE. In the left SPL, there were interactions between cMLEr and: MLEr, Age, while in the right SPL there was an interaction with HpW-IE. In the left medPPC, there were significant interactions between cMLEr and: AIS, Age, and MLEr, all of which had significant or near significant main effects.

In the left MTG, there were interaction effects with Days-IE and TotHours-IE, while in the right MTG, there were interaction effects with Age, MLEr, AIS, and TSI.

Subcortical Correlations

Subcortically, BOLD activity in the cerebellum during the AK task also correlated with baseline ASIA somatomotor functional measures, as well as with changes in ASIA motor scores. Activity in the right (ipsilateral) cerebellum correlated negatively with bilateral ASIA Touch/Pin score, bilateral ASIA combined motor score, bilateral ASIA LEMS. Lower activity in the right cerebellum during the AK task also predicted better functional motor improvement in the lower extremities, assessed by a change in bilateral (including right) ASIA LEMS from the baseline measure to the same measure taken 6 months later. Increasing

hours per week of exercise in the IE program also decreased activity in the ipsilateral cerebellum, to resemble a more normal activation pattern. In the contralateral cerebellum, similar correlations were observed (negative correlation between BOLD activity and bilateral ASIA LEMS and change in right ASIA LEMS).

Effect of ASIA Impairment Scale (AIS) on brain activity

Linear correlation analyses revealed relationships between the level of BOLD activity in several ROIs engaged during imagined leg movement and the degree of "completeness" of the spinal cord injury. However, we also subdivided the SCI group into two subgroups to increase the power of comparisons between "more complete" and "less complete" injuries.

The first SCI subgroup consisted of 11 AIS A/B subjects. AIS A classification means that the subject's injury is complete, with no sensory or motor function preserved in sacral segments S4-S5. AIS B classification means that a subject's injury is incomplete, with sensory but no motor function preserved below the injury level and extending through sacral segments S4-S5. A second SCI subgroup consisted of 5 AIS subjects. AIS C classification means that a subject's injury is incomplete, with some motor function preserved below the site of injury.

In both tasks, subjects with "less complete" injuries (AIS C) exhibit the most normal pattern of task-related brain activity (Figure 14). In the IL task, subjects with AIS A/B classification still recruit PMd, SMA, medPPC and aIPS, but the overall spread of activity is reduced compared to HC subjects, and the level of activity is also reduced (not shown). In the AK task, subjects with AIS A/B classification activate a greater area of somatomotor cortex than HC subjects, while this network shrinks in subjects with AIS C classification.

Effect of time-since-injury (TSI) on brain activity

Linear correlation analyses did not reveal robust relationships between TSI and BOLD activity and many of the main somatomotor and motor association ROIs in the two experimental tasks. To improve the power of our investigation of the effect of TSI, we

subdivided the SCI subjects into two groups based on the total elapsed time between their spinal cord injury and the date of their fMRI and clinical exam.

The Early-SCI subgroup consisted of eight SCI subjects with TSIs less than 4.5 years. The Late-SCI subgroup consisted of eight SCI subjects with TSIs of greater than 4.5 years. Group activation maps for the two tasks are pictured in Figure 15. There seems to be an early depression and a later expansion of the spread of the network engaged during imagined leg movement in SCI subjects, while during attempted knee movement, there is local and inter-hemispheric spread of activity in the Early-SCI group, compared to the HC group, and this activity spread contracts again in the Late-SCI group.

We also directly compared the Early- and the Late-SCI groups controlling for possible covariates like hours per week of exercise, total hours spent in an intense exercise program, and spinal cord cross-sectional area. These random-effects ANCOVA analyses found one ROI with a particularly strong relationship with time-since-injury: the M1/PMd knee area located in the medial-most portion of the precentral sulcus, just anterior to the primary knee representation in M1 (Figure 16).

This ROI was hyperactive in the Early-SCI subgroup and hypoactive in the Late-SCI subgroup, compared to HC subjects. However, we also observed a robust relationship between spinal cord cross-sectional area (CSA) and BOLD activity in this ROI. CSA is a measure of spinal cord area used to assess shrinkage of the spinal cord following injury. CSA values for the spinal cord subjects in this study are lower than those for healthy controls. Larger CSA means that a subject's spinal cord is more healthy/normal in size. In the Low-CSA subgroup, M1/PMd was hypoactive relative to HC subjects. In the High-CSA subgroup, M1/PMd was hyperactive relative to HC subjects.

The strong modulation of BOLD activity by both TSI and CSA is not unexpected, since we hypothesized that TSI and CSA would be correlated. This is indeed the case (Figure 17), with CSA decreasing as TSI increases. However, a smaller portion of the M1/PMd ROI survived the ANCOVA analysis with a between-subjects factor of TSI subgroup and a covariate of

CSA, suggesting that at least a portion of the variance in the BOLD signal observed in this ROI is an effect of TSI that doesn't covary with CSA.

Effect of preserved sensory and proprioceptive abilities on brain activity

The main task-related ROIs in both the IL and the AK tasks receive somatosensory and proprioceptive inputs in healthy control subjects. However, these inputs are severely disrupted in SCI subjects. To examine the effect of severe disruption to these sensory input pathways, we looking at linear correlations between ASIA somatosensory touch, ASIA pin-prick, and proprioception scores and brain activity.

During the IL task, BOLD activity in parts of the medPPC correlated positively with all three variables, reflecting preserved sensory function, while activity in parts of the SMA correlated with both ASIA pin and proprioception scores. There were no significant linear correlations between these variables and BOLD activity in the AK task.

We increased the statistical power for our investigation of proprioceptive ability and effects on brain activity by dividing the SCI group into two subgroups based on their right proprioception score. Subjects with a right proprioception score of zero, indicating no residual proprioceptive ability, were included in the SCI-P0 group (n=13). Only three of the SCI subjects included in the study had non-zero right proprioception scores, and these subjects were included in the SCI-P1 group.

Comparing the IL task activation maps for the SCI-P0 and HC groups (Figure 18A), it is clear that even if proprioceptive ability scales with brain activity in the medPPC and SMA, these ROIs and the rest of the frontoparietal association, motor planning network remain active above baseline in subjects with no preserved proprioception. Figures 18B shows the BOLD timecourses from PMd, SMA and medPPC with separate activation curves for the SCI-P0 and SCI-P1 subgroups. A least a portion of the activity in these brain areas seems to be accounted for by residual proprioceptive ability (difference between the SCI-P1 and SCI-

P0 curves), but all three ROIs are still active even if a subject's proprioceptive inputs are completely disrupted (SCI-P0 curve vs. baseline).

Similar investigations of the ROIs engaged during the AK task reveal a major spread of the activation map in the SCI-P0 group compared to the HC and SCI-P1 groups. Attempted knee movement activity recruited more of the neighboring and opposite-hemisphere somatomotor cortex in the SCI-P0 group, indicating that at least some of the compensatory hyper-activations observed in the overall SCI subject group could be correlated with the absence of proprioceptive inputs from the limb.

DISCUSSION

We investigated changes in neural activity and the organization of cortical networks for action planning and execution following SCI. A relatively normal pattern of brain activity was observed in SCI subjects during both the planning and execution phases of movements of the disconnected limb. However, we did find evidence of neural compensatory mechanisms during attempted knee movement. Similar changes were not observed during motor planning and execution for imagined lower limb movement, suggesting differential task-related plasticity in the primary motor system and motor association areas.

Attempted self-paced knee movement task

The first experimental task investigated plasticity in the neural circuits involved in movement execution, including primary somatomotor cortex (M1, S1, and CMA) and the cerebellum. Following SCI, the somatomotor cortex contralateral to the limb employed and central to right knee movement in healthy controls remained active (Left M1 leg, Left S1 leg, and Left CMA). However, surrounding left- and homologous right-somatomotor cortex was hyper-active in the SCI group compared with the HC group. We observed local 'spreading' of activity in the M1/S1 and onto the medial wall in SCI subjects, such that parts of the somatomotor cortex responsible for movements of other body parts of or synergistic muscle groups in the leg, and even the adjacent arm representations, were recruited. In addition, the right motor cortex, ipsilateral to the right knee effector, was engaged, again suggesting that SCI subjects may compensate for the severely disrupted functional connectivity of the knee

M1-to-spinal cord by attempting to recruit additional corticospinal fibers for neighboring body parts and muscle groups, and for the analogous limb in the opposite hemisphere. Subcortically, this hyper-activity effect was also observed in the bilateral cerebellum and the posterior corpus callosum.

Similar over-activations are common following injury to the motor output pathway, particularly in the earlier stages of injury. In cortical stroke subjects, functional impairments of both the upper and the lower limbs are associated with increased recruitment somatomotor cortex in both the lesioned and the unlesioned hemisphere (Enzinger et al. 2008, Schaechter & Perdue 2008, Gerloff et al. 2005, for review: Rossini et al. 2007). Compensatory over-activity has also been reported in earlier-stage spinal cord injured subjects (Alkahdi et al 2005).

From a cognitive perspective, significant impairments in M1-to-spinal cord communication could translate into a higher task difficulty for the SCI subjects. Attempted knee movement can be extremely frustrating for these subjects, and is often fruitless, and this could lead to compensatory recruitment of surrounding cortex and the upregulation in cerebellar activity. Physiologically, reduced M1-to-spinal cord excitability as a result of injury to the descending corticospinal fibers could manifest as the need to recruit additional primary motor cortex and other surviving fibers (Ward et al. 2006) to complete the task. Severe disruptions to both motor output and afferent feedback could also lead to disorganization of motor or action representations in primary motor cortex. Thus, the differences observed between HC and SCI subjects could represent task difficulty and temporary network regulation, or could indicate more long-term functional and physiological changes.

We investigated the possibility that reduced afferent feedback during movement execution could explain the overall activation enhancement and spread in the SCI group. We looked at BOLD activity sorted by clinical proprioception scores for the lower limbs. Subjects with proprioception scores of zero had no residual proprioceptive abilities (subgroup SCI-P0). Only 3/16 subjects had a non-zero right limb proprioception score (subgroup SCI-P1), indicating some level of residual proprioceptive ability. Compensatory recruitment of the

dorsal premotor cortex, superior frontal gyrus, supplementary motor cortex, M1 arm/hand areas, corpus callosum, and cerebellum was only apparent in the SCI-P0 subject group. In contrast, no differences between the HC and SCI groups, or between the SCI-P0 and SCI-P1 subgroups, were observed in the M1 knee area. However, between-group differences were observed extending medially in M1 from the knee area, and this effect generalized across the whole SCI group, regardless of proprioception score. These findings indicate that at least some of the compensatory hyper-activations observed in the SCI subject group could be correlated with the absence of proprioceptive inputs from the limb.

Our finding of enhanced recruitment of somatomotor cortex ipsilateral to the limb used is consistent with studies of stroke subjects (Enzinger et al. 2008, Schaechter et al. 2008, Cramer & Crafton 2006, Foltys et al. 2003, Ward et al. 2003, for review see Cramer 2004). These previous studies suggested that the activation of ipsilateral motor cortex could be compensatory, but was also often associated with the severity of the impairment and linked to poorer clinical outcome. Mirror movements of the opposite limb are common during attempted limb movement in SCI subjects, particularly when the function of one limb is more disrupted than the other. These mirror movements could be mediated by the disinhibition of the opposite motor cortex as the limb-brain mapping in motor cortex changes following SCI, or by compensatory recruitment mechanisms. In either case, increases in interhemispheric communication are likely to accompany and facilitate mirror movements. In the current study, SCI subjects exhibited increased activity in the posterior corpus callosum (pCC) compared to healthy controls. The corpus callosum, which mediates interhemispheric transfer of information, is not ordinarily task-related in the HC group. The upregulation of pCC activity in SCI subjects could reflect heightened communication between the contralateral and ipsilateral primary motor cortices, especially since it correlated with increased right hemisphere somatomotor activity. We ruled out the possibility of differential head movement between groups as an explanation of the functional activity differences (see Methods). The pattern of brain activity observed in this task, including enhanced pCC activity and over-activity in the right hemisphere (ipsilateral to limb) provides evidence of a neural basis that could explain the propensity for and generation of mirrored actions following SCI.

Imagined goal-directed leg movement task

The second experimental task investigated plasticity in the neural circuits involved in planning and executing goal-directed limb movements. We employed imagined limb movement in this task to avoid any confounds of involuntary head movement during attempted limb movement, and because a previous study in healthy control subjects found that imagined movements were as effective at recruiting motor association areas as real movements (Glidden et al. submitted). In the current study, imagined, goal-directed leg movement planning and execution robustly activated the frontoparietal motor association network (including PMd, SMA, aIPS and PRR) in both healthy control and SCI subjects. We found no evidence of compensatory over-activations or activation spread in the SCI group. However there were some significant differences in the level of BOLD activity between HC and SCI subjects, with the overall trend that SCI subjects recruit these brain areas to a lesser degree than HC subjects.

As in the attempted knee movement task, SCI subjects with some degree of preserved proprioceptive ability retained a more healthy/normal level of BOLD activity, while SCI subjects with proprioception scores of zero demonstrated a reduced BOLD activity level relative to healthy control subjects. Therefore, an assessment of preserved proprioceptive feedback in SCI subjects, such as the proprioception score, may be a tangible clinical marker correlating with the degree of brain reorganization and plasticity in both the primary motor execution network and the motor association network following spinal cord injury. The observed correlation between proprioception score and brain activity also suggests that proprioceptive feedback may play a role in maintaining healthy motor and action representations in the brain.

The motor association network involved in imagined leg movement, including the SMA, PMd, and PPC, is also recruited by real and imagined goal-directed limb movement planning and execution, as well as by saccadic eye movement planning and execution (Glidden et al. submitted). In the current study, we controlled for visual stimulation and eye movements; therefore, the preservation of the motor association network following SCI suggests that SCI subjects can still plan and internally simulate movements of a functionally disconnected

limb. Regular motor imagery or attempted movements of the affected limbs, movements of unaffected limbs, and even saccades could all help contribute to activity-dependent maintenance of a healthy/normal motor association network following spinal cord injury.

Motor association areas may reorganize less than primary motor areas

We observed a greater disruption in the organization of the primary somatomotor network than in the motor association network. This difference could reflect either disparities in difficulty between the attempted knee movement and imagined goal-direct leg movement tasks, or could be indicative of network-specific plasticity. If the activation spread during attempted knee movement is not an effect of task-difficulty, then it is possible that it has a more long-term, physiological basis. Compared to primary somatomotor cortex, motor association areas including PMd, SMA and PPC are further removed from the site of injury with few direct connections with the spinal cord, still receive many sensory inputs following SCI (e.g. visual, auditory, vestibular), and are also regularly engaged during a variety of cognitive and motor tasks. These differences between the primary somatomotor network and the motor association network could explain differences in the degree of reorganization and plasticity in each network following spinal cord injury. A future experiment employing attempted goal-directed limb movements to drive both the primary motor execution network as well as motor association areas could disambiguate between task difficulty and network-specific plasticity.

Time-since-injury

In the current study of chronic, high-level SCI subjects an average of 4.7 years post-injury, the brain networks subserving both paced attempted knee extension and goal-directed, imagined leg movement planning and execution remained largely intact, even though the injury effectively disconnects the lower limb from the cortex. However, several recent fMRI studies of SCI subjects have reported both hyper- and hypo-activations (Alkadhi et al 2005, Cramer et al 2005, Hotz-Boendermaker et al 2008). The divergent results of these previous studies could be unified if time-since-injury (TSI) plays a significant role in shaping brain activity. This variable might be critical to the stability of cortical motor representations (the preservation of which may not be entirely activity-dependent, at least if the limb is still

physically attached to the body), and could also influence the cognitive and functional processes engaged during imagined and attempted movements of the affected limbs.

We did not find significant correlations between continuous TSI, measured as the number of days between the date of the spinal cord injury and the date of the fMRI session, and BOLD activity in the primary and association motor system ROIs in either experimental task. However, when SCI subjects were grouped into an Early-SCI and a Late-SCI group, a few interesting effects of time-since-injury emerged. In the AK task, hyperactivity in parts of the PMd/SFG decreased with increasing TSI, i.e., activity became more normal. In contrast, the corpus callosum became more active, or less normal, with increasing TSI. In the primary M1 and S1 knee areas, there was no significant difference in activity level between the HC and SCI groups. However, when the SCI group was subdivided based on TSI, a hyper-activation was apparent in the Early-SCI group while a hypo-activation relative to HC subjects was observed in the Late-SCI group. This finding helps unify the divergent results of previous studies of SCI subjects (Alkadhi et al 2005, Cramer et al 2005, Hotz-Boendermaker et al 2008), suggesting that during the first few years after SCI, primary somatomotor cortex becomes hyperactive and there is enhanced recruitment of neighboring as well as opposite-hemispheric, homologous cortex. However, once the injury stabilizes with severe functional impairments remaining, later SCI subjects exhibit hypo-activations in primary somatomotor cortex.

Two recent fMRI papers investigating attempted foot flexion/extension in SCI subjects, reporting divergent results early (2.7 years), and very late (22 years) after spinal cord injury. Alkadhi and colleagues (2005) investigated imagined foot movement in SCI subjects, at an average of 2.7 years-post-injury, compared to both motor imagery and movement execution in healthy control subjects. They reported stable cortical representations in M1/S1 during imagined movement in the SCI subjects (compared to real movement execution in controls) as well as over-activation of surrounding cortical areas and the cerebellum during foot imagery of foot flexion/extension in SCI subjects compared to both motor imagery and motor execution in healthy controls. They also reported strong linear correlations between measures of the vividness of motor imagery (including kinesthetic elements) and brain activity in M1

and the SMA/CMA. In contrast, the paper by Cramer and colleagues (2005) investigated later-stage SCI subjects, at an average of 22 years-post-injury. While Cramer et al. reported stable cortical representations during attempted movement of the foot, they also found reduced overall activation volume, consistent with the hypotheses that either 1) the motor cortex becomes less excitable many years after the injury, 2) subjects lose touch with the concept of motor execution involving the affected limb, or 3) they are less motivated in their life, during rehabilitation, and/or during specific task engagement.

Our experimental findings are in greatest accord with the work of Alkadhi et al (2005), as are the specifics of our patient population. Cramer et al (2005) studied SCI subjects with dense ASIA A impairment, who averaged over 20 years since their last voluntary leg movements. In contrast, the SCI subjects scanned in our experimental paradigm were an average of 4.7 years-post-injury and exercised for an average of 6.3 hours per week, indicating a high degree of motivation and commitment to rehabilitation, which we hope translated into a high degree of subject engagement during our fMRI tasks. However, our findings are also in accord with the hypothesis that many early SCI subjects may 'try hard' and are more likely to be undergoing more intensive rehabilitative strategies than subjects with longer TSI. With increasing TSI, a subject's condition is likely to have stabilized and a multitude of other factors, including overall satisfaction with life or level of independence, could affect the subject's mood and motivation. This in turn could affect their ability to engage in the experimental tasks and manifest as a different pattern or level of BOLD activity.

Another recent study investigated complete lower thoracic and lumbar-level SCI subjects at an average of 10 years-post-injury, an intermediate stage between the subject groups of Alkadhi et al 2005 and Cramer et al 2005 (Hotz-Boendermaker et al 2008). The authors reported that attempted self-paced foot flexion in SCI subjects activated largely the same brain network as motor execution in healthy control subjects. The foci of the local maxima of BOLD activity in M1 did not differ between the SCI and control groups, suggesting that the cortical map representation of the foot was still intact and had not been absorbed by other, neighboring maps of preserved body parts/muscle groups. However, they also observed a reduced spread of activation in primary somatosensory cortices and both an activity spread

and a pattern of over-activity in the bilateral cerebellum. Like Hotz-Boendermaker and colleagues (2008), we also found little evidence of a shift in the location of the local maxima in M1 and S1, but in contrast saw evidence of spreading, compensatory activity. The SCI subjects included in our study were an average of 4.7 years-post-injury, which may explain the increase in cortical volume recruited during the attempted movement task, compared with the reduction observed by Hotz-Boendermaker and colleagues (2008) in a later-stage SCI subject group.

When average time-since-injury of the subject populations participating in previous fMRI studies of SCI is considered, a unified view of changes in the cortical motor system emerges, with early stage hyperactivity and later stage hypoactivity. The ecological, clinical and behavioral importance of these deviations from "normal" levels and patterns of activity is still under consideration. However, if these changes are maladaptive, strategies for "normalizing" would be imperative. Several possible "normalizing" strategies are discussed later.

Brain activity correlates with current and future measures of clinical severity and exercise history in the imagined goal-directed leg movement task

Linear correlation analyses between clinical or behavioral variables and BOLD activity in SCI subjects yielded interesting results. Within the frontoparietal motor association network engaged during the imagined goal-directed leg movement task, no significant correlations were observed in the left PMd, though there was a trend ($p<0.08$) towards a positive correlation between brain activity and hours/week exercise. In the SMA, total hours spent in an intense exercise program (exercise history) correlated positively with BOLD activity. In the aIPS, there were significant correlations with hours/week exercise and functional motor improvements six months later. However, the strongest linear correlations were observed in the medial SPL (medSPL), near and including human PRR.

BOLD activity in the medSPL correlated with current variables, such as the ASIA lower extremity motor scores and ASIA Impairment Scale assessed same day, but also with prior and future variables, such as the history of exercise prior to the fMRI exam (hours/week of

exercise, days and total hours spent in an intense exercise program) as well as future functional motor improvements, assessed as positive changes in ASIA motor scores between the day of the fMRI exam and a second measure of the same ASIA scores taken six months later. Higher (more normal) BOLD activity at the single subject level in this part of the brain significantly correlated with better current motor functionality, more exercise, and greater improvements in motor functionality over the next six months.

At the single subject level, the paired clinical (ASIA motor scores, ASIA impairment scale, and changes in ASIA motor scores) and behavioral variables (exercise history) did not significantly correlate with each other, except for a significant correlation ($r=0.51$, $p<0.054$) between a change in bilateral ASIA lower motor extremity score and hours per week spent in the intense exercise program at Project Walk. A recent study by Harness et al (2008), which included the same SCI subjects presented in the current study (as well as additional subjects), demonstrated that functional motor gains assessed as changes in ASIA motor scores in the IE-SCI group (Project Walk participants) correlated significantly with the number of hours/week spent in the intense exercise program, and particularly with load bearing exercises. They concluded that "multimodal intense exercise can significantly improve motor function in subjects with chronic SCI." Load-bearing exercises are likely to activate any residual ascending proprioceptive pathways; therefore, their finding is consistent with the hypothesis that there is a strong link between residual proprioception, clinical outcome, and brain activity in primary motor and motor association cortical areas.

Interestingly, medial posterior parietal brain activity (including hPRR) assessed via fMRI during the imagined leg movement task not only correlated with current clinical status, exercise history, and future functional motor gains, but as effectively or more robustly predicted functional motor improvements than traditional clinical/behavioral variables. The linear correlation r-values for hPRR activity as a predictor of future functional motor gains ranged from 0.75-0.88.

Table II.2.D – Correlations between brain activity or clinical and behavioral variables and subsequent functional motor gains. Functional motor gains were assessed via changes in ASIA motor scores from T1, the day of fMRI

exam and baseline measurements, to T2, six months later, when a second a clinical assessment of ASIA motor scores was made.

	Correlation with functional motor gains (lower extremity bilateral, lower extremity right, lower and upper extremity bilateral)
medPPC/hPRR BOLD Activity	max r=0.75-0.88
Exercise History (hours/week exercise)	max r=0.51
ASIA Impairment Scale	r=0.55-0.7
B. ASIA Lower Extremity Motor Score	r=0.6-0.83
R. ASIA Lower Extremity Motor Score	r=0.3-0.44

Activity level in the posterior parietal cortex signals not only the current clinical condition, but also future functional motor gains, suggesting that it could serve as a viable marker of the potential for clinical "plasticity." A future study involving longitudinal functional neuroimaging of SCI subjects could confirm whether the functional motor gains predicted by current PPC activity level are accompanied by physiological plasticity in BOLD activity in the PPC, as well as changes at the level of injury in the spinal cord.

Implications for neural prosthetics

The success of neural prosthetic devices capitalizing on a subject's ability to formulate action plans or outputs, reading out these intentions and translating them into inputs to an external device, may depend crucially on the preservation of motor and action representations in the brain. Our findings suggest that these representations are largely intact for functionally disconnected limbs in SCI subjects. The fidelity of these representations may also be influenced by subject motivation, time-since-injury, or interventions such as exercise therapy. Pre-surgical functional neuroimaging of candidate recipients of neural prosthetic devices could not only aid in customization and optimal placement of the device, but could also serve as a screening tool to vet candidates based on the probability of success of the device, improving the risk/benefit analysis.

CONCLUSIONS

FMRI of real reaching can be used to localize PRR in healthy subjects, but patients with upper limb paralysis are unable to reach. Thus, it is possible that imagined reaching could be used as a proxy for real reaching, driving activity in brain areas involved in real reach planning to localize potential neural prosthetic implant sites like PRR (see Part I: Chapter II).

For the purposes of the Caltech Neural Prosthetic project, we also wanted to investigate whether potential neural prosthetic implant targets, including PRR and PMd, are still active following injury to the motor output pathway.

Unlike our previous fMRI studies in healthy participants, the study of SCI subjects at the University of California, Irvine (UCI) utilized an imagined leg-reaching task. Data from healthy control subjects were used to confirm that imagined leg-reaching activates brain areas involved in real and imagined reach planning, including our potential neural prosthetic implant sites. Leg movements were used instead of arm movements because most of our SCI subjects still retained some use of the upper arms or shoulders, and we wanted to investigate neural plasticity and reorganization following complete injury to the motor output pathway. None of the SCI subjects scanned at UCI had preserved leg function. Pre-fMRI, we recorded activity from several muscles in the leg while subjects attempted real right knee extension, and also conducted transcranial magnetic stimulation of the knee area of primary motor cortex, again to assess the degree of remaining motor function below the spinal cord lesion site. These additional tests confirmed that none of the SCI subjects scanned in the fMRI experiment retained function of their lower limbs.

The results from our second fMRI study of SCI subjects performing an imagined leg-reaching task revealed that brain areas involved in planning imagined leg movements in healthy controls, including SMA, PMd, and PRR, remain active in SCI subjects. There is little evidence of cortical reorganization in these pre-motor brain areas following spinal cord injury, even up to 10 years post-injury. Compared to arm-reach planning and execution, leg-reach planning and execution activates a more bilateral network in healthy controls. This pattern is preserved in patients with high-level SCI. The main results of this study and the previous fMRI study are shown in Figure II.2.D.

Figure II.2.D – a. Comparison of fMRI study of SCI subjects and imagined leg-reaching and previous fMRI study of real and imagined arm-reaching. Imagined leg-reaching activates pre-motor areas selective for real reach planning, including SMA, PMd, and PRR. Real right arm reaching activates the hand/arm region of primary motor cortex (M1). Real right knee movement in healthy control subjects is shown in gold, and activated the knee/leg area of M1; compare with Figure II.2.Db. b. There is strong overlap of activation patterns during imagined right leg-reach planning and execution between healthy control subjects (yellow) and SCI subjects (purple), including in SMA, PMd, and PRR.

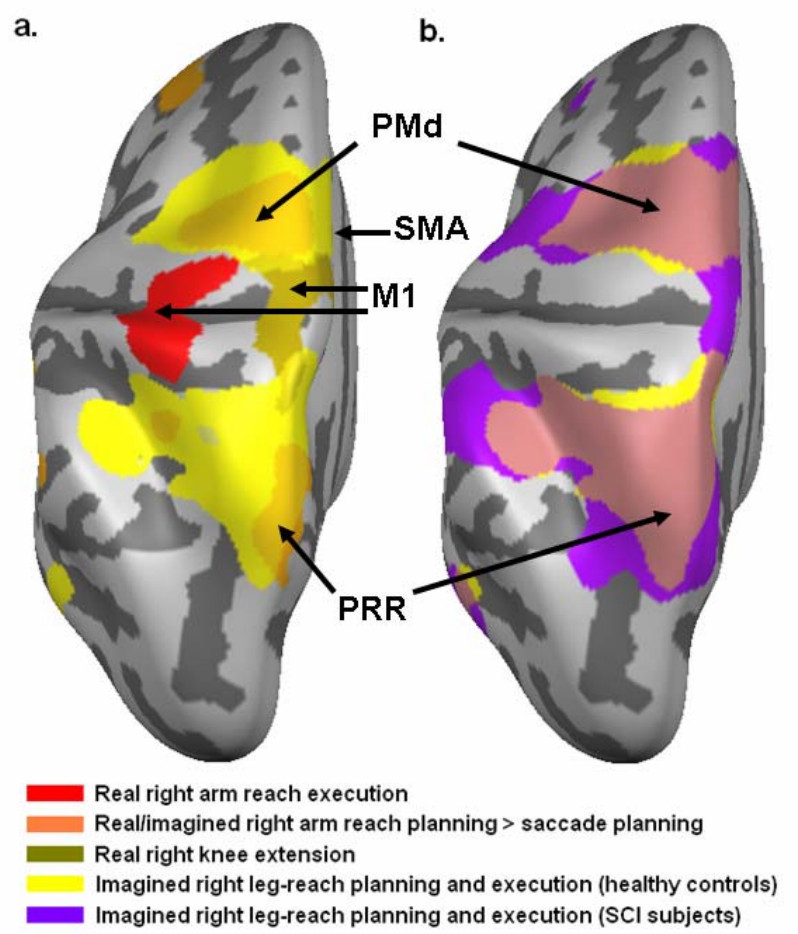

From the activation of human PRR and PMd by imagined movements in SCI subjects, we conclude that lower- or upper-limb motor imagery may be a viable proxy for real limb movement in the pre-surgical localization of candidate neural prosthetic implant targets in severely paralyzed patients. Our finding that the pattern of brain activity observed in SCI subjects strongly mirrors that of healthy controls is very promising. It demonstrates that even in the case of stable, complete disruption of the motor output pathway below the lesion site, merely thinking about and imagining movements of the paralyzed limbs activates a relatively

normal brain network, including our candidate implant sites of PRR, PMd, and SMA. Additionally, there was also no correlation between the level of activity in these areas and time-since-injury, indicating that they are still active in SCI subjects even up to 10 years-post-injury. These findings, as well as the positive correlations between PRR activity and amount and history of exercise, current motor functionality, and future functional motor improvements, have implications for the implantation and implementation of a neural prosthetic device in severely paralyzed patients, discussed further in the next chapter (Part II: Discussion).

METHODS

Subjects

Spinal cord-injured (SCI) subjects (n=16, see Table 1) and age-matched healthy control subjects (n=12) were included in this study. An additional five SCI subjects underwent neurological, behavioral and fMRI testing. However, these subjects were excluded from analyses for the following reasons: excessive head motion (n=3), subject non-compliance with task instructions (n=1), and undisclosed brain lesion (n=1). All subjects gave informed consent in accordance with the University of California, Irvine Institutional Review Board guidelines.

Inclusion criteria for study enrollment as an SCI subject were: the subject had to be in the age range 18-70 years, have a history of spinal cord injury (greater than 2 months prior to baseline neurological, behavioral and fMRI testing) resulting in quadriplegia or paraplegia between C2 and T12 levels, and be ASIA Impairment Scale A-D. Exclusion criteria included: ventilator-dependence and other major neurological disease or traumatic brain injury, which was operationally defined as trauma associated with loss of consciousness for > 24 hours.

Prior to experimental testing, a variety of clinical neurological, psychological and behavioral measures were taken. Both handedness (Oldfield 1971) and footedness (Coren 1993) were tested. A single experimenter (N.Y.) conducted neurological assessments, including ASIA motor score of the lower extremities (ASIA LEMS), ASIA motor score of the upper extremities (ASIA UEMS), and level of injury, which was defined as the most caudal segment with normal sensation and motor function.

Two groups of SCI subjects were including in the study. Subjects were either recruited from an intense exercise (IE) program, Project Walk in Carlsbad, CA to be in the IE-SCI group (n=11), or were recruited as control SCI (C-SCI, n=5) subjects who were not participants in Project Walk. Because 2/7 C-SCI subjects scanned were excluded from further analysis due

to excessive head motion, direct comparative statistical power between the IE-SCI and C-SCI subject groups was limited.

Pre-fMRI Transcranial Magnetic Stimulation (TMS) and Electro-myogram (EMG) Recording

Prior to the fMRI experiment, all SCI subjects underwent TMS of the M1 knee area. Electrodes were placed over three leg muscles (right leg: tibialis anterior and rectus femoris; left leg: rectus femoris, to check for mirror movements) to record EMG during TMS, to measure the amplitude of any TMS-evoked muscle responses and characterize the degree of remaining descending corticospinal projections. If TMS did not elicit evoked-responses at the 100% thresholds, SCI subjects were asked to attempt right knee extension (a "kicking" motion) during TMS to check for motor-evoked potentials.

EMG was also recorded while subjects attempted forcible extension of the right knee, in the absence of TMS. No significant motor-evoked potentials were recorded, even during TMS, confirming effective functional disconnection of the right leg.

FMRI Experimental Setup and Behavior

Subjects were trained in both fMRI experimental tasks outside of the scanner, while recording EMG of the right and the left leg (to check for mirror movements), and trained again in the scanner prior to fMRI. Once the experimenters were satisfied that each subject was complying with task instructions (including visual fixation on the IL task), MRI scanning commenced.

Subjects' behavior was visually monitored by the experimenters during scanning, and eye position was video-recorded from the eye camera during the imagined leg movement task. If a subject was unable to maintain central visual fixation during the main experimental task or did not appear alert on the video monitor, the subject was classified as 'non-compliant' and excluded from the data analysis (n=1).

Subjects lay supine on the scanner bed and viewed the task through video goggles, which included an infrared eye camera for observing eye movements. Padding was inserted around the head in the head coil to help minimize head movement during scanning. Subjects' legs were placed on top of a wooden board and their lower legs and feet were fixed in MRI-compatible boots, which standardized and stabilized leg position during scanning. A cushion was placed under the right knee to slightly raise and flex the right leg, and to serve as resting, starting position for real and imagined knee/leg movements. The right leg was then strapped to the wooden board in 2 places along the lower leg and also along the thigh, to fix the leg and provide resistance against which the subjects' would attempt to extend the knee in the control knee extension task.

The main experimental task employed imagined 'reaching' movement of the right leg (IL task). When instructed to do so, subjects were asked to imagine what it would look like and feel like to reach their right leg towards a remembered target location and 'step' on that location, as if stepping to squash a bug. Following this outward movement, subjects were instructed to imagine returning their right leg to resting position. Central eye fixation was required at all times during the main experimental task.

In a second experimental task, subjects were instructed to pace real/attempted right knee extension to a video representation of the leg extending and flexing, viewed through the goggles (AK task). There was no requirement for eye fixation during this task.

Experimental Task

The main experiment (IL task, see Fig. 1, left) was a typical delayed response (DR) task. Each trial began with an initial fixation period (2s), during which the central fixation stimulus became a colored circle. The color of the circle indicated whether the trial was an 'active' or 'rest' trial. This stimulus stayed on for the duration of the trial. Next, a small gray circle briefly flashed (500ms) to the left or right of the central fixation stimulus, indicated the target location. A delay period of 7.5s intervened between target presentation and the start of the response period (2.5s), indicated by the central filled fixation circle becoming a hollow circle. When the hollow fixation circle became a fixation cross, this indicated the end of the

response period and the beginning of the intertrial interval (10s). On ‘active’ trials, indicated by a green central fixation circle, subjects were required to remember the location of the flashed target and to plan an upcoming imagined leg reach to the remembered target location during the delay period. During the response period, subjects were instructed to imagine both what it would look like and feel like to reach out their right leg towards the remembered target location and ‘step’ on this location, before imagining returning their leg to resting position. On ‘rest’ trials, indicated by a red central fixation circle, subjects were instructed to rest and were not required to plan or execute an imagined movement. These trials controlled for visual stimulation, since the visual stimulation was the same, except for the color of the central fixation cue, across ‘active’ and ‘rest’ trials. Blocks of ‘Rest’ (trials/block=3) and ‘Active/Imagined Leg’ (trials/block=5) trials were alternatively presented, and repeated three times in the experimental run.

A second experimental task required attempted extension and flexion of the right knee paced to a videoed cartooned representation of the subjects’ leg extending and flexing once every seven seconds (AK task, see Fig. 1, right). Blocks of ‘Active’ right knee extension/flexion (3 movements/block) were alternated with blocks of ‘Rest’. As in the main experimental task, the same video was presented in both ‘Active’ and ‘Rest’ blocks, to serve as a built-in control for visual stimulation effects.

Functional and Anatomical Imaging

T2* Echo-planar functional images were acquired in a Philips 1.5-Tesla MRI scanner at the University of California Irvine. The scan volume covered the whole brain in 25 axial slices (slice thickness=4mm, gap=1mm, in-plane voxel size=1.95x1.95mm FOV=250x250, matrix=128x128), with a TR of 2500ms (sample rate) and TE=40ms, flip angle 80 degrees. Anatomical images for the whole brain volume were acquired using a T1-weighted MP-RAGE sequence with the same head coil used for functional image collection. The whole brain volume was scanned (a variable number of slices, ~150 dependent on individual subject brain size and geometry) at voxel resolution of 1x1x1mm, with a FOV/matrix size of 256x256, TR=13ms, TE=4.5ms, Flip Angle=20 degrees, FOV=250x250.

Data Preprocessing and Analysis

Preprocessing

Anatomical images were reconstructed into a 3D brain with voxel resolution of 1x1x1mm and transformed first to AC-PC then to Talairach space via an 8-parameter affine transformation in BrainVoyager QX (Brain Innovation B.V., Maastricht, The Netherlands). Functional images were imported into BrainVoyager QX as ANALYZE images. Functional runs were carefully coregistered to the anatomical scan using BrainVoyager QX's initial alignment and manual fine alignment. Functional data preprocessing included slice scan time correction, trilinear 3D motion correction, spatial smoothing (8mm Gaussian kernel), linear trend removal and temporal high pass filtering (0.005Hz). Functional data were converted to Talairach space, to facilitate analyses across subjects.

To minimize inter-subject cortical anatomical variability, cortex-based alignment (CBA) of functional and anatomical data was performed in BrainVoyager QX. For each individual subject, gray matter was segmented from white matter to obtain a cortical surface for each hemisphere. Next, these folded cortical surfaces were mapped onto a standard sphere, so that each resulting surface has the same number of vertices. After mapping of each individual hemisphere to the standard sphere, these hemispheres were aligned to a dynamic across-subjects group average. The resulting aligned cortical surfaces minimize the variation in sulcal patterns across subjects. Functional data were also registered to the CBA surfaces. For better surface-based viewing of statistical maps, an average group-aligned cortical surface was calculated for each hemisphere, and results are projected onto these surfaces.

Data Analyses

The experimental data were analyzed using across-subjects general linear models (GLM, Friston et al. 1995) with 1 block condition/predictor of interest for each task: *Active*. The *Rest* condition served as a built-in control for visual stimulation, and because it was a predictor of no interest, visual stimulation modulations are captured in baseline BOLD activity. Thus, the main experimental contrast to test for brain activity related to the planning and execution of goal-directed leg reaches (IL task), or to attempted knee movement (AK task), compared to visual controls was [Active+], where the "+"indicates that the predictor has a significant

positive beta value (positively contributes to the GLM). Reported statistics were either uncorrected, or corrected for multiple comparisons via Bonferroni or False Discovery Rate (Genovese et al. 2002) at q(FDR)<0.05, as stated in the text. GLMs were either calculated in 3D-Talairach space (in order to look at subcortical structures), or in cortical surface-aligned space (see details of CBA above, to look at cortex).

For subject-group comparisons, random-effects GLMs were used for both tasks; and direct comparisons were made between groups using the contrasts described below.

Regions of interest (ROIs) were identified by the following random-effects contrasts:

1) Task-related in healthy subjects: [Active+] for HC subjects in either task
2) Task-related in SCI subjects: [Active+] for SCI subjects in either task
3) Differentially activated in HC and SCI subject-groups: [HC Active+] > [SCI Active+], or [SCI Active+] > [HC Active+]. Both of these contrasts were run separately for each task.

These ROIs were defined at a threshold of p<0.05 uncorrected on the cortical surface, and included the extent of all significantly active voxels.

Event-related average (ERA) timecourses were calculated by extracting the average BOLD timecourse within an ROI. ERAs are averaged across Active blocks and across subjects (or subsets of subjects), and timecourses are shown as % BOLD signal change (with standard error) relative to baseline, where the baseline period included the 6 TRs (15s) prior to the Active condition blocks. There were the same number of Active blocks per subject; hence each subject contributes equally to these plots.

Relative Contribution (RC) analyses were calculated in BrainVoyager QX, according to methods described previously (in Munk et al. 2002, Cohen Kadosh et al. 2005). The advantage of RC analyses is that, while the maps do not directly test for significant statistical differences between predictors, even task-related voxels with similar contributions of both

predictors are visible. This allows for the visualization of a “latency” map, which shows how the differential relative contributions of two experimental predictors change across the cortical surface.

The color of a voxels in the RC maps depicts the relative weighting of two predictors (P1 and P2) in terms of their contribution to explaining the variance in a given voxel (e.g. HC Active predictor vs. SCI Active predictor, or IL Active predictor vs. AK Active predictor). The minimum multiple correlation coefficient of voxels shown in the maps is listed in the RC figure legends (as the R-value), and the color code for each RC figure is also described. The RC value for each voxel is calculated as:

$$RC\ value = (Pb1 - Pb2)/(Pb1 + Pb2)$$

where Pbi is calculated as an incremental multiple correlation coefficient according to the extra sum of squares principle (see Cohen Kadosh et al. 2005 and Draper & Smith 1998). The RC value can range between +1 (only predictor P1 contributes to the model) and -1 (only predictor P2 contributes to the model), and an RC value of 0 indicates that both predictors P1 and P2 contribute equally to the model. Statistical differences between predictors P1 and P2 can be confirmed by performing a t-test of the beta-weights for P1 and P2, such as was done in the subject-group RFX comparisons described above.

Linear Correlation (LC) analyses were calculated to check for significant relationships between externally measured clinical and behavioral variables (covariates) and BOLD activity in SCI subjects. LC analyses were calculated separately for each experimental task. Each covariate was normalized to have zero mean across SCI subjects, and the LC between each covariate and the Active predictor in each voxel was calculated. These LC maps were calculated in Talairach-space and viewed on the 2D unsegmented across-subjects average anatomical brain, or were calculated in CBA-space and viewed on the average group-aligned cortical surface. ROI-based LC analyses were also calculated by extracting the Active predictor beta values for each SCI subject, averaged across voxels within a single ROI, and by correlating these beta values with the covariates. ANOVAs were used to check for

interaction effects between covariates in ROIs, and we also separately calculated the linear correlation between covariates.

GLM statistical parametric maps, RC maps, and LC maps were either projected onto average segmented and group-aligned 3D cortical surfaces (cortex-based group alignment was performed in BrainVoyager QX, neurological image convention: left hemisphere on the left, right hemisphere on the right), or onto 2D un-segmented brain slices of the subject-averaged anatomical image (flipped to be in neurological image convention) for viewing.

CHAPTER 2: TABLES AND FIGURES

Table 1 – Profile of SCI subjects including clinical variables (**on next page**)

Abbreviations:
IE-SCI = Participants in Project Walk's intense exercise programs (see Methods); C-SCI = Control group of SCI subjects not participating in Project Walk; ASIA = American Spinal Injury Association; Bilat. = Bilateral; UEMS = Upper extremity motor score; LEMS = Lower extremity motor score; IE = Intense exercise (see Methods)

Table 1 – Profile of SCI subjects including clinical variables

SCI Subjects (n=16)	Mean; Mode	Min.	Max.	IE-SCI	C-SCI	Sig. Diff. IE-SCI vs. C-SCI?
SPINAL CORD INJURY						
Level of SCI (C1=1 for linear correlations)	C6/C7; C5 (n=6)	C4 (n=3)	T8 (n=1)	C4-C8	C4-T8	see 1.
Days Injury to fMRI	1718	358	3970	1535	2122	no
Normalized spinal cord cross-sectional area (mm^3)	216.2	139.3	299.4	206.7	231.6	no
Adjusted spinal cord cross-sectional area (mm^3)	217.5	139.7	294	215.3	221.1	no
BASELINE ASIA SCORES						
ASIA Impairment Scale (A=1 for linear correlations)	B; A (n=6)	A	C	A/B/C: 3/4/4	A/B/C: 3/1/1	see 2.
Bilat. ASIA Touch/Pin Score	89.5	32	142	89.5	89.6	no
Bilat. ASIA UEMS	32.5	18	50	30	38	no
Right ASIA LEMS	0.7; 0	0	6	0.9	0.2	no
Left ASIA LEMS	2.8; 0	0	19	3.6	0.8	no
CHANGE IN ASIA MOTOR SCORES OVER 6 MONTHS						
Change Bilat. ASIA Motor Score	2.5; 2	-3	11	4	-0.4	yes, $p<0.04$
Change Bilat. ASIA UEMS	0.4; 0	-3	4	0.7	-0.4	no
Change Right ASIA LEMS	1.2; 0	-1	7	1.8	0	near sig., $p<0.15$
Change ASIA Left LEMS	1; 1	-1	6	1.5	0	near sig., $p<0.1$
EXERCISE VARIABLES						
SCI Group (IE-SCI=1, C-SCI=2)	na	na	na	n=11	n=5	na
Hours per week of IE Prog. Exercise	4.4	0	11.8	6.3	0	no
Hours per week ANY exercise	6.3	0	11.9	6.3	6.4	no
Days in IE Prog. prior to fMRI	98	0	440	143	0	no
Total hours in IE Prog. prior to fMRI	106.5	0	742	155	0	no
OTHER VARIABLES						
Age	32.75	22	59	32.8	32.6	no
Handedness	1.4	-2	2	1.7	0.76	no
Footedness	1.2	0	2	1.3	1.1	no

1. IE-SCI group all cervical injuries; C-SCI group includes 2 thoracic injuries
2. C-SCI group has more complete injury

Figure 1 – FMRI experimental paradigms. Left: The main experimental task was a spatial delayed-response task required imagined leg movement (IL task). Blocks of "Rest" (3 trials/block) and "Active" (5 trials/block) condition trials were presented alternating throughout the experimental run, with each condition presented three times per run. A single trial structure/timing is shown. Within each trial, the initial fixation period (2.0s) cued the start of the trial, and the color of the central fixation stimulus indicated the trial condition ("Active"=green, "Rest"=red). Next, a gray peripheral visual target was flashed for 500ms to the left or the right of the central fixation stimulus. Subjects had to remember the target location and plan the upcoming imagined leg movement during the delay period (7.5s) of "Active" trials, or passively fixate on "Rest" trials. Upon presentation of the "Go" stimulus (hollow fixation circle), subjects were required to imagined what it would look like and feel like to reach the right leg to "step" on the remembered target location in "Active" trials, or to maintain passive central fixation in "Rest" trials.

Right: The second experimental task was an attempted knee movement (AK) task, and also alternated blocks of "Rest" and "Active" conditions that repeated two times per experimental run. A single experimental run structure is shown. In any single block (25s), a video cartoon representation of the leg extended and flexed the knee once every seven seconds, such that the cartoon leg completed three "movements" per block. The color of the cartoon leg indicated whether the subject was in a "Rest" (red) or an "Active" (green) block. In "Rest" blocks, subjects were required to passively view the video, while in "Active" blocks, subjects were required to pace attempted right knee extension with the video representation of a leg. The black arrow in this figure indicates the dynamic video extension motion of the cartoon knee.

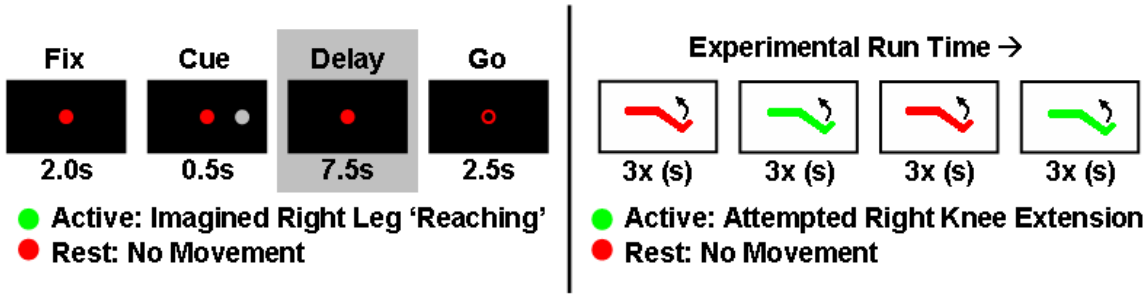

Figure 2 - Overlap of imagined arm and imagined leg "reaching" activity in normal subjects (n=4). Left: Imagined arm and imagined leg reaching activity a largely overlapping network of brain activity. Right: A direct comparison between the two conditions reveals that imagined arm reaching activates the left M1 hand knob, IFG, IPL, and MTG more than imagined leg reaching, while imagined leg reaching activates the left M1 leg area and SMA, as well as several areas in the right hemisphere (see Table 2).

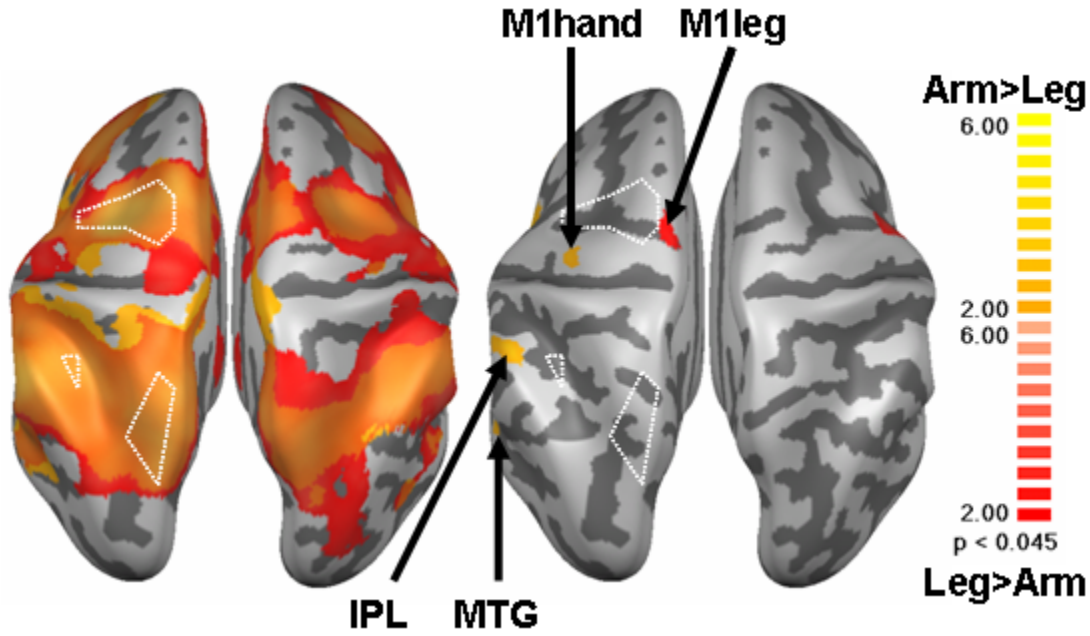

Table 2 – Direct comparison of imagined right arm and imagined right leg movement conditions. ROIs with significant differences at $p<0.05$ across subjects (n=4).

Imagined Right Arm > Imagined Right Leg

ROI Name	Hemi.	BA	Tal X	Tal Y	Tal Z
IFG	Left	9	-43	5	22
M1 Hand/PMd (p<0.1)	Left	4,6	-33	-16	56
M1 Hand (p<0.1)	Left	4	-31	-20	52
IPL	Left	40	-53	-35	49
MTG	Left	22	-52	-40	1
IFG	Right	47	43	16	-6

Imagined Right Leg > Imagined Right Arm

ROI Name	Hemi.	BA	Tal X	Tal Y	Tal Z
Ant. Commissure	Mid	na	0	4	-5
Globus Pallidus	Left	na	-15	-3	1
SMA	Left	6	-8	-6	53
M1 Leg	Left	4	-10	-28	64
IFG	Right	9	57	17	25
latPrCS	Right	6	46	0	40
Insula	Right	13	39	0	15
Thal (Ant. Nuc.)	Right	na	8	-14	17

Figure 3 – Imagined leg task RFX activation maps for HC subjects (n=12, left), and SCI subjects (n=16, right), with overlap in the middle. While there appears to be mild left-lateralization bias in the HC subject group, this bias disappears in the SCI subject group. Outlined in white are brain areas previously identified to be involved in planning real and imagined right arm reaches (Glidden et al. submitted.)

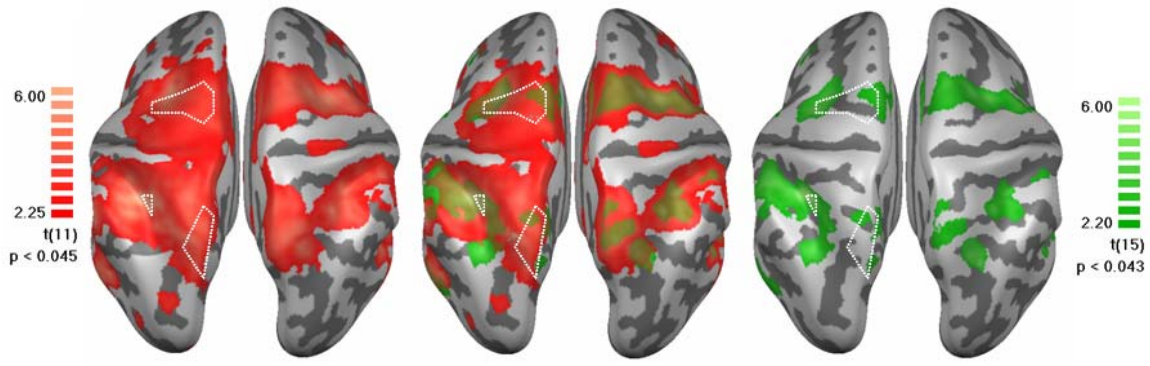

Table 3 – Main Task-Related ROIs in Both Experimental Tasks (continued on next page)

HC Imagined Leg [Active+]

ROI Name	Hemi.	BA	Tal X	Tal Y	Tal Z
dlPFC/MiFG	Right	9	36	37	26
ACC	Right	32	8	25	34
PMv/IFG	Right	44	52	9	10
SMA	Left	6	-3	-6	53
SMA/Cing.	Right	6,24	6	-4	47
PMd	Left	6	-25	-7	55
PMd	Right	6	27	-8	57
SFG/M1	Left	6	-12	-17	70
M1 Hand Knob	Left	4	-32	-26	52
M1 Hand Knob	Right	4	29	-29	54
pCing	Left	7	-9	-46	60
MTG/STG	Right	21	51	-23	-5
aIPS/IPL	Left	40	-38	-43	43
aIPS/IPL	Right	40	40	-39	42
SMG/IPL	Left	40	-56	-42	31
SMG/IPL	Right	40	56	-34	31
MTG	Left	22	-54	-50	4
MTG	Right	21	50	-41	7
medPPC	Left	7	-17	-57	57
SPL	Left	7	-24	-62	51
medPPC	Right	7	15	-62	54

SCI Imagined Leg [Active+]

ROI Name	Hemi.	BA	Tal X	Tal Y	Tal Z
dlPFC/MiFG	Left	9	-39	29	30
ACC	Left	32	-7	10	38
ACC	Right	32	8	27	34
PMv/IFG	Left	6	-47	0	36
PMv/IFG	Right	44	51	8	11
SMA	Left	6	-3	-6	51
SMA	Right	6	7	-3	46
latPrCS	Right	6	42	-5	49
SFG/SMA	Left	6	-8	-10	70
SFG/SMA	Right	6	17	-6	69
PMd	Left	6	-30	-8	51
PMd	Right	6	25	-8	54
Cing.	Right	24	3	-16	35
STG	Right	21	51	-24	-4
latPoCS	Right	2,40	49	-29	39
SMG/IPL	Right	40	55	-35	29
aIPS/IPL	Left	40	-45	-37	41
aIPS/IPL	Right	40	36	-44	44

MTG	Left	21	-56	-51	0
MTG	Right	21	50	-41	7
medPPC (mSPL)	Left	7	-16	-58	56
medPPC (med. wall)	Left	7	-6	-58	51
medPPC (aPOS)	Left	7	-8	-72	42
IPL	Left	39	-33	-61	38
medPPC/medPoCS	Right	7	14	-61	55
SPL	Right	7	25	-64	42

HC Attempted Knee [Active+]

ROI Name	Hemi.	BA	Tal X	Tal Y	Tal Z
PMv/IFG	Right	6,44	51	5	22
latPrCS	Right	6	44	-4	49
SFG/SMA	Right	6	12	-10	70
M1/PrCG	Right	6	18	-16	70
M1 Leg	Left	4	-13	-30	69
CMA	Left	6	-1	-31	61
M1/S1 Leg	Right	4,5	3	-35	60
S1 Leg	Left	5	-10	-46	67
IPL	Left	40	-57	-21	25
medPoCS	Right	7,5	19	-45	66
medPoCS/medPPC	Right	7	19	-53	59

SCI Attempted Knee [Active+]

ROI Name	Hemi.	BA	Tal X	Tal Y	Tal Z
preSMA	Right	32	6	6	44
SMA	Left	6	-3	-2	50
latPrCS	Right	6	50	-6	47
SFG/SMA	Left	6	-7	-8	69
PMdc	Right	6	40	-10	56
M1/PrCG/CMA	Right	6	4	-12	51
SFG/M1	Right	6	10	-12	69
M1/PrCG	Right	4	21	-21	70
M1 Leg	Left	4	-11	-33	70
M1/S1 Leg	Right	4	8	-35	69
S1 Leg/Arm	Right	3	21	-37	69
S1 Leg	Left	5	-11	-40	70
pCC	Right	na	0	-32	14
medPoCS	Right	7	14	-55	62
medPPC	Right	7	15	-69	51

Table 4 – Direct RFX Comparison of HC and SCI groups in the IL and the AK tasks

HC Imagined Leg > SCI Imagined Leg

ROI Name	Hemi.	BA	Tal X	Tal Y	Tal Z
PMd (at SFS/PrCS)	Left	6	-24	-3	52
Cingulate	Left	24	-4	-7	38
M1/S1 Hand	Left	4	-36	-25	55
PoCG	Left	3	-21	-31	64
aSPL	Left	5	-31	-41	54
medPoCS	Left	7	-14	-51	65
retIPS	Left	7	-23	-63	53
posCing	Right	31	6	-45	41
STG	Right	22	62	-35	18
STG/MTG	Right	22,39	48	-57	8
MTG	Right	39	37	-72	27

SCI Attempted Knee > HC Attempted Knee

ROI Name	Hemi.	BA	Tal X	Tal Y	Tal Z
MiFG	Left	9	-43	20	32
SFG	Left	6	-7	-6	70
CMA	Left	31, 6	-5	-20	46
Corpus Callosum (post)	Left	na	0	-28	14
M1/S1 Leg	Left	4,5	-3	-42	65
medPPC	Left	7	-7	-65	42
M1/PrCG	Right	4	23	-22	68
M1 Hand	Right	4	37	-23	55
Corpus Callosum (post)	Right	na	0	-32	14
M1/S1 Leg	Right	4,5	6	-40	68
medPPC	Right	7	4	-59	49
medSPL	Right	7	17	-69	51
Cuneus	Right	18	6	-85	14

HC Attempted Knee > SCI Attempted Knee (ns)

ROI Name	Hemi.	BA	Tal X	Tal Y	Tal Z
latPrCS	Right	6	45	-3	47

HC Attempted Knee = SCI Attempted Knee

ROI Name	Hemi.	BA	Tal X	Tal Y	Tal Z
CMA (HC center)	Left	6	-1	-31	61
M1 Leg (HC center)	Left	4	-13	-30	69
S1 Leg (HC center)	Left	5	-10	-46	67

Figure 4 – Direct RFX comparison of HC and SCI groups in the IL task. HC>SCI in red, SCI>HC in green. The transparent light pink overlay is the RFX activation map for the 12 HC subjects in the IL task, showing the task-related brain network. There are no significant RFX differences between HC and SCI groups in the main ROIs related to movement planning (outlined in white), including the PMd, SMA, medPPC and aIPS.

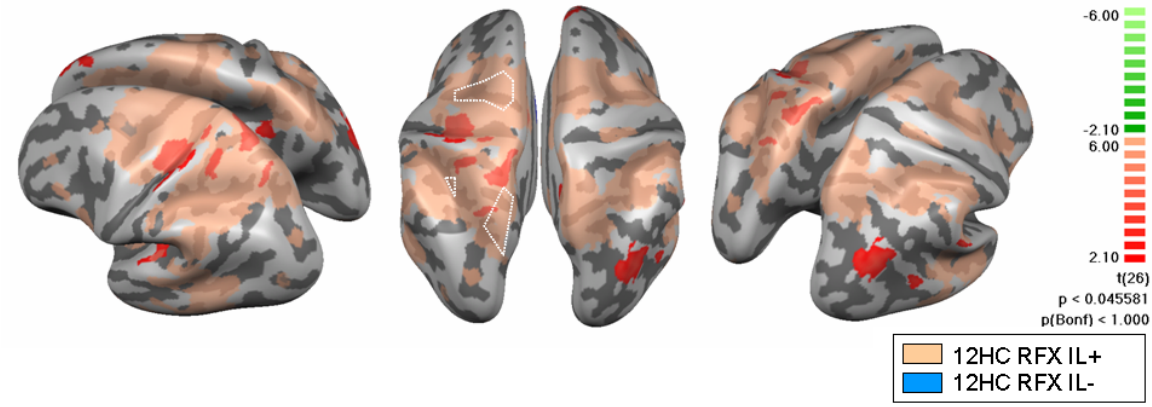

Figure 5 – Timecourses of BOLD activity (raw data) in IL task-related ROIs, comparing subject groups (HC=red, SCI=green). Standard error bars are plotted. Left: Centers of HC task-related ROIs show that both HC and SCI groups have positive activity during active imagined leg "reaching" blocks. Right: Task-related ROIs with significantly higher BOLD activity in the SCI than in the HC group, or vice versa (aPOS). Also see Table 4.

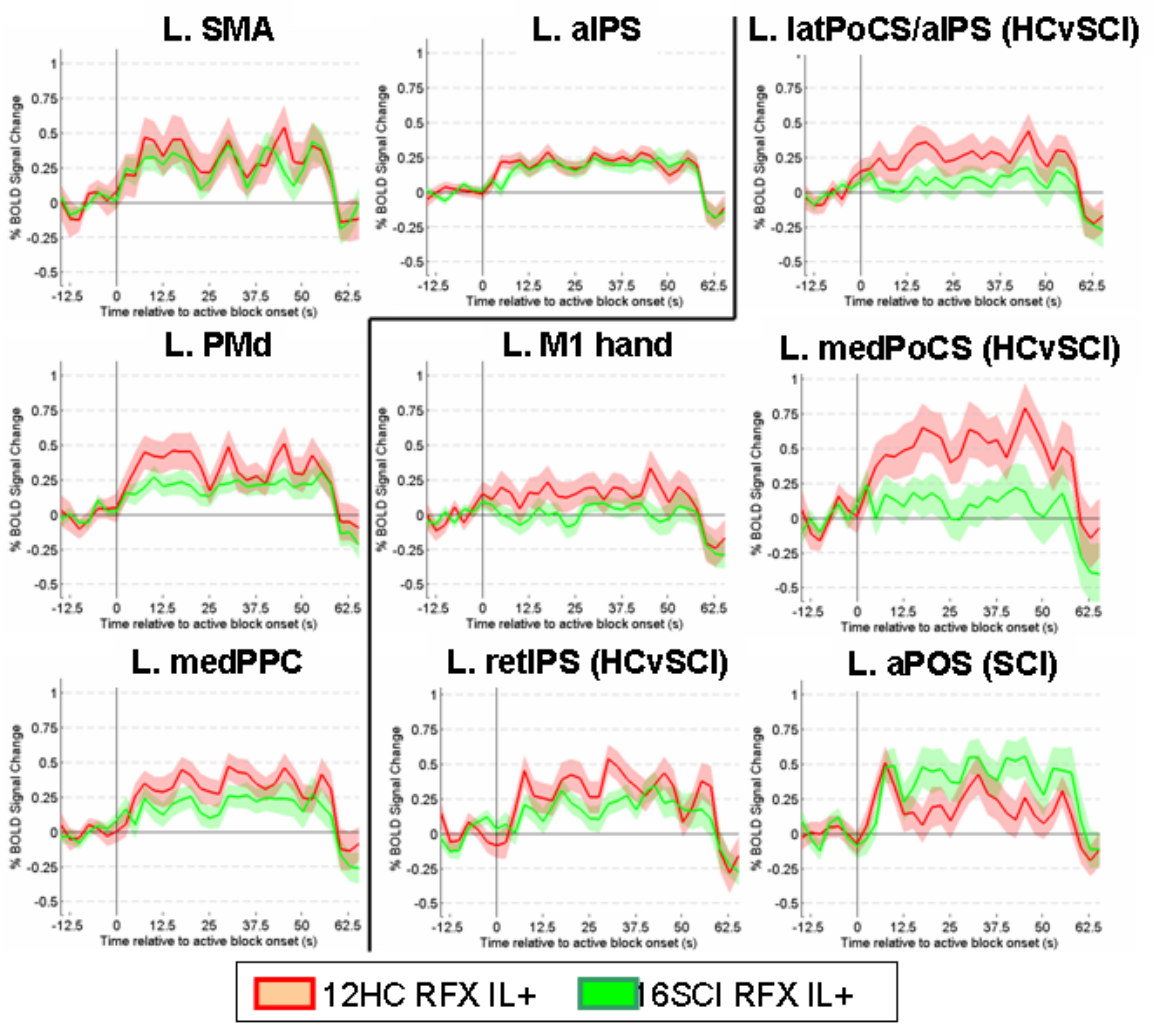

Figure 6 – Attempted knee extension task RFX activation maps for HC subjects (n=12, left), and SCI subjects (n=16, right), with overlap in the middle. While there appears to be mild left-lateralization bias in the HC subject group, this bias disappears in the SCI subject group and may even shift to a right-lateralization. Outlined in white are brain areas previously identified to be involved in planning real and imagined right arm reaches (Glidden et al., submitted).

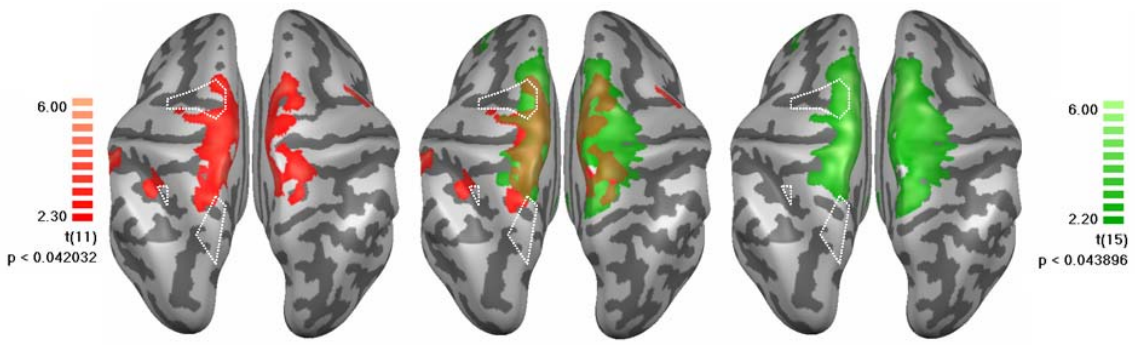

Figure 7 – Timecourses of BOLD activity (raw data) in AK task-related ROIs, comparing subject groups (HC=red, SCI=green). Standard error bars are plotted. Left: Centers of HC task-related ROIs show no significant differences in % BOLD signal change between HC and SCI groups. Right: Task-related ROIs with significantly higher BOLD activity in the SCI than in the HC group. Also see Table 4.

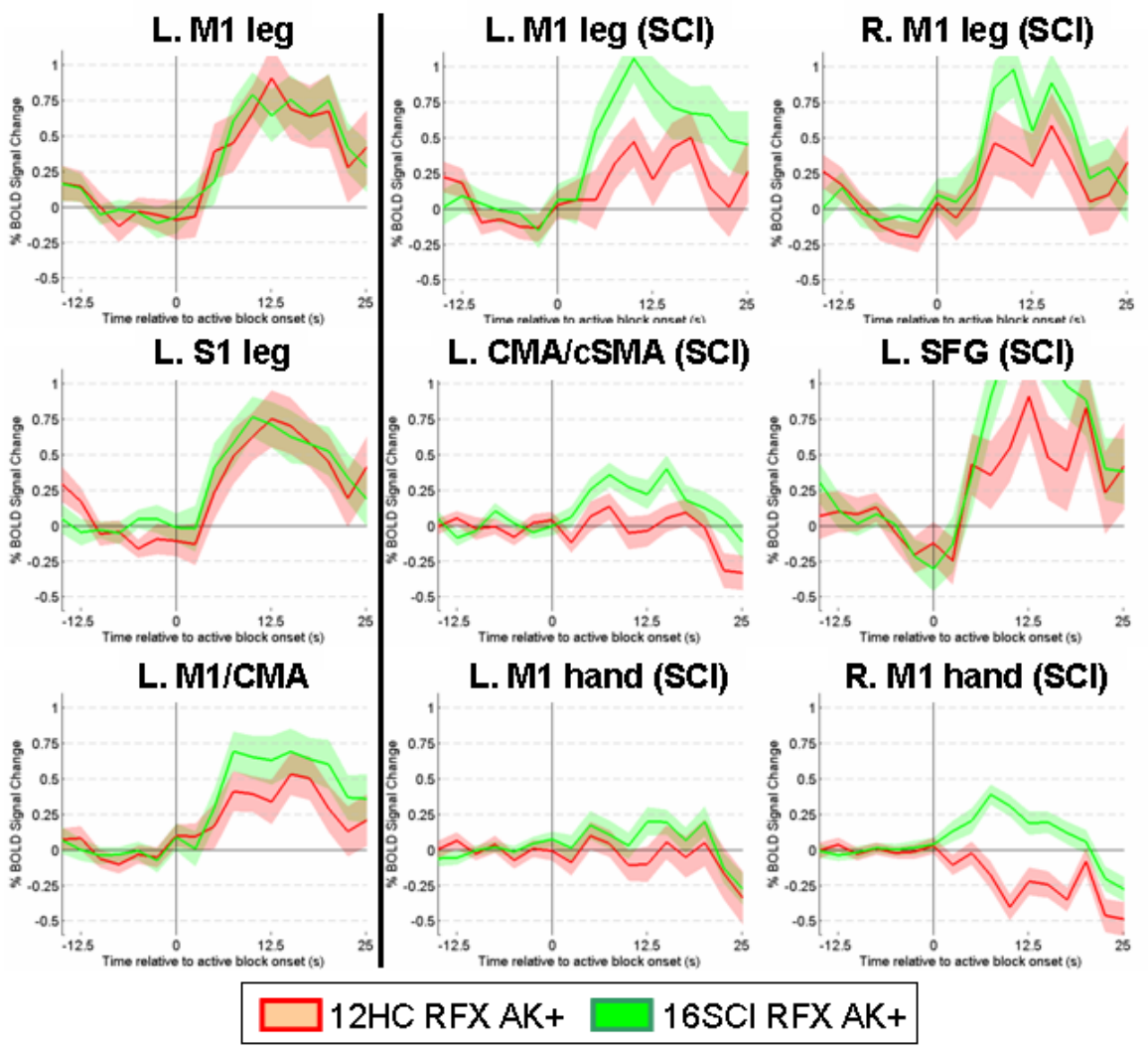

Figure 8 – Timecourses of BOLD activity in subcortical AK task-related ROIs. Both pCC and the bilateral cerebellum, including rCereb (26,-31,-22), are more active in SCI than in HC subjects.

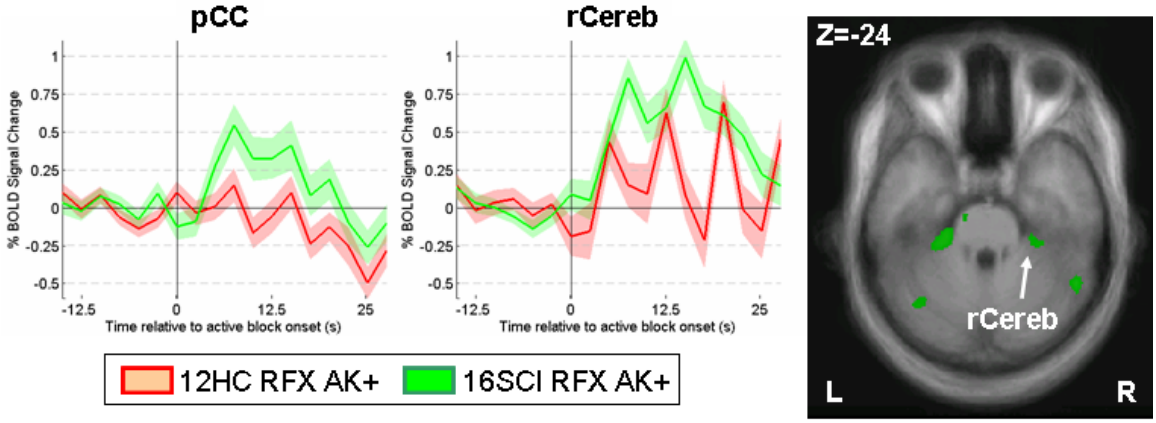

Figure 9 – Relative contribution (RC) analysis of the HC and SCI subject group recruitment across the task-related brain network for the IL task (left), and the AK task (right). The orange-to-purple map shows increasing relative contribution of the HC group compared to the SCI group, while the green-to-blue map shows increasing relative contribution of the SCI group compared to the HC group. Maps are corrected with p(bonferroni)<0.000. In the IL task, the HC group activates the medial SPL to a greater degree than the SCI group, while the reverse is true of the medial PMd/M1 leg area. In the AK task, the SCI group recruits much of bilateral somatomotor cortex to a greater degree than the HC group. In the SCI group compared to the HC group, there is extension of the activation map anterior into the SFG and onto the medial wall in the left hemisphere, and additional extension into the right somatomotor cortex.

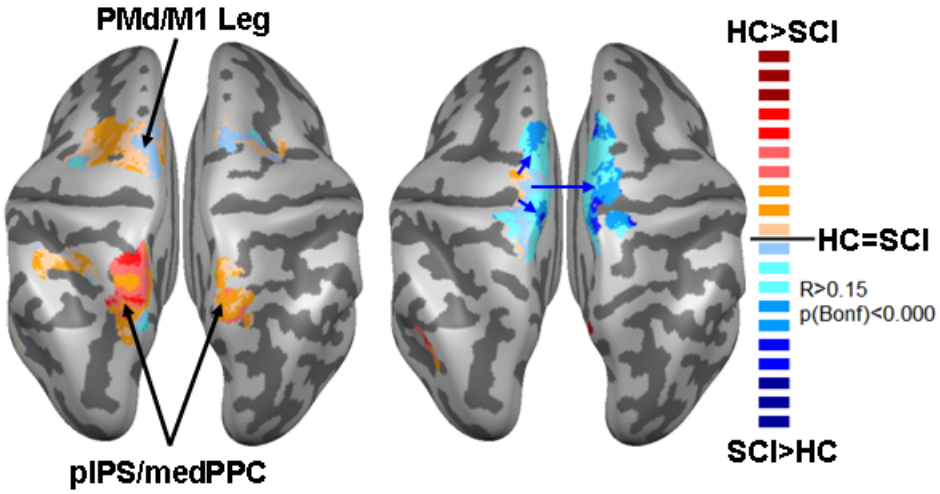

Figure 10 – RC analysis of IL and AK task predictors separated by subject group, for the left hemisphere. Left: IL task-related ROIs are outlined in pink, while AK task-related ROIs are outlined in blue. Middle: HC group (n=12). Right: SCI group (n=16). The orange-to-purple map shows increasing relative contribution of the IL task predictor compared to the AK task predictor, while the green-to-blue map shows increasing relative contribution of the AK task predictor compared to the IL task predictor. RC maps are at q(FDR)<0.001.

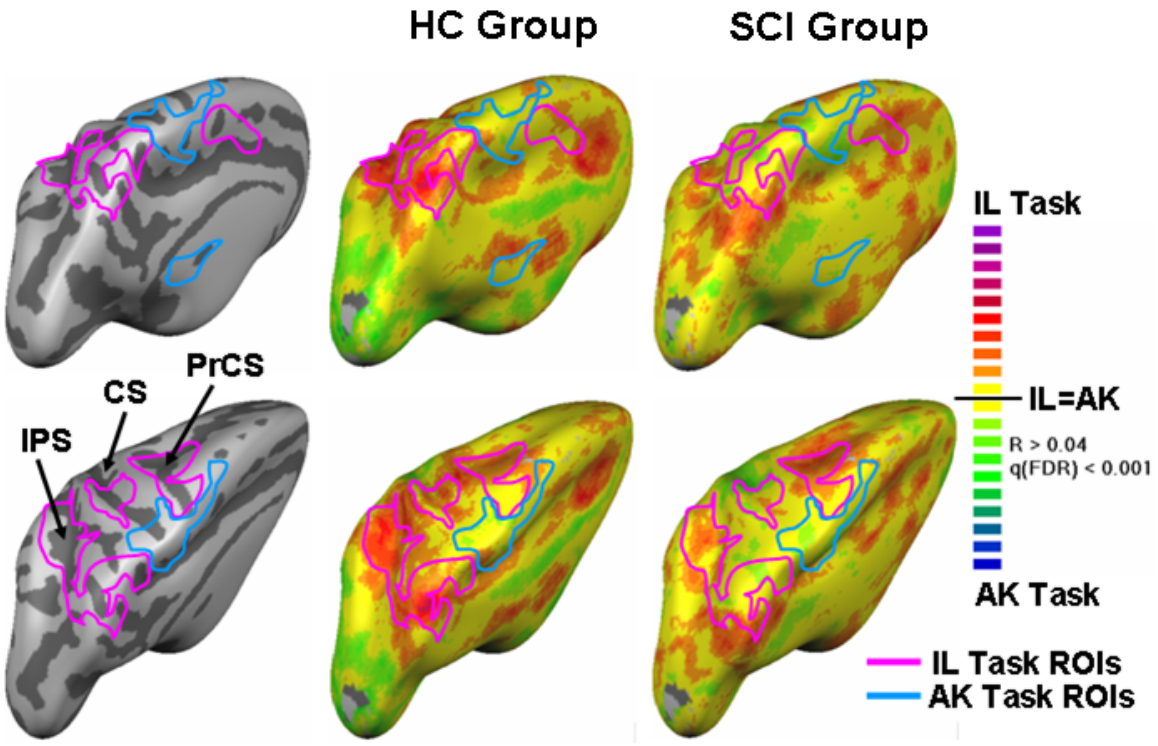

Figure 11 – RC analysis of IL and AK task predictors separated by subject group, for the right hemisphere. The images have been flipped horizontally to facilitate comparison with the left hemisphere maps. Left: IL task-related ROIs are outlined in pink, while AK task-related ROIs are outlined in blue. Middle: HC group (n=12). Right: SCI group (n=16). The orange-to-purple map shows increasing relative contribution of the IL task predictor compared to the AK task predictor, while the green-to-blue map shows increasing relative contribution of the AK task predictor compared to the IL task predictor. RC maps are at q(FDR)<0.001.

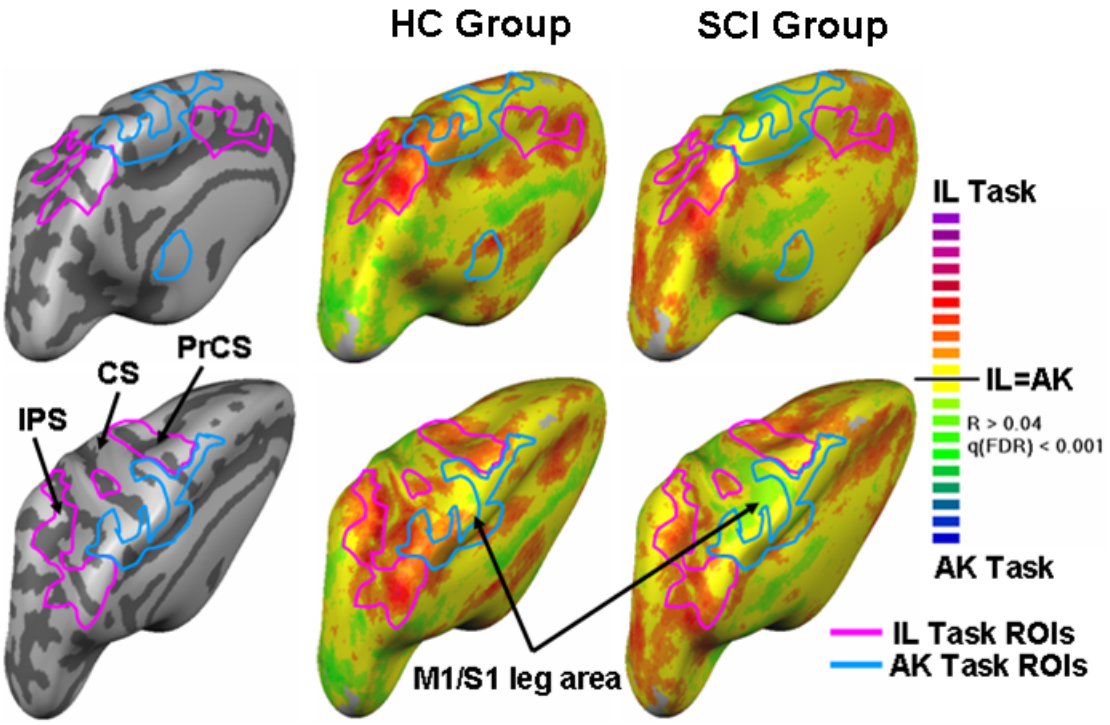

Figure 12 – Linear correlations in the IL task between SCI subject BOLD activity and clinical and behavioral variables. Linear correlation maps are significant at $p<0.046$, at a linear correlation coefficient of greater than or equal to r=0.54 for positive correlations, and less than or equal to r=-0.54 for negative correlations (i.e., greater than 30% of variance explained). Leg-related somatomotor cortex is outlined in purple, while the medial PPC (medPPC) involved in planning real and imagined limb movements (see Glidden et al. submitted) is outlined in green. Note that medPPC BOLD activity correlates with many clinical variables. MedPPC BOLD activity increases with a greater degree of current motor functionality (assessed via the current bilateral ASIA lower motor extremity score: ASIA LEMS B) and with less complete SCI (assessed using the ASIA Impairment Scale: AIS). Activity in this ROI also correlates positively with future functional motor gains, indexed as a positive change in lower right limb motor functionality between the time of the fMRI scan and a second ASIA assessment made six months later (cASIA LEMS R). However, medPPC BOLD activity driven by a task involving lower limb movement does not predict future functional motor gains for the upper limbs (cASIA UEMS B), i.e., it is limb-specific. MedPPC activity also relates positively with the amount of weekly exercise completed by SCI subjects.

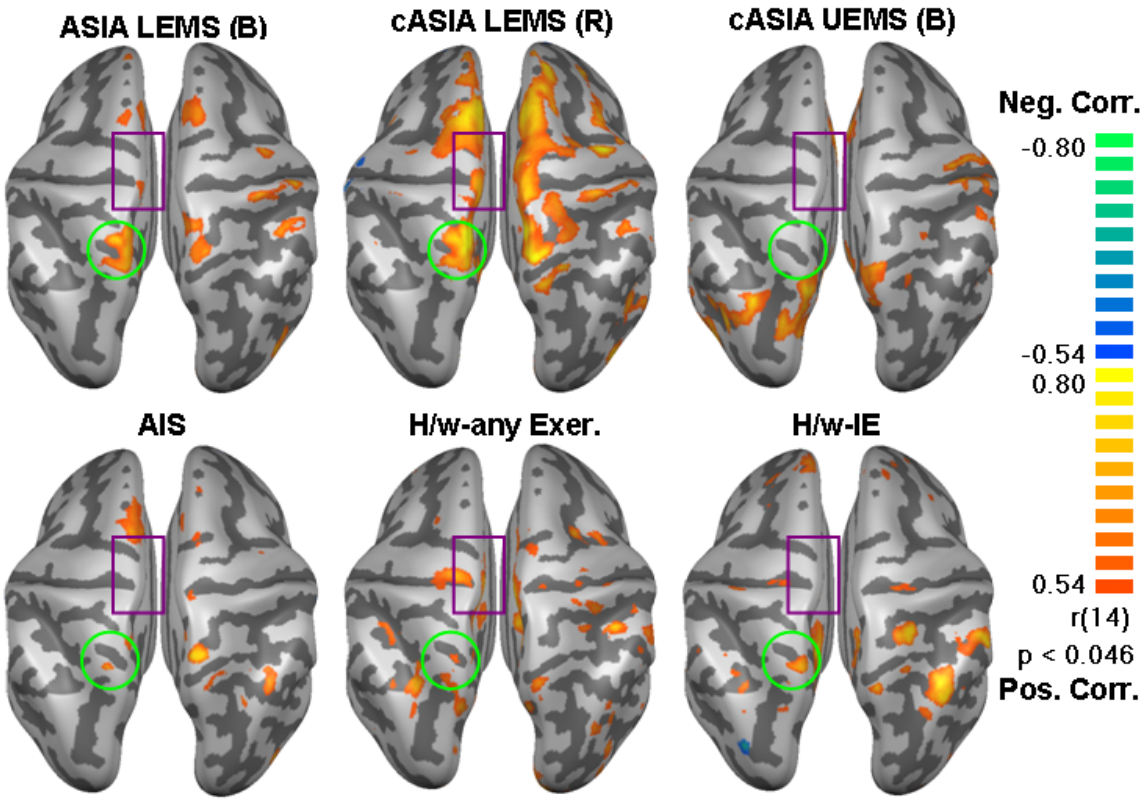

Table 5 – Linear Correlations between BOLD activity and clinical variables in main task-related ROIs.

Abbreviations:

c = Change from day of fMRI to second measurement six-months later

LEMS = Lower extremity motor score; UEMS = Upper extremity motor score

R = Right side; L = Left side; B = Bilateral

AIS = ASIA Impairment scale (AIS "A" = 1, AIS "B" = 2, AIS "C" = 3)

IE = Intense exercise (see Methods and table 1)

H/w = Hours per week

SCI/exer. Group = IE-SCI vs. C-SCI (see Methods and Table 1)

Imagined Leg Task Correlations

ROI	COVARIATE	R	P
L. ACC	Total hours IE	0.55	0.03
	Time since injury	0.52	0.05
R. ACC	Hours/week IE	0.57	0.03
	Total hours IE	0.56	0.03
	cASIA Motor Score (B)	0.44	0.1
	cASIA UEMS (R)	0.43	0.11
	SCI/exer. Group	-0.41	0.13
L. SMA	Total Hours IE	0.51	0.05
	Hours/week any exer.	0.43	0.11
	Time since injury	0.43	0.11
	cASIA LEMS (R)	0.39	0.15
	cLEMS-R x Age	**int.**	**0.01**
	cLEMS-R x AIS	**int.**	**0.02**
	cLEMS-R x TSI	**int.**	**0.05**
R. SMA	Total Hours IE	0.68	0
	Hours/week any exer.	0.5	0.06
	cASIA Motor Score (B)	0.43	0.11
	cASIA LEMS (R)	0.36	0.19
	Hours/week IE	0.36	0.19
	cLEMS-R x Age	**int.**	**0.1**
L. SFG/SMA	cASIA LEMS (R)	0.55	0.03
	AIS	0.54	0.04
	Hours/week any exer.	0.45	0.09
	cASIA Motor Score (B)	0.41	0.13
	Total Hours IE	0.38	0.17
	cLEMS-R x TSI	**int.**	**0.03**
R. SFG/SMA	cASIA LEMS (R)	0.61	0.02
	cASIA Motor Score (B)	0.45	0.09

ROI	COVARIATE	R	P
L. aIPS	Total Hours IE	0.62	0.01
	Hours/week any exer.	0.45	0.09
	Time since injury	0.44	0.1
	cASIA Motor Score (B)	0.42	0.12
	cLEMS-R x Age	**int.**	**0.04**
	cLEMS-R x AIS	**int.**	**0.03**
R. aIPS	cASIA Motor Score (B)	0.63	0.01
	cASIA UEMS (R)	0.53	0.04
	Hours/week any exer.	0.49	0.06
	ASIA Motor Score (B)	0.46	0.09
	Total Hours IE	0.45	0.09
	Hours/week IE	0.37	0.17
	ASIA LEMS (R)	0.37	0.18
	cASIA LEMS (R)	0.36	0.19
	cLEMS-R x H/w-IE	**int.**	**0.08**
L. SPL	cASIA LEMS (R)	0.68	0.01
	cASIA Motor Score (B)	0.62	0.01
	AIS	0.53	0.04
	SCI/exer. Group	-0.49	0.06
	Hours/week any exer.	0.49	0.06
	ASIA LEMS (R)	0.48	0.07
	Hours/week IE	0.48	0.07
	ASIA Motor Score (B)	0.41	0.13
	Total Hours IE	0.38	0.16
	cLEMS-R x LEMS-R	**int.**	**0.07**
	cLEMS-R x Age	**int.**	**0.09**
R. SPL	AIS	0.38	0.16
	cLEMS-R x H/w-IE	**int.**	**0.09**

	Hours/week any exer.	0.45	0.09	L. medPoCS	cASIA LEMS (R)	0.69	0
	Hours/week IE	0.35	0.2		ASIA Motor Score (B)	0.62	0.01
	cLEMS-R x Age	**int.**	**0.01**		AIS	0.5	0.06
	cLEMS-R x AIS	**int.**	**0.03**		Age	-0.46	0.08
	cLEMS-R x TSI	**int.**	**0.06**		ASIA LEMS (R)	0.36	0.19
L. PMd	Hours/week any exer.	0.46	0.08	R. medPoCS	none	na	na
	Total Hours IE	0.38	0.16	L. medPPC	cASIA Motor Score (B)	0.81	0
	cLEMS-R x Age	**int.**	**0**		SCI/exer. Group	-0.39	0.15
	cLEMS-R x AIS	**int.**	**0.02**		Age	-0.38	0.17
	cLEMS-R x Level	**int.**	**0.06**		cASIA LEMS (R)	0.75	0
	cLEMS-R x cUEMS-R	**int.**	**0.08**		cASIA UEMS (R)	0.71	0
R. PMd	Total Hours IE	0.46	0.08		Total Hours IE	0.66	0.01
	Hours/week any exer.	0.43	0.11		Hours/week IE	0.55	0.03
	cASIA Motor Score (B)	0.43	0.11		AIS	0.54	0.04
	cLEMS-R x Age	**int.**	**0.11**		ASIA Motor Score (B)	0.49	0.07
	cLEMS-R x AIS	**int.**	**0.11**		Hours/week any exer.	0.48	0.07
L. latPrCS	none	na	na		ASIA LEMS (R)	0.45	0.09
R. latPrCS	cASIA Motor Score (B)	0.6	0.02		**cLEMS-R x AIS**	**int.**	**0.02**
	Total Hours IE	0.5	0.06		**cLEMS-R x Age**	**int.**	**0.03**
	Hours/week IE	0.43	0.11		**cLEMS-R x LEMS-R**	**int.**	**0.04**
	Hours/week any exer.	0.36	0.18	R. medPPC	cASIA Motor Score (B)	0.77	0
	cASIA LEMS (R)	0.36	0.18		Hours/week any exer.	0.38	0.16
	Time since injury	0.35	0.2		SCI/exer. Group	-0.35	0.2
	SCI/exer. Group	-0.35	0.21		cASIA LEMS (R)	0.65	0.01
	cLEMS-R x H/w-IE	**int.**	**0.08**		cASIA UEMS (R)	0.55	0.03
L. PMv/IFG	none	na	na		ASIA Motor Score (B)	0.52	0.04
R. PMv/IFG	ASIA Motor Score (B)	0.54	0.04		ASIA LEMS (R)	0.51	0.05
	ASIA LEMS (R)	0.48	0.07		Age	0.46	0.08
	cASIA Motor Score (B)	0.44	0.1		Total Hours IE	0.42	0.12
	cASIA UEMS (R)	0.42	0.12		Hours/week IE	0.41	0.13
	SCI Level	0.4	0.14		AIS	0.41	0.13
	ASIA UEMS (R)	0.4	0.14	L. IPL/MTG	Hours/week any exer.	0.6	0.02
L. M1/S1 hand area	Total Hours IE	0.66	0.01		Total Hours IE	0.54	0.04
	Hours/week IE	0.45	0.09		Hours/week IE	0.48	0.07
	Hours/week any exer.	0.42	0.12		cASIA UEMS (R)	0.45	0.09

	cLEMS-R x H/w-AE	**int.**	**0.03**
R. M1/S1 hand area	Total Hours IE	0.67	0.01
	Hours/week any exer.	0.47	0.08
	SCI Level	0.47	0.08
	Hours/week IE	0.42	0.12
L. Cing	Time since injury	0.42	0.12
	Total Hours IE	0.39	0.15
R. Cing	Total Hours IE	0.56	0.03
L. pCing	cASIA LEMS (R)	0.67	0.01
	cASIA Motor Score (B)	0.54	0.04
	Hours/week any exer.	0.5	0.06
	ASIA Motor Score (B)	0.47	0.07
	AIS	0.39	0.15
	Total Hours IE	0.38	0.17
R. pCing	Hours/week IE	0.68	0.01
	SCI/exer. Group	-0.59	0.02
	cASIA Motor Score (B)	0.57	0.03
	Total Hours IE	0.54	0.04
	AIS	0.44	0.1
	cASIA LEMS (R)	0.43	0.11
	Hours/week any exer.	0.37	0.17
	cLEMS-R x AIS	**int.**	**0.09**
	cLEMS-R x Level	**int.**	**0.11**
	cLEMS-R x cUEMS-R	**int.**	**0.12**

	cASIA Motor Score (B)	0.44	0.1
R. IPL/MTG	Hours/week any exer.	0.61	0.02
	Time since injury	-0.43	0.11
L. SMG/ IPL/ MTG	cASIA Motor Score (B)	0.59	0.02
	ASIA Motor Score (B)	0.55	0.03
	cASIA UEMS (R)	0.53	0.04
	ASIA UEMS (R)	0.52	0.05
	ASIA LEMS (R)	0.44	0.1
	SCI Level	0.38	0.16
	cLEMS-R x Days-IE	**int.**	**0.09**
	cLEMS-R x Tot.Hrs-IE	**int.**	**0.09**
R. SMG/ IPL/ MTG	cASIA Motor Score (B)	0.64	0.01
	cASIA LEMS (R)	0.58	0.02
	ASIA Motor Score (B)	0.54	0.04
	ASIA UEMS (R)	0.53	0.04
	ASIA LEMS (R)	0.48	0.07
	SCI Level	0.46	0.08
	cASIA UEMS (R)	0.46	0.09
	Hours/week any exer.	0.4	0.14
	Age	0.4	0.14
	AIS	0.37	0.17
	cLEMS-R x Age	**int.**	**0.03**
	cLEMS-R x LEMS-R	**int.**	**0.03**
	cLEMS-R x AIS	**int.**	**0.06**
	cLEMS-R x TSI	**int.**	**0.08**

Attempted Knee Extension Task Correlations

ROI	COVARIATE	R	P
L. SMA	none	na	na
R. SMA	cASIA LEMS (R)	-0.61	0.01
	Hours/week IE	-0.45	0.09
	Hours/week any exer.	-0.41	0.13
	ASIA LEMS (R)	-0.33	0.23
	Age	0.3	0.27

ROI	COVARIATE	R	P
L. M1/S1 hand area	none	na	na
R. M1/S1 hand area	ASIA LEMS (R)	0.47	0.08
	Age	-0.35	0.2
	AIS	0.26	0.34
	ASIA Motor Score (B)	0.26	0.34
	Time since injury	0.25	0.37

	Total hours IE	-0.29	0.29		SCI/exer. Group	0.24	0.38
	AIS	-0.29	0.29		ASIA UEMS (R)	0.24	0.38
	ASIA Motor Score (B)	-0.28	0.31		**cLEMS-R x Age**		**0.1**
	cASIA Motor Score (B)	-0.24	0.39	L. latCS	none	na	na
L. PMdc	none	na	na	R. latCS	SCI/exer. Group	0.52	0.05
R. PMdc	SCI Level	-0.31	0.26		SCI Level	0.46	0.08
	Hours/week IE	-0.31	0.27		cASIA LEMS (R)	-0.37	0.17
	Age	-0.26	0.34		ASIA UEMS (R)	0.32	0.25
	SCI/exer. Group	0.24	0.38		ASIA LEMS (R)	-0.29	0.3
	cLEMS-R x LEMS-R		**0.09**		Hours/week IE	-0.28	0.32
	cLEMS-R x Age		**0.03**		cASIA Motor Score (B)	-0.27	0.33
L. latPrCS	none	na	na		Hours/week any exer.	0.26	0.34
R. latPrCS	cASIA LEMS (R)	-0.47	0.08		**cLEMS-R x LEMS-R**		**0.19**
	Hours/week IE	-0.3	0.27	L. PMv/IFG	none	na	na
	SCI/exer. Group	0.26	0.35	R. PMv/IFG	Hours/week IE	-0.47	0.08
	ASIA Motor Score (B)	-0.23	0.4		SCI/exer. Group	0.46	0.09
	cLEMS-R x LEMS-R		**0.05**		cASIA LEMS (R)	-0.38	0.16
L. SFG/SMA	Hours/week any exer.	0.42	0.12		cASIA Motor Score (B)	-0.36	0.19
	cASIA UEMS (R)	-0.4	0.13		SCI Level	0.3	0.28
	Age	-0.38	0.16		ASIA LEMS (R)	-0.26	0.34
	ASIA UEMS (R)	-0.29	0.3		AIS	-0.24	0.39
	SCI/exer. Group	0.28	0.32	L. PoCG	none	na	na
	cASIA Motor Score (B)	-0.27	0.32	R. PoCG	cASIA LEMS (R)	-0.31	0.26
R. SFG/SMA	ASIA LEMS (R)	0.34	0.22		cASIA UEMS (R)	0.31	0.27
	Hours/week IE	-0.33	0.24		SCI Level	0.25	0.36
	AIS	0.31	0.27		ASIA UEMS (R)	0.24	0.39

	Age	-0.26	0.36		**cLEMS-R x Age**		**0.01**
	cLEMS-R x Age		**0.01**	L. pCC	Total hours IE	-0.34	0.21
R. SFG/M1	ASIA UEMS (R)	-0.43	0.11		Time since injury	-0.27	0.33
	ASIA LEMS (R)	0.43	0.11		cASIA UEMS (R)	0.26	0.35
	SCI Level	-0.38	0.16		Hours/week IE	-0.25	0.37
	Age	-0.38	0.17	R. pCC	cASIA UEMS (R)	0.56	0.03
	ASIA Motor Score (B)	-0.36	0.19		cASIA Motor Score (B)	0.4	0.14
	AIS	0.34	0.21		ASIA Motor Score (B)	0.39	0.15
	Hours/week IE	-0.28	0.32		ASIA UEMS (R)	0.32	0.24
	Hours/week any exer.	-0.24	0.39		SCI Level	0.32	0.24
	cLEMS-R x AIS		**0.06**		AIS	0.31	0.27
	cLEMS-R x Age		**0**		Age	0.25	0.36
L. CMA	cASIA LEMS (R)	-0.26	0.35	L. IPL	ASIA LEMS (R)	0.44	0.1
	cLEMS-R x AIS		**0.08**		Age	-0.32	0.24
	cLEMS-R x Age		**0**		cASIA UEMS (R)	0.25	0.36
R. CMA	none	na	na		**cLEMS-R x Age**		**0.05**
L. M1/CMA	Hours/week IE	-0.53	0.04	R. IPL	none	na	na
	SCI/exer. Group	0.44	0.1	L. medPoCS	none	na	na
	Total hours IE	-0.41	0.13	R. medPoCS	cASIA UEMS (R)	0.39	0.15
	cASIA UEMS (R)	0.4	0.14		Hours/week IE	-0.37	0.17
	SCI Level	0.4	0.14		Hours/week any exer.	-0.37	0.18
	ASIA UEMS (R)	0.38	0.16		Total hours IE	-0.34	0.21
	ASIA Motor Score (B)	0.37	0.18		ASIA LEMS (R)	0.27	0.33
	Hours/week any exer.	-0.26	0.36		Age	-0.25	0.37
R. M1/CMA	Age	-0.3	0.28		**cLEMS-R x AIS**		**0.04**
	ASIA LEMS (R)	0.24	0.4		**cLEMS-R x Age**		**0**
	cLEMS-R x AIS		**0.05**	L. medPPC	cASIA UEMS (R)	0.55	0.03
	cLEMS-R x Age		**0**		ASIA LEMS (R)	0.52	0.05

L. M1 Leg	cASIA UEMS (R)	0.35	0.2
	Hours/week IE	-0.33	0.23
	ASIA LEMS (R)	0.31	0.26
	Time since injury	-0.27	0.34
	cLEMS-R x cUEMS-R		**0.12**
	cLEMS-R x AIS		**0.04**
	cLEMS-R x Age		**0**
	cLEMS-R x H/w IE		**0.07**
R. M1/S1 leg	cASIA UEMS (R)	0.52	0.05
	Age	0.34	0.21
	ASIA LEMS (R)	0.34	0.22
	cASIA LEMS (R)	-0.24	0.39
	cASIA Motor Score (B)	0.24	0.39
	cLEMS-R x AIS		**0.04**
	cLEMS-R x Age		**0**
	cLEMS-R x H/w IE		**0.11**
	cLEMS-R x Tot.Hrs-IE		**0.11**
L. S1 leg	Hours/week IE	-0.54	0.04
	cASIA UEMS (R)	0.41	0.13
	SCI/exer. Group	0.41	0.13
	AIS	0.37	0.17
	Time since injury	0.35	0.19
	ASIA Motor Score (B)	0.35	0.2
	cASIA Motor Score (B)	0.34	0.22
	Age	0.33	0.23
	ASIA LEMS (R)	-0.3	0.29
	SCI Level	0.28	0.31
	Total hours IE	-0.24	0.38
	ASIA UEMS (R)	0.24	0.39
	cLEMS-R x Age		**0.02**
R. S1 leg	ASIA LEMS (R)	0.27	0.33
	cLEMS-R x Age		**0.02**

	SCI/exer. Group	-0.35	0.21
	cASIA Motor Score (B)	0.3	0.28
	ASIA Motor Score (B)	0.27	0.34
	AIS	0.24	0.4
R. medPPC	Hours/week IE	-0.4	0.14
	ASIA LEMS (R)	0.37	0.17
	Age	-0.36	0.19
	Total hours IE	-0.33	0.23
	SCI/exer. Group	0.28	0.31
	AIS	0.28	0.31
	cASIA UEMS (R)	0.28	0.31
	SCI Level	0.28	0.32
	cASIA LEMS (R)	-0.25	0.36
	Hours/week any exer.	0.24	0.39
	cLEMS-R x AIS		**0.04**
	cLEMS-R x Age		**0.01**
L. SPL	none	na	na
R. SPL	ASIA UEMS (R)	0.49	0.06
	SCI/exer. Group	0.47	0.07
	SCI Level	0.43	0.11
	Hours/week IE	-0.43	0.11
	ASIA Motor Score (B)	0.4	0.14
	cASIA UEMS (R)	0.24	0.38

Figure 13 – MedPPC activity during the IL task better predicts future functional motor gains than a clinical assessment of current motor status. Left: Linear correlation between medPPC activity and future change in Right ASIA Lower Extremity Motor Score (R. ASIA LEMS). Average beta value for imagined leg reaching is shown for the HC and SCI groups (gray bar and black bar, respectively). Subjects with normal or above normal medPPC activity exhibited the largest functional motor improvements for the right leg six months later. Right: Linear correlation between current R. ASIA LEMS and future change in R. ASIA LEMS.

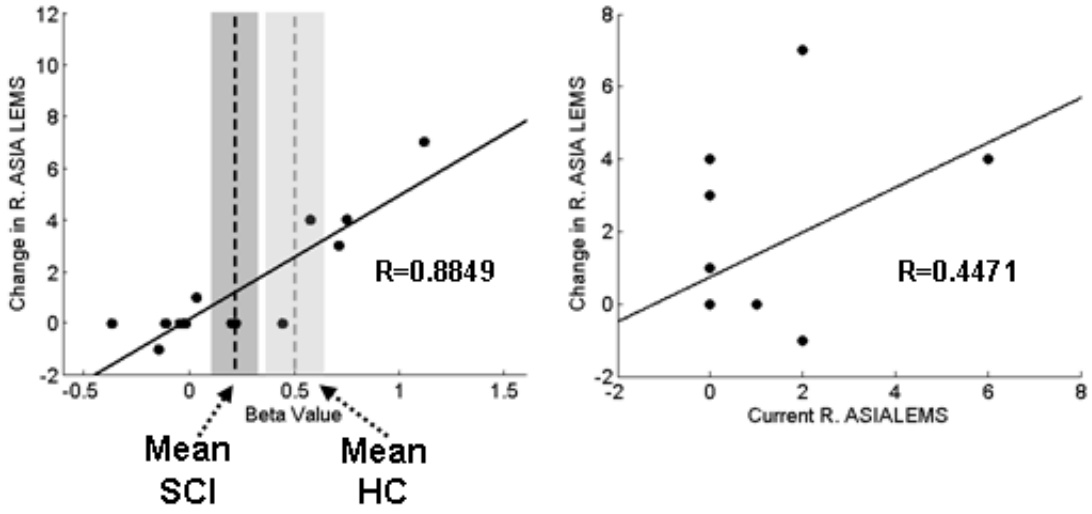

Figure 14 – Effect of ASIA Impairment Scale (AIS) on brain activity. Group statistical maps for Healthy Control (left), AIS C (middle), and AIS A/B (right) subgroups during the IL task (top row) and AK task (bottom row). Q(FDR)<0.05. AIS A classification means that the subject's injury is complete, with no sensory or motor function preserved in sacral segments S4-S5. AIS B classification means that a subject's injury is incomplete, with sensory but no motor function preserved below the injury level and extending through sacral segments S4-S5. AIS C classification means that a subject's injury is incomplete, with some motor function preserved below the site of injury. In both tasks, subjects with less-complete injury (AIS C) exhibit the most normal pattern of task-related brain activity. In the IL task, subjects with AIS A/B classification still activate PMd, SMA, medPPC and aIPS, but the spread of activity is reduced compared to HC subjects, and the level of activity is also reduced (not shown). In the AK task, subjects with AIS A/B classification activate a greater area of somatomotor cortex than HC subjects, while this network shrinks in subjects with AIS C classification.

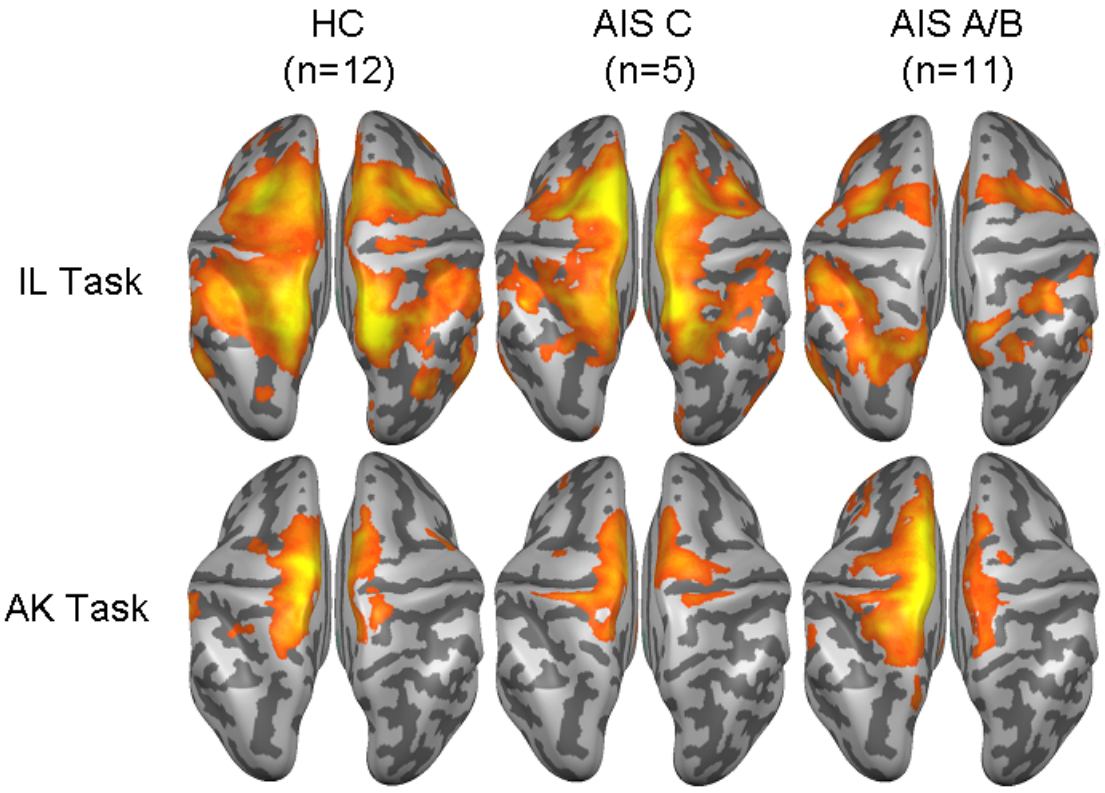

Figure 15 – Effect of time-since-injury on brain activity. Group statistical maps for Healthy Control (left, n=12), Early SCI (middle, n=8), and Late SCI (right, n=8) subgroups during the IL task (top row) and AK task (bottom row). Q(FDR)<0.05.

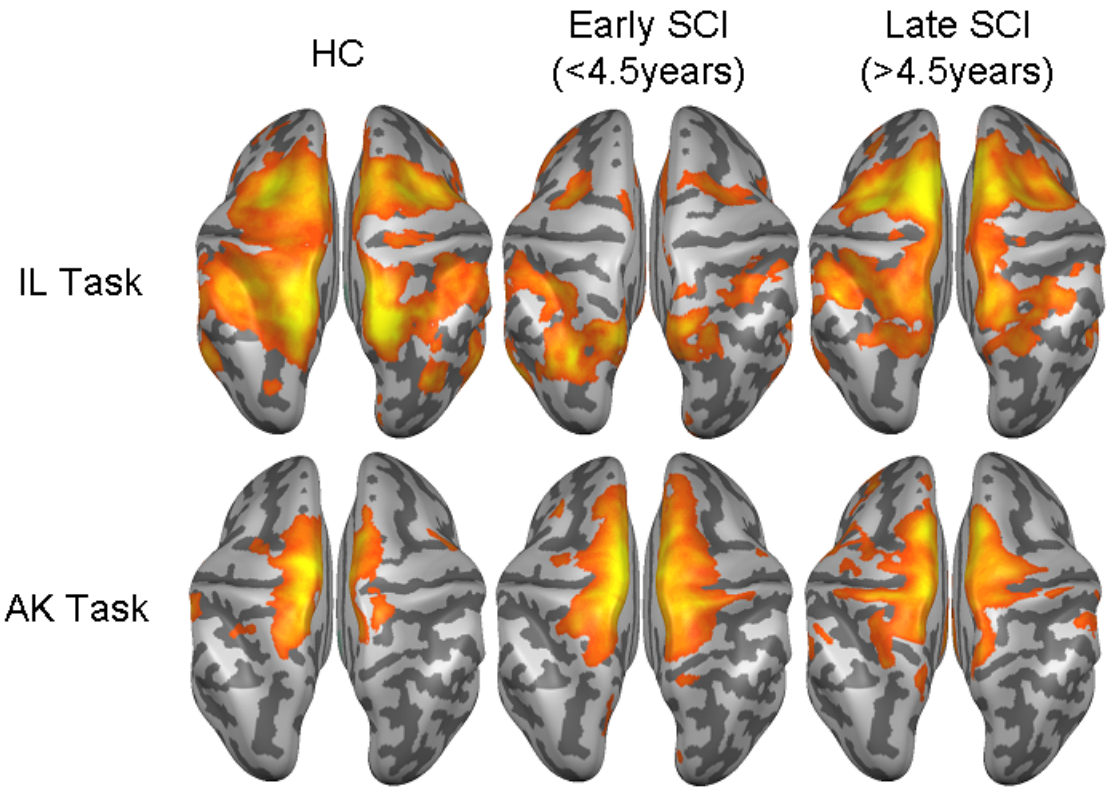

Figure 16 – Effect of time-since-injury (TSI) and spinal cord cross-sectional area (CSA) on brain activity in the M1/PMd knee area, just anterior to the primary motor knee representation. In the Early-SCI subgroup this ROI is hyperactive, while in the Late-SCI subgroup this ROI is hypoactive. CSA is a measure of spinal cord area and is used to assess shrinkage of the spinal cord following injury. CSA values for the spinal cord subjects in this study are lower than those for healthy controls. Larger CSA means that a subject's spinal cord is more healthy/normal in size. We hypothesized that TSI and CSA would be correlated (see Figure 17), with CSA decreasing as TSI increases. In the Low-CSA subgroup, M1/PMd was hypoactive relative to HC subjects. In the High-CSA subgroup, M1/PMd was hyperactive relative to HC subjects.

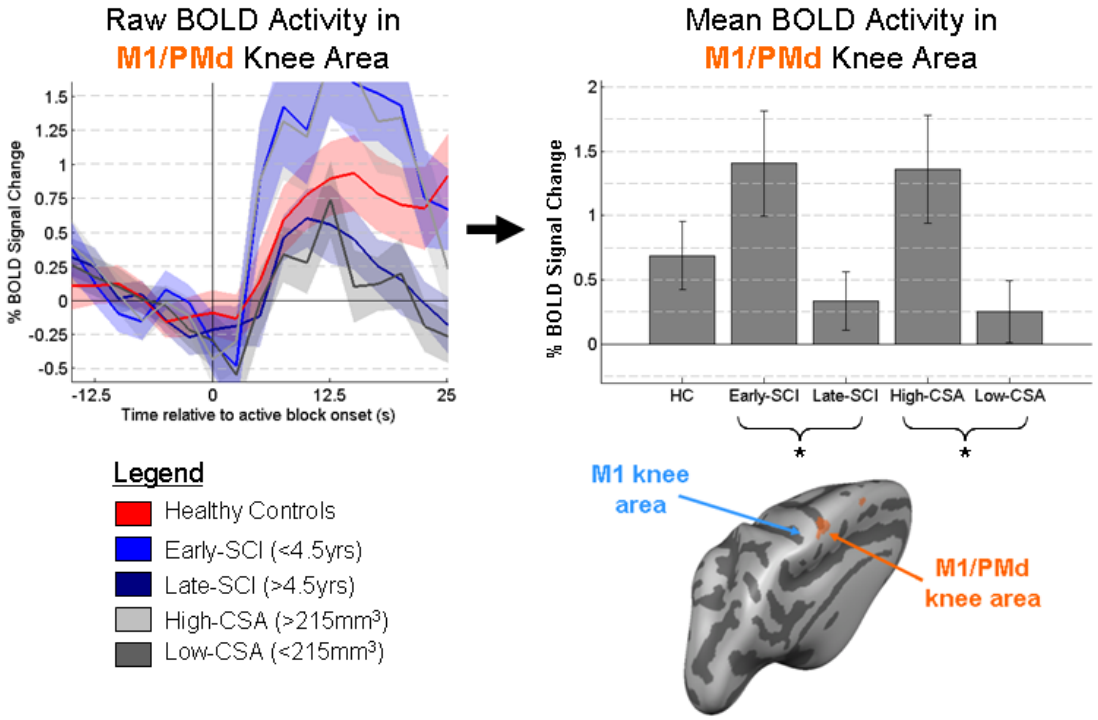

Figure 17 – Effect of time-since-injury (TSI) on spinal cord size. For every subject, we measured the cross-sectional area (CSA, in mm^3) of the spinal cord, calculating both normalized and adjusted CSA. As hypothesize, there is a significant negative linear correlation between TSI and CSA.

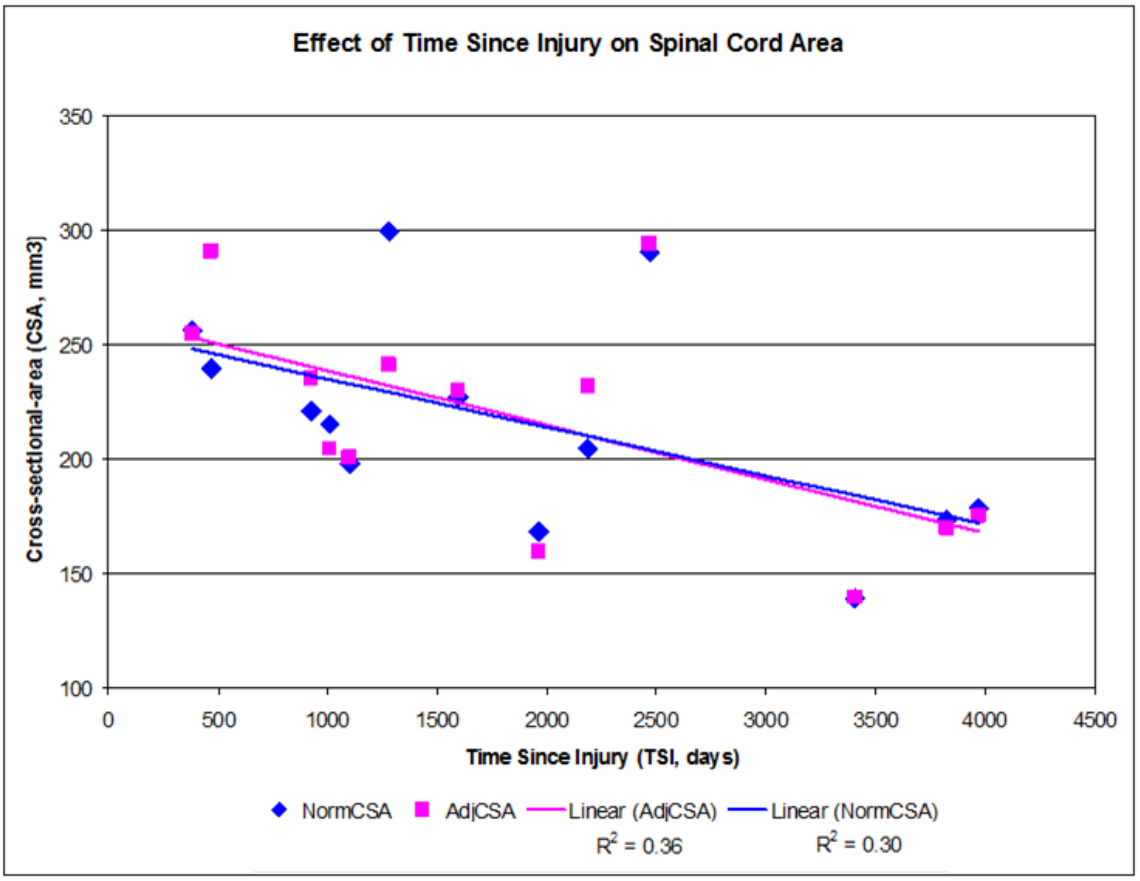

Figure 18 – Effect of preserved proprioceptive ability on brain activity. SCI-P0 = Group of 13 SCI subjects with a right proprioception score of zero, indicating no retained proprioceptive ability. SCI-P1 = Group of three SCI subjects with a non-zero right proprioception score, indicating some degree of retained proprioceptive ability. A) IL task-related group statistical maps for Healthy Control and SCI-P0 groups. Q(FDR)<0.05. Even subjects with no right-sided proprioceptive ability retain a fairly normal pattern of brain activity including motor association areas like PMd, SMA, medPPC and aIPS. B) BOLD timecourses of activity during the IL task for three motor association ROIs: PMd, SMA, and medPPC. SCI subjects with preserved proprioceptive ability activated these brain areas as much or greater than HC subjects. In contrast, BOLD activity in these ROIs in SCI subjects with no preserved proprioceptive function was decreased relative to HC subjects, but still above baseline.

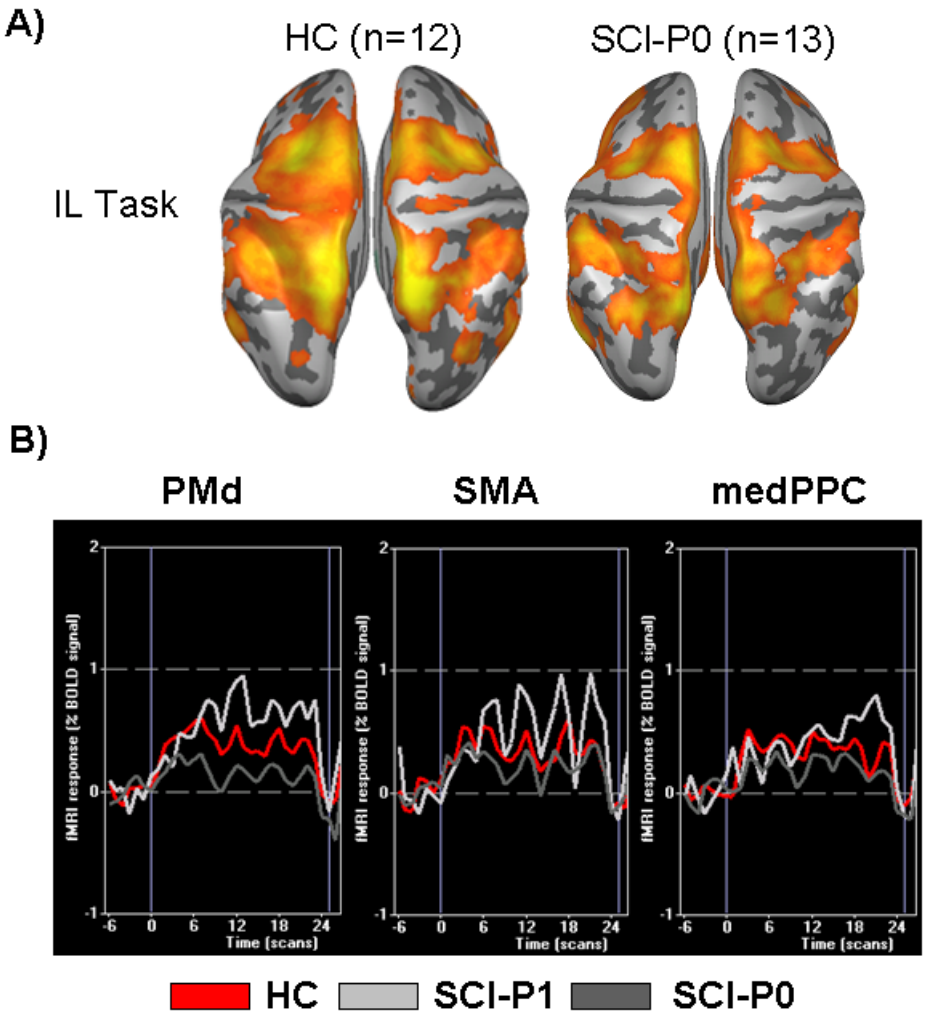

CONSIDERATIONS FOR THE DESIGN AND IMPLEMENTATION OF NEURAL PROSTHETIC DEVICES

Control Signals for Cortical Neural Prosthetic Devices (NPDs)

Reach plans have been successfully decoded from monkey PRR (Musallam et al. 2004), while Hwang and colleagues (unpublished results) have also decoded a "go" state signal that reflects movement initiation. A decode of discrete movement goals could be implemented by recording these directional and state signals from the human homologue of monkey PRR. Mulliken et al. (2008) have demonstrated the presence of both static goal angle and dynamic movement angle signals in neurons in monkey PRR and Area 5 during a joystick reaching task, with goal angle representations located deeper in parietal cortex than movement angle representations. The presence of a forward estimate of the dynamic cursor position supports a role for these PPC brain areas in the online control of movement trajectories, in addition to specifying the end goal of a movement. Another study by Mulliken and colleagues successfully implemented a continuous decode of cursor position in a joystick task, decoding movement trajectories from monkey PRR/Area 5 (Mulliken et al. 2004 and Mulliken et al. submitted). Additional cognitive signals related to the consequences of action are also present in the PPC. Variables related to reward probability and magnitude are encoded in monkey PRR (Musallam et al. 2004), and performance-weighted action value (absolute value, encodes both upcoming rewards and punishments) modulates action planning activity in human PPC (Iyer et al., submitted). The multitude of cognitive, motor intentional, and state variables represented in PRR render it an ideal candidate for the implantation of a NPD. Both continuous and discrete decodes would allow for the flexible control of an external device.

We now have converging functional and anatomical evidence in normal, healthy subjects that our parietal region of interest (medPPC/pIPS) is the human homologue of monkey PRR (see Part I of this thesis). We've also identified two additional reach-specific, pre-motor brain

areas in the human frontal cortex with robust motor planning activity: SMA and PMd (Fig. II.D.1). Since PRR, SMA, and PMd all play a role in planning real arm reaches and show greater activity for arm vs. eye movements, they are all candidate neural prosthetic implant sites (Glidden et al. 2005, Glidden et al. submitted). Because these brain areas are also activated by imagined reach planning, this finding opens up the possibility of obtaining precise electrode targeting maps for paralyzed patients using fMRI during an imagined-reach task.

The presence of independent arm-intentional and eye-intentional signals in the human brain increases the number of potential control signals for a NPD. In addition to decoding real or imagined reaches from human PRR and PMd, it may be possible to record neural activity in human LIP or FEF and decode eye movements. LIP and FEF may encode covert shifts of visual attention (see: Chapter 3.1), which would allow for both motor intentional and attentional signals to be utilized in the brain control of external devices. Decoded motor intentional signals could be used to interact with the external device. In the case of a computer interface, these intentional signals could be used to control the position of a cursor, and open/close or use computer applications. However, additional directional or positional eye- and attentional-signals could also be used to intuitively navigate a larger interactive space. For instance, a covert voluntary shift of attention could be used to shift or select an interactive window, to “foveate” and facilitate user interaction with different snapshots of a larger scene (Fig. II.D.2). Increasing the number of potential independent control signals could greatly boost the flexibility and speed of the user-device interface, as multiple user-device interactions could be processed in parallel.

In addition to the possibility of decoding independent control signals from different brain regions, decoding of “redundant” information could improve decode reliability and provide a backup failsafe if two NPDs are implanted and one fails. Both PRR and PMd preferentially encode reach plans and specify the “goal” of the movement. Two NPDs, one located in PRR and one in PMd, could be used to simultaneously decode reach plans. An error-check algorithm could then compare the decoded plans from the two brain areas, incorporating information about the reliability and quality of neural signals recorded from the device

implanted in each area. A “best estimate” of the intentional signal could then be used as the control signal to improve overall decode performance. Pesaran, Nelson & Andersen (2006) showed that neurons in MIP (includes PRR) encode the position of the target in an eye-centered reference frame, while neurons in PMd encode the relative position of the target, eye and hand; a more complex reference frame which may be useful for coordinating arm and eye movements. Another study by Batista and colleagues (2007) demonstrated the presence of neurons in PMd that encode in eye-centered, limb-centered, and combined references frames. PMd and PRR may simultaneously encode intentional information, but at least some of the information is non-redundant. The integration of these two sources of information regarding intended arm movements could potentially be used to optimize the performance of a decode algorithm.

Location of PRR and impact on prosthetic design and implantation

Due to the high degree of inter-subject anatomical variability, localization of PRR in individual subjects using our fMRI task is crucial for customized device design (as the location and geometry of PRR could affect electrode length and geometry), pre-surgical planning, and image-guided surgery.

Our current depth estimates of the center of human PRR range between ~0.5-1.5cm from the surface of parietal cortex. A more direct route to PRR achieved by opening up the intraparietal sulcus may also be possible, though opening up the sulcus could complicate both the surgery and surgical recovery processes and impact device performance. These depth estimates of human PRR have influenced the design of the implantable Caltech Neural Prosthetic device.

Human PRR is located quite close to the midline, and near the superior sagittal sinus. The superior sagittal sinus is the major draining vein of the brain, and the neurosurgeon will need to carefully navigate around it and the nearby vasculature in order to implant a NPD into PRR, which could complicate the surgery. Obtaining images of individual patient brain anatomy and an overlay of the cerebral vasculature would enable optimal surgical path planning and image-guided surgery, decreasing the risks involved with the surgery and

potentially improving patient outcome and device performance. Intra-operative recording of neural activity could also help ensure accurate placement of the implanted device, as many functional properties of the human area and homologous monkey PRR are now known.

Selection of Patients for Clinical Implantation of the Caltech Neural Prosthetic (CNP)

The works presented in this thesis could also influence the selection of potential recipients of the CNP. The localization of PRR via the fMRI task described in Part I could allow for pre-screening of potential surgical patients. Patients could be selected based on accessibility of their individual PRR, as PRR accessibility will affect device customization, surgical risk, and the degree of uncertainty in placement of the CNP.

The CNP electrode array is limited in how long the electrodes can be without breaking or causing too much brain dimpling during implantation. Because of the increased risks of electrode breakage and brain dimpling with increasing electrode length, a device with shorter electrodes is likely to be more viable after implantation. Ideal candidates for implantation of the CNP into PRR are patients whose PRR is located further from the superior sagittal sinus, with an intra-cortical surgical path shorter than ~1cm while avoiding the surrounding vasculature.

The study of patients with SCI presented in Part II of this thesis also has implications for the selection of potential CNP patients. While relatively normal brain activity was observed across the group of SCI patients, we did observe a spectrum of plastic changes within the group. Plastic deviations from a normal amplitude or network pattern of activity correlated with clinical variables such as ASIA motor scores, ASIA impairment score, and behavioral variables such as the hours/week spent exercising. Therefore, selecting patients with less anatomically/functionally complete lesions or impairments might bias the selection process towards patients who retain the most healthy, normal pattern of brain activity, which in turn may facilitate the operation and efficacy of an implanted neural prosthetic device.

DISCUSSION FIGURES

Figure II.D.1 – a. fMRI time courses from SMA, PMd, and PRR show greater activity for real and imagined reach planning compared to eye movement planning and a visual control. b. The locations of left-hemisphere SMA, PMd, and PRR are marked. Orange indicates brain activity greater for reach compared to saccade planning. Blue indicates brain activity higher for saccades than for reaching.

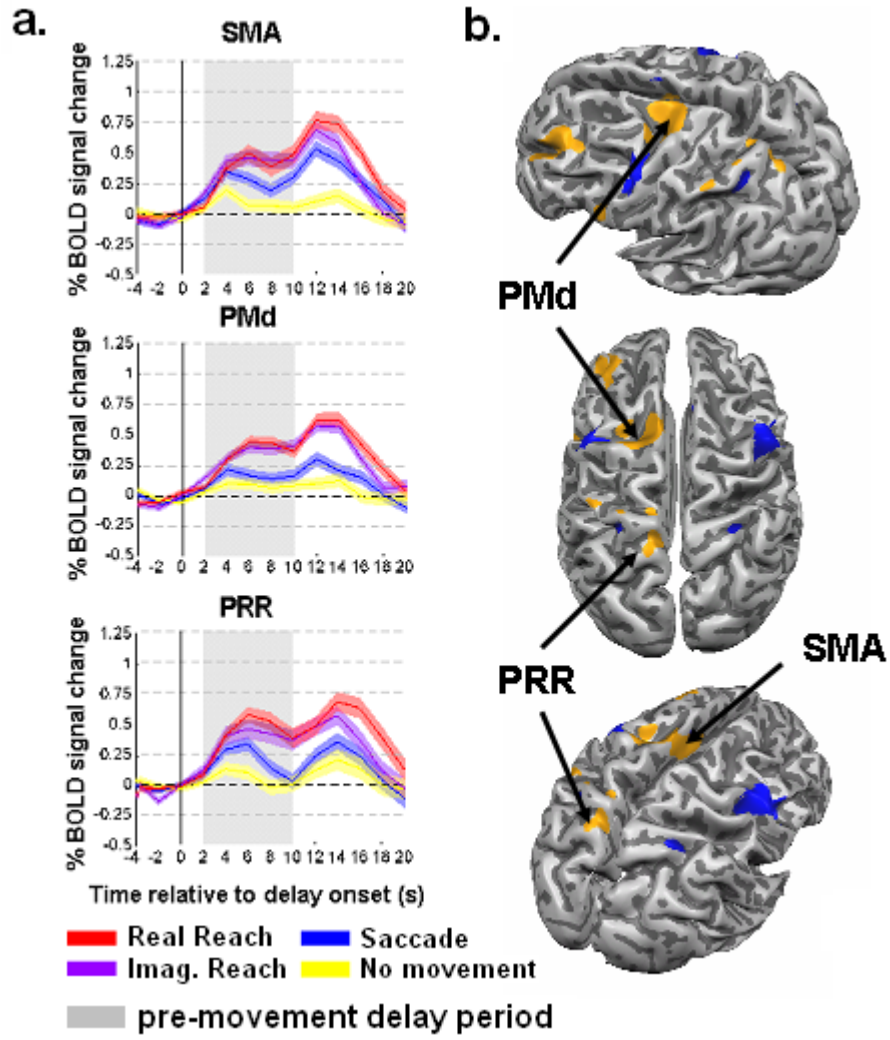

Figure II.D.2 - Dynamic interactive "scene" shift enabled by neural decode of change in the locus of gaze or spatial attention. Top: The subject could be asked to shift their gaze (or attempt/imagine a gaze shift if the patient is severely "locked in") or covertly shift their spatial attention. Decoding these gaze- or attention-shifts from human LIP or FEF could be used to shift the interactive scene relative to the subject, allowing the subject to navigate the scene. Independent motor intentional signals could be used to interact with elements or objects in the scene. Navigational and interactive decodes could be processed in parallel, speeding the user interface compared to a purely serial process implemented by decode of only intentional or navigational signals.

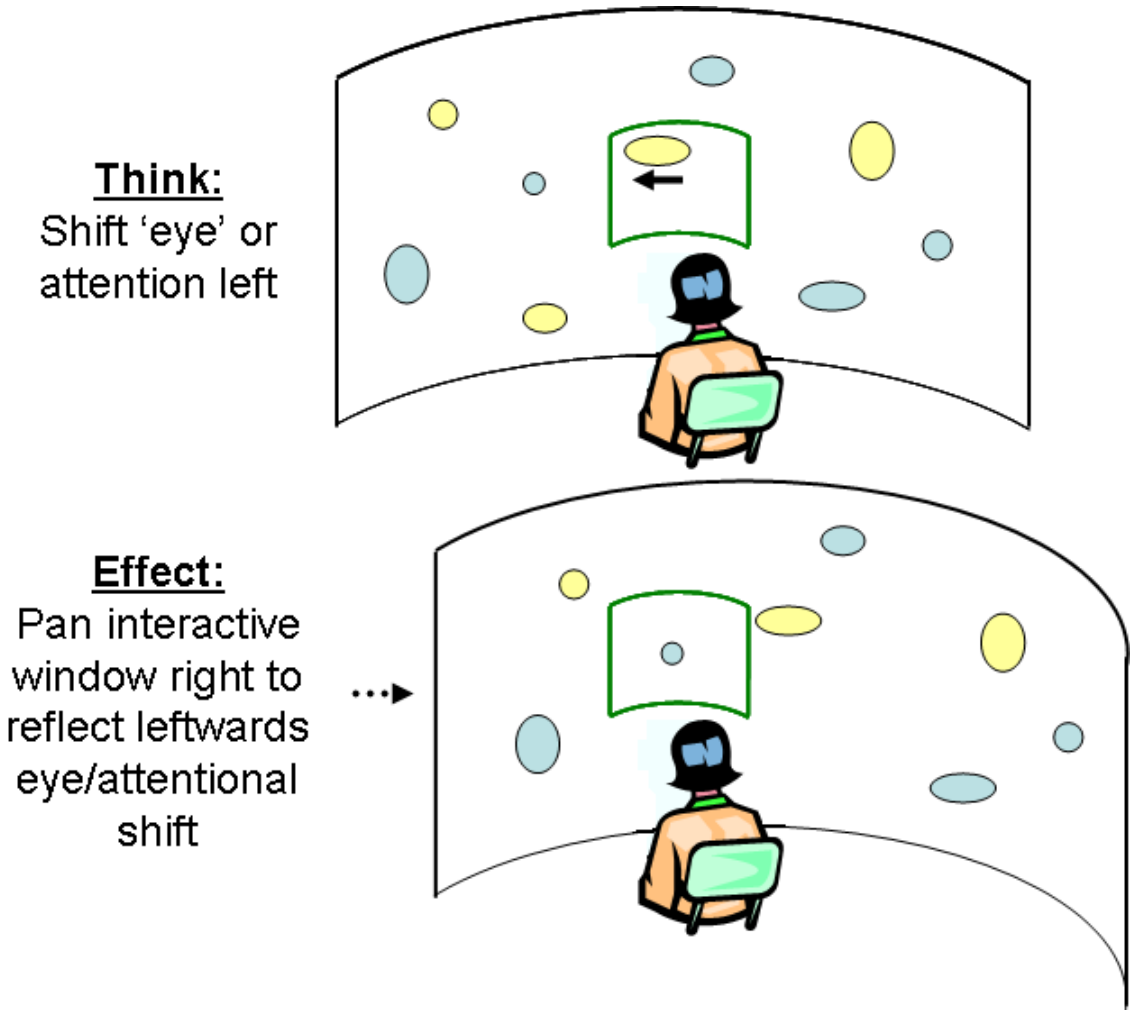

CONCLUSIONS

A little knowledge that acts is worth infinitely more than much knowledge that is idle.
- Kahlil Gibran, poet

The body of work presented in this thesis elucidates how the brain represents goal-directed arm and eye movements such as the handshake introduced in the *Preface*, with basic science and clinical applications. Part I: Chapter 1 dissociated two frontoparietal brain networks involved in motor planning for independent control of the arms and the eyes, discussed human-monkey interspecies functional homologies, and resolved the debate on effector-specificity in the human brain. In short, there are effector-specific cortical areas, but effector-specificity is relative. The PMd, SMA, aIPS, and pIPS/medPPC (putative homologue of monkey PRR) all preferentially encoded reach plans, while the infFEF and midIPS (putative homologue of monkey LIP) preferentially encoded saccade plans. Despite the fact that significant BOLD signal amplitude differences distinguished these two networks, all of the nodes previously listed were also active during a pre-movement, preparatory phase for movements with the non-preferred effector. The substantial overlap of arm- and eye-movement preparatory activations in the human brain could be the signature of the tight coupling between these two movement-types in natural behaviors and the need for eye-hand coordination (I might already be looking at you if I intend to shake your hand, but if I am not, I will most certainly meet your gaze while shaking hands). It could also be a hallmark of the representation of behavioral flexibility in the brain. In a dynamic environment, our behavioral priorities may rapidly change, necessitating modifications to existing movement plans, or the specification of new motor intentions. Rapid, optimal behavioral flexibility could be implemented not only through the neural representation of a selected movement plan, but also by the encoding of alternatives. In the case that behavioral priorities update, a "ready" alternative action plan could then be selected for execution.

Empirically, it makes sense that whenever a behaviorally relevant target is instructed (or attended within a scene), the brain should immediately engage both arm and eye movement planning networks and formulate default motor plans. Then, additional contextual cues

(either external or internal) may bias the selection of one type of movement over another. However, it would also be advantageous to maintain these default plans in the event that behavioral priorities change. The engagement of reach-planning areas on saccade trials and saccade-planning areas on reach trials in the first experiment presented in Part I may reflect the formation and maintenance of default motor plans generate in response to a behaviorally-relevant visual target.

The subsequent experiment investigated the interaction between effector-specificity and both motor planning and related processes. Compared to BOLD delay-period activity when a movement is fully-instructed, delay-period activity in partially instructed trials (when a spatial target is instructed but no effector is known, or when an effector is instructed and the spatial target is not yet known) indicates that the effector-specific PMd, SMA, infFEF, aIPS, medPPC/pIPS and midIPS preferentially encode a selected motor plan compared to a default motor plan. However, BOLD activity during the delay period of these partially-instructed trials could also indicate the presence of a less potent (compared to a selected action plan) default motor plan. I am currently further investigating default motor plans and the representation of selected vs. potential actions in the human brain in a free-choice (effector-choice) experiment.

The study presented in Part I: Chapter 2 investigated the cognitive basis of the BOLD signal observed during a pre-movement delay period. By varying the behaviorally-relevant information available to the subject prior to this delay, we were able to disentangle activity specifically attributable to motor planning from activity reflected of other, related processes like the processing of relevant visual cues, spatial attention/working memory, effector preparation in the absence of information about the goal of the movement, and a general "action-readiness." The results of this study indicated that the PMd, SMA, and PPC are involved in motor planning, and that their delay-period activity cannot be fully explained by other related processes. This supports a motor role for these brain areas in the preparation of goal-directed action, and not just an attentional role (Part I: Chapter 2). Additional support for a motor role in these brain areas stems from the encoding of additional variables related

to arm-movement, including movement type, limb posture, and some contralaterality for the limb employed (Part I: Chapter 3).

In Part II, a comparison of real vs. imagined movements demonstrated that the imagined arm is nearly as effective a driver of preparatory activity in frontoparietal motor planning areas as the real arm. In contrast, the imagined arm was not effective in driving activity in motor execution-related areas such as M1, S1, and the CMA, and was less effective than the real arm in driving execution period activity in frontoparietal areas. Therefore, at least a portion of the go period activity in the PMd, SMA, and PPC is critically linked to action execution. Real vs. imagined arm execution did not differentially activate V1; thus, these go-period differences are probably due to somatosensory and proprioceptive feedback during movement, and could also be related to efference copy and forward state estimation (see Mulliken, Musallam & Andersen 2008). One final difference was that internal simulation of a movement increased activity in the dlPFC, pre-SMA, and IPL compared to actual movement execution.

These experimental results suggest that imagined movements can be used as a viable proxy for real arm movements to activate cortical motor planning areas, and this finding has implications for the localization and implementation of cortical neural prosthetic devices in patients with severe paralysis. The fact that it was difficult to distinguish a real from an imagined arm movement during the planning phase of the task indicates that while real and imagined intentions coexist, there are many internal intentions that never bear action in the real world. The ethical and legal implications of this finding are interesting, as it highlights the danger of developing technologies that read peoples' "intentions" before they become actions, a la the movie *Minority Report*, since an internal intention is not always causally linked to real action output. However, the coexistence of real and imagined intentions is not a problem in the context of cortical neural prosthetic devices, as a "go" trigger signal, or state change from delay/plan → go/execute, could be used to selectively decode and implement only actions that the patient wishes to execute.

The implementation of the Caltech Neural Prosthetic is predicated upon the ability to successfully record and decode neural signals from the human PRR and/or PMd. Thus, it is important to determine the viability of recording from human PRR and PMd in severely paralyzed patients. An fMRI experiment comparing goal-directed action planning and execution activity in healthy control and spinal cord-injured (SCI) subjects revealed that a fairly normal pattern and amplitude of BOLD activity is maintained in the SCI subjects, indicating that the brain still represents movements of the disconnected limbs. One explanation for the preservation of normal BOLD activity is that the frontoparietal network is further removed from the site of injury than the primary motor cortex, which directly projects to neurons in the spinal cord. Another possible explanation is that the redundancy/overlap in the brain maps for goal-directed real and imagined arm and leg movements (and even eye movements) helps to reduce cortical plasticity and reorganization. Even if SCI subjects can no longer execute real goal-directed movements of the lower limbs, the internal simulation of leg movements or the preparation and execution of arm and eye movements should continue to activate the frontoparietal network, reducing activity-dependent plastic changes related to disuse of the lower limb effectors. In either case, the fact that our delayed response task is able to activate and locate the human PRR and PMd in high-level SCI subjects indicates that recording neural signals from these brain areas using an implantable cortical neural prosthetic should still yield viable control signals for the control of an external device.

Action is eloquence

- William Shakespeare, Coriolanus, Act III, scene ii

REFERENCES

Bálint R (1909) Seelenlähmung des ‘schauens’, optische ataxie, raümliche störung der aufmerksam. Monatschr. Psychiat. Neurol. 25:51–81.

Alkadhi H, Brugger P, Boendermaker SH, Crelier G, Curt A, Hepp-Reymond MC, Kollias SS (2005) What disconnection tells about motor imagery: evidence from paraplegic patients. Cereb Cortex 15(2):131-40.

Amiez C, Kostopoulos P, Champod AS, Petrides M (2006) Local morphology predicts functional organization of the dorsal premotor region in the human brain. J Neurosci 26(10):2724-31.

Astafiev SV, Shulman GL, Stanley CM, Snyder AZ, Van Essen DC, Corbetta M (2003) Functional organization of human intraparietal and frontal cortex for attending, looking, and pointing. J Neurosci 23(11):4689-99.

Batista AP, Buneo CA, Snyder LH, Andersen RA (1999) Reach plans in eye-centered coordinates. Science 285(5425):257-60.

Batista AP, Santhanam G, Yu BM, Ryu SI, Afshar A, Shenoy KV (2007) Reference frames for reach planning in macaque dorsal premotor cortex. J Neurophysiol 98(2):966-83.

Beevor CE, Horsley V (1890) An experimental investigation into the arrangement of the excitable fibers of the internal capsule of the bonnet monkey (Macacus sinicus). Philos Trans R Soc Lond 181(B):49–88.

Berman RA, Colby CL, Genovese CR, Voyvodic JT, Luna B, Thulborn KR, Sweeney JA (1999) Cortical networks subserving pursuit and saccadic eye movements in humans: an FMRI study. Hum Brain Mapp 8(4):209-25.

Beurze SM, de Lange FP, Toni I, Medendorp WP (2007) Integration of target and effector information in the human brain during reach planning. J Neurophysiol 97(1):188-99.

Bisley JW, Goldberg ME (2003) Neuronal activity in the lateral intraparietal area and spatial attention. Science 299(5603):81-86.

Boussaoud D (1995) Primate premotor cortex: modulation of preparatory neuronal activity by gaze angle. J Neurophysiol 73(2):886-90.

Boussaoud D (2001) Attention versus intention in the primate premotor cortex. Neuroimage 14(1 Pt 2):S40-5.

Bracewell RM, Mazzoni P, Barash S, Andersen RA (1996) Motor intention activity in the macaque's lateral intraparietal area. II. Changes of motor plan. J Neurophysiol 76(3):1457-64.

Brown MR, Goltz HC, Vilis T, Ford KA, Everling S (2006) Inhibition and generation of saccades: rapid event-related fMRI of prosaccades, antisaccades, and nogo trials. Neuroimage 33(2):644-59.

Brown MR, Vilis T, Everling S (2007) Frontoparietal activation with preparation for antisaccades. J Neurophysiol. 2007 Jun 27; [Epub ahead of print].

Bruce CJ, Goldberg ME (1985) Primate frontal eye fields. I. Single neurons discharging before saccades. J Neurophysiol 53(3):603-35.

Bruce CJ, Goldberg ME, Bushnell MC, Stanton GB (1985) Primate frontal eye fields. II. Physiological and anatomical correlates of electrically evoked eye movements. J Neurophysiol 54(3):714-34.

Buneo CA, Andersen RA (2008) The posterior parietal cortex: sensorimotor interface for the planning and online control of visually guided movements. Neuropsychologia 44(13):2594-606.

Calton JL, Dickinson AR, Snyder LH (2002) Non-spatial, motor-specific activation in posterior parietal cortex. Nat Neurosci 5(6):580-8.

Chang SW, Dickinson AR, Snyder LH (2008) Limb-specific representations for reaching in the posterior parietal cortex. J Neurosci 28(24):6128-40.

Cisek P, Kalaska JF (2002) Simultaneous encoding of multiple potential reach directions in dorsal premotor cortex. J Neurophysiol 87(2):1149-54.

Cohen Kadosh R, Henik A, Rubinsten O, Mohr H, Dori H, van de Ven V, Zorzi M, Hendler T, Goebel R, Linden DE (2005) Are numbers special? The comparison systems of the human brain investigated by fMRI. Neuropsychologia 43(9):1238-48.

Colby CL, Duhamel JR, Goldberg ME (1996) Visual, presaccadic, and cognitive activation of single neurons in monkey lateral intraparietal area. J Neurophysiol 76(5):2841-52.

Connolly JD, Andersen RA, Goodale MA (2003) FMRI evidence for a 'parietal reach region' in the human brain. Exp Brain Res 153(2):140-5.

Connolly JD, Goodale MA, Cant JS, Munoz DP (2007) Effector-specific fields for motor preparation in the human frontal cortex. Neuroimage 34(3):1209-19.

Connolly JD, Goodale MA, Desouza JF, Menon RS, Vilis T (2000) A comparison of frontoparietal fMRI activation during anti-saccades and anti-pointing. J Neurophysiol 84(3):1645-55.

Coren S (1993) The lateral preference inventory for measurement of handedness, footedness, eyedness, and earedness: norms for young adults. Bull Psychon Soc 31:1-3.

Coull JT, Vidal F, Nazarian B, Macar F (2004) Functional anatomy of the attentional modulation of time estimation. Science 303(5663):1506-8.

Cramer SC (2004) Changes in motor system function and recovery after stroke. Restor Neurol Neurosci 22(3-5):231-8.

Cramer SC, Crafton KR (2006) Somatotopy and movement representation sites following cortical stroke. Exp Brain Res 168(1-2):25-32.

Cramer SC, Lastra L, Lacourse MG, Cohen MJ (2005) Brain motor system function after chronic, complete spinal cord injury. Brain 128(Pt 12):2941-50.

Culham JC, Cavina-Pratesi C, Singhal A (2006) The role of parietal cortex in visuomotor control: what have we learned from neuroimaging? Neuropsychologia 44(13):2668-84.

Cunnington R, Windischberger C, Deecke L, Moser E (2003) The preparation and readiness for voluntary movement: a high-field event-related fMRI study of the Bereitschafts-BOLD response. Neuroimage 20(1):404-12.

Cunnington R, Windischberger C, Robinson S, Moser E (2006) The selection of intended actions and the observation of others' actions: a time-resolved fMRI study. Neuroimage 29(4):1294-302.

Curtis CE (2006) Prefrontal and parietal contributions to spatial working memory. Neuroscience 139(1):173-80.

Curtis CE, D'Esposito M (2006) Selection and maintenance of saccade goals in the human frontal eye fields. J Neurophysiol 95(6):3923-7.

de Lange FP, Helmich RC, Toni I (2006) Posture influences motor imagery: an fMRI study. Neuroimage 33(2):609-17.

Deecke L, Kornhuber HH (1978) An electrical sign of participation of the mesial 'supplementary' motor cortex in human voluntary finger movement. Brain Res 159(2):473-6.

Deiber MP, Ibanez V, Honda M, Sadato N, Raman R, Hallett M (1998) Cerebral processes related to visuomotor imagery and generation of simple finger movements studied with positron emission tomography. Neuroimage 7(2):73-85.

Deiber MP, Ibanez V, Sadato N, Hallett M (1996) Cerebral structures participating in motor preparation in humans: a positron emission tomography study. J Neurophysiol 75(1):233-47.

Diedrichsen J, Hashambhoy Y, Rane T, Shadmehr R (2005) Neural correlates of reach errors. J Neurosci 25(43):9919-31.

Draper NR, Smith H (1998) Applied Regression Analysis, 3rd edition. New York: Wiley-Interscience.

Enzinger C, Johansen-Berg H, Dawes H, Bogdanovic M, Collett J, Guy C, Ropele S, Kischka U, Wade D, Fazekas F, Matthews PM (2008) Functional MRI correlates of limb function in stroke victims with gait impairment. Stroke 39(5):1507-13.

Fernandez-Ruiz J, Goltz HC, Desouza JF, Vilis T, Crawford JD (2007) Human parietal "reach region" primarily encodes intrinsic visual direction, not extrinsic movement direction, in a visual-motor dissociation task. Cereb Cortex 17(10):2283-92.

Foltys H, Krings T, Meister IG, Sparing R, Boroojerdi B, Thron A, Topper R (2003) Motor representation in patients rapidly recovering after stroke: a functional magnetic resonance imaging and transcranial magnetic stimulation study. Clin Neurophysiol 114(12):2404-15.

Friston KJ, Holmes AP, Worsley KJ, Poline JB, Frith C, Frackowiak RSJ (1995) Statistical parametric maps in functional imaging: A general linear approach. Hum Brain Mapp 2:189-210.

Fujii N, Mushiake H, Tanji J (2000) Rostrocaudal distinction of the dorsal premotor area based on oculomotor involvement. J Neurophysiol 83(3):1764-9.

Fujii N, Mushiake H, Tanji J (2002) Distribution of eye- and arm-movement-related neuronal activity in the SEF and in the SMA and Pre-SMA of monkeys. J Neurophysiol 87(4):2158-66.

Gail A, Andersen RA (2006) Neural dynamics in monkey parietal reach region reflect context-specific sensorimotor transformations. J Neurosci 26(37):9376-84.

Genovese CR, Lazar NA, Nichols T (2002) Thresholding of statistical maps in functional neuroimaging using the false discovery rate. Neuroimage 15(4):870-8.

Gerloff C, Bushara K, Sailer A, Wassermann EM, Chen R, Matsuoka T, Waldvogel D, Wittenberg GF, Ishii K, Cohen LG, Hallett M (2006) Multimodal imaging of brain reorganization in motor areas of the contralesional hemisphere of well recovered patients after capsular stroke. Brain 129(Pt 3):791-808.

Glidden HK, Rizzuto DS, Andersen RA (2005) Localizing neuroprosthetic implant targets with fMRI: Premotor, supplementary motor, and parietal regions. Program No. 520.2. 2005 Abstract Viewer/Itinerary Planner. Washington, DC: Society for Neuroscience, 2005. Online.

Glidden HK, Rizzuto DS, Fineman I, Andersen RA. Effector-specific motor planning in human parietal and frontal cortices. [submitted]

Goense JB, Logothetis NK (2008) Neurophysiology of the BOLD fMRI signal in awake monkeys. Curr Biol 18(9):631-40.

Goodale MA, Milner AD (1992) Separate visual pathways for perception and action. Trends Neurosci 15(1):20-5.

Gottlieb JP, Kusunoki M, Goldberg ME (1998) The representation of visual salience in monkey parietal cortex. Nature 391(6666):481-4.

Graziano MS, Aflalo TN (2007) Mapping behavioral repertoire onto the cortex. Neuron 56(2)239-51.

Grosbas MH, Leonards U, Lobel E, Poline JB, LeBihan D, Berthoz A (2001) Human cortical networks for new and familiar sequences of saccades. Cereb Cortex 11(10):936-45.

Hagler DJ Jr, Riecke L, Sereno MI (2007) Parietal and superior frontal visuospatial maps activated by pointing and saccades. Neuroimage 35(4):1562-77.

Hagler DJ Jr, Sereno MI (2006) Spatial maps in frontal and prefrontal cortex. Neuroimage 29(2):567-77.

Hahn B, Ross TJ, Stein EA (2006) Neuroanatomical dissociation between bottom-up and top-down processes of visuospatial selective attention. Neuroimage 32(2):842-53.

Hanakawa T, Immisch I, Toma K, Dimyan MA, Van Gelderen P, Hallett M (2003) Functional properties of brain areas associated with motor execution and imagery. J Neurophysiol 89(2):989-1002.

Harness ET, Yozbatiran N, Cramer SC (2008) Effects of intense exercise in chronic spinal cord injury. Spinal Cord. 2008 Jun 3. [Epub ahead of print].

Heiser LM, Colby CL (2006) Spatial updating in area LIP is independent of saccade direction. J Neurophysiol 95(5):2751-67.

Hinton SC, Harrington DL, Binder JR, Durgerian S, Rao SM (2004) Neural systems supporting timing and chronometric counting: an FMRI study. Brain Res Cogn Brain Res 21(2):183-92.

Hoshi E, Sawamura H, Tanji J (2005) Neurons in the rostral cingulate motor area monitor multiple phases of visuomotor behavior with modest parametric selectivity. J Neurophysiol 94(1):640-56.

Hoshi E, Tanji J (2000) Integration of target and body-part information in the premotor cortex when planning action. Nature 408(6811):466-70.

Hoshi E, Tanji J (2002) Contrasting neuronal activity in the dorsal and ventral premotor areas during preparation to reach. J Neurophysiol 87(2):1123-8.

Hoshi E, Tanji J (2004) Differential roles of neuronal activity in the supplementary and presupplementary motor areas: from information retrieval to motor planning and execution. J Neurophysiol 92(6):3482-99.

Hoshi E, Tanji J (2006) Differential involvement of neurons in the dorsal and ventral premotor cortex during processing of visual signals for action planning. J Neurophysiol 95(6):3596-616.

Hotz-Boendermaker S, Funk M, Summers P, Brugger P, Hepp-Reymond MC, Curt A, Kollias SS (2008) Preservation of motor programs in paraplegics as demonstrated by attempted and imagined foot movements. Neuroimage 39(1):383-94.

Hu D, Yan L, Liu Y, Zhou Z, Friston KJ, Tan C, Wu D (2005) Unified SPM-ICA for fMRI analysis. Neuroimage 25(3):746-55.

Johnson PB, Ferraina S, Bianchi L, Caminiti R (1996) Cortical networks for visual reaching: physiological and anatomical organization of frontal and parietal lobe arm regions. Cereb Cortex 6(2):102-19.

Johnson SH, Rotte M, Grafton ST, Hinrichs H, Gazzaniga MS, Heinze HJ (2002) Selective activation of a parietofrontal circuit during implicitly imagined prehension. Neuroimage 17(4):1693-704.

Karnath HO, Perenin MT (2005) Cortical control of visually guided reaching: evidence from patients with optic ataxia. Cereb Cortex 15(10):1561-9.

Kastner S, DeSimone K, Konen CS, Szczepanski SM, Weiner KS, Schneider KA (2007) Topographic maps in human frontal cortex revealed in memory-guided saccade and spatial working-memory tasks. J Neurophysiol 97(5):3494-507.

Kincade JM, Abrams RA, Astafiev SV, Shulman GL, Corbetta M (2005) An event-related functional magnetic resonance imaging study of voluntary and stimulus-driven orienting of attention. J Neurosci 25(18):4593-604.

Koyama M, Hasegawa I, Osada T, Adachi Y, Nakahara K, Miyashita Y (2004) Functional magnetic resonance imaging of macaque monkeys performing visually guided saccade tasks: comparison of cortical eye fields with humans. Neuron 41(5):795-807.

Kwong KK, Belliveau JW, Chesler DA, Goldberg IE, Weisskoff RM, Poncelet BP, Kennedy DN, Hopel BE, Cohen MS, Turner R, et al. (1992) Dynamic magnetic resonance imaging of human brain activity during primary sensory stimulation. Proc Natl Acad Sci USA 89(12):5675-9.

Lachaux JP, Hoffman D, Minotti L, Berthoz A, Kahane P (2006) Intracerebral dynamics of saccade generation in the human frontal eye field and supplementary eye field. Neuroimage 30(4):1302-12.

Lawrence BM, Snyder LH (2006) Comparison of effector-specific signals in frontal and parietal cortices. J Neurophysiol 96(3):1393-400.

Lawrence BM, White RL 3rd, Snyder LH (2005) Delay-period activity in visual, visuomovement, and movement neurons in the frontal eye fields. J Neurophysiol 94(2):1498-508.

Levy I, Schluppeck D, Heeger DJ, Glimcher PW (2007) Specificity of human cortical areas for reaches and saccades. J Neurosci 27(17):4687-96.

Lobel E, Kahane P, Leonards U, Grosbas M, Lehéricy S, Le Bihan D, Berthoz A (2001) Localization of human frontal eye fields: anatomical and functional findings of functional magnetic resonance imaging and intracerebral electrical stimulation. J Neurosurg 95(5):804-15.

Luna B, Thulborn KR, Strojwas MH, McCurtain BJ, Berman RA, Genovese CR, Sweeney JA (1998) Dorsal cortical regions subserving visually guided saccades in humans: an fMRI study. Cereb Cortex 8(1):40-7.

Macar F, Anton JL, Bonnet M, Vidal F (2004) Timing functions of the supplementary motor area: an event-related fMRI study. Brain Res Cogn Brain Res 21(2):206-15.

Macar F, Coull J, Vidal F (2006) The supplementary motor area in motor and perceptual time processing: fMRI studies. Cogn Process 7(2):89-94.

Macar F, Lejeune H, Bonnet M, Ferrara A, Pouthas V, Vidal F, Maquet P (2002) Activation of the supplementary motor area and of attentional networks during temporal processing. Exp Brain Res 142(4):475-85.

Mazzoni P, Bracewell RM, Barash S, Andersen RA (1996) Motor intention activity in the macaque's lateral intraparietal area. I. Dissociation of motor plan from sensory memory. J Neurophysiol 76(3):1439-56.

Medendorp WP, Goltz HC, Crawford JD, Vilis T (2005a) Integration of target and effector information in human posterior parietal cortex for the planning of action. J Neurophysiol 93(2):954-62.

Medendorp WP, Goltz HC, Vilis T (2005b) Remapping the remembered target location for anti-saccades in human posterior parietal cortex. J Neurophysiol 94(1):734-40.

Medendorp WP, Goltz HC, Vilis T, Crawford JD (2003) Gaze-centered updating of visual space in human parietal cortex. J Neurosci 23(15):6209-14.

Michelon P, Vettel JM, Zacks JM (2006) Lateral somatotopic organization during imagined and prepared movements. J Neurophysiol 95(2):811-22.

Mulliken GH, Musallam S, Andersen RA (2004) Decoding trajectories in real-time from posterior parietal cortex. Program No. 263.4. 2004 Abstract Viewer/Itinerary Planner. Washington, DC: Society for Neuroscience. Online.

Mulliken GH, Musallam S, Andersen RA (2008) Forward estimation of movement state in posterior parietal cortex. Proc Natl Acad Sci USA 105(24):8170-7.

Munk MH, Linden DE, Muckli L, Lanfermann H, Zanella FE, Singer W, Goebel R (2002) Distributed cortical systems in visual short-term memory revealed by event-related functional magnetic resonance imaging. Cereb Cortex 12(8):866-76.

Musallam S, Corneil BD, Greger B, Scherberger H, Andersen RA (2004) Cognitive control signals for neural prosthetics. Science 305(5681):258-62.

Mushiake H, Fujii N, Tanji J (1996) Visually guided saccade versus eye-hand reach: contrasting neuronal activity in the cortical supplementary and frontal eye fields. J Neurophysiol 75(5):2187-91.

Nair DG, Purcott KL, Fuchs A, Steinberg F, Kelso JA (2003) Cortical and cerebellar activity of the human brain during imagined and executed unimanual and bimanual action sequences: a functional MRI study. Brain Res Cogn Brain Res 15(3):250-60.

Nudo RJ, Milliken GW, Jenkins WM, Merzenich MM (1996) Use-dependent alterations of movement representations in primary motor cortex of adult squirrel monkeys. J Neurosci 16(2):785-807.

Oldfield RC (1971) The assessment and analysis of handedness: the Edinburgh inventory. Neuropsychologia 9(1):97-113.

Ogawa S, Lee TM, Kay AR, Tank DW (1990a) Brain magnetic resonance imaging with contrast dependent on blood oxygenation. Proc Natl Acad Sci USA 87(24):9868-9872.

Ogawa S, Lee TM, Nayak AS, Glynn P (1990b) Oxygenation-sensitive contrast in magnetic resonance image of rodent brain at high magnetic fields. Magn Reson Med 14(1):68-78.

Pellijeff A, Bonilha L, Morgan PS, McKenzie K, Jackson SR (2006) Parietal updating of limb posture: an event-related fMRI study. Neuropsychologia 44(13):2685-90.

Pesaran B, Nelson MJ, Andersen RA (2006) Dorsal premotor neurons encode the relative position of the hand, eye, and goal during reach planning. Neuron 51(1):125-34.

Quian Quiroga R, Snyder LH, Batista AP, Cui H, Andersen RA (2006) Movement intention is better predicted than attention in the posterior parietal cortex. J Neurosci 26(13):3615-20.

Rossini PM, Altamura C, Ferreri F, Melgari JM, Tecchio F, Tombini M, Pasqualetti P, Vernieri F (2007) Neuroimaging experimental studies on brain plasticity in recovery from stroke. Eura Medicophys 43(2):241-54.

Rizzuto DR. Glidden HK, Fineman I, Andersen RA (2004) Motor imagery activates human parietal reach region. Program No. 263.5. 2004 Abstract Viewer/Itinerary Planner. Washington, DC: Society for Neuroscience, 2004. Online.

Rowe JB, Toni I, Josephs O, Frackowiak RS, Passingham RE (2000) The prefrontal cortex: response selection or maintenance within working memory? Science 288(5471):1656-60.

Rushworth MF, Behrens TE, Johansen-Berg H (2006) Connection patterns distinguish 3 regions of human parietal cortex. Cereb Cortex 16(10):1418-30.

Schaechter JD, Perdue KL (2008) Enhanced cortical activation in the contralesional hemisphere of chronic stroke patients in response to motor skill challenge. Cereb Cortex 18(3):638-47.

Schaechter JD, Perdue KL, Wang R (2008) Structural damage to the corticospinal tract correlates with bilateral sensorimotor cortex reorganization in stroke patients. Neuroimage 39(3):1370-82.

Scherberger H, Andersen RA (2007) Target selection signals for arm reaching in the posterior parietal cortex. J Neurosci 27(8):2001-12.

Scherberger H, Jarvis MR, Andersen RA (2005) Cortical local field potential encodes movement intentions in the posterior parietal cortex. Neuron 46(2):347-54.

Schieber MH, Fuglevand AJ (2003) Motor areas of the cerebral cortex. *Encyclopedia of Cognitive Science, Volume 3*. London: Nature Publishing Group. 111-121.

Schluppeck D, Curtis CE, Glimcher PW, Heeger DJ (2006) Sustained activity in topographic areas of human posterior parietal cortex during memory-guided saccades. J Neurosci 26(19):5098-108.

Schluppeck D, Glimcher P, Heeger DJ (2005) Topographic organization for delayed saccades in human posterior parietal cortex. J Neurophysiol 94(2):1372-84.

Sereno MI, Pitzalis S, Martinez A (2001) Mapping of contralateral space in retinotopic coordinates by a parietal cortical area in humans. Science 294(5545):1350-4.

Shadmehr R, Wise SP (2005) *Computation Neurobiology of Reaching and Pointing: A Foundation for Motor Learning*. Cambridge MA: MIT Press.

Silver MA, Ress D, Heeger DJ (2005) Topographic maps of visual spatial attention in human parietal cortex. J Neurophysiol 94(2):1358-71.

Simon O, Mangin JF, Cohen L, Le Bihan D, Dehaene S (2002) Topographical layout of hand, eye, calculation, and language-related areas in the human parietal lobe. Neuron 33(3):475-87.

Sirigu A, Daprati E, Pradat-Diehl P, Franck N, Jeannerod M (1999) Perception of self-generated movement following left parietal lesion. Brain 122(Pt 10):1867-74.

Snyder LH, Batista AP, Andersen RA (1997) Coding of intention in the posterior parietal cortex. Nature 386(6621):167-70.

Snyder LH, Batista AP, Andersen RA (1998) Change in motor plan, without a chance in the spatial locus of attention, modulates activity in posterior parietal cortex. J Neurophysiol 79(5):2814-9.

Snyder LH, Batista AP, Andersen RA (2000) Saccade-related activity in the parietal reach region. J Neurophysiol 83(2):1099-102.

Sweeney JA, Mintun MA, Kwee S, Wiseman MB, Brown DL, Rosenberg DR, Carl JR (1996) Positron emission tomography study of voluntary saccadic eye movements and spatial working memory. J Neurophysiol 75(1):454-68.

Swisher JD, Halko MA, Merabet LB, McMains SA, Somers DC (2007) Visual topography of human intraparietal sulcus. J Neurosci 27(20):5326-37.

Szameitat AJ, Shen S, Sterr A (2007) Motor imagery of complex everyday movements. An fMRI study. Neuroimage 34(2):702-13.

Torres EB, Andersen RA (2006) Computing time from space in the parietal reach region. Program No. 370.3. 2006 Neuroscience Meeting Planner. Atlanta, GA: Society for Neuroscience. Online.

Vesia M, Monteon JA, Sergio LE, Crawford JD (2006) Hemispheric asymmetry in memory-guided pointing during single-pulse transcranial magnetic stimulation of human parietal cortex. J Neurophysiol 96(6):3016-27.

Ward NS, Brown MM, Thompson AJ, Frackowiak RS (2003) Neural correlates of outcome after stroke: a cross-sectional fMRI study. Brain 126(Pt 6):1430-48.

Ward NS, Newton JM, Swayne OB, Lee L, Thompson AJ, Greenwood RJ, Rothwell JC, Frackowiak RS (2006) Motor system activation after subcortical stroke depends on corticospinal system integrity. Brain 129(Pt 3):809-19.

Wilson KD, Woldorff MG, Mangun GR (2005) Control networks and hemispheric asymmetries in parietal cortex during attentional orienting in different spatial reference frames. Neuroimage 25(3):668-83.